EXHIBITS 22-30

Exhibits to Center for Biological Diversity Comments
EPA Call for Information on Greenhouse Gas Emissions
Associated with Bioenergy and Other Biogenic Sources
Docket No. EPA-HQ-OAR-2010-0560
September 13, 2010

The Copenhagen Diagnosis

Updating the World on the Latest Climate Science

2009

EXHIBIT 22

UNSW Sydney NSW 2052
Australia

Title: ***The Copenhagen Diagnosis***

Subtitle: *Updating the World on the Latest Climate Science*

This report should be cited as:

The Copenhagen Diagnosis, *2009: Updating the World on the Latest Climate Science.*
I. Allison, N.L. Bindoff, R.A. Bindschadler, P.M. Cox, N. de Noblet, M.H. England, J.E. Francis, N. Gruber, A.M. Haywood, D.J. Karoly, G. Kaser, C. Le Quéré, T.M. Lenton, M.E. Mann, B.I. McNeil, A.J. Pitman, S. Rahmstorf, E. Rignot, H.J. Schellnhuber, S.H. Schneider, S.C. Sherwood, R.C.J. Somerville, K. Steffen, E.J. Steig, M. Visbeck, A.J. Weaver. The University of New South Wales Climate Change Research Centre (CCRC), Sydney, Australia, 60pp.

Acknowlegdements:

Stephen Gray from the UNSW Climate Change Research Centre (CCRC) provided support in the compilation of this report and contributed as Technical Editor. Robert Beale (UNSW Faculty of Science) and Michael Molitor (UNSW CCRC) provided editorial advice on sections of the report. Alex Sen Gupta (UNSW CCRC) provided Figure 15 and Darrell Kaufman (Northern Arizona University) provided Figure 20.

Design: Heléna Brusić, P^3 Design Studio, UNSW, Ref: 43413

Printing: SOS Print + Media, Sydney

Photographs:
Text: p3 ©Rainer Prinz *Weissbrunnferner, Italian Alps, 18 July 2006, showing a glacier that has lost its firm body. Extended dark ice surfaces accelerate the melt rate,* p6 ©evirgen & NASA - iStockphoto®, p8 ©Domen Colja - Photospin®, p12 ©Darren Green - Photospin®, p14 ©kavram - Photospin®, p16 ©Brian Press *Tornado* - Photospin®, p17 ©kavram - Photospin®, p18 ©Luoman *Amazon rainforest deforestation* - iStockphoto®, p22 ©Charles Westerlage *Ice carving from Hubbard Glacier* - Photospin®, p28 ©Stephen Schneider *Sunset giant iceberg at Ilulissat*, p31 ©Jan Martin Will - iStockphoto®, p32 ©Phil Dickson *Ice stack collapsing off the Perito Moreno Glacier, Patagonia Argentina* - iStockphoto®, p34 ©Photospin® *South Pacific Islands*, p39 ©Sebastian D'Souza *Indian commuters walk through floodwater* - Getty Images®, p42 ©kavram *Death Valley* - Photospin®, p45 ©Maxim Tupikov *Arctic icebreaker* - iStockphoto®, p46 ©Alexander Hafeman (Mlenny) *Dead Vlei Namibia* - iStockphoto®, ©p47 ©E. Steig, p48 ©Ian Joughin *Meltwater on the Greenland Ice Sheet*, p51 ©Gary Bydlo - Photospin®, p58 Muammer Mujdat Uzel *Marl and dry land on recent lake Denizili Turkey* - iStockphoto®, p60 ©Kirill Putchenko - iStockphoto®.

Cover: (front and inside back) ©Beverley Vycital *Exit Glacier Alaska* - iStockphoto®; front cover images: ©Alexander Hafeman (Mlenny) *Dead Vlei Namibia* - iStockphoto®, ©evirgen & NASA - iStockphoto®, ©Jens Carsten Rosemann *Stormy ocean* - iStockphoto®; back cover: ©Paige Falk *Mud in the Sierra* - iStockphoto®.

Format: Paperback
ISBN: [978-0-9807316-0-6]

Format: Online
ISBN: [978-0-9807316-1-3]

Publication Date: 11/2009

UNSW CRICOS Provider No: 00098G

Climate Change Research Centre

UNSW
THE UNIVERSITY OF NEW SOUTH WALES

The Copenhagen Diagnosis

Updating the World on the Latest Climate Science

2009

CONTRIBUTING AUTHORS

Ian Allison
Nathan Bindoff
Robert Bindschadler
Peter Cox
Nathalie de Noblet-Ducoudré
Matthew England
Jane Francis
Nicolas Gruber
Alan Haywood
David Karoly
Georg Kaser
Corinne Le Quéré
Tim Lenton
Michael Mann
Ben McNeil
Andy Pitman
Stefan Rahmstorf
Eric Rignot
Hans Joachim Schellnhuber
Stephen Schneider
Steven Sherwood
Richard Somerville
Konrad Steffen
Eric Steig
Martin Visbeck
Andrew Weaver

CONTENTS

Preface 5

Executive Summary 7

Greenhouse Gases and the Carbon Cycle 9

The Atmosphere 11

Extreme Events 15

Land Surface 19

Permafrost and Hydrates 21

Glaciers and Ice-Caps 23

Ice-Sheets of Greenland and Antarctica 24

Ice Shelves 27

Sea-Ice 29

The Oceans 35

Global Sea Level 37

Abrupt Change and Tipping Points 40

Lessons from the Past 43

The Future 49

References 52

Biographies 59

PREFACE

It is over three years since the drafting of text was completed for the Intergovernmental Panel on Climate Change (IPCC) Fourth Assessment Report (AR4). In the meantime, many hundreds of papers have been published on a suite of topics related to human-induced climate change. The purpose of this report is to synthesize the most policy-relevant climate science published since the close-off of material for the last IPCC report. The rationale is two-fold. Firstly, this report serves as an interim evaluation of the evolving science midway through an IPCC cycle – IPCC AR5 is not due for completion until 2013. Secondly, and most importantly, the report serves as a handbook of science updates that supplements the IPCC AR4 in time for Copenhagen in December, 2009, and any national or international climate change policy negotiations that follow.

This report covers the range of topics evaluated by Working Group I of the IPCC, namely the Physical Science Basis. This includes:

- an analysis of greenhouse gas emissions and their atmospheric concentrations, as well as the global carbon cycle;
- coverage of the atmosphere, the land-surface, the oceans, and all of the major components of the cryosphere (land-ice, glaciers, ice shelves, sea-ice and permafrost);
- paleoclimate, extreme events, sea level, future projections, abrupt change and tipping points;
- separate boxes devoted to explaining some of the common misconceptions surrounding climate change science.

The report has been purposefully written with a target readership of policy-makers, stakeholders, the media and the broader public. Each section begins with a set of key points that summarises the main findings. The science contained in the report is based on the most credible and significant peer-reviewed literature available at the time of publication. The authors primarily comprise previous IPCC lead authors familiar with the rigor and completeness required for a scientific assessment of this nature.

This report is freely available on the web at:

www.copenhagendiagnosis.com

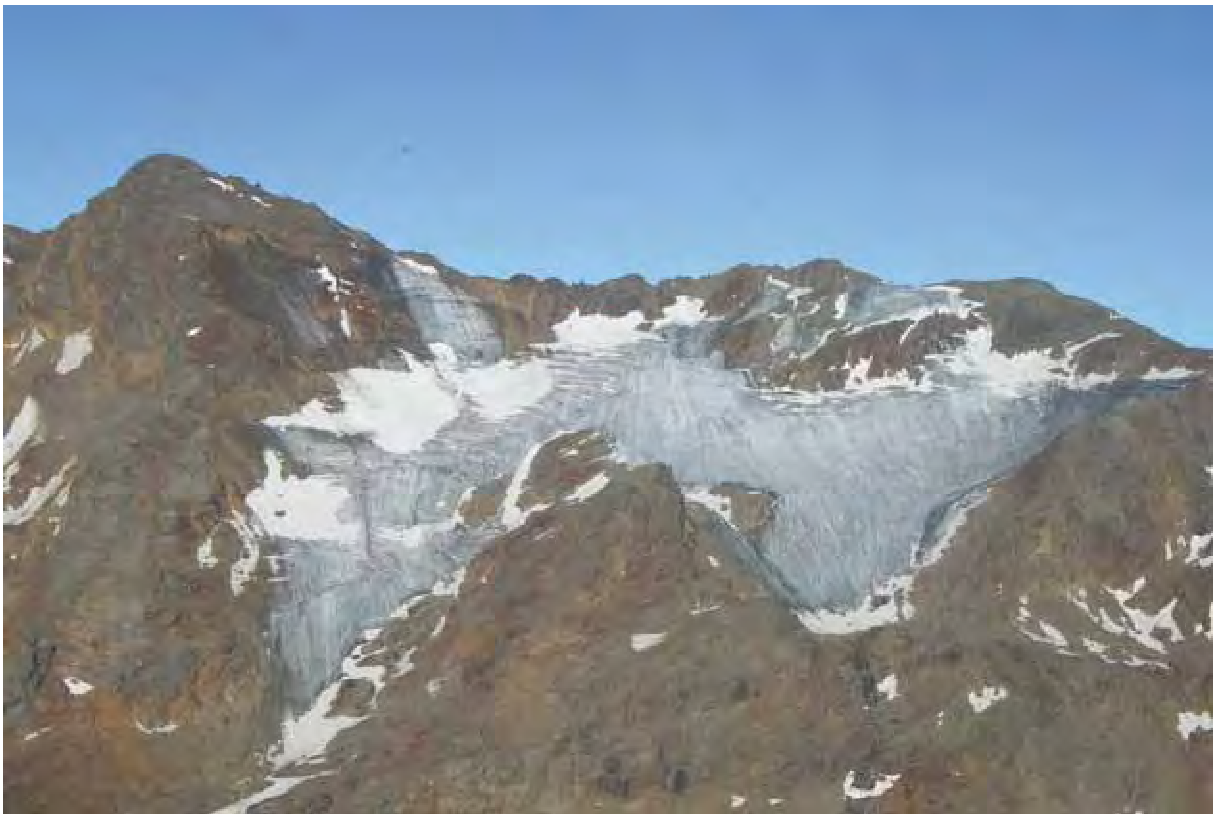

^ *Weissbrunnferner, Italian Alps, 18 July 2006, showing a glacier that has lost its firm body. Extended dark ice surfaces accelerate the melt rate.*

EXECUTIVE SUMMARY

The most significant recent climate change findings are:

Surging greenhouse gas emissions: Global carbon dioxide emissions from fossil fuels in 2008 were 40% higher than those in 1990. Even if global emission rates are stabilized at present-day levels, just 20 more years of emissions would give a 25% probability that warming exceeds 2°C, even with zero emissions after 2030. Every year of delayed action increases the chances of exceeding 2°C warming.

Recent global temperatures demonstrate human-induced warming: Over the past 25 years temperatures have increased at a rate of 0.19°C per decade, in very good agreement with predictions based on greenhouse gas increases. Even over the past ten years, despite a decrease in solar forcing, the trend continues to be one of warming. Natural, short-term fluctuations are occurring as usual, but there have been no significant changes in the underlying warming trend.

Acceleration of melting of ice-sheets, glaciers and ice-caps: A wide array of satellite and ice measurements now demonstrate beyond doubt that both the Greenland and Antarctic ice-sheets are losing mass at an increasing rate. Melting of glaciers and ice-caps in other parts of the world has also accelerated since 1990.

Rapid Arctic sea-ice decline: Summer-time melting of Arctic sea-ice has accelerated far beyond the expectations of climate models. The area of summertime sea-ice melt during 2007-2009 was about 40% less than the average prediction from IPCC AR4 climate models.

Current sea-level rise underestimated: Satellites show recent global average sea-level rise (3.4 mm/yr over the past 15 years) to be ~80% above past IPCC predictions. This acceleration in sea-level rise is consistent with a doubling in contribution from melting of glaciers, ice caps, and the Greenland and West-Antarctic ice-sheets.

Sea-level predictions revised: By 2100, global sea-level is likely to rise at least twice as much as projected by Working Group 1 of the IPCC AR4; for unmitigated emissions it may well exceed 1 meter. The upper limit has been estimated as ~ 2 meters sea level rise by 2100. Sea level will continue to rise for centuries after global temperatures have been stabilized, and several meters of sea level rise must be expected over the next few centuries.

Delay in action risks irreversible damage: Several vulnerable elements in the climate system (e.g. continental ice-sheets, Amazon rainforest, West African monsoon and others) could be pushed towards abrupt or irreversible change if warming continues in a business-as-usual way throughout this century. The risk of transgressing critical thresholds ("tipping points") increases strongly with ongoing climate change. Thus waiting for higher levels of scientific certainty could mean that some tipping points will be crossed before they are recognized.

The turning point must come soon: If global warming is to be limited to a maximum of 2 °C above pre-industrial values, global emissions need to peak between 2015 and 2020 and then decline rapidly. To stabilize climate, a decarbonized global society – with near-zero emissions of CO_2 and other long-lived greenhouse gases – needs to be reached well within this century. More specifically, the average annual per-capita emissions will have to shrink to well under 1 metric ton CO_2 by 2050. This is 80-95% below the per-capita emissions in developed nations in 2000.

GREENHOUSE GASES AND THE CARBON CYCLE

❏ *Global carbon dioxide (CO_2) emissions from fossil fuel burning in 2008 were 40% higher than those in 1990, with a three-fold acceleration over the past 18 years.*

❏ *Global CO_2 emissions from fossil fuel burning are tracking near the highest scenarios considered so far by the IPCC.*

❏ *The fraction of CO_2 emissions absorbed by the land and ocean CO_2 reservoirs has likely decreased by ~5% (from 60 to 55%) in the past 50 years, though interannual variability is large.*

Global Carbon Dioxide Emissions

In 2008, combined global emissions of carbon dioxide (CO_2) from fossil fuel burning, cement production and land use change (mainly deforestation) were 27% higher than in the year 1990 (Le Quéré et al. 2009). Of this combined total, the CO_2 emissions from fossil fuel burning and cement production were 40% higher in 2008 compared to 1990. The global rate of increase of fossil fuel CO_2 emissions has accelerated three-fold over the last 18 years, increasing from 1.0% per year in the 1990s to 3.4% per year between 2000-2008 (Figure 1). The accelerated growth in fossil fuel CO_2 emissions since 2000 was primarily caused by fast growth rates in developing countries (particularly China) in part due to increased international trade of goods (Peters and Hertwich 2008), and by the slowdown of previous improvements in the CO_2 intensity of the global economy (Raupach et al. 2007). The observed acceleration in fossil fuel CO_2 emissions is tracking high-end emissions scenarios used by IPCC AR4 (Nakicenovic et al. 2000). In contrast, CO_2 emissions from land use change were relatively constant in the past few decades. Preliminary figures suggest total CO_2 emissions have dropped in 2009, but this is a temporary effect resulting from the global recession and no sign of the transformation required for stabilizing greenhouse gases in the atmosphere.

Carbon Dioxide

The concentration of CO_2 in the atmosphere reached 385 parts per million (ppm) in 2008 (Figure 2). The atmospheric CO_2 concentration is more than 105 ppm above its natural pre-industrial level. The present concentration is higher than at any time in the last 800,000 years, and potentially the last 3 to 20 million years (Luthi et al. 2008; Tripati et al. 2009; Raymo et al. 1996). CO_2 levels increased at a rate of 1.9 ppm/year between 2000 and 2008, compared to 1.5 ppm/yr in the 1990s. This rate of increase of atmospheric CO_2 is more than ten times faster than the highest rate that has been detected in ice core data; such high rates would be discernable in ice cores if they had occurred at any time in the last 22,000 years (Joos and Spahni 2008).

Methane

The concentration of methane (CH_4) in the atmosphere increased since 2007 to 1800 parts per billion (ppb) after almost a decade of little change (Figure 2). The causes of the recent increase in CH_4 have not yet been determined. The spatial distribution of the CH_4 increase shows that an increase in Northern Hemisphere CH_4 emissions has played a role and could dominate the signal

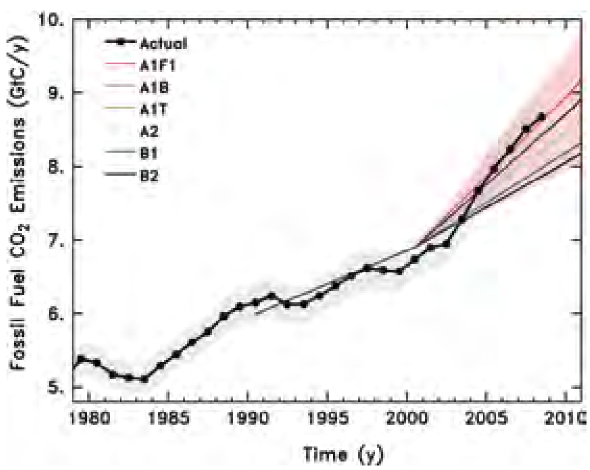

Figure 1. Observed global CO_2 emissions from fossil fuel burning and cement production compared with IPCC emissions scenarios (Le Quéré et al. 2009). Observations are from the US Department of Energy Carbon Dioxide Information Center (CDIAC) up to 2006. 2007 and 2008 are based on BP economic data. The emission scenarios are averaged over families of scenarios presented in Nakicenovic et al (2000). The shaded area covers all scenarios used to project climate change by the IPCC. Emissions in 2009 are projected to be ~3% below 2008 levels, close to the level of emissions in 2007. This reduction is equivalent to a temporary halt in global emissions for a period of only 2-4 weeks.

(Rigby et al. 2008), but the source of the increase is unknown. CH_4 is emitted by many industrial processes (ruminant farming, rice agriculture, biomass burning, coal mining, and gas & oil industry) and by natural reservoirs (wetlands, permafrost and peatlands). Annual industrial emissions of CH_4 are not available as they are difficult to quantify. CH_4 emissions from natural reservoirs can increase under warming conditions. This has been observed from permafrost thawing in Sweden (see Permafrost section), but no large-scale evidence is available to clearly connect this process to the recent CH_4 increase. If the CH_4 increase is caused by the response of natural reservoirs to warming, it could continue for decades to centuries and enhance the greenhouse gas burden of the atmosphere.

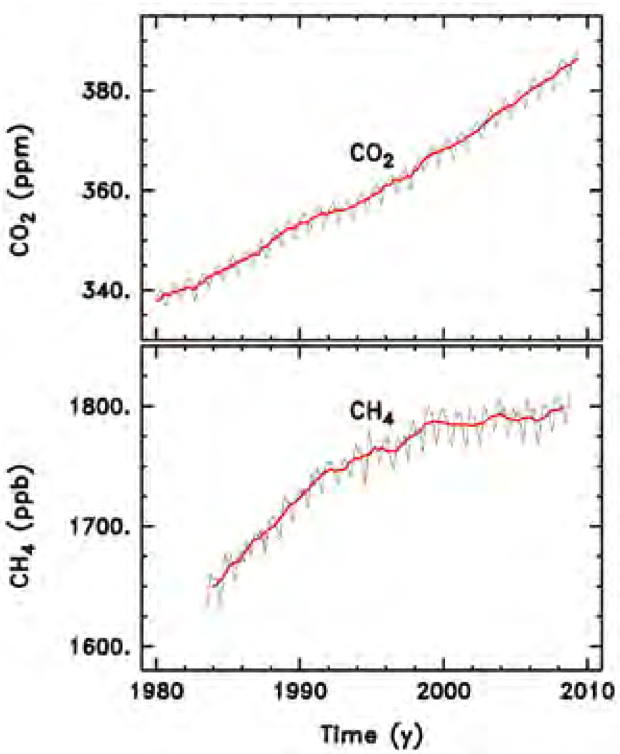

Figure 2. Concentration of CO_2 (top) and CH_4 (bottom) in the atmosphere. The trends with seasonal cycle removed are shown in red. CO_2 and CH_4 are the two most important anthropogenic greenhouse gases. Data are from the Earth System Laboratory of the US National Oceanic and Atmospheric Administration. CO_2 is averaged globally. CH_4 is shown for the Mauna Loa station only.

Carbon Sinks and Future Vulnerabilities

The oceanic and terrestrial CO_2 reservoirs – the 'CO_2 sinks'– have continued to absorb more than half of the total emissions of CO_2. However the fraction of emissions absorbed by the reservoirs has likely decreased by ~5% (from 60 to 55%) in the past 50 years (Canadell et al. 2007). The uncertainty in this estimate is large because of the significant background interannual variability and because of uncertainty in CO_2 emissions from land use change.

The response of the land and ocean CO_2 sinks to climate variability and recent climate change can account for the decrease in uptake efficiency of the sinks suggested by the observations (Le Quéré et al. 2009). A long-term decrease in the efficiency of the land and ocean CO_2 sinks would enhance climate change via an increase in the amount of CO_2 remaining in the atmosphere. Many new studies have shown a recent decrease in the efficiency of the oceanic carbon sink at removing anthropogenic CO_2 from the atmosphere. In the Southern Ocean, the CO_2 sink has not increased since 1981 in spite of the large increase in atmospheric CO_2 (Le Quéré et al. 2007; Metzl 2009; Takahashi et al. 2009). The Southern Ocean trends have been attributed to an increase in winds, itself a likely consequence of ozone depletion (Lovenduski et al. 2008). Similarly, in the North Atlantic, the CO_2 sink decreased by ~50% since 1990 (Schuster et al. 2009), though part of the decrease has been associated with natural variability (Thomas et al. 2008).

Future vulnerabilities of the global CO_2 sinks (ocean and land) have not been revised since the IPCC AR4. Our current understanding indicates that the natural CO_2 sinks will decrease in efficiency during this century, and the terrestrial sink could even start to emit CO_2 (Friedlingstein et al. 2006). The response of the sinks to elevated CO_2 and climate change is shown in models to amplify global warming by 5-30%. The observations available so far are insufficient to provide greater certainty, but they do not exclude the largest global warming amplification projected by the models (Le Quéré et al. 2009).

Is the greenhouse effect already saturated, so that adding more CO_2 makes no difference?

No, not even remotely. It isn't even saturated on the runaway greenhouse planet Venus, with its atmosphere made up of 96% CO_2 and a surface temperature of 467 °C, hotter even than Mercury (Weart and Pierrehumbert 2007). The reason is simple: the air gets ever thinner when we go up higher in the atmosphere. Heat radiation escaping into space mostly occurs higher up in the atmosphere, not at the surface – on average from an altitude of about 5.5 km. It is here that adding more CO_2 does make a difference. When we add more CO_2, the layer near the surface where the CO_2 effect is largely saturated gets thicker – one can visualize this as a layer of fog, visible only in the infrared. When this "fog layer" gets thicker, radiation can only escape to space from higher up in the atmosphere, and the radiative equilibrium temperature of -18 °C therefore also occurs higher up. That upward shift heats the surface, because temperature increases by 6.5 °C per kilometer as one goes down through the atmosphere due to the pressure increase. Thus, adding 1 km to the "CO_2 fog layer" that envelopes our Earth will heat the surface climate by about 6.5 °C.

THE ATMOSPHERE

- ❑ *Global air temperature, humidity and rainfall trend patterns exhibit a distinct fingerprint that cannot be explained by phenomena apart from increased atmospheric greenhouse gas concentrations.*
- ❑ *Every year this century (2001-2008) has been among the top 10 warmest years since instrumental records began, despite solar irradiance being relatively weak over the past few years.*
- ❑ *Global atmospheric temperatures maintain a strong warming trend since the 1970s (~0.6°C), consistent with expectations of greenhouse induced warming.*

Global Temperature Trends

IPCC AR4 presented "an unambiguous picture of the ongoing warming of the climate system." The atmospheric warming trend continues to climb despite 2008 being cooler than 2007 (Figure 3). For example, the IPCC gave the 25-year trend as 0.177 ± 0.052 °C per decade for the period ending 2006 (based on the HadCRUT data). Updating this by including the last two years (2007 and 2008), the trend becomes 0.187 ± 0.052 °C per decade for the period ending 2008. The recent observed climate trend is thus one of ongoing warming, in line with IPCC predictions.

Year-to-year differences in global average temperatures are unimportant in evaluating long-term climate trends. During the warming observed over the 20th century, individual years lie above or below the long-term trend line due to internal climate variability (like 1998); this is a normal and natural phenomenon. For example, in 2008 a La Niña occurred, a climate pattern which naturally causes a temporary dip in the average global temperature. At the same time, solar output was also at its lowest level of the satellite era, another temporary cooling influence. Without anthropogenic warming these two factors should have resulted in the 2008 temperature being among the coolest in the instrumental era, while in fact 2008 was the 9th warmest on record. This underpins the strong greenhouse warming that has occurred in the atmosphere over the past century. The most recent ten-year period is warmer than the previous ten-year period, and the longer-term warming trend is clear and unambiguous (Figure 3).

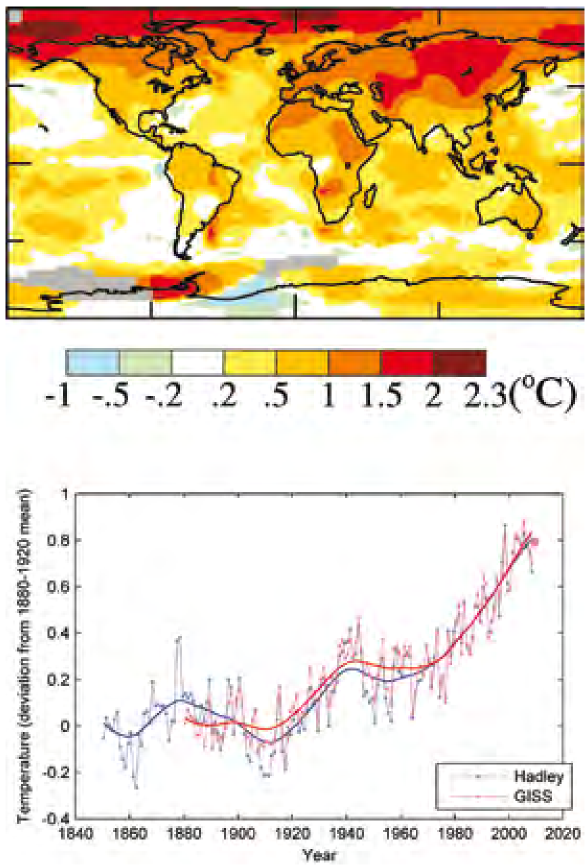

Figure 3. (top) Mean surface temperature change (°C) for 2001-2007 relative to the baseline period of 1951-1980 and (bottom) global average temperature 1850-2009 relative to the baseline period 1880-1920 estimated from the (top) NASA/GISS data set and (bottom) NASA/GISS and Hadley data. Data from the NOAA reconstructed sea surface temperature show similar results. In the lower panel the final bold-face points (they lie on top of each other) are the preliminary values for 2009 based on data up to and including August.

Is the Warming Natural or Human-Induced?

Our understanding of the causes of the recent century-scale trend has improved further since the IPCC AR4. By far the greatest part of the observed century-scale warming is due to human factors. For example, Lean and Rind (2008) analyzed the role of natural factors (e. g., solar variability, volcanoes) versus human influences on temperatures since 1889. They found that the sun contributed only about 10% of surface warming in the last century and a negligible amount in the last quarter century, less than in earlier assessments. No credible scientific literature has been published since the AR4 assessment that supports alternative hypotheses to explain the warming trend.

Is Warming Occurring Higher up in the Atmosphere?

The IPCC AR4 noted a remaining uncertainty in temperature trends in the atmosphere above the lowest layers near the Earth's surface. Most data sets available at that time showed weaker than expected warming in the atmospheric region referred to as the tropical upper troposphere, ten to fifteen kilometers above the surface. However, the observations suffered from significant stability issues especially in this altitude region. Researchers have since performed additional analyses of the same data using more rigorous techniques, and developed a new method of assessing temperature trends from wind observations (Allen and Sherwood 2008). The new observational estimates show greater warming than the earlier ones, and the new, larger set of estimates taken as a whole now bracket the trends predicted by the models (Thorne 2008). This resolves a significant ambiguity expressed in AR4 (Santer et al. 2008).

Water Vapor, Rainfall and the Hydrological Cycle

New research and observations have resolved the question of whether a warming climate will lead to an atmosphere containing more water vapor, which would add to the greenhouse effect and enhance the warming. The answer is yes, this amplifying feedback has been detected: water vapor does become more plentiful in a warmer atmosphere (Dessler et al. 2008). Satellite data show that atmospheric moisture content over the oceans has increased since 1998, with greenhouse emissions being the cause (Santer at al. 2007).

No studies were cited in IPCC AR4 linking observed rainfall trends on a fifty-year time scale to anthropogenic climate change. Now such trends can be linked. For example, Zhang et al. (2007) found that rainfall has reduced in the Northern Hemisphere subtropics but has increased in middle latitudes, and that this can be attributed to human-caused global warming. Models project that such trends will amplify as temperatures continue to rise.

Recent research has also found that rains become more intense in already-rainy areas as atmospheric water vapor content increases (Wentz et al. 2007; Allan and Soden 2008). Their conclusions strengthen those of earlier studies. However, recent changes have occurred even faster than predicted, raising the possibility that future changes could be more severe than predicted. This is a common theme from the recent science: uncertainties existing in AR4, once resolved, point to a more rapidly changing and more sensitive climate than we previously believed.

Has global warming recently slowed down or paused?

No. There is no indication in the data of a slowdown or pause in the human-caused climatic warming trend. The observed global temperature changes are entirely consistent with the climatic warming trend of ~0.2 °C per decade predicted by IPCC, plus superimposed short-term variability (see Figure 4). The latter has always been – and will always be – present in the climate system. Most of these short-term variations are due to internal oscillations like El Niño – Southern Oscillation, solar variability (predominantly the 11-year Schwabe cycle) and volcanic eruptions (which, like Pinatubo in 1991, can cause a cooling lasting a few years).

If one looks at periods of ten years or shorter, such short-term variations can more than outweigh the anthropogenic global warming trend. For example, El Niño events typically come with global-mean temperature changes of up to 0.2 °C over a few years, and the solar cycle with warming or cooling of 0.1 °C over five years (Lean and Rind 2008). However, neither El Niño, nor solar activity or volcanic eruptions make a significant contribution to longer-term climate trends. For good reason the IPCC has chosen 25 years as the shortest trend line they show in the global temperature records, and over this time period the observed trend agrees very well with the expected anthropogenic warming.

Nevertheless global cooling has not occurred even over the past ten years, contrary to claims promoted by lobby groups and picked up in some media. In the NASA global temperature data, the past ten 10-year trends (i.e. 1990-1999, 1991-2000 and so on) have all been between 0.17 and 0.34 °C warming per decade, close to or above the expected anthropogenic trend, with the most recent one (1999-2008) equal to 0.19 °C per decade. The Hadley Center data most recently show smaller warming trends (0.11 °C per decade for 1999-2008) primarily due to the fact that this data set is not fully global but leaves out the Arctic, which has warmed particularly strongly in recent years.

It is perhaps noteworthy that despite the extremely low brightness of the sun over the past three years (see next page); temperature records have been broken during this time (see NOAA, State of the Climate, 2009). For example, March 2008 saw the warmest global land temperature of any March ever measured in the instrumental record. June and August 2009 saw the warmest land and ocean temperatures in the Southern Hemisphere ever recorded for those months. The global ocean surface temperatures in 2009 broke all previous records for three consecutive months: June, July and August. The years 2007, 2008 and 2009 had the lowest summer Arctic sea ice cover ever recorded, and in 2008 for the first time in living memory the Northwest Passage and the Northeast Passage were simultaneously ice-free. This feat was repeated in 2009. Every single year of this century (2001-2008) has been among the top ten warmest years since instrumental records began.

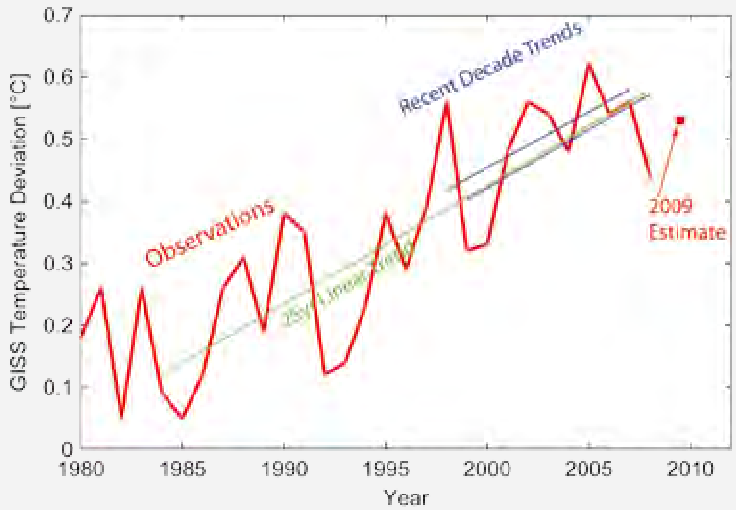

Figure 4. Global temperature according to NASA GISS data since 1980. The red line shows annual data, the red square shows the preliminary value for 2009, based on January-August. The green line shows the 25-year linear trend (0.19 °C per decade). The blue lines show the two most recent ten-year trends (0.18 °C per decade for 1998-2007, 0.19 per decade for 1999-2008) and illustrates that these recent decadal trends are entirely consistent with the long-term trend and IPCC predictions. Misunderstanding about warming trends can arise if only selected portions of the data are shown, e.g. 1998 to 2008, combined with the tendency to focus on extremes or end points (e.g. 2008 being cooler than 1998) rather than an objective trend calculation. Even the highly "cherry-picked" 11-year period starting with the warm 1998 and ending with the cold 2008 still shows a warming trend of 0.11 °C per decade.

Can solar activity or other natural processes explain global warming?

No. The incoming solar radiation has been almost constant over the past 50 years, apart from the well-known 11-year solar cycle (Figure 5). In fact it has slightly decreased over this period. In addition, over the past three years the brightness of the sun has reached an all-time low since the beginning of satellite measurements in the 1970s (Lockwood and Fröhlich 2007, 2008). But this natural cooling effect was more than a factor of ten smaller than the effect of increasing greenhouse gases, so it has not noticeably slowed down global warming. Also, winters are warming more rapidly than summers, and overnight minimum temperatures have warmed more rapidly than the daytime maxima – exactly the opposite of what would be the case if the sun were causing the warming.

Other natural factors, like volcanic eruptions or El Niño events, have only caused short-term temperature variations over time spans of a few years, but cannot explain any longer-term climatic trends (e.g., Lean and Rind 2008).

Figure 5. (below) Time-series of solar irradiance alongside the net effect of greenhouse gas emissions (the latter relative to the year 1880; using Meehl et al. 2004) calculated in terms of total estimated impact on global air temperatures; observed from 1970-2008; and projected from 2009-2030 (adapted from Lean and Rind 2009).

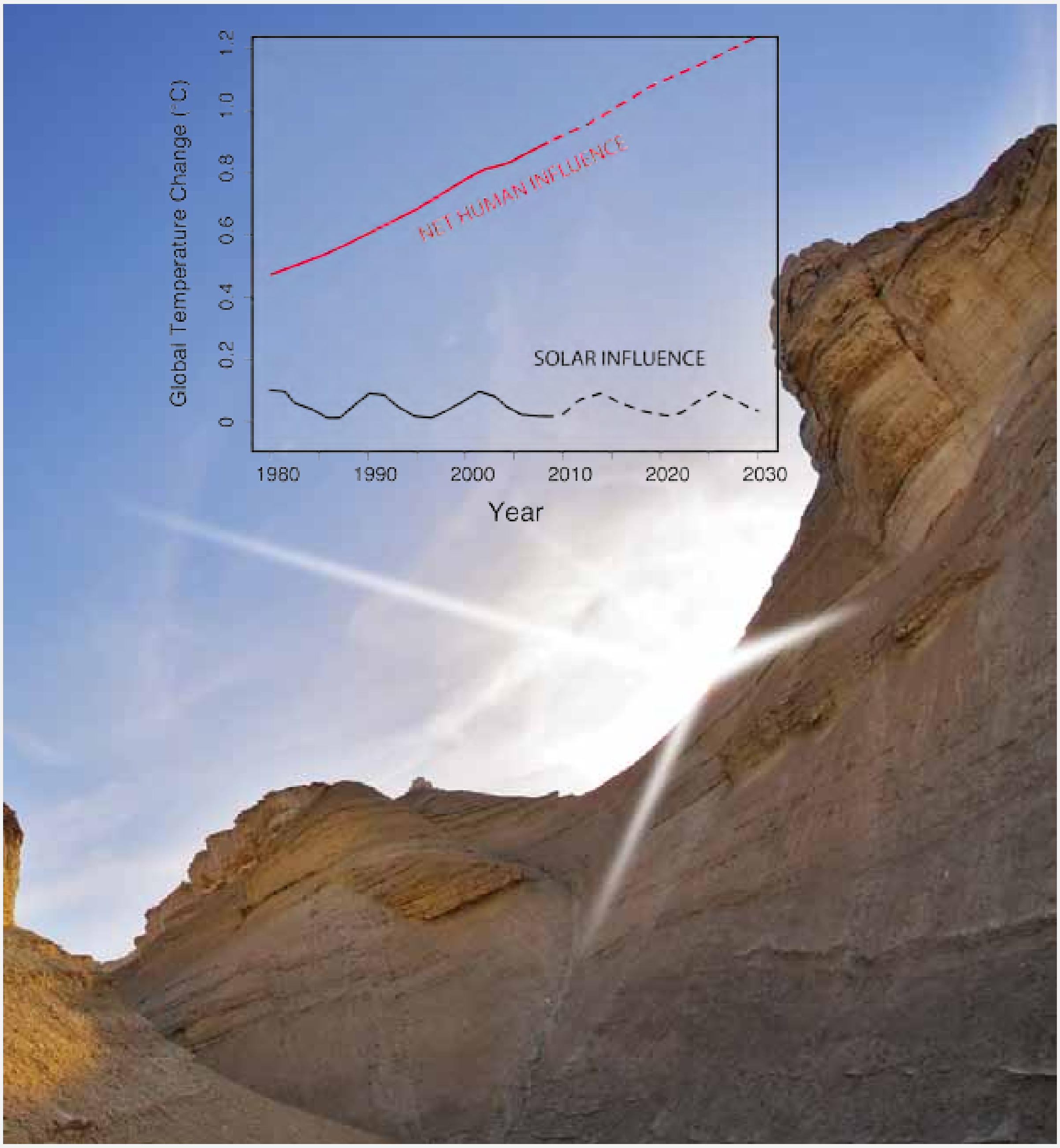

EXTREME EVENTS

- *Increases in hot extremes and decreases in cold extremes have continued and are expected to amplify further.*
- *Anthropogenic climate change is expected to lead to further increases in precipitation extremes, both increases in heavy precipitation and increases in drought.*
- *Although future changes in tropical cyclone activity cannot yet be modeled, new analyses of observational data confirm that the intensity of tropical cyclones has increased in the past three decades in line with rising tropical ocean temperatures.*

Many of the impacts of climate variations and climate change on society, the environment and ecosystems arise through changes in the frequency or intensity of extreme weather and climate events. The IPCC Fourth Assessment Report (IPCC 2007) concluded that many changes in extremes had been observed since the 1970s as part of the warming of the climate system. These included more frequent hot days, hot nights and heat waves; fewer cold days, cold nights and frosts; more frequent heavy precipitation events; more intense and longer droughts over wider areas; and an increase in intense tropical cyclone activity in the North Atlantic but no trend in total numbers of tropical cyclones.

Temperature extremes

Recent studies have confirmed the observed trends of more hot extremes and fewer cold extremes and shown that these are consistent with the expected response to increasing greenhouse gases and anthropogenic aerosols at large spatial scales (CCSP 2008a; Meehl et al. 2007a; Jones et al. 2008; Alexander and Arblaster 2009). However, at smaller scales, the effects of land-use change and variations of precipitation may be more important for changes in temperature extremes in some locations (Portmann et al. 2009). Continued marked increases in hot extremes and decreases in cold extremes are expected in most areas across the globe due to further anthropogenic climate change (CCSP 2008a; Kharin et al. 2007; Meehl et al. 2007a; Jones et al. 2008; Alexander and Arblaster 2009).

Precipitation extremes and drought

Post IPCC AR4 research has also found that rains become more intense in already-rainy areas as atmospheric water vapor content increases (Pall et al. 2007; Wentz et al. 2007; Allan and Soden 2008). These conclusions strengthen those of earlier studies and are expected from considerations of atmospheric thermodynamics. However, recent changes have occurred faster than predicted by some climate models, raising the possibility that future changes will be more severe than predicted.

An example of recent increases in heavy precipitation is found in the United States, where the area with a much greater than normal proportion of days with extreme rainfall amounts has increased markedly (see Figure 6). While these changes in precipitation extremes are consistent with the warming of the climate system, it has not been possible to attribute them to anthropogenic climate change with high confidence due to the very large variability of precipitation extremes (CCSP 2008a; Meehl et al. 2007b; Alexander and Arblaster 2009).

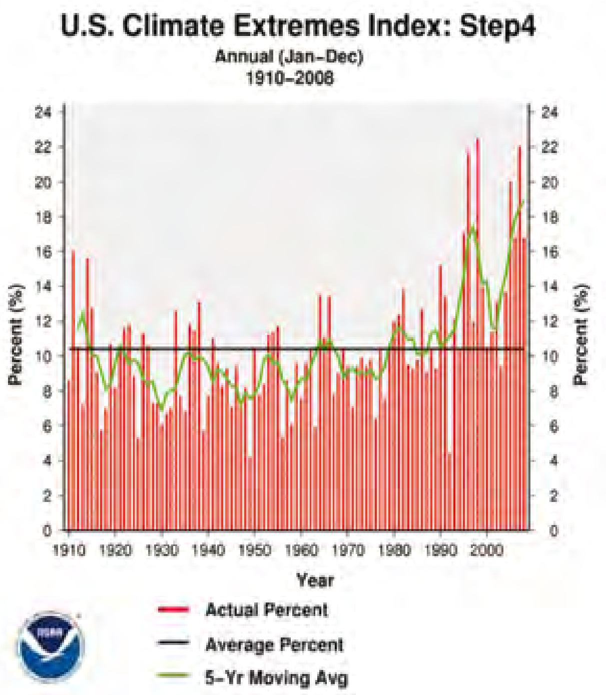

Figure 6. An increasing area of the US is experiencing very heavy daily precipitation events. Annual values of the percentage of the United States with a much greater than normal proportion of precipitation due to very heavy (equivalent to the highest tenth percentile) 1-day precipitation amounts. From Gleason et al. (2008) updated by NOAA at /www.ncdc.noaa.gov/oa/climate/research/cei/cei.html.

In addition to the increases in heavy precipitation, there have also been observed increases in drought since the 1970s (Sheffield and Wood 2008), consistent with the decreases in mean precipitation over land in some latitude bands that have been attributed to anthropogenic climate change (Zhang et al. 2007).

The intensification of the global hydrological cycle with anthropogenic climate change is expected to lead to further increases in precipitation extremes, both increases in very heavy precipitation in wet areas and increases in drought in dry areas. While precise figures cannot yet be given, current studies suggest that heavy precipitation rates may increase by 5% - 10% per °C of warming, similar to the rate of increase of atmospheric water vapor.

Tropical cyclones

The IPCC Fourth Assessment found a substantial upward trend in the severity of tropical cyclones (hurricanes and typhoons) since the mid-1970s, with a trend towards longer storm duration and greater storm intensity, strongly correlated with the rise in tropical sea surface temperatures. It concluded that a further increase in storm intensity is likely.

Several studies since the IPCC report have found more evidence for an increase in hurricane activity over the past decades. Hoyos et al. (2006) found a global increase in the number of hurricanes of the strongest categories 4 and 5, and they identified rising sea surface temperatures (SST) as the leading cause. Warming tropical SST has also been linked to increasingly intense tropical cyclone activity – and an increasing number of tropical cyclones – in the case of certain basins such as the North Atlantic (Mann and Emanuel 2006; Emanuel et al. 2008; Mann et al. 2009).

Scientific debate about data quality has continued, especially on the question of how many tropical cyclones may have gone undetected before satellites provided a global coverage of observations. Mann et al. (2007) concluded that such an undercount bias would not be large enough to question the recent rise in hurricane activity and its close connection to sea surface warming. A complete reanalysis of satellite data since 1980 (Elsner et al. 2008) confirms a global increase of the number of category 4 and 5 (i.e., the strongest) tropical cyclones: they found a 1°C global warming corresponding to a 30% increase in these storms. While evidence has thus firmed up considerably that recent warming has been associated with stronger tropical cyclones, modeling studies (e.g. Emanuel et al. 2008; Knutson et al. 2008, Vecchi et al. 2008) have shown that we have as yet no robust capacity to project future changes in tropical cyclone activity.

Other severe weather events

The IPCC Fourth Assessment concluded that there were insufficient studies available to make an assessment of observed changes in small-scale severe weather events or of expected future changes in such events. However, recent research has shown an increased frequency of severe thunderstorms in some regions, particularly the tropics and south-eastern US, is expected due to future anthropogenic climate change (Trapp et al. 2007; Aumann et al. 2008; Marsh et al. 2009; Trapp et al. 2009). In addition, there have been recent increases in the frequency and intensity of wildfires in many regions with Mediterranean climates (e.g. Spain, Greece, southern California, south-east Australia) and further marked increases are expected due to anthropogenic climate change (Westerling et al. 2006; Pitman et al. 2008).

LAND SURFACE

- *Land cover change, particularly deforestation, can have a major impact on regional climate, but at the global scale its biggest impact comes from the CO_2 released in the process.*
- *Observations through the 2005 drought in Amazonia suggest that the tropical forests could become a strong carbon source if rainfall declines in the future.*
- *Carbon dioxide changes during the Little Ice Age indicate that warming may in turn lead to carbon release from land surfaces, a feedback that could amplify 21st century climate change.*
- *Avoiding tropical deforestation could prevent up to 20% of human-induced CO_2 emissions and help to maintain biodiversity.*

How does land-use change affect climate?

Earth's climate is strongly affected by the nature of the land-surface, including the vegetation and soil type and the amount of water stored on the land as soil moisture, snow and groundwater. Vegetation and soils affect the surface albedo, which determines the amount of sunlight absorbed by the land. The land surface also affects the partitioning of rainfall into evapotranspiration (which cools the surface and moistens the atmosphere) and runoff (which provides much of our freshwater). This partitioning can affect local convection and therefore rainfall. Changes in land-use associated with the spread of agriculture and urbanization and deforestation can alter these mechanisms. Land use change can also change the surface roughness, affect emissions of trace gases, and some volatile organic compounds such as isoprene. Despite the key role of land cover change at regional scales, climate model projections from IPCC AR4 excluded anthropogenic land-cover change.

There has been significant progress on modeling the role of land cover change since the IPCC AR4 (Piekle et al. 2007), with the first systematic study demonstrating that large-scale land cover change directly and significantly affects regional climate (Pitman et al. 2009). This has important implications for understanding future climate change; climate models need to simulate land cover change to capture regional changes in regions of intense land cover change. However, failing to account for land cover change has probably not affected global-scale projections (Pitman et al. 2009), noting that emissions from land cover change are included in projections.

Land-cover change also affects climate change by releasing CO_2 to the atmosphere and by modifying the land carbon sink (Bondeau et al. 2007; Fargione et al. 2008). The most obvious example of this is tropical deforestation which contributes about a fifth of global CO_2 emissions and also influences the land-to-atmosphere fluxes of water and energy (Bala et al. 2007). Avoiding deforestation therefore eliminates a significant fraction of anthropogenic CO_2 emissions, and maintains areas like the Amazon rainforest which supports high biodiversity and plays a critically important role in the climate system (Malhi et al. 2008).

Climate Change and the Amazon Rainforest

The distribution and function of vegetation depends critically on the patterns of temperature and rainfall across the globe. Climate change therefore has the potential to significantly alter land-cover even in the absence of land-use change. A key area of concern has been the remaining intact Amazonian rainforest which is susceptible to 'dieback' in some climate models due to the combined effects of increasing greenhouse gases and reducing particulate or 'aerosol' pollution in the northern hemisphere (Cox et al. 2008). However, these projections are very dependent on uncertain aspects of regional climate change, most notably the sign and magnitude of rainfall change in Amazonia in the 21st century (Malhi et al. 2008, 2009).

There have also been some doubts raised as to whether the Amazonian rainforest is as sensitive to rainfall reductions as large-scale models suggest. The drought in Western Amazonia in 2005 provided a test of this hypothesis using long-term monitoring of tree growth in the region (Phillips et al. 2009), and a massive carbon source was detected in the region in 2005 against the backdrop of a significant carbon sink in the decades before. The forests of Amazonia are therefore sensitive to '2005-like' droughts and these are expected to become more common in the 21st century (Cox et al. 2008).

A similar story emerges from the analysis of satellite and CO_2 flux measurements during the European drought of 2003 (Reichstein et al. 2007). The IPCC AR4 tentatively suggested a link between global warming and the 2003 drought, and this analysis showed that the drought had an enormous impact on the health and functioning of both natural and managed landscapes in the region.

How large are feedbacks linking land-surface and climate?

The response of the land-surface to climatic anomalies feeds back on the climate by changing the fluxes of energy, water and CO_2 between the land and the atmosphere. For example, it seems likely that changes in the state of the land-surface, which in turn changed the energy and water fluxes to the atmosphere, played an important part in the severity and length of the 2003 European drought (Fischer et al. 2007). In some regions, such as the Sahel, land-atmosphere coupling may be strong enough to support two alternative climate-vegetation states; one wet and vegetated, the other dry and desert-like. There may be other "hot-spot" regions where the land-atmosphere coupling significantly controls the regional climate; indeed it appears that the land is a strong control on climate in many semi arid and Mediterranean-like regions.

However, the strongest feedbacks on global climate in the 21st century are likely to be due to changes in the land carbon sink. The climate-carbon cycle models reported in the IPCC AR4 (Friedlingstein et al. 2006) reproduced the historical land carbon sink predominantly through `CO_2 fertilization'. There is evidence of CO_2 fertilization being limited in nitrogen-limited ecosystems (Hyvonen et al. 2007), but the first generation coupled climate-carbon models did not include nutrient cycling.

The IPCC AR4 climate-carbon cycle models also represented a counteracting tendency for CO_2 to be released more quickly from the soils as the climate warms, and as a result these models predicted a reducing efficiency of the land carbon sink under global warming. There is some suggestion of a slow-down of natural carbon sinks in the recent observational record (Canadell et al. 2007), and strong amplifying land carbon-climate feedback also seems to be consistent with records of the little ice-age period (Cox and Jones 2008).

Does the land-surface care about the causes of climate change?

Yes. Vegetation is affected differently by different atmospheric pollutants, and this means that the effects of changes in atmospheric composition cannot be understood purely in terms of their impact on global warming.

CO_2 increases affect the land through climate change, but also directly through CO_2-fertilization of photosynthesis, and 'CO_2-induced stomatal closure' which tends to increase plant water-use efficiency. Observational studies have shown a direct impact of CO_2 on the stomatal pores of plants, which regulate the fluxes of water vapor and CO_2 at the leaf surface. In a higher CO_2 environment, stomata reduce their opening since they are able to take up CO_2 more efficiently. By transpiring less, plants increase their water-use efficiency, which consequently affects the surface energy and water balance. If transpiration is suppressed via higher CO_2, the lower evaporative cooling may also lead to higher temperatures (Cruz et al. 2009). There is also the potential for significant positive impacts on freshwater resources, but this is still an area of active debate (Gedney et al. 2006, Piao et al. 2007, Betts et al. 2007).

By contrast, increases in near surface ozone have strong negative impacts on vegetation by damaging leaves and their photosynthetic capacity. As a result historical increases in near surface ozone have probably suppressed land carbon uptake and therefore increased the rate of growth of CO_2 in the 20th century. Sitch et al. (2007) estimate that this indirect forcing of climate change almost doubles the contribution that near-surface ozone made to 20th century climate change.

Atmospheric aerosol pollution also has a direct impact on plant physiology by changing the quantity and nature of the sunlight reaching the land-surface. Increasing aerosol loadings from around 1950 to 1980, associated predominantly with the burning of sulphurous coal, reduced the amount of sunlight at the surface, which has been coined 'global dimming' (Wild et al. 2007). Since plants need sunlight for photosynthesis, we might have expected to see a slow-down of the land carbon sink during the global dimming period, but we didn't. Mercado et al. (2009) offer an explanation for this based on the fact that plants are more light-efficient if the sunlight is 'diffuse'. Aerosol pollution would certainly have scattered the sunlight, making it more diffuse, as well as reducing the overall quantity of sunlight reaching the surface. It seems that 'diffuse radiation fertilization' won this battle, enhancing the global land-carbon sink by about a quarter from 1960 to 2000 (Mercado et al. 2009). This implies that the land carbon sink will decline if we reduce the amount of potentially harmful particulates in the air.

These recent studies since IPCC AR4 argue strongly for metrics to compare different atmospheric pollutants that go beyond radiative forcing and global warming, to impacts on the vital ecosystem services related to the availability of food and water.

PERMAFROST AND HYDRATES

- *New insights into the Northern Hemisphere permafrost (permanently frozen ground) suggest a large potential source of CO_2 and CH_4 that would amplify atmospheric concentrations if released.*
- *A recent increase in global methane levels cannot yet be attributed to permafrost degradation.*
- *A separate and significant source of methane exists as hydrates beneath the deep ocean floor and in permafrost. It has recently been concluded that release of this type of methane is very unlikely to occur this century.*

As noted in the IPCC AR4 and more recent studies, the southern boundary of the discontinuous permafrost zone has shifted northward over North America in recent decades. Rapid degradation and upward movement of the permafrost lower limit has continued on the Tibetan plateau (Jin et al. 2008, Cui and Graf 2009). In addition, observations in Europe (Åkerman and Johansson 2008; Harris et al. 2009) have noted permafrost thawing and a substantial increase in the depth of the overlying active layer exposed to an annual freeze/thaw cycle, especially in Sweden.

As permafrost melts and the depth of the active layer deepens, more organic material can potentially start to decay. If the surface is covered with water, methane-producing bacteria break down the organic matter. But these bacteria cannot survive in the presence of oxygen. Instead, if the thawed soils are exposed to air, carbon dioxide-producing bacteria are involved in the decay process. Either case is an amplifying feedback to global warming. In fact, the magnitude of the feedback represents an important unknown in the science of global warming; this feedback has not been accounted for in any of the IPCC projections. The total amount of carbon stored in permafrost has been estimated to be around 1672 Gt (1 Gt = 10^9 tons), of which ~277 Gt are contained in peatlands (Schuur et al. 2008; Tarnocai et al. 2009). This represents about twice the amount of carbon contained in the atmosphere. A recent analysis by Dorrepaal et al. (2009) has found strong direct observational evidence for an acceleration of carbon emissions in association with climate warming from a peat bog overlying permafrost at a site in northern Sweden. Whether or not recent observations of increasing atmospheric methane concentration (Rigby et al. 2008), after nearly a decade of stable levels, are caused by enhanced northern hemisphere production associated with surface warming is still uncertain.

Another amplifying feedback to warming that has recently been observed in high northern latitudes involves the microbial transformation of nitrogen trapped in soils to nitrous oxide. By measuring the nitrous oxide emissions from bare peat surfaces, Repo et al. (2009) inferred emissions per square meter of the same magnitude as those from croplands and tropical soils. They point out that as the Arctic warms, regions of bare exposed peat will increase, thereby amplifying total nitrous oxide emissions.

Between 500 and 10,000 Gt of carbon are thought to be stored under the sea floor in the form methane hydrates (or clathrates), a crystalline structure of methane gas and water molecules (Brook et al. 2008). Another 7.5 to 400 Gt of carbon are stored in the form of methane hydrates trapped in permafrost (Brook et al. 2008). Some have argued that anthropogenic warming could raise the possibility of a catastrophic release of methane from hydrates to the atmosphere. In a recent assessment by the US Climate Change Science Program (CCSP 2008b), it was deemed to be very unlikely that such a release would occur this century, although the same assessment deemed it to be very likely that methane sources from hydrate and wetland emissions would increase as the climate warmed. This is supported by a recent analysis that found that the observed increase in atmospheric methane 11,600 years ago had a wetland, as opposed to hydrate, origin (Petrenko et al. 2009); as was also found in studies using Earth models of intermediate complexity (Fyke and Weaver 2006; Archer et al. 2009).

Few studies with AR4-type climate models have been undertaken. One systematic study used the Community Climate System Model, version 3 (CCSM3) with explicit treatment of frozen soil processes. The simulated reduction in permafrost reached 40% by ~2030 irrespective of emission scenario (a reduction from ~10 million km^2 to 6 million km^2). By 2050, this reduces to 4 million km^2 (under B1 emissions) and 3.5 million km^2 (under A2 emissions). Permafrost declines to ~1 million km^2 by 2100 under A2. In each case, the simulations did not include additional feedbacks triggered by the collapse of permafrost including out-gassing of methane, a northward expansion of shrubs and forests and the activation of the soil carbon pool. These would each further amplify warming.

GLACIERS AND ICE-CAPS

- *There is widespread evidence of increased melting of glaciers and ice-caps since the mid-1990s.*
- *The contribution of glaciers and ice-caps to global sea-level has increased from 0.8 millimeters per year in the 1990s to be 1.2 millimeters per year today.*
- *The adjustment of glaciers and ice caps to present climate alone is expected to raise sea level by ~18 centimeters. Under warming conditions they may contribute as much as ~55 centimeters by 2100*

Glaciers and mountain ice-caps can potentially contribute a total of approximately 0.7 meters to global sea-level. Glaciers and mountain ice-caps also provide a source of freshwater in many mountain regions worldwide. The IPCC AR4 assessed the contribution from worldwide shrinking glaciers and ice caps to sea level rise at the beginning of the 21st Century at about 0.8 millimeters per year (Lemke et al. 2007, Kaser et al. 2006). Since then, new estimates of the contribution from glaciers and ice caps have been made using new data and by exploring new assessment methods.

These new assessments are shown in Figure 7. They show glacier and ice cap contributions to sea level rise that are generally slightly higher than those reported in IPCC AR4. They also extend from 1850 up to 2006. These new estimates show that the mass loss of glaciers and ice caps has increased considerably since the beginning of the 1990s and now contribute about 1.2 millimeters per year to global sea level rise.

Glaciers and ice caps are not in balance with the present climate. Recent estimates show that adjustment to that alone will cause a mass loss equivalent to ~18 centimeters sea level rise (Bahr et al. 2009) within this century. Under ongoing changes consistent with current warming trends, a mass loss of up to ~55 centimeters sea level rise is expected by 2100 (Pfeffer et al. 2008).

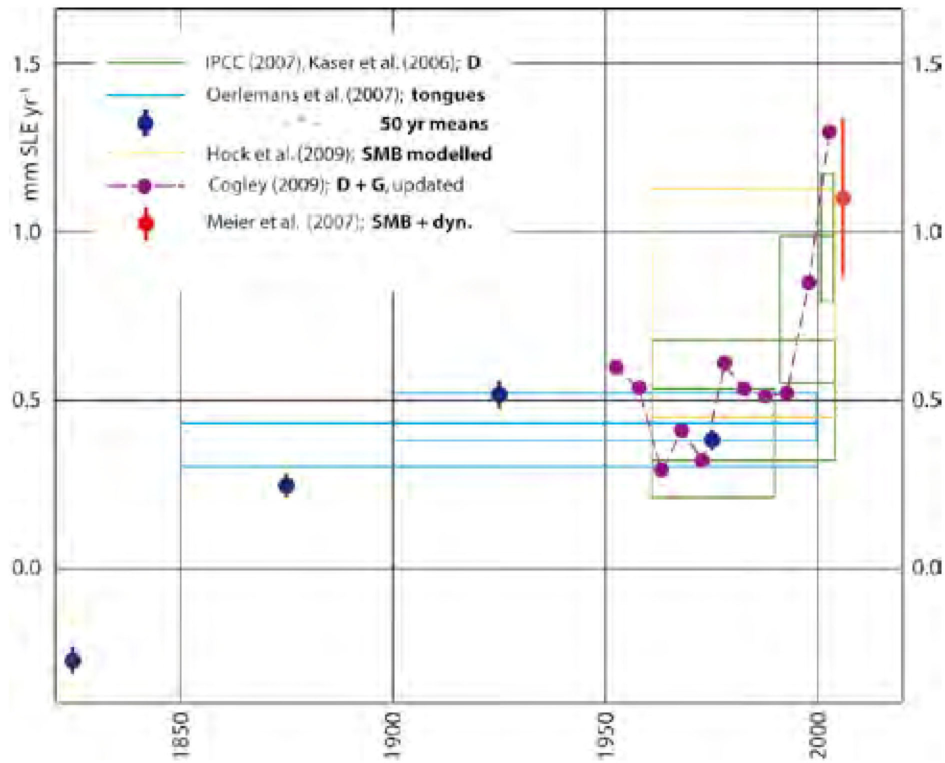

Figure 7. Estimates of the contribution of glaciers and ice-caps to global change in sea-level equivalent (SLE), in millimeters SLE per year.

ICE-SHEETS OF GREENLAND AND ANTARCTICA

- *The surface area of the Greenland ice sheet which experiences summer melt has increased by 30% since 1979, consistent with warming air temperatures. Melt covered 50% of the ice sheet during the record season in 2007.*
- *The net loss of ice from the Greenland ice sheet has accelerated since the mid-1990s and is now contributing as much as 0.7 millimeters per year to sea level rise due to both increased melting and accelerated ice flow.*
- *Antarctica is also losing ice mass at an increasing rate, mostly from the West Antarctic ice sheet due to increased ice flow. Antarctica is currently contributing to sea level rise at a rate nearly equal to Greenland.*

Antarctica and Greenland maintain the largest ice reservoirs on land. If completely melted, the Antarctic ice-sheet would raise global sea-level by 52.8 meters, while Greenland would add a further 6.6 meters. Loss of only the most vulnerable parts of West Antarctica would still raise sea level by 3.3 meters (Bamber et al,. 2009). IPCC AR4 concluded that net ice loss from the Greenland and Antarctic ice sheets together contributed to sea level rise over the period 1993 to 2003 at an average rate estimated at 0.4 millimeters per year. Since IPCC AR4, there have been a number of new studies observing and modelling ice-sheet mass budget that have considerably enhanced our understanding of ice-sheet vulnerabilities (Allison et al. 2009). These assessments reinforce the conclusion that the ice sheets are contributing to present sea level rise, and show that the rate of loss from both Greenland and Antarctica has increased recently. Furthermore, recent observations have shown that changes in the rate of ice discharge into the sea can occur far more rapidly than previously suspected (e.g. Rignot 2006).

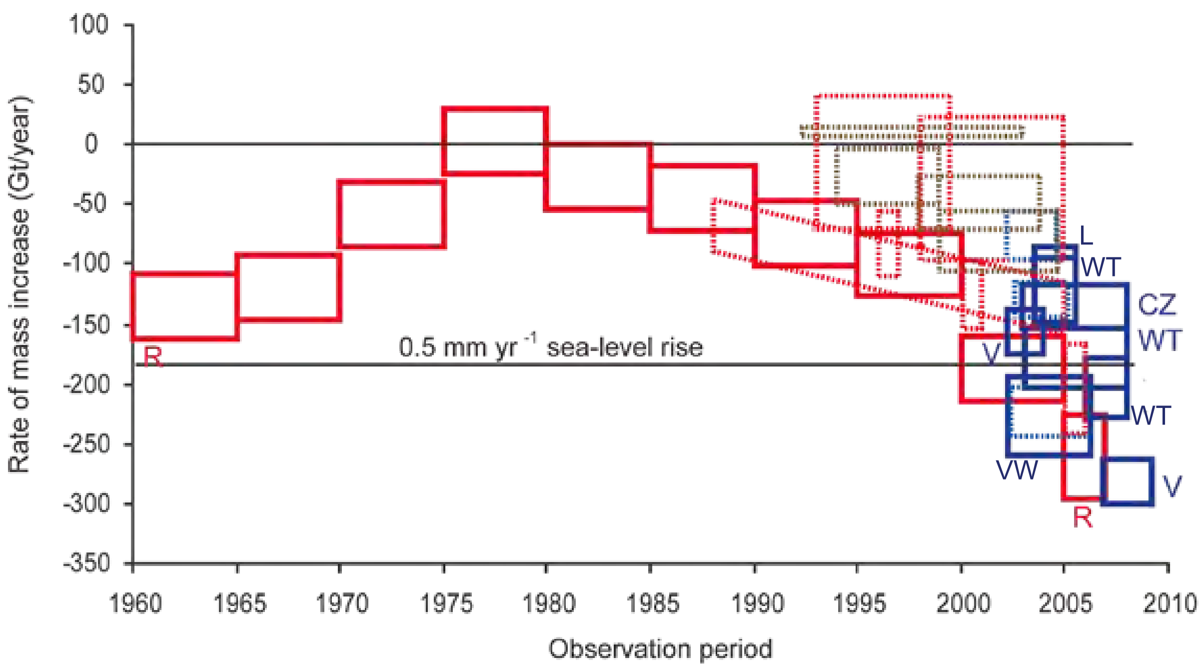

Figure 8. Estimates of the net mass budget of the Greenland Ice Sheet since 1960. A negative mass budget indicates ice loss and sea level rise. Dotted boxes represent estimates used by IPCC AR4 (IPCC, 2007). The solid boxes are post-AR4 assessments (R = Rignot et al. 2008a; VW = Velicogna & Wahr 2006; L = Luthcke et al. 2006; WT = Wouters et al. 2008; CZ = Cazenave et al. 2009; V = Velicogna 2009).

Greenland

Figure 8 shows estimates of the mass budget of the Greenland Ice Sheet since 1960. In this representation, the horizontal dimension of the boxes shows the time period over which the estimate was made, and the vertical dimension shows the upper and lower limits of the estimate. The colors represent the different methods that were used: estimates derived from satellite or aircraft altimeter measurements of height change of the ice sheet surface are brown; estimates of mass loss from satellite gravity measurements are blue; and estimates derived from the balance between mass influx and discharge are red.

The data in Figure 8 indicate that net ice mass loss from Greenland has been increasing since at least the early 1990s, and that in the 21st Century, the rate of loss has increased significantly. Multiple observational constraints and the use of several different techniques provide confidence that the rate of mass loss from the Greenland ice-sheet has accelerated. Velicogna (2009) used GRACE satellite gravity data to show that the rate of Greenland mass loss doubled over the period from April 2002 to February 2009.

Near-coastal surface melt and run-off have increased significantly since 1960 in response to warming temperature, but total snow precipitation has also increased (Hanna et al. 2008). The average Greenland surface temperature rose by more than 1.5°C over the period 2000 to 2006 and mass loss estimated from GRACE gravity data occurred within 15 days of the initiation of surface melt, suggesting that the water drains rapidly from the ice sheet (Hall et al. 2008). Passive microwave satellite measurements of the area of the Greenland ice sheet subject to surface melt indicate that the melt area has been increasing since 1979 (Steffen et al. 2008; Figure 9). There is a good correlation between total melt area extent and the number of melt days with total volume of run off, which has also increased.

The pattern of ice sheet change in Greenland is one of near-coastal thinning, primarily in the south along fast-moving outlet glaciers. Accelerated flow and discharge from some major outlet glaciers (also called dynamic thinning) is responsible for much of the loss (Rignot & Kanagaratnam 2006; Howat et al. 2007). In southeast Greenland many smaller drainage basins, especially the catchments of marine-terminating outlet glaciers, are also contributing to ice loss (Howat et al. 2008). Pritchard et al. (2009) used high resolution satellite laser altimetry to show that dynamic thinning of fast-flowing coastal glaciers is now widespread at all latitudes in Greenland. Greenland glaciers flowing faster than 100 meters per year thinned by an average of 0.84 meters per year between 2003 and 2007.

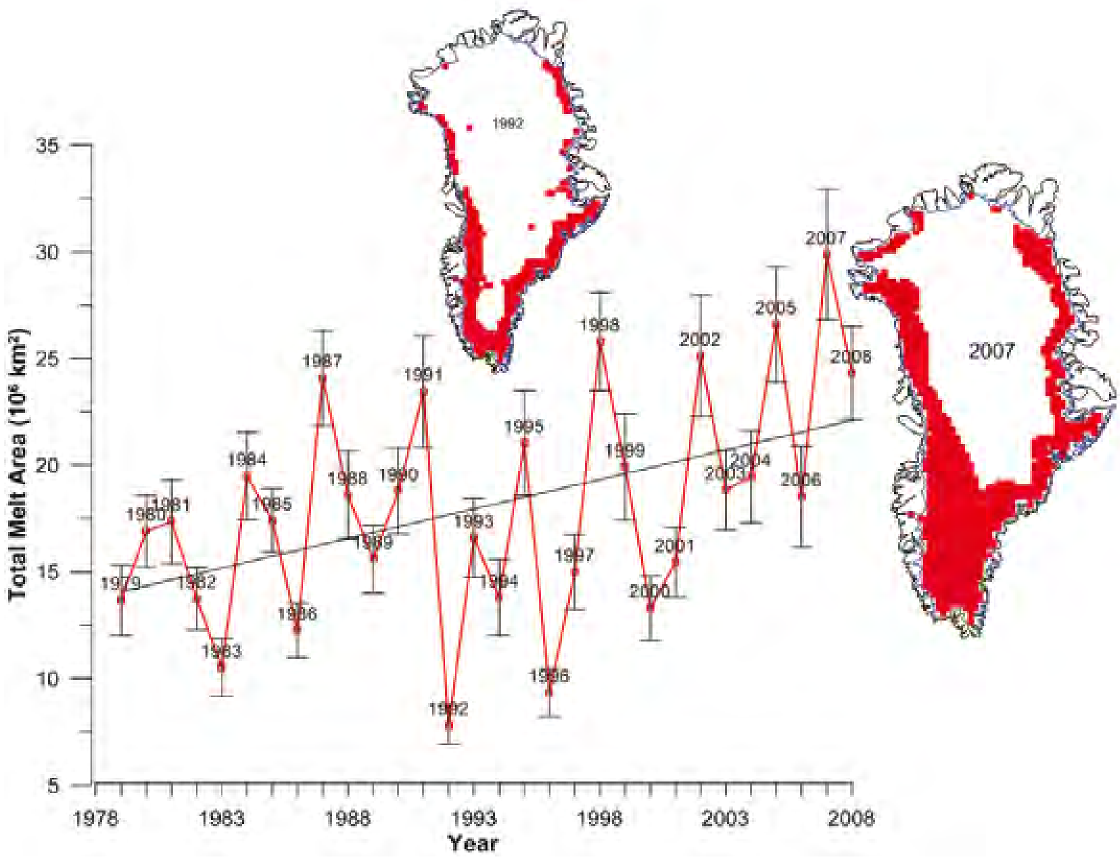

Figure 9. The total melt area of the Greenland ice sheet increased by 30% between 1979 and 2008 based on passive microwave satellite data, with the most extreme melt in 2007. In general 33-55% of the total mass loss from the Greenland ice sheet is caused by surface melt and runoff. For 2007, the area experiencing melt was around 50% of the total ice sheet area. The low melt year in 1992 was caused by the volcanic aerosols from Mt. Pinatubo causing a short-lived global cooling (updated from Steffen et al. 2008).

Antarctica

New estimates of the mass budget of the Antarctic Ice Sheet are shown in Figure 10. Comprehensive estimates for Antarctica are only available since the early 1990s. Several new studies using the GRACE satellite gravity data (blue boxes in Figure 10) all show net loss from the Antarctic since 2003 with a pattern of near balance for East Antarctica, and greater mass loss from West Antarctica and the Antarctic Peninsula (e.g. Chen et al. 2006; Cazenave et al. 2009). The GRACE assessment of Velicogna (2009) indicates that, like Greenland, the rate of mass loss from the Antarctic ice sheet is accelerating, increasing from 104 Gt per year for 2002-2006 to 246 Gt per year for 2006-2009 (the equivalent of almost 0.7 millimeters per year of sea level rise). Gravity and altimeter observations require correction for uplift of the Earth's crust under the ice sheets (glacial isostatic adjustment): this is poorly known for Antarctica.

The largest losses occurred in the West Antarctic basins draining into the Bellingshausen and Amundsen Seas. Satellite glacier velocity estimates from 1974 imagery show that the outlet glaciers of the Pine Island Bay region have accelerated since then, changing a region of the ice sheet that was in near-balance to one of considerable loss (Rignot 2008). Rignot et al. (2008b) show that the ice discharge in this region further increased between 1996 and 2006, increasing the net mass loss over the period by 59%, and Pritchard et al. (2009) show from laser altimetry that dynamic thinning in some parts of the Amundsen Sea embayment has exceeded 9 meters per year. The recent acceleration of ice streams in West Antarctica explains much of the Antarctic mass loss, but narrow fast-moving ice streams in East Antarctica are also contributing to the loss (Pritchard et al. 2009).

The Antarctic Peninsula region has experienced much greater warming than the continent as a whole. This has led to widespread retreat (Cook et al. 2005) and acceleration (Pritchard & Vaughan 2007) of the tidewater glaciers in that region.

The Risk of Ice-Sheet Collapse

The largest unknown in the projections of sea level rise over the next century is the potential for rapid dynamic collapse of ice sheets. The most significant factor in accelerated ice discharge in both Greenland and Antarctica over the last decade has been the un-grounding of glacier fronts from their bed, mostly due to submarine ice melting. Changes to basal lubrication by melt water, including surface melt draining through moulins (vertical conduits) to the bottom of the ice sheet, may also affect the ice sheet dynamics in ways that are not fully understood. The major dynamic ice sheet uncertainties are largely one-sided: they can lead to a faster rate of sea-level rise, but are unlikely to significantly slow the rate of rise. Although it is unlikely that total sea level rise by 2100 will be as high as 2 meters (Pfeffer et al. 2008), the probable upper limit of a contribution from the ice sheets remains uncertain.

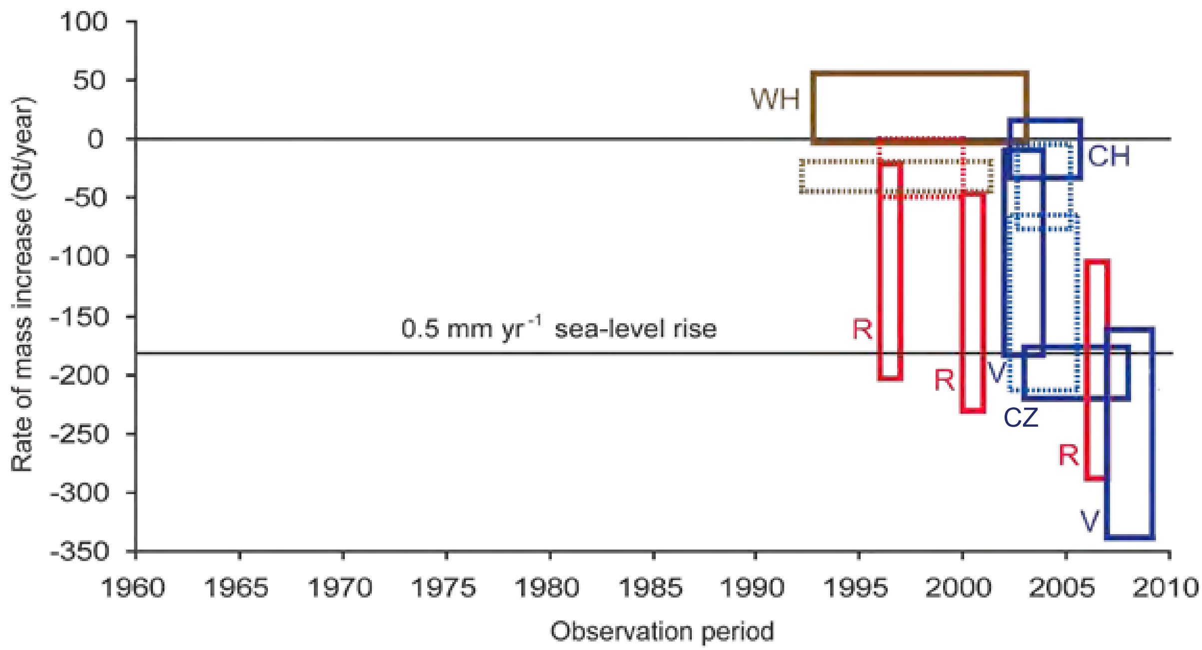

Figure 10. Estimates of the net mass budget of the Antarctic Ice Sheet since 1992. Dotted boxes represent estimates used by IPCC AR4 (IPCC 2007). The solid boxes are more recent estimates (CH = Chen et al. 2006; WH = Wingham et al. 2006; R = Rignot et al. 2008b; CZ = Cazenave et al. 2009; V = Velicogna 2009).

ICE SHELVES

- ❏ *Ice-shelves connect continental ice-sheets to the ocean. Destabilization of ice-shelves along the Antarctic Peninsula has been widespread with 7 collapses over the past 20 years.*
- ❏ *Signs of ice shelf weakening have been observed elsewhere than in the Antarctic Peninsula, e.g. in the Bellingshausen and Amundsen seas, indicating a more widespread influence of atmospheric and oceanic warming than previously thought.*
- ❏ *There is a strong influence of ocean warming on ice sheet stability and mass balance via the melting of ice-shelves.*

Ice shelves are floating sheets of ice of considerable thickness that are attached to the coast. They are mostly composed of ice that has flowed from the interior ice sheet, or that has been deposited as local snowfall. They can be found around 45% of the Antarctic coast, in a few bays off the north coast of Ellesmere Island near Greenland, and in a few fiords along the northern Greenland coast (where they are termed ice tongues). Over the last few years, the six remaining ice shelves (Serson, Petersen, Milne, Ayles, Ward Hunt and Markham) off Ellesmere Island have either collapsed entirely (Ayles on August 13, 2005 and Markham during the first week of August, 2008) or undergone significant disintegration.

Along the coast of Greenland, the seaward extent of the outlet glacier Jakobshavn Isbrae provides a striking example of a floating ice tongue in retreat (Figure 11). Holland et al. (2008) suggest

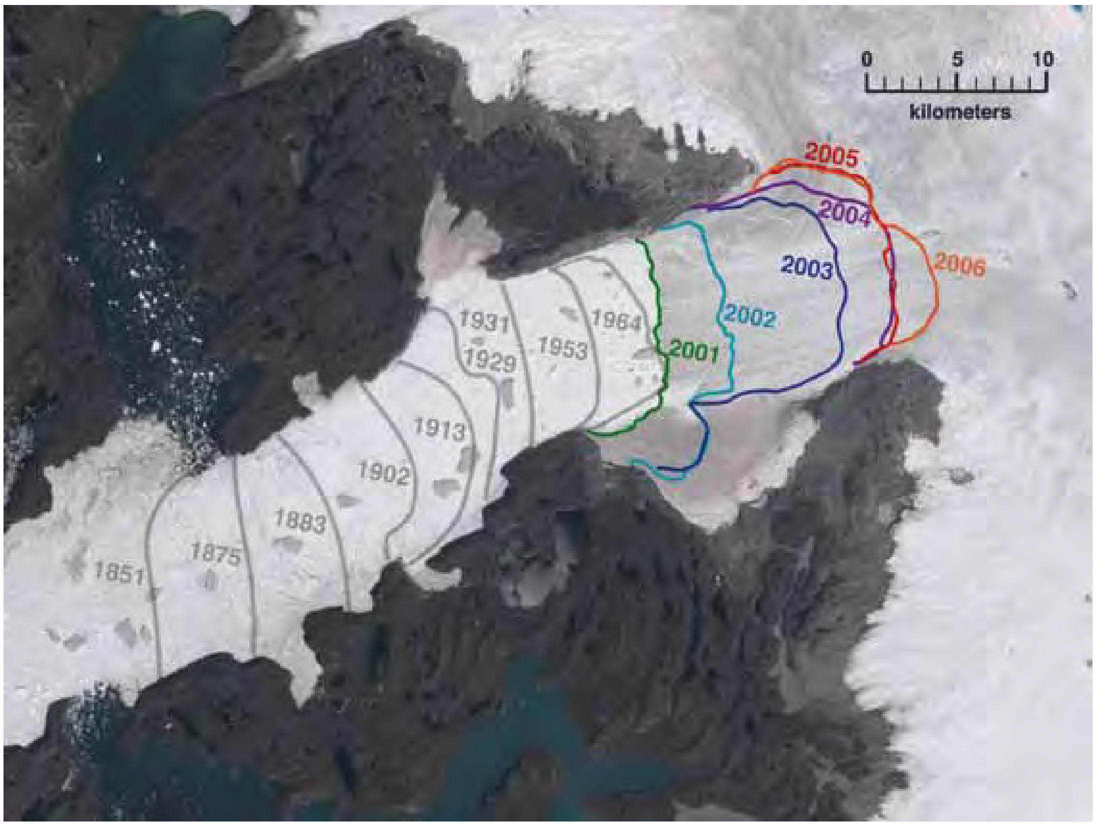

Figure 11. The floating ice tongue representing the seaward extent of Jakobshavn Isbræ on July 7, 2001. Changes in the position of the calving front from 1851 to 2006 are indicated. Credit: NASA/Goddard Space Flight Center Scientific Visualization Studio (http://svs.gsfc.nasa.gov/vis/a000000/a003300/a003395/).

that the observed recent acceleration (Rignot and Kanagaratnam 2006) of Jakobshavn Isbrae may be attributed to thinning from the arrival of warm waters in the region.

Destabilization of floating ice shelves has been widespread along the Antarctic Peninsula with seven collapsing in the last 20 years. Warming along the Peninsula has been dramatic, and on the western side has been substantially above the global average. Most recently, in March 2009, more than 400 square kilometers collapsed off the Wilkins Ice Shelf on the western side of the Antarctic Peninsula. A number of mechanisms are thought to play important roles in destabilizing floating Antarctic ice shelves. These include: surface warming leading to the creation of melt ponds and subsequent fracturing of existing crevasses (van den Broeke 2005); subsurface ice shelf melting from warming ocean waters (Rignot et al. 2008b); and internal ice shelf stresses (Bruan and Humbert 2009). While the collapse of a floating ice shelf does not itself raise sea level, its collapse is followed by rapid acceleration of glacier outflow – which does raise sea level – due to the removal of the ice shelf buttressing effect (e.g. Rignot et al. 2004; Scambos et al. 2004).

There is evidence for the melting of ice shelves in the Amundsen Sea, with impacts on the flow speed of glaciers draining this part of West Antarctica. A recent modeling study has suggested that the West Antarctic Ice Sheet would begin to collapse when ocean temperatures in the vicinity of any one of the ice shelves that surround it warm by about 5°C (Pollard and DeConto 2009). There is also evidence that these changes are not limited to West Antarctica and may also affect the coastline of East Antarctica, for example in Wilkes Land (Pritchard et al. 2009; Shepherd and Wingham 2007). The widespread thinning and acceleration of glaciers along the Antarctic coast may indicate a significant impact of oceanic changes on glacier dynamics, a factor that has received little attention in past IPCC reports due to the lack of observational data on ice-ocean interactions and how climate change might influence coastal ocean waters.

SEA-ICE

- The observed summer-time melting of Arctic sea-ice has far exceeded the worst-case projections from climate models of IPCC AR4.
- The warming commitment associated with existing atmospheric greenhouse gas levels means it is very likely that in the coming decades the summer Arctic Ocean will become ice-free, although the precise timing of this remains uncertain.
- Satellite observations show a small increase of Antarctic sea-ice extent and changes to seasonality, although there is considerable regional variability. This is most likely due to changes in Southern Ocean winds associated with stratospheric ozone-depletion.

Arctic Sea Ice

Perhaps the most stunning observational change since the IPCC AR4 has been the shattering of the previous Arctic summer minimum sea ice extent record – something not predicted by climate models. Averaged over the five-day period leading up to September 16, 2007, the total extent of sea ice in the Arctic was reduced to an area of only 4.1 million square kilometers (see Figure 12), surpassing the previous minimum set in 2005 by 1.2 million square kilometers (about the same size as France, Spain, Portugal, Belgium and Netherlands combined). The median September minimum sea ice extent since observations with the current generation of multi-frequency passive microwave sensors commenced in 1979 to 2000 was 6.7 million square kilometers. Compared to the median, the 2007 record involved melting 2.6 million square kilometers more ice (~40% of the median).

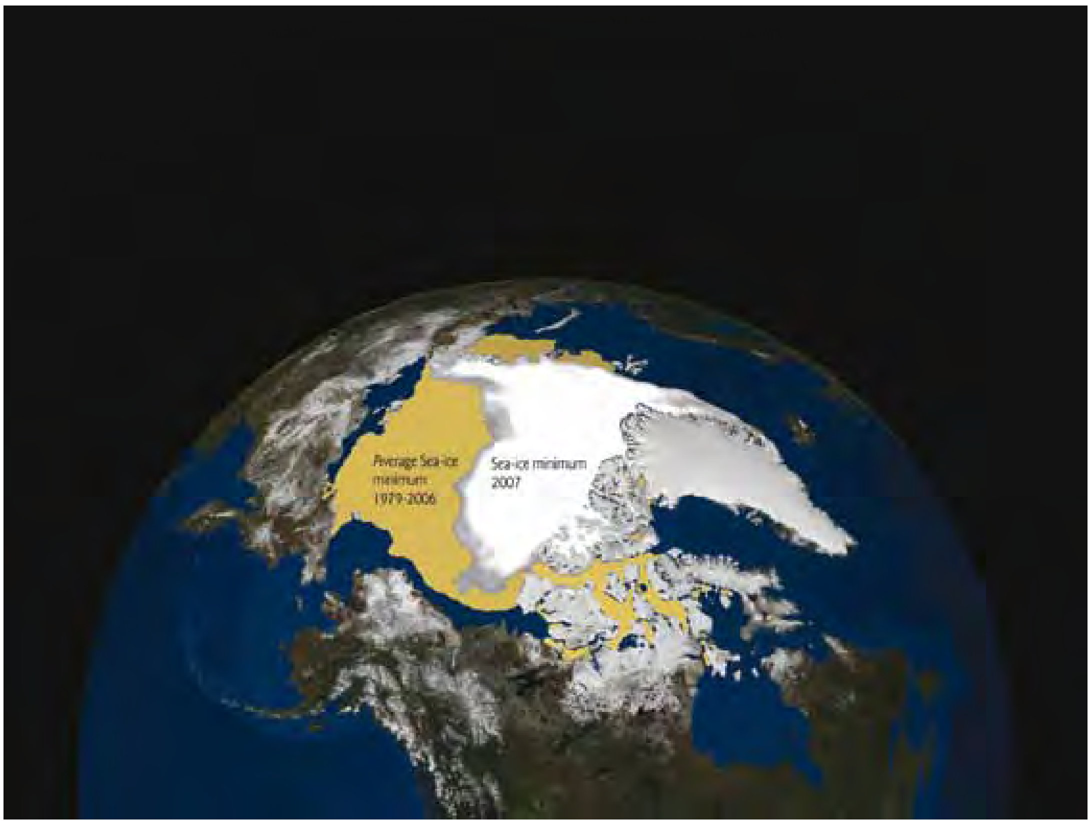

Figure 12. Arctic sea ice extent over the five days leading up to and including September 16, 2007 compared to the average sea-ice minimum extent for the period 1979- 2006. Sourced from the NASA/Goddard Space Flight Center Scientific Visualization Studio.

The September Arctic sea ice extent over the last several decades has decreased at a rate of 11.1 ± 3.3%/decade (NSIDC 2009). This dramatic retreat has been much faster than that simulated by any of the climate models assessed in the IPCC AR4 (Figure 13). This is likely due to a combination of several model deficiencies, including: 1) incomplete representation of ice albedo physics, including the treatment of melt ponds (e.g., Pedersen et al. 2009) and the deposition of black carbon (e.g. Flanner et al. 2007; Ramanathan and Carmichael 2008); and 2) incomplete representation of the physics of vertical and horizontal mixing in the ocean (e.g. Arzel et al. 2006). Winter Arctic sea ice extent has also decreased since 1979, but at a slower rate than in summer. The February extent has decreased at a rate of 2.9 ± 0.8%/decade (NSIDC 2009).

The thickness of Arctic sea ice has also been on a steady decline over the last several decades. For example, Lindsay et al. (2009) estimated that the September sea ice thickness has been decreasing at a rate of 57 centimeters per decade since 1987. Similar decreases in sea-ice thickness have been detected in winter. For example, within the area covered by submarine sonar measurements, Kwok and Rothrock (2009) show that the overall mean winter thickness of 3.64 meters in 1980 decreased to only 1.89 meters by 2008 — a net decrease of 1.75 meters, or 48%. By the end of February 2009, less than 10% of Arctic sea ice was more than two years old, down from the historic values of 30%.

When Will the Arctic Ocean be Ice-Free?

Due to the existence of natural variability within the climate system, it is not possible to predict the precise year that the Arctic Ocean will become seasonally ice free. Nevertheless, the warming commitment associated with existing atmospheric greenhouse gas levels very likely means that a summer ice-free Arctic is inevitable. Evidence is also emerging to suggest that the transition to an ice-free summer in the Arctic might be expected to occur abruptly, rather than slowly (Holland et al. 2006), because of amplifying feedbacks inherent within the Arctic climate system. In fact, in one of the simulations of the NCAR Climate System Model version 3 (CCSM3) discussed in Holland et al (2006), the Arctic summer became nearly ice-free by 2040. As noted by Lawrence et al. (2008), an abrupt reduction in Arctic summer sea ice extent also triggers rapid warming on land and subsequent permafrost degradation.

Antarctic Sea Ice

Unlike the Arctic, Antarctic sea-ice extent changes have been more subtle, with a net annual-mean area increase of ~1% per decade over the period 1979–2006 (Cavalieri and Parkinson 2008; Comiso and Nishio 2008). There have however been large regional changes in Antarctic sea-ice distribution: for example, the Weddell and Ross Sea areas have shown increased extent linked to changes in large-scale atmospheric circulation, while the western Antarctic Peninsula region and the coast of West Antarctica (Amundsen and Bellingshausen Seas) show a significant decline consistent with more northerly winds and surface warming observed there (Lefebvre et al. 2004; Turner et al. 2009; Steig et al. 2009). These regional changes are linked to a major change in the seasonality of the ice; that is, its duration and the timing of the annual advance and retreat (Stammerjohn et al. 2008).

Since Antarctica is a land mass surrounded by the vast Southern Ocean, whereas the Arctic is a small ocean surrounded by vast amounts of land, and as oceans respond less rapidly than land to warming because of their thermal stability, one would expect, and indeed climate models show, a delayed

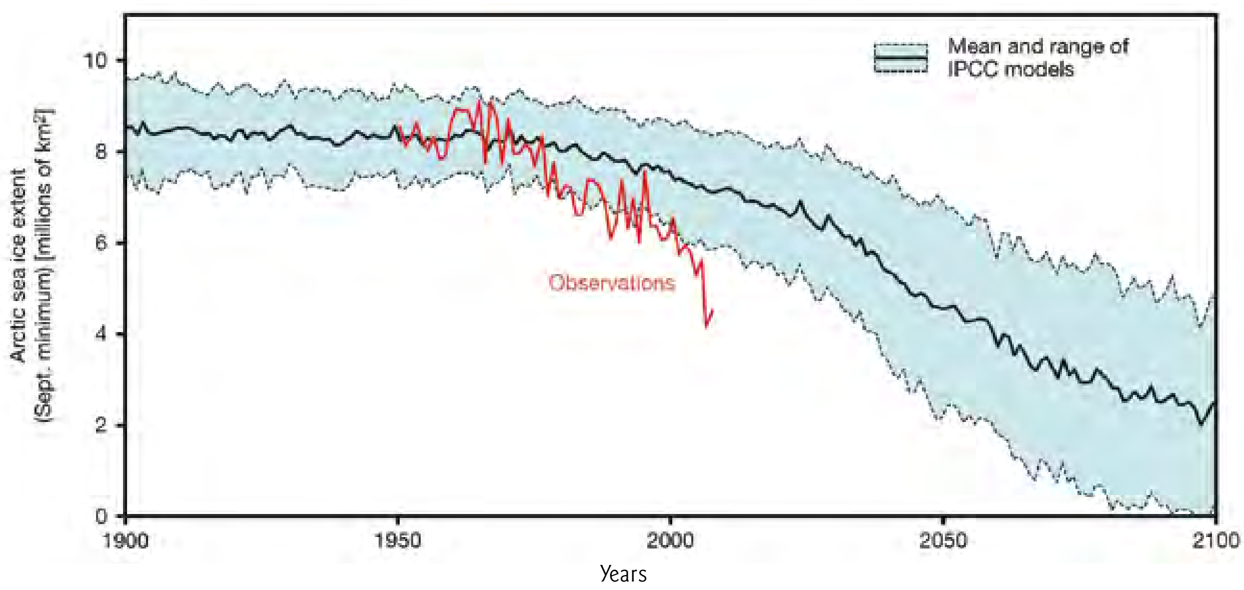

Figure 13. Observed (red line) and modeled September Arctic sea ice extent in millions of square kilometers. The solid black line gives the ensemble mean of the 13 IPCC AR4 models while the dashed black lines represent their range. From Stroeve et al. (2007) updated to include data for 2008. The 2009 minimum has recently been calculated at 5.10 million km², the third lowest year on record, and still well below the IPCC worst case scenario.

warming response around Antarctica. In addition, Turner et al. (2009) note that stratospheric ozone depletion arising from the anthropogenic release of chlorofluorocarbons (CFCs) has led to the strengthening of surface winds around Antarctica during December to February (summer). They argue that these strengthened winds are in fact the primary cause for the slight positive trend in Antarctic sea ice extent observed over the last three decades. However, as CFCs are regulated under the Montreal Protocol and have declining atmospheric concentrations, the ozone hole over Antarctica is expected to recover and hence one anticipates an acceleration of sea ice melt in the Southern Hemisphere in the decades ahead.

There are few data available on the thickness distribution of Antarctic pack ice, and no information on any changes in the thickness of Antarctic sea ice.

Isn't Antarctica cooling and Antarctic sea ice increasing?

Antarctica is not cooling: it has warmed overall over at least the past 50 years. Although the weather station at the South Pole shows cooling over this period, this single weather station is not representative. For example, there is a warming trend at Vostok, the only other long-term monitoring station in the interior of the continent. Several independent analyses (Chapman and Walsh 2008; Monaghan et al. 2008; Goosse et al. 2009; Steig et al. 2009) show that on average, Antarctica has warmed by about 0.5°C since wide-scale measurements began in the 1957 International Geophysical Year, with particularly rapid warming around the Antarctic Peninsula region and over the West Antarctic Ice Sheet (Figure 14 shows the mean trend from 1957-2006). Furthermore, there is direct evidence from borehole measurements that warming in West Antarctica began no later than the 1930s (Barrett et al. 2009).

Since the development of the Antarctic ozone hole in the late 1970s, there has been a strengthening of the circumpolar winds around Antarctica, which tends to reduce the amount of warmer air reaching the interior of the continent. The stronger winds are due to cooling in the upper atmosphere, which are in turn a result of ozone depletion caused by chlorofluorocarbons. As a consequence, much of East Antarctica has cooled in the summer and autumn seasons since the late 1970s. Ironically, human emissions of CFCs are thus helping to partly offset interior Antarctic warming, analogous to the global dimming due to sulphate aerosols. As the ozone hole gradually repairs over the coming century, the cooling offset is likely to diminish.

The factors that determine sea ice extent around Antarctica are very different from those in the Arctic, because Antarctica is a continent sited around the pole and surrounded by water, just the opposite of the Arctic geography. The extent of sea ice around Antarctica is strongly determined by the circumpolar winds which spread the ice out from the continent, and by the position of the polar front where the ice encounters warmer ocean waters. Sea ice cover in Antarctica shows a slight upward trend, consistent with the increase in circumpolar winds mentioned above. In West Antarctica, where the temperature increases are the greatest, sea ice has declined at a statistically significant rate since at least the 1970s.

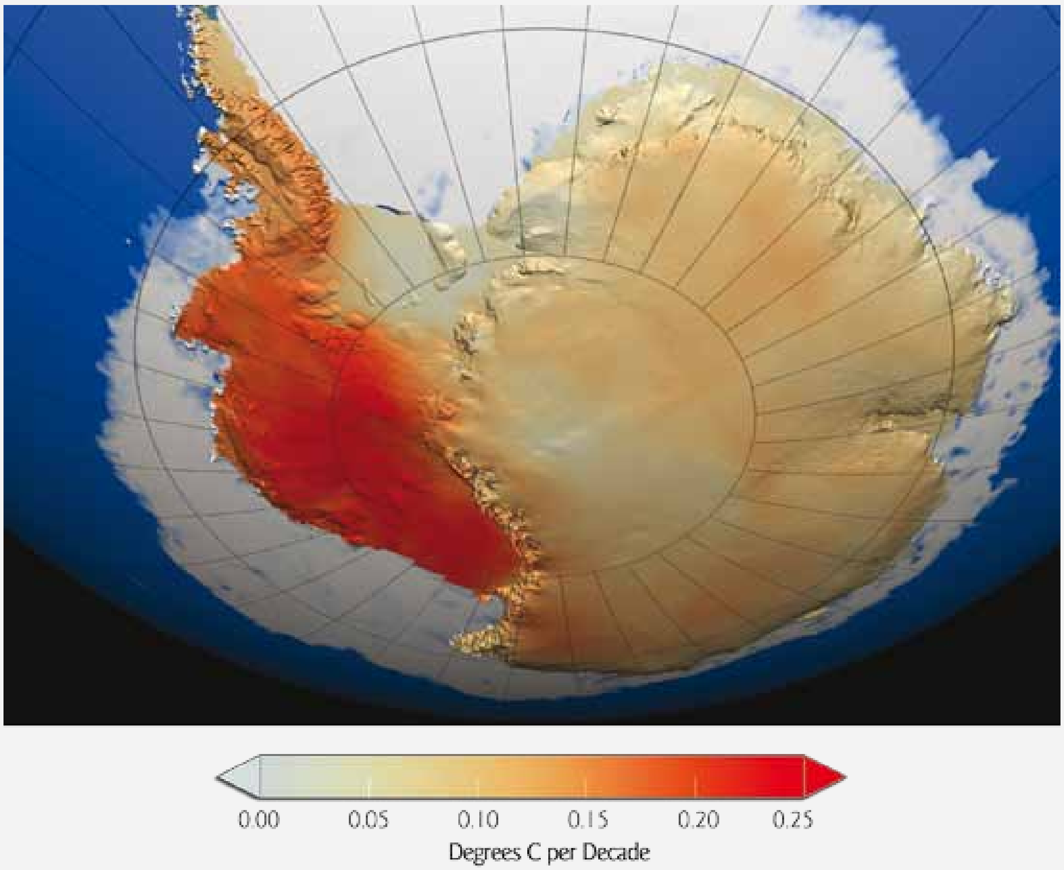

Figure 14. Annual mean air temperature trend in °C/decade during 1957-2006 from Steig et al. [2009].

THE OCEANS

- *Estimates of ocean heat uptake have converged and are found to be 50% higher than previous calculations.*
- *Global ocean surface temperature reached the warmest ever recorded for each of June, July and August 2009.*
- *Ocean acidification and ocean de-oxygenation have been identified as potentially devastating for large parts of the marine ecosystem.*

Detection of how climate change is impacting the oceans has improved markedly since the IPCC AR4. Significant changes in temperature, salinity and biogeochemical properties have been measured. These changes are consistent with the observed 50-year warming, rainfall and CO_2 trends in the atmosphere. There have also been important new analyses of the trends in a broader range of properties since the IPCC AR4, including acidification and oxygen. This has improved our understanding of the changing state of the oceans and also identified new issues. Where new estimates of ocean change exist since IPCC AR4, they tend to be larger and also more consistent with projections of climate change (e.g., global heat content).

Ocean Warming

There has been a long-term sustained warming trend in ocean surface temperatures over the past 50 years (Figure 15). Satellite measurements for the surface ocean showed 2007 to be the warmest year ever recorded, despite the extremely strong El Niño of 1997/1998. The year 2008 was cooler due to an intense temporary La-Niña event, whereas ocean temperatures up until the time of publication are tracking toward record warmth in 2009. For example, global ocean surface temperature was the warmest ever recorded for June, for July and for August in 2009.

Increases in oceanic heat content in the upper ocean (0-700m) between 1963 and 2003 have been found to be 50% higher than previous estimates (Domingues et al. 2008, Bindoff et al. 2007). The higher estimates of heat content change are now consistent with observations of sea-level rise over the last 50 years, resolving a long standing scientific problem in understanding the contribution of thermal expansion to sea-level (Domingues et al. 2008). Observations also show deep-ocean warming that is much more widespread in the Atlantic and Southern Oceans (Johnson et al. 2008a, Johnson et al. 2008b) than previously appreciated.

Salinity and the Hydrological Cycle

More comprehensive analyses of ocean salinity show a freshening of high latitudes, while regions of excess evaporation over precipitation have become saltier. The salinity changes are consistent with a strengthening of the hydrological cycle. The patterns of salinity change are also consistent with regional circulation and inter-basin exchanges. We now have increased evidence that the long-term trends in patterns of rainfall over the global ocean, as reflected in salinity, can be attributed to human influence (Stott et al. 2008).

Climate Change and Ocean Circulation

Surprising salinity changes in Antarctic bottom waters provide additional evidence of increased melt from the ice-sheets and ice shelves (Rintoul 2007). The Arctic shows strong evidence for increased precipitation and river run-off. Intermediate layers in the Arctic Ocean have warmed notably (Polyakov et al. 2004). Consistent with current model results, observations are yet to detect any indication of a sustained change in the North Atlantic Ocean circulation (e.g. Hansen and Østerhus 2007).

Regional climate change is often organized and expressed around the main patterns of variation such as the North Atlantic Oscillation, El Niño, and the Southern Annular Mode. These patterns themselves may be affected by greenhouse gases, leading to either larger fluctuations, or a preferred state in coming decades (e.g., a trend toward a different type of El Niño event, Yeh et al. 2009; Latif and Keenlyside 2009). Currently the influence of regional climate modes on ocean circulation is larger than the underlying trends attributable to anthropogenic climate change.

The stability of the North Atlantic Ocean circulation is vitally important for North American and European climate. For example, a slowdown of these ocean currents could lead to a more rapid rise of regional sea level along the northeast US coast (Yin et al. 2009). The IPCC AR4 concluded that there is greater than 90% probability of a slowdown of this ocean current system, and less than 10% risk of a "large abrupt transition" by the year 2100. As noted in the Synthesis and Assessment Project 3.4 of the US Climate Change Science Program (Delworth et al. 2008), no comprehensive climate model projects such a transition within this century. However, given uncertainty in our ability to model nonlinear threshold behaviour, and the recent suggestion that models may be too stable (Hofman and Rahmstorf 2009) we cannot completely exclude the possibility of such an abrupt transition.

Ocean Acidification, Carbon Uptake and Ocean De-oxygenation

The CO_2 content of the oceans increased by 118 ± 19 Gt (1 Gt = 10^9 tons) between the end of the pre-industrial period (about 1750) and 1994, and continues to increase by about 2 Gt each year (Sabine et al. 2004). The increase in ocean CO_2 has caused a direct decrease in surface ocean pH by an average of 0.1 units since 1750 and an increase in acidity by more than 30% (Orr et al. 2005: McNeil and Matear 2007; Riebesell, et al. 2009). Calcifying organisms and reefs have been shown to be particularly vulnerable to high CO_2, low pH waters (Fabry et al. 2008).

New in-situ evidence shows a tight dependence between calcification and atmospheric CO_2, with smaller shells evident during higher CO_2 conditions over the past 50,000 years (Moy et al. 2009). Furthermore, due to pre-existing conditions, the polar regions of the Arctic and Southern Oceans are expected to start dissolving certain shells once the atmospheric levels reach 450ppm (~2030 under business-as-usual; McNeil and Matear 2008: Orr et al. 2009).

There is new evidence for a continuing decrease in dissolved oxygen concentrations in the global oceans (Oschlies et al. 2008), and there is for the first time significant evidence that the large equatorial oxygen minimum zones are already expanding in a warmer ocean (Stramma et al. 2008). Declining oxygen is a stress multiplier that causes respiratory issues for large predators (Rosa and Seibel 2008) and significantly compromises the ability of marine organisms to cope with acidification (Brewer 2009). Increasing areas of marine anoxia have profound impacts on the marine nitrogen cycle, with yet unknown global consequences (Lam et al. 2009). A recent modeling study (Hofmann and Schellnhuber 2009) points to the risk of a widespread expansion of regions lacking in oxygen in the upper ocean if increases in atmospheric CO_2 continue.

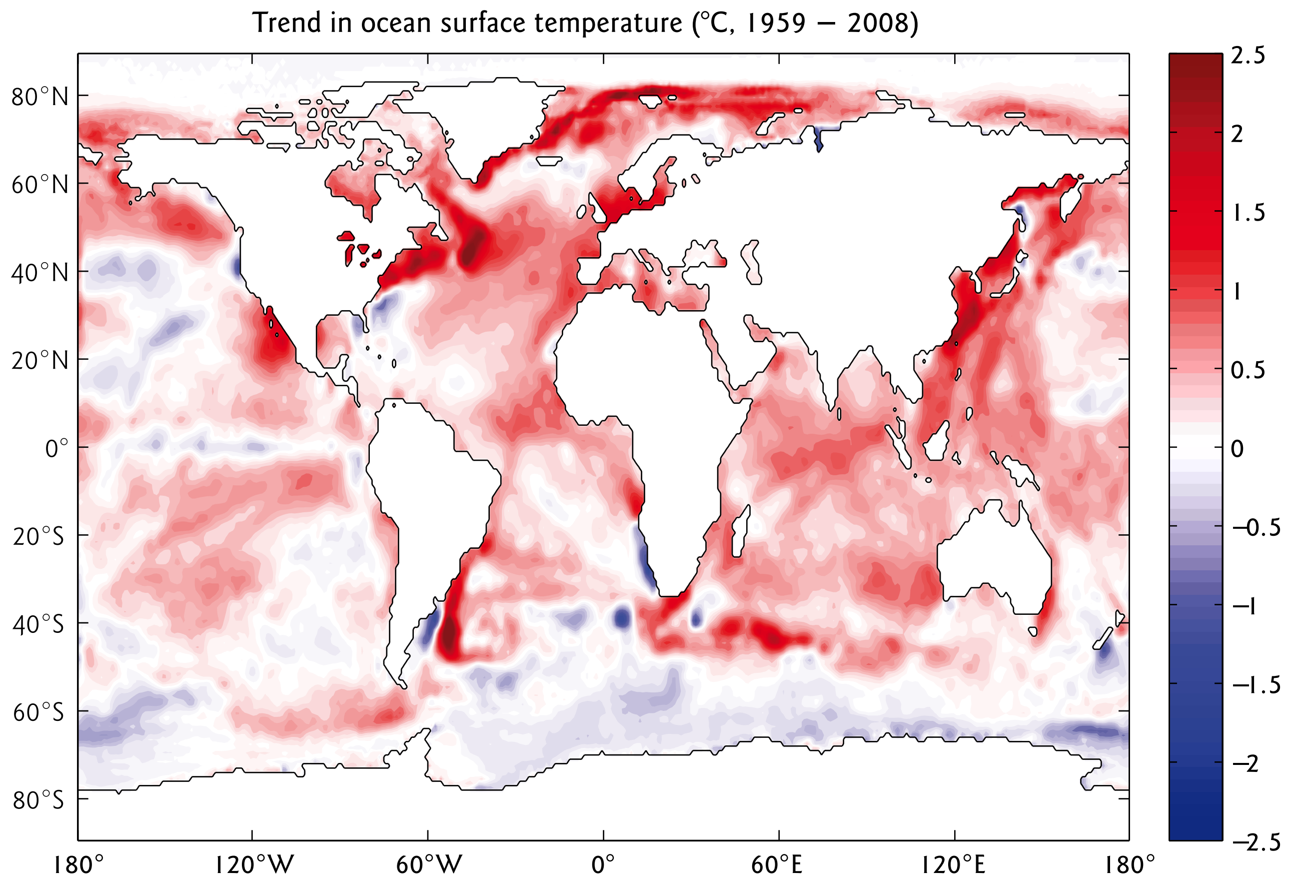

Figure 15. Long-term 50-year change in sea surface temperature (SST) during 1959-2008 calculated by fitting a linear trend to 50 years of monthly SST data at each grid point. The SST fields are from the Hadley Centre data set as described by Rayner et al. (2006).

GLOBAL SEA LEVEL

- ❑ *Satellite measurements show sea-level is rising at 3.4 millimeters per year since these records began in 1993. This is 80% faster than the best estimate of the IPCC Third Assessment Report for the same time period.*
- ❑ *Accounting for ice-sheet mass loss, sea-level rise until 2100 is likely to be at least twice as large as that presented by IPCC AR4, with an upper limit of ~2m based on new ice-sheet understanding.*

Population densities in coastal regions and on islands are about three times higher than the global average. Currently 160 million people live less than 1 meter above sea level. This allows even small sea level rise to have significant societal and economic impacts through coastal erosion, increased susceptibility to storm surges and resulting flooding, ground-water contamination by salt intrusion, loss of coastal wetlands, and other issues.

Since 1870, global sea level has risen by about 20 centimeters (IPCC AR4). Since 1993, sea level has been accurately measured globally from satellites. Before that time, the data come from tide gauges at coastal stations around the world. Satellite and tide-gauge measurements show that the rate of sea level rise has accelerated. Statistical analysis reveals that the rate of rise is closely correlated with temperature: the warmer it gets, the faster sea level rises (Rahmstorf 2007).

Sea level rise is an inevitable consequence of global warming for two main reasons: ocean water expands as it heats up, and additional water flows into the oceans from the ice that melts on land. For the period 1961-2003, thermal expansion contributed ~40% to the observed sea level rise, while shrinking mountain glaciers and ice sheets have contributed ~60% (Domingues et al. 2008).

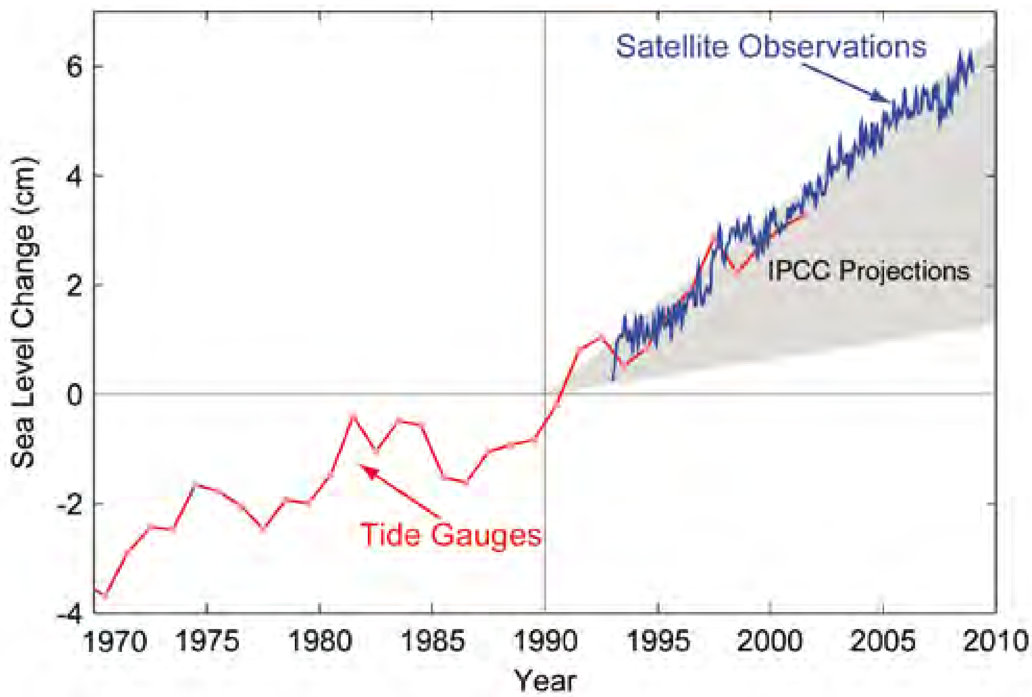

Figure 16. Sea level change during 1970-2010. The tide gauge data are indicated in red (Church and White 2006) and satellite data in blue (Cazenave et al. 2008). The grey band shows the projections of the IPCC Third Assessment report for comparison.

Sea level has risen faster than expected (Rahmstorf et al. 2007), see Figure 16. The average rate of rise for 1993-2008 as measured from satellite is 3.4 millimeters per year (Cazenave et al. 2008), while the IPCC Third Assessment Report (TAR) projected a best estimate of 1.9 millimeters per year for the same period. Actual rise has thus been 80% faster than projected by models. (Note that the more recent models of the 2007 IPCC report still project essentially the same sea level rise as those of the TAR, to within 10%.)

Future sea level rise is highly uncertain, as the mismatch between observed and modeled sea level already suggests. The main reason for the uncertainty is in the response of the big ice sheets of Greenland and Antarctica.

Sea level is likely to rise much more by 2100 than the often-cited range of 18-59 centimeters from the IPCC AR4. As noted in the IPCC AR4, the coupled models used in developing the 21st century sea level projections did not include representations of dynamic ice sheets. As such, the oft-cited 18-59 centimeters projected sea level rise only included simple mass balance estimates of the sea level contribution from the Greenland and Antarctic ice sheets. As a consequence of an assumed positive mass balance over the Antarctic ice sheet in the AR4, Antarctica was estimated to have contributed to global sea level decline during the 21st century in that report. However, the Antarctic Ice Sheet is currently losing mass as a consequence of dynamical processes (see Figure 10 in this report). Based on a number of new studies, the synthesis document of the 2009 Copenhagen Climate Congress (Richardson et al. 2009) concluded that "updated estimates of the future global mean sea level rise are about double the IPCC projections from 2007."

Sea level will continue to rise for many centuries after global temperature is stabilized, since it takes that much time for the oceans and ice sheets to fully respond to a warmer climate. Some recent estimates of future rise are compiled in Figure 17. These estimates highlight the fact that unchecked global warming is likely to raise sea level by several meters in coming centuries, leading to the loss of many major coastal cities and entire island states.

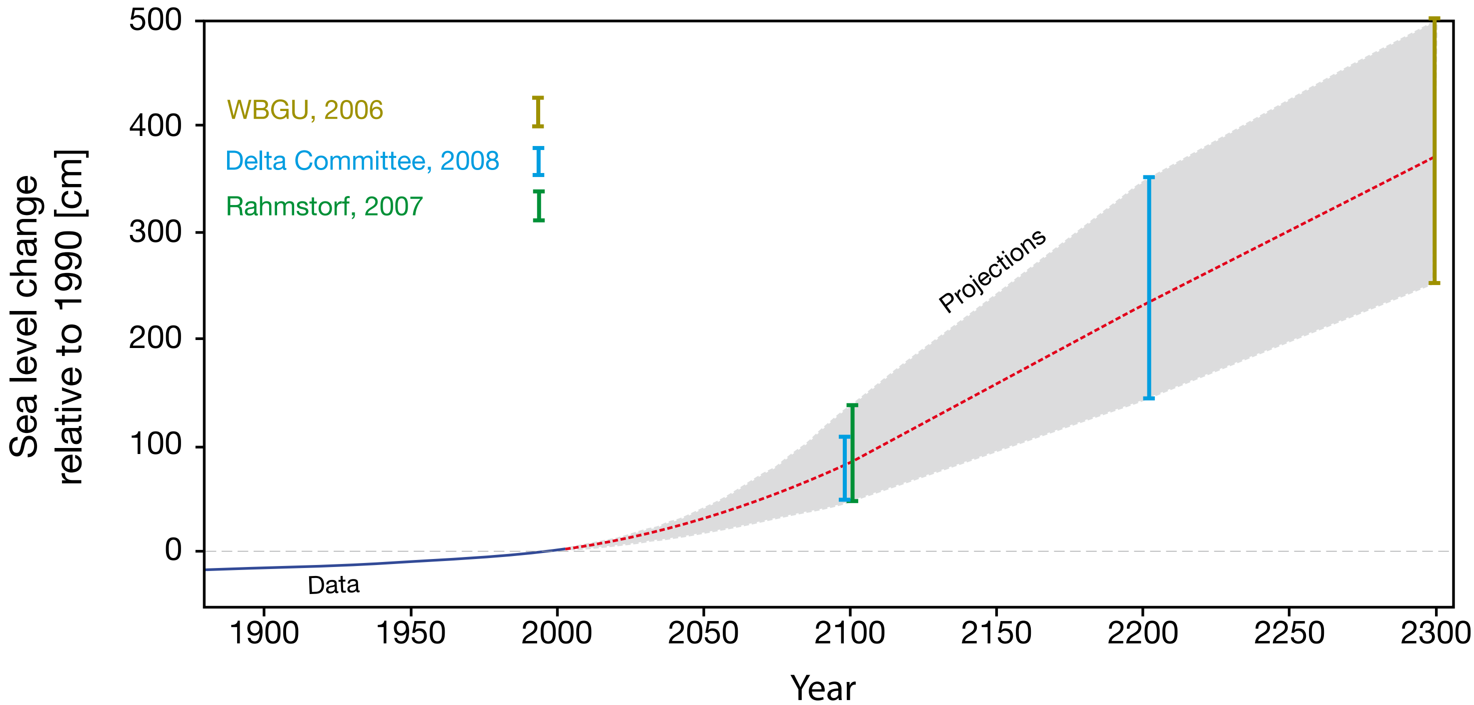

Figure 17. Some recent projections of future sea level rise. Historical data from Church and White (2006). Future projections are from Rahmstorf (2007) and WBGU (2006), while those projections represented here as 'Delta Committee' are from Vellinga et al., (2008).

ABRUPT CHANGE AND TIPPING POINTS

- *There are several elements in the climate system that could pass a tipping point this century due to human activities, leading to abrupt and/or irreversible change.*
- *1 °C global warming (above 1980-1999) carries moderately significant risks of passing large-scale tipping points, and 3 °C global warming would give substantial or severe risks.*
- *There are prospects for early warning of approaching tipping points, but if we wait until a transition begins to be observed, in some cases it would be unstoppable.*

What is a tipping point?

A tipping point is a critical threshold at which the future state of a system can be qualitatively altered by a small change in forcing (Lenton et al. 2008; Schellnhuber 2009). A tipping element is a part of the Earth system (at least sub-continental in scale) that has a tipping point (Lenton et al. 2008). Policy-relevant tipping elements are those that could be forced past a tipping point this century by human activities. Abrupt climate change is the subset of tipping point change which occurs faster than its cause. Tipping point change also includes transitions that are slower than their cause (in both cases the rate is determined by the system itself). In either case the change in state may be reversible or irreversible. Reversible means that when the forcing is returned below the tipping point the system recovers its original state, either abruptly or gradually. Irreversible means that it does not (it takes a larger change in forcing to recover). Reversibility in principle does not mean that changes will be reversible in practice. A tipping element may lag anthropogenic forcing such that once a transition begins to be observed, a much larger change in state is already inevitable.

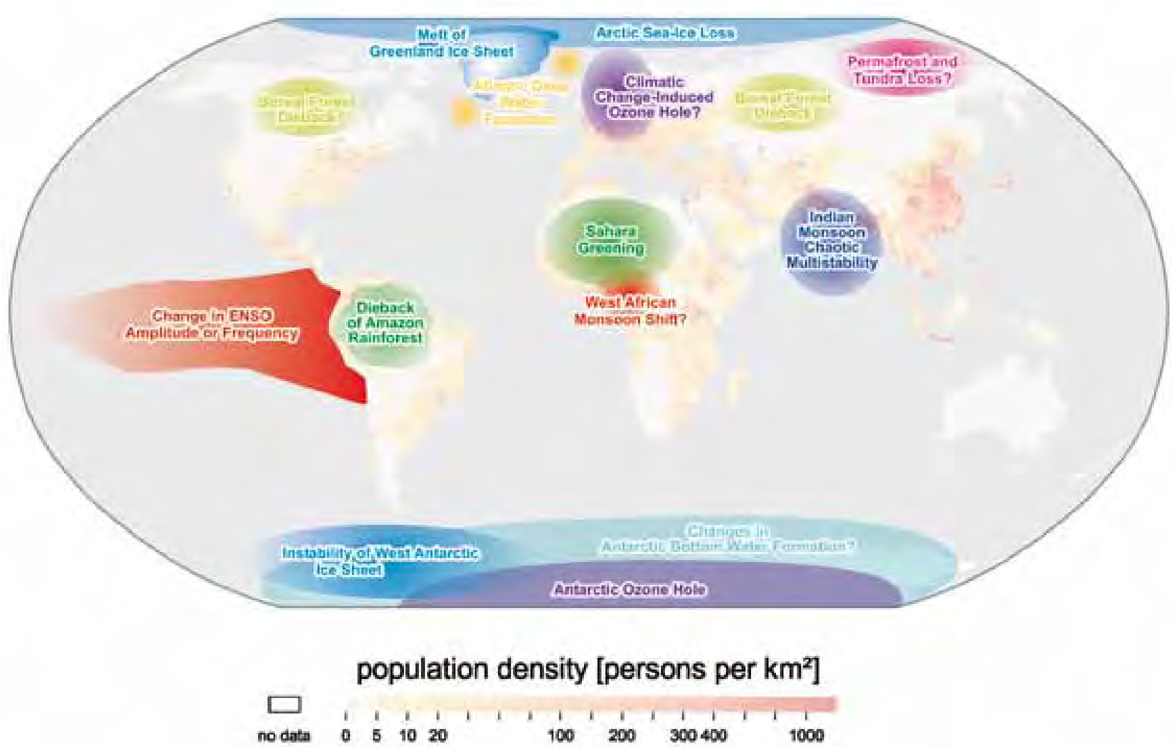

Figure 18. Map of some of the potential policy-relevant tipping elements in the Earth's climate system overlain on population density. Question marks indicate systems whose status as tipping elements is particularly uncertain. There are other potential tipping elements that are missing from the map, for example shallow-water coral reefs (Veron et al. 2009) threatened in part by ocean acidification (see Oceans chapter).

Are there tipping points in the Earth's climate system?

There are a number of tipping points in the climate system, based on understanding of its non-linear dynamics, and as revealed by past abrupt climate changes and model behavior (Pitman and Stouffer 2007; Schellnhuber 2009). Some models pass tipping points in future projections, and recent observations show abrupt changes already underway in the Arctic. Recent work has identified a shortlist of nine potential policy-relevant tipping elements in the climate system that could pass a tipping point this century and undergo a transition this millennium under projected climate change (Lenton et al. 2008). These are shown with some other candidates in Figure 18.

Which ones are of the greatest concern? How has this been assessed?

The tipping points of greatest concern are those that are the nearest (least avoidable) and those that have the largest negative impacts. Generally, the more rapid and less reversible a transition is, the greater its impacts. Additionally, any amplifying feedback to global climate change may increase concern, as can interactions whereby tipping one element encourages tipping another. The proximity of some tipping points has been assessed through expert elicitation (Lenton et al. 2008; Kriegler et al. 2009). Proximity, rate and reversibility have been also assessed through literature review (Lenton et al. 2008), but there is a need for more detailed consideration of impacts. Some of the most concerning regions and their tipping elements are now discussed:

Arctic: The Greenland ice sheet (GIS) may be nearing a tipping point where it is committed to shrink (Lenton et al. 2008; Kriegler et al. 2009). Striking amplification of seasonal melt was observed in 2007 associated with record Arctic summer sea-ice loss (Mote 2007). Once underway the transition to a smaller Greenland ice cap will have low reversibility, although it is likely to take several centuries (and is therefore not abrupt). The impacts via sea level rise will ultimately be large and global, but will depend on the rate of ice sheet shrinkage.

Antarctic: The West Antarctic ice sheet (WAIS) is currently assessed to be further from a tipping point than the GIS, but this is more uncertain (Lenton et al. 2008; Kriegler et al. 2009). The WAIS has the potential for more rapid change and hence greater impacts. The loss of ice-shelves around the Antarctic Peninsula, such as Larsen B, followed by the acceleration of glaciers they were buttressing, highlights a mechanism that could threaten parts of the WAIS. The main East Antarctic ice sheet (EAIS) is thought to be more stable than the WAIS. However, there is evidence that changes are taking place along its marine sector, which drains more ice than all of West Antarctica.

Amazonia: The Amazon rainforest experienced widespread drought in 2005 turning the region from a sink to a source (0.6 - 0.8 Gt C per year) of carbon (Phillips et al. 2009). If anthropogenic-forced lengthening of the dry season continues (Vecchi et al. 2006), and droughts increase in frequency or severity (Cox et al. 2008), the system could reach a tipping point resulting in dieback of up to ~80% of the rainforest (Cox et al. 2004; Scholze et al. 2006; Salazar et al. 2007; Cook and Vizy 2008), and its replacement by savannah. This could take a few decades, would have low reversibility, large regional impacts, and knock-on effects far away. Widespread dieback is expected in a >4 °C warmer world (Kriegler 2009), and it could be committed to at a lower global temperature, long before it begins to be observed (Jones et al. 2009).

West Africa: The Sahel and West African Monsoon (WAM) have experienced rapid but reversible changes in the past including devastating drought from the late 1960s through the 1980s. Forecast future weakening of the Atlantic thermohaline circulation contributing to 'Atlantic Niño' conditions, including strong warming in the Gulf of Guinea (Cook and Vizy 2006), could disrupt the seasonal onset of the WAM (Chang et al. 2008) and its later 'jump' northwards (Hagos 2007) into the Sahel. Perversely, if the WAM circulation collapses, this could lead to wetting of parts of the Sahel as moist air is drawn in from the Atlantic to the West (Cook and Vizy 2006; Patricola and Cook 2008), greening the region in what would be a rare example of a positive tipping point.

India: The Indian Summer Monsoon is probably already being disrupted (Ramanathan et al. 2005; Meehl et al. 2008) by an atmospheric brown cloud haze that sits over the sub-continent and, to a lesser degree, the Indian Ocean. This haze is comprised of a mixture of soot, which absorbs sunlight, and some reflecting sulfate. It causes heating of the atmosphere rather than the land surface, weakening the seasonal establishment of a land-ocean temperature gradient which is critical in triggering monsoon onset (Ramanathan 2005). In some future projections, brown cloud haze forcing could lead to a doubling of drought frequency within a decade (Ramanathan 2005) with large impacts, although transitions should be highly reversible.

Several other candidate tipping elements and mechanisms could become a major concern, for example, carbon loss from permafrost. Recently it has been suggested that a region of permafrost known as the Yedoma, which stores up to ~500 Gt C (Zimov et al. 2006) could be tipped into irreversible breakdown driven by internal, biochemical heat generation (Khvorostyanov et al. 2008a, 2008b). However, the tipping point is estimated to be relatively distant.

How do tipping points relate to amplifying feedbacks on climate change?

Tipping points are often confused with the phenomenon of amplifying feedbacks on climate change. All tipping elements must have some strong amplifying feedback – detailed elsewhere (Lenton et al. 2008) – in their own internal or regional climate dynamics in order to exhibit a threshold, but they need not have an amplifying feedback to global climate change. Tipping elements that could have an amplifying feedback to global climate change include the Amazon rainforest (dieback would make it a CO_2 source, which could ultimately release up to ~100 Gt C), the thermohaline circulation (weakening or collapse would lead to net out-gassing of CO_2), and the Yedoma permafrost (release of up to ~500 Gt C). Tipping elements that could have a diminishing feedback on global climate change include boreal forest (dieback would release CO_2 but this would be outweighed by cooling due to increased land surface albedo from unmasked snow cover; Betts 2000), and the Sahel/Sahara (greening would take up CO_2 and probably increase regional cloud cover).

Should we be concerned about global amplifying feedbacks?

Amplifying feedbacks from individual tipping elements are mostly fairly weak at the global scale. However, other (non tipping element) amplifying feedbacks, including a potential future switch in the average response of the land biosphere from a CO_2 sink to a CO_2 source, could significantly amplify CO_2 rise and global temperature on the century timescale (Friedlingstein et al. 2006). The Earth's climate system is already in a state of strong amplifying feedback from relatively fast physical climate responses (Bony et al. 2006) (e.g. water vapor feedback). In any system with strong amplifying feedback, relatively small additional feedbacks can have a disproportionate impact on the global state (in this case, temperature), because of the non-linear way in which amplifiers work together.

Is there a global tipping point?

A global tipping point can only occur if a net amplifying feedback becomes strong enough to produce a threshold whereby the global system is committed to a change in state, carried by its own internal dynamics. Despite much talk in the popular media about such 'runaway' climate change there is as yet no strong evidence that the Earth as a whole is near such a threshold. Instead 'amplified' climate change is a much better description of what we currently observe and project for the future.

Which anthropogenic forcing agents are dangerous?

The total cumulative emissions of CO_2 (and other long-lived greenhouse gases) determine long-term committed climate changes and hence the fate of those tipping elements that are sensitive to global mean temperature change, are slow to respond, and/or have more distant thresholds. Key examples are the large ice sheets (GIS and WAIS). Uneven sulfate (Rotstatyn and Lohmann 2002) and soot (Ramanathan 2005; Ramanathan and Carmichael 2008) aerosol forcing are most dangerous for monsoons. Soot deposition on snow and ice (Ramanathan and Carmichael 2008; Flanner et al. 2007) is a key danger to Arctic tipping elements as it is particularly effective at forcing melting (Flanner et al. 2007). Increasing soot aerosol, declining sulfate aerosol (Shindell and Faluvegi 2009), and increasing short-lived greenhouse gases (Hansen et al. 2007) (methane and tropospheric ozone) have also contributed to rapid Arctic warming, and together far outweigh the CO_2 contribution. The current mitigation of SO_2 emissions and hence sulfate aerosol is a mixed blessing for climate tipping elements, it may for example be benefiting the Sahel region (Rotstayn and Lohmann 2002) but endangering the Amazon (Cox et al. 2008) and the Arctic sea-ice (Shindell and Faluvegi 2009). Land cover change may also drive large areas of continents from being relatively robust to climate change to being highly vulnerable.

Is there any prospect for early warning of an approaching tipping point?

Recent progress has been made in identifying and testing generic potential early warning indicators of an approaching tipping point (Lenton et al. 2008; Livina and Lenton 2007; Dakos et al. 2008; Lenton et al. 2009; Scheffer et al. 2009). Slowing down in response to perturbation is a nearly universal property of systems approaching various types of tipping point (Dakos et al. 2008; Scheffer et al. 2009). This has been successfully detected in past climate records approaching different transitions (Livina and Lenton 2007; Dakos et al. 2008), and in model experiments (Livina and Lenton 2007; Dakos et al. 2008; Lenton et al. 2009). Flickering between states may also occur prior to a more permanent transition (Bakke et al. 2009). Other early warning indicators are being explored for ecological tipping points (Biggs et al. 2009), including increasing variance (Biggs et al. 2009), skewed responses (Biggs et al. 2009; Guttal and Jayaprakash 2008) and their spatial equivalents (Guttal and Jayaprakash 2009). These could potentially be applied to anticipating climate tipping points.

LESSONS FROM THE PAST

- *The reconstruction of past climate reveals that the recent warming observed in the Arctic, and in the Northern Hemisphere in general, are anomalous in the context of natural climate variability over the last 2000 years.*
- *New ice-core records confirm the importance of greenhouse gases for past temperatures on Earth, and show that CO_2 levels are higher now than they have ever been during the last 800,000 years.*

Reconstructing the last two millennia

Knowledge of climate during past centuries can help us to understand natural climate change and put modern climate change into context. There have been a number of studies to reconstruct trends in global and hemispheric surface temperature over the last millennium (e.g. Mann et al. 1998; Esper et al. 2002; Moberg et al. 2005), all of which show recent Northern Hemisphere warmth to be anomalous in the context of at least the past millennium, and likely longer (Jansen et al. 2007). The first of these reconstructions has come to be known as the 'hockey stick' reconstruction (Mann et al. 1998, 1999). Some aspects of the hockey stick reconstruction were subsequently questioned, e.g. whether the 20th century was the warmest at a hemispheric average scale (Soon and Baliunas 2003), and whether the reconstruction is reproducible, or verifiable (McIntyre and McKitrick 2003), or might be sensitive to the method used to extract information from tree ring records (McIntyre and McKitrick 2005a,b). Whilst these criticisms have been rejected in subsequent work (e.g. Rutherford et al. 2005; Wahl and Ammann 2006, 2007; Jansen et al. 2007) the US National Research Council convened a committee to examine the state of the science of reconstructing the climate of the past millennium. The NRC report published in 2006 largely supported the original findings of Mann et al. (1998, 1999) and recommended a path toward continued progress in this area (NRC, 2006).

Mann et al. (2008) addressed the recommendations of the NRC report by reconstructing surface temperature at a hemispheric and global scale for much of the last 2,000 years using a greatly expanded data set for decadal-to-centennial climate changes, along with recently updated instrumental data and complementary methods that have been thoroughly tested and

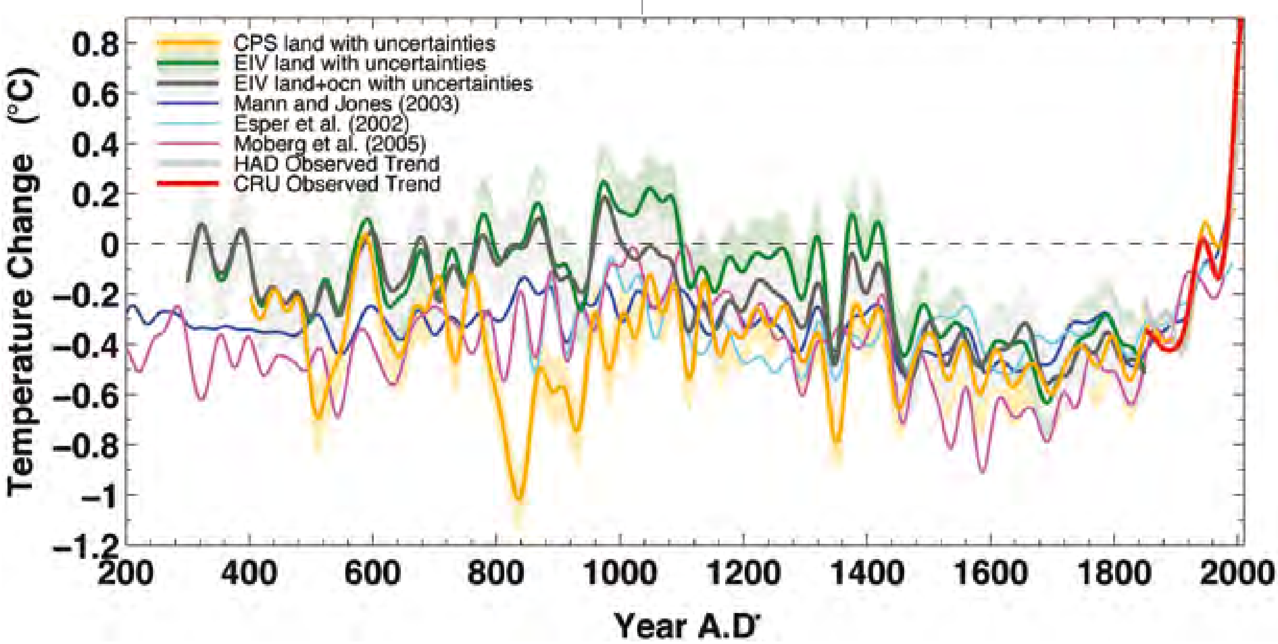

Figure 19. Comparison of various Northern Hemisphere temperature reconstructions, with estimated 95% confidence intervals shown (from Mann et al. 2008).

validated with climate model simulations. Their results extend previous studies and conclude that recent Northern Hemisphere surface temperature increases are likely anomalous in a long-term context (Figure 19).

Kaufman et al. (2009) independently concluded that recent Arctic warming is without precedent in at least 2000 years (Figure 20) reversing a long-term millennial-scale cooling trend caused by astronomical forcing (i.e. orbital cycles). Warmth during the peak of the "Medieval Climate Anomaly" of roughly AD 900-1100 may have rivalled modern warmth for certain regions such as the western tropical Pacific (Oppo et al. 2009), and some regions neighbouring the North Atlantic (Mann et al. in-press). However, such regional warming appears to reflect a redistribution of warmth by changes in atmospheric circulation, and is generally offset by cooling elsewhere (e.g. the eastern and central tropical Pacific) to yield hemispheric and global temperatures that are lower than those of recent decades.

Ice Core Records of Greenhouse Gases

Changes in past atmospheric Carbon Dioxide (CO_2) and Methane (CH_4) concentrations can be determined by measuring the composition of air trapped in ice cores and through the analyses of leaf stomata density and geochemical analyses of marine sediment cores.

The Dome Concordia (Dome C) ice core CO_2 and CH_4 records, drilled by the European Project for Ice Coring in Antarctica (EPICA), were published in 2004 and 2005 detailing events back to 440,000 years and 650,000 years respectively (EPICA community members 2004; Siegenthaler et al. 2005). In 2008 the record was extended to 800,000 years (Lüthi et al. 2008; Loulergue et al. 2008). The newly extended records reveal that current greenhouse gas levels (~385ppm) are at least 40% higher than at any time over the past 800,000 years. We must travel back at least two to three million years, and perhaps as far as fifteen million years, to the Pliocene and Miocene epochs of geological time to find equivalent greenhouse gas levels in the atmosphere (Haywood et al. 2007; Raymo et al. 1996; Kürschner et al. 1996; Tripati et al. 2009).

Strong correlations of CH_4 and CO_2 with temperature reconstructions are maintained throughout the new 800,000 year record (Lüthi et al. 2008; Loulergue et al. 2008). Temperature warming typically comes before increases in atmospheric CO_2 over the ice-core record. This finding is consistent with the view that natural CO_2 variations constitute a feedback in the glacial-interglacial cycle rather than a primary cause (Shackleton 2000); something that has recently been explained in detail with the help of climate model experiments (Ganopolski and Roche 2009). Changes in the Earth's orbit around the Sun are the pacemaker for glacial-interglacial cycles (Hays et al. 1976; Berger 1978), but these rather subtle orbital changes must be amplified by climate feedbacks in order to explain the large differences in global temperature and ice volume, and the relative abruptness of the transitions between glacial and interglacial periods (Berger et al. 1998; Clark et al. 1999).

Palaeo Constraints on Climate and Earth System Sensitivity

One of the key questions for climate research is to determine how sensitively the Earth's climate responds to a given change

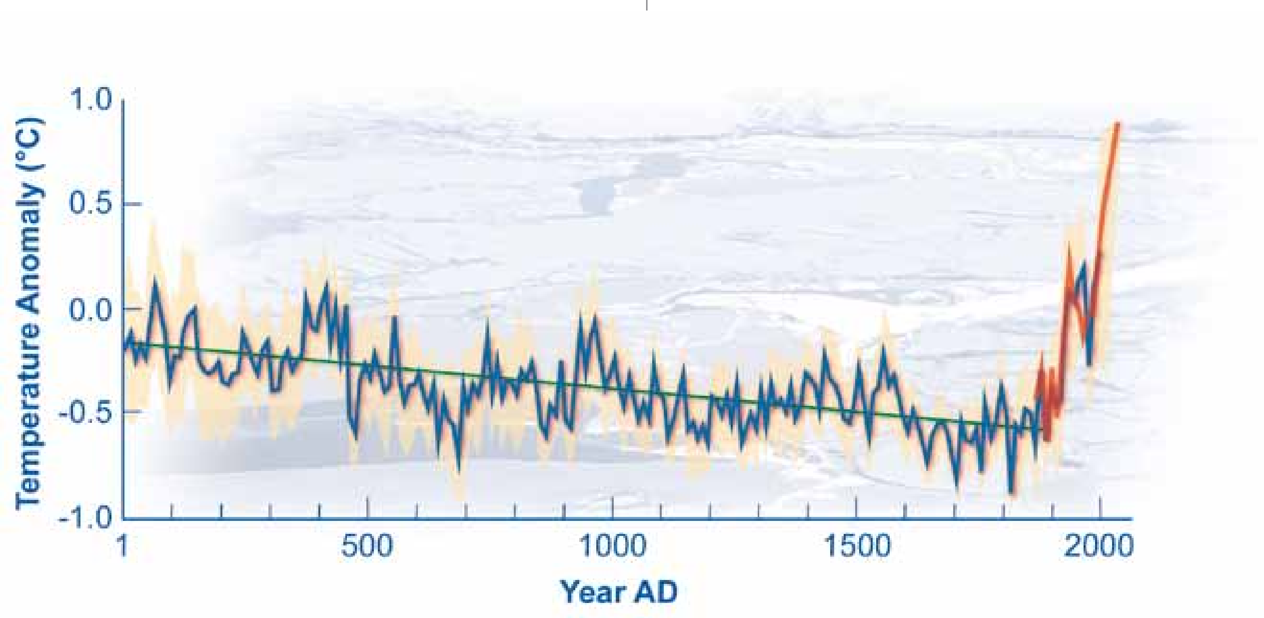

Figure 20. Blue line: estimates of Arctic air temperatures over the last 2,000 years based on proxy records from lake sediments, ice cores and tree rings. The green line shows the best fit long-term cooling trend for the period ending 1900. The red line shows the recent warming based on actual observations. (Courtesy Science, modified by the University Corporation for Atmospheric Research).

in our planet's radiation budget. This is often described by the "Climate Sensitivity", defined as the equilibrium global temperature response to a doubling of atmospheric CO_2 concentration.

IPCC AR4 summarizes the research aimed at characterizing the uncertainty in climate sensitivity (e.g. Andronova and Schlesinger 2001; Frame et al. 2005; Annan and Hargreaves 2006) by stating that "climate sensitivity is likely to lie in the range 2°C to 4.5°C, with a most likely value of about 3°C". More recent studies have agreed with this assessment (e.g. Knutti and Hegerl 2008). These estimates of climate sensitivity have also been used to determine the likely impacts, both environmental and social/economic, of various CO_2 stabilization scenarios, or the level of greenhouse gas emissions consistent with stabilization of the global mean temperature below a certain value (e.g. Meinshausen et al. 2009; this document section "Mitigating global warming").

Isn't climate always changing, even without human interference?

Of course. But past climate changes are no cause for complacency; indeed, they tell us that the Earth's climate is very sensitive to changes in forcing. Two main conclusions can be drawn from climate history:

Climate has always responded strongly if the radiation balance of the Earth was disturbed. That suggests the same will happen again, now that humans are altering the radiation balance by increasing greenhouse gas concentrations. In fact, data from climate changes in the Earth's history have been used to quantify how strongly a given change in the radiation balance alters the global temperature (i.e., to determine the *climate sensitivity*). The data confirm that our climate system is as sensitive as our climate models suggest, perhaps even more so.

Impacts of past climate changes have been severe. The last great Ice Age, when it was globally 4-7 °C colder than now, completely transformed the Earth's surface and its ecosystems, and sea level was 120 meters lower. When the Earth last was 2-3 °C warmer than now, during the Pliocene 3 million years ago, sea level was 25-35 meters higher due to the smaller ice sheets present in the warmer climate.

Despite the large natural climate changes, the recent global warming does stick out already. Climate reconstructions suggest that over the past two millennia, global temperature has never changed by more than 0.5 °C in a century (e.g. Mann et al. 2008; and references therein).

Are we just in a natural warming phase, recovering from the "little ice age"?

No. A "recovery" of climate is not a scientific concept, since the climate does not respond like a pendulum that swings back after it was pushed in one direction. Rather, the climate responds like a pot of water on the stove: it can only get warmer if you add heat, according to the most fundamental law of physics, conservation of energy. The Earth's heat budget (its *radiation balance*) is well understood. By far the biggest change in the radiation balance over the past 50 years, during which three quarters of global warming has occurred, is due to the human-caused increase in greenhouse gas concentrations (see above). Natural factors have had a slightly cooling effect during this period.

Global temperatures are now not only warmer than in the 16th-19th centuries, sometimes dubbed the "the little ice age" (although this term is somewhat misleading in that this largely regional phenomenon has little in common with real ice ages). Temperatures are in fact now globally warmer than any time in the past 2000 years – even warmer than in the "medieval optimum" a thousand years ago (see Figure 19). This is a point that all global climate reconstructions by different groups of researchers, based on different data and methods, agree upon.

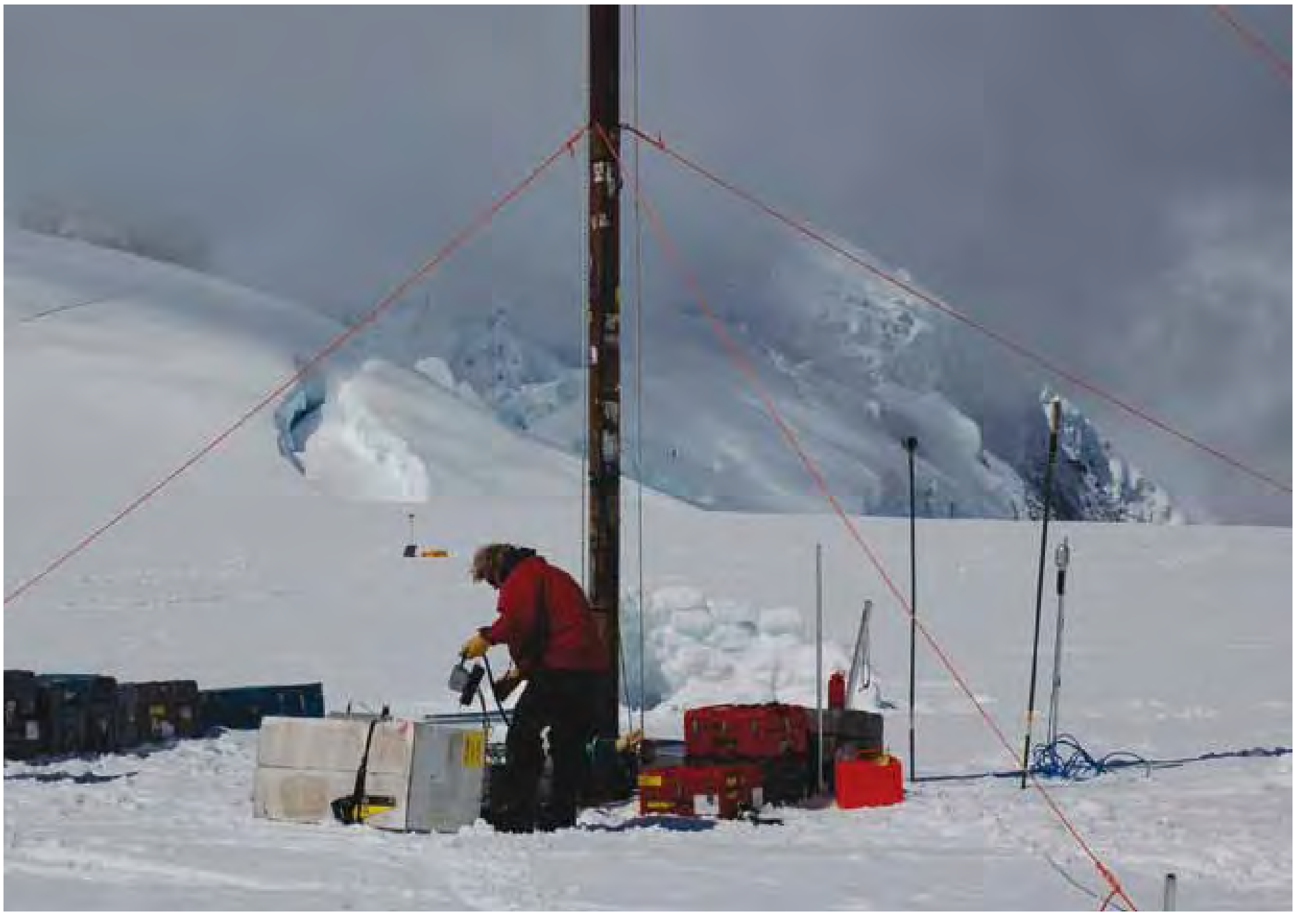

In climate history, didn't CO_2 change in response to temperature, rather than the other way round?

It works both ways: CO_2 changes affect temperature due to the greenhouse effect, while temperature changes affect CO_2 concentrations due to the carbon cycle response. This is what scientists call a feedback loop.

If global temperatures are changed, the carbon cycle will respond (typically with a delay of centuries). This can be seen during the ice age cycles of the past 3 million years, which were caused by variations in the Earth's orbit (the so-called Milankovich cycles). The CO_2 feedback amplified and globalized these orbital climate changes: without the lowered CO_2 concentrations and reduced greenhouse effect, the full extent of ice ages cannot be explained, nor can the fact that the ice ages occurred simultaneously in both hemispheres. The details of the lag-relationship of temperature and CO_2 in Antarctic records have recently been reproduced in climate model experiments (Ganopolski and Roche 2009) and they are entirely consistent with the major role of CO_2 in climate change. During the warming at the end of ice ages, CO_2 was released from the oceans – just the opposite of what we observe today, where CO_2 is increasing in both the ocean and the atmosphere.

If the CO_2 concentration in the atmosphere is changed, then the temperature follows because of the greenhouse effect. This is what is happening now that humans release CO_2 from fossil sources. But this has also happened many times in Earth's history. CO_2 concentrations have changed over millions of years due to natural carbon cycle changes associated with plate tectonics (continental drift), and climate has tracked those CO_2 changes (e.g. the gradual cooling into ice-age climates over the past 50 million years).

A rapid carbon release, not unlike what humans are causing today, has also occurred at least once in climate history, as sediment data from 55 million years ago show. This "Paleocene-Eocene thermal maximum" brought a major global warming of ~ 5 °C, a detrimental ocean acidification and a mass extinction event. It serves as a stark warning to us today.

THE FUTURE

- *Global mean air-temperature is projected to warm 2°C – 7°C above pre-industrial by 2100. The wide range is mainly due to uncertainty in future emissions.*
- *There is a very high probability of the warming exceeding 2°C unless global emissions peak and start to decline rapidly by 2020.*
- *Warming rates will accelerate if positive carbon feedbacks significantly diminish the efficiency of the land and ocean to absorb our CO_2 emissions.*
- *Many indicators are currently tracking near or above the worst case projections from the IPCC AR4 set of model simulations.*

Climate Projections

There has been no new coordinated set of future climate model projections undertaken since the IPCC AR4. Instead, much of the new research over the past few years has focused on preparation for the next round of IPCC simulations for AR5, and continued evaluation of the AR4 model runs. This includes new analyses of the observed rate of climate change in comparison to the IPCC AR4 projections (e.g., Rahmstorf 2007; Stroeve et al. 2007), and new calculations that take existing simulations and incorporate coupled carbon feedbacks and other processes (e.g. Zickfeld et al. 2009; Allen et al. 2009). While models exhibit good skill at capturing the mean present-day climate, some recent observed changes, notably sea-level rise and Arctic sea-ice melt, are occurring at a faster rate than anticipated by IPCC AR4. This is a cause for concern as it suggests that some amplifying feedbacks and processes, such as land-ice melt, are occurring faster than first predicted.

The latest estimates of global mean air temperature projected out to 2100 are shown in Figure 21. The wide range in the projection envelope is primarily due to uncertainty in future emissions. At the high end of emissions, with business as usual for several decades to come, global mean warming is estimated to reach 4-7°C by 2100, locking in climate change at a scale that would profoundly and adversely affect all of human civilization and all of the world's major ecosystems. At the lower end of emissions, something that would require urgent, deep and long-lasting cuts in fossil fuel use, and active preservation of the world's forests, global mean warming is projected to reach 2-3°C by century's end. While clearly a better outcome than the high emissions route, global mean warming of even just 1.5-2.0°C still carries a significant risk of adverse impacts on ecosystems and human society. For example, 2°C global temperature rise could lead to sufficient warming over Greenland to eventually melt much of its ice sheet (Oppenheimer and Alley 2005), raising sea level by over six meters and displacing hundreds of millions of people worldwide.

Despite the certainty of a long-term warming trend in response to rising greenhouse gases, there is no expectation that the warming will be monotonic and follow the emissions pathway on a year-to-year basis. This is because natural variability and the 11-year solar cycle, as well as sporadic volcanic eruptions, generate short-term variations superimposed on the long term trend (Lean and Rind 2009). Even under a robust century-long warming trend of around 4°C, we still expect to see the temperature record punctuated by isolated but regular ten-year periods of no trend, or even modest cooling (Easterling and Wehner 2009). Such decades therefore do not spell the end of global warming – emissions must peak and decline well before that is to occur. In fact, the peak in global temperature might not be reached until several centuries after emissions peak (e.g., Allen et al. 2009). Even after emissions stop completely, atmospheric temperatures are not expected to decline much for many centuries to millennia (Matthews and Caldeira 2008; Solomon et al. 2009; Eby et al. 2009) because of the long lifetime of CO_2 in the atmosphere. Furthermore, dry season rainfall reductions in several regions are expected to become irreversible (Solomon et al. 2009).

< Meltwater lake on the Greenland Ice Sheet

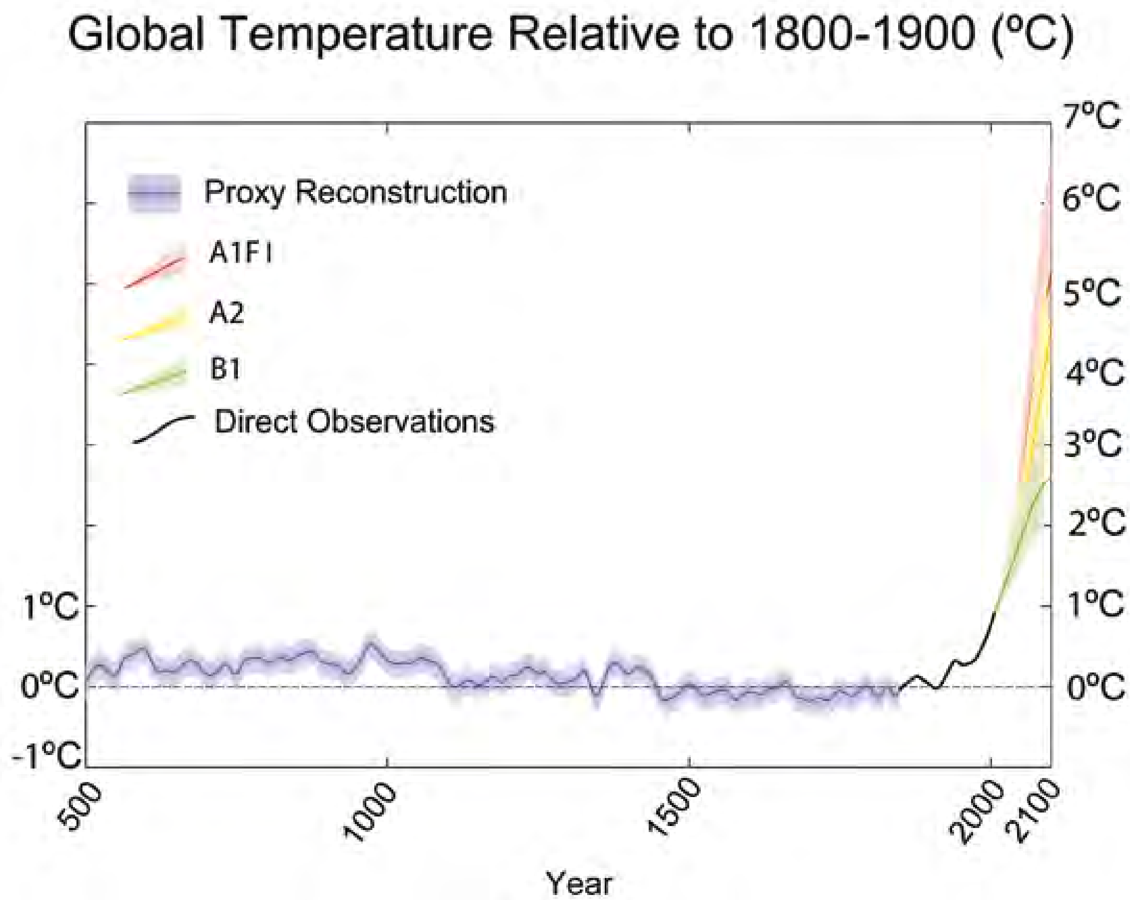

Figure 21. Reconstructed global-average temperature relative to 1800-1900 (blue) and projected global-average temperature out to 2100 (the latter from IPCC AR4). The envelopes B1, A2, A1FI refer to the IPCC AR4 projections using those scenarios. The reconstruction record is taken from Mann et al. (2008).

Mitigating global warming

While global warming can be stopped, it cannot easily be reversed due to the long lifetime of carbon dioxide in the atmosphere (Solomon et al. 2009; Eby et al. 2009). Even a thousand years after reaching a zero-emission society, temperatures will remain elevated, likely cooling down by only a few tenths of a degree below their peak values. Therefore, decisions taken now have profound and practically irreversible consequences for many generations to come, unless affordable ways to extract CO_2 from the atmosphere in massive amounts can be found in the future. The chances of this do not appear to be promising.

The temperature at which global warming will finally stop depends primarily on the total amount of CO_2 released to the atmosphere since industrialization (Meinshausen et al. 2009, Allen et al. 2009, Zickfeld et al. 2009). This is again due to the long life-time of atmospheric CO_2. Therefore if global warming is to be stopped, global CO_2 emissions must eventually decline to zero. The sooner emissions stop, the lower the final warming will be. From a scientific point of view, a cumulative CO_2 budget for the world would thus be a natural element of a climate policy agreement. Such an agreed global budget could then be distributed amongst countries, for example on the basis of equity principles (e.g., WBGU 2009).

The most widely supported policy goal is to limit global warming to at most 2 °C above the preindustrial temperature level (often taken for example as the average 19th Century temperature, although the exact definition does not matter much due to the small variations in preindustrial temperatures). Many nations have publically recognized the importance of this 2°C limit. Furthermore, the group of Least Developed Countries as well as the 43 small island states (AOSIS) are calling for limiting global warming to only 1.5°C. The Synthesis Report of the Copenhagen climate congress (Richardson et al. 2009), the largest climate science conference of 2009, concluded that "Temperature rises above 2 °C will be difficult for contemporary societies to cope with, and are likely to cause major societal and environmental disruptions through the rest of the century and beyond."

A number of recent scientific studies have investigated in detail what global emissions trajectories would be compatible with limiting global warming to 2 °C. The answer has to be given in terms of probabilities, to reflect the remaining uncertainty in the climate response to elevated CO_2, and the uncertainty in the stability of carbon stored in the land and ocean systems. Meinshausen et al. (2009) found that if a total of 1000 Gigatons of CO_2 is emitted for the period 2000-2050, the likelihood of exceeding the 2-degree warming limit is around 25%. In 2000-2009, about 350 Gigatons have already been emitted, leaving only 650 Gigatons for 2010-2050. At current emission rates this budget would be used up within 20 years.

An important consequence of the rapidly growing emissions rate, and the need for a limited emissions budget, is that any delay in reaching the peak in emissions drastically increases the required rapidity and depth of future emissions cuts (see Figure 22 and also England et al. 2009). In Figure 22, emissions in the green exemplary path are 4 Gt CO_2 in the year 2050, which, with a projected world population of around 9 billion, would leave only less than half a ton per person per year. While the exact number will depend strongly on the path taken, the required decline in emissions combined with a growing population will mean that by 2050, annual per capita CO_2 emissions very likely will need to be below 1 ton.

Although CO_2 is the most important anthropogenic climate forcing, other greenhouse gases as well as aerosols also play a non-negligible role. Successful limitation of the non- CO_2 climate forcing would therefore create more leeway in the allowable CO_2 emissions budget. Studies have shown that attractive options for particularly rapid and cost-effective climate mitigation are the reduction of black carbon (soot) pollution and tropospheric low-level ozone (Wallack and Ramanathan 2009). In contrast to CO_2, these are very short-lived gases in the atmosphere, and therefore respond rapidly to policy measures.

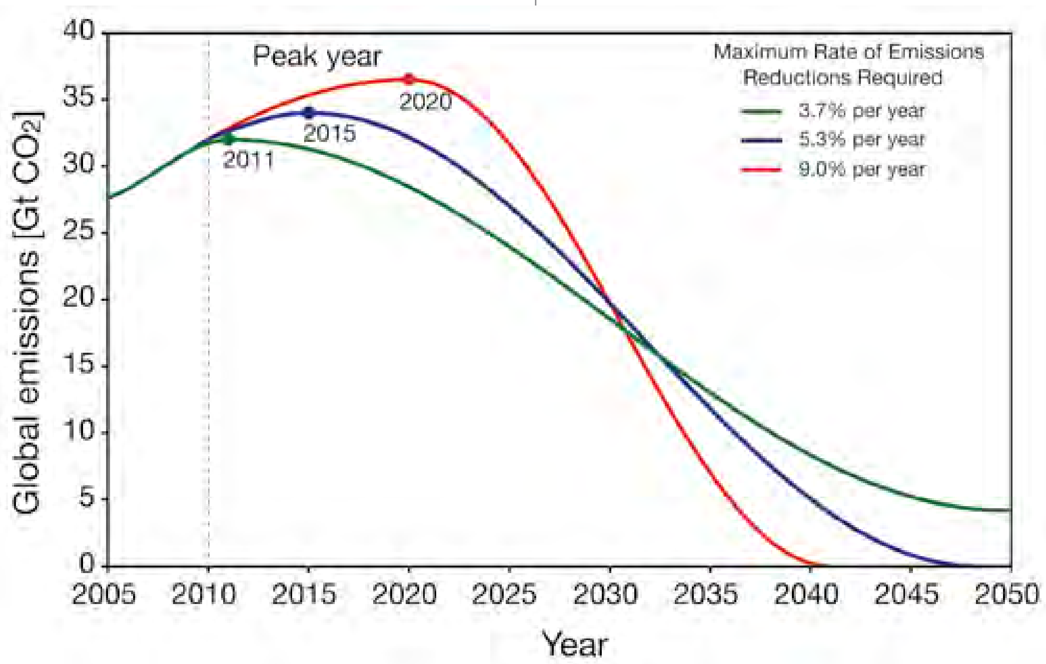

Figure 22. Examples of global emission pathways where cumulative CO_2 emissions equal 750 Gt during the time period 2010-2050 (1 Gt C = 3.67 Gt CO_2). At this level, there is a 67% probability of limiting global warming to a maximum of 2°C. The graph shows that the later the peak in emissions is reached, the steeper their subsequent reduction has to be. The figure shows variants of a global emissions scenario with different peak years: 2011 (green), 2015 (blue) and 2020 (red). In order to achieve compliance with these curves, maximum annual reduction rates of 3.7 % (green), 5.3 % (blue) or 9.0 % (red) would be required (relative to 2008). (Source: German Advisory Council on Global Change; WBGU 2009).

REFERENCES

Åkerman, H. J. & M. Johansson, (2008) Thawing permafrost and thicker active layers in sub-arctic Sweden. *Permafrost and Periglacial Processes* **19**, 279-292.

Alexander, L. V. & J. M. Arblaster, (2009) Assessing trends in observed and modelled climate extremes over Australia in relation to future projections. *International Journal of Climatology* **29**, 417-435.

Allan, R. P. & B. J. Soden, (2008) Atmospheric warming and the amplification of precipitation extremes. *Science* **321**, 1481-1484.

Allen, R. J. & S. C. Sherwood, (2008) Warming maximum in the tropical upper troposphere deduced from thermal winds. *Nature Geoscience* **1**, 399-403.

Allen, M. R. et al., (2009) Warming caused by cumulative carbon emissions toward the trillionth tonne. *Nature* **458**, 1163-1166.

Alley, R. B. et al., (2003) Abrupt Climate Change. *Science* **299**, 2005-2010.

Allison, I. et al., (2009) Ice sheet mass balance and sea level. *Antarctic Science*, **21**, 413-426.

Andronova, N. & M. E. Schlesinger, (2001) Objective estimation of the probability distribution for climate sensitivity. *Journal of Geophysical Research* **106**, 22605-22612.

Annan, J. D. & J. C. Hargreaves, (2006) Using multiple observationally-based constraints to estimate climate sensitivity. *Geophysical Research Letters* **33**, L06704.

Archer, D. et al., (2009) Ocean methane hydrates as a slow tipping point in the global carbon cycle. *Proceedings of the National Academy of Sciences*, doi:10.1073/pnas.0800885105.

Arzel, O. et al., (2006) Sea ice evolution over the 20th and 21st centuries as simulated by the current AOGCMs. *Ocean Modelling* **12**, 401-415.

Aumann, H. H. et al., (2008) Frequency of severe storms and global warming. *Geophysical Research Letters* **35**, L19805.

Bahr, D. B. et al., (2009) Sea-level rise from glaciers and ice caps: A lower bound. *Geophysical Research Letters* **36**, L03501.

Bakke, J. et al., (2009) Rapid oceanic and atmospheric changes during the Younger Dryas cold period. *Nature Geoscience* **2**.

Bala, G. et al., (2007) Combined climate and carbon-cycle effects of large-scale deforestation. *Proceedings of the National Academy of Sciences* **104**, 6550-6555.

Barnett, T. P. et al., (2008) Human induced changes in the hydrology of the western United States. *Science* **319**, 1080-1083.

Barrett B. E. et al., (2009) Rapid recent warming on Rutford Ice Stream, West Antarctica, from borehole thermometry, *Geophysical Research Letters*, **36**, L02708.

Benestad, R. E. & G. A. Schmidt, (2009) Solar trends and global warming. *Journal of Geophysical Research* **114**, D14101.

Berger, A., (1978) Long-term variations of daily insolation and Quaternary climatic changes. *Journal of the Atmospheric Sciences* **35**, 2362-2367.

Berger, A. & M. F. Loutre, (1991) Insolation values for the climate of the last 19 million years. *Quaternary Science Reviews* **10**, 297—317.

Berger, A. et al., (1998) Sensitivity of the LLN climate model to the astronomical and CO_2 forcings over the last 200 ky. *Climate Dynamics* **14**, 615-629.

Betts, R. A., (2000) Offset of the potential carbon sink from boreal afforestation by decreases in surface albedo. *Nature* **408**, 187-190.

Betts, R. A. et al., (2007) Projected increases in continental river runoff due to plant responses to carbon dioxide. *Nature* **448**, 1037-1041.

Biggs, R. et al., (2009) Turning back from the brink: Detecting an impending regime shift in time to avert it. *Proceedings of the National Academy of Sciences* **106**, 826-831, doi:10.1073/pnas.0811729106.

Bindoff, N. L. et al., (2007) Observations: Oceanic Climate Change and Sea Level. In *Climate Change 2007: The Physical Science Basis. Contribution of Working Group I to the Fourth Assessment Report of the Intergovernmental Panel on Climate Change* S. Solomon et al. eds (Cambridge University Press).

Bondeau, A. et al., (2007) Modelling the role of agriculture for the 20th century global terrestrial carbon balance. *Global Change Biology* **13**, 679-706.

Bony, S. et al., (2006) How well do we understand and evaluate climate change feedback processes? *Journal of Climate* **19**, 3445–3482.

Booth, B. B. et al., (2009 submitted) Global warming uncertainties due to carbon cycle feedbacks exceed those due to CO2 emissions. *Nature*.

Braun, M. & A. Humbert, (2009) Recent retreat of Wilkins Ice Shelf reveals new insights in ice shelf breakup mechanisms. *IEEE Geoscience and Remote Sensing Letters* **6**, 263-267.

Brewer, P. G., (2009) A changing ocean seen with clarity. *Proceedings of the National Academy of Sciences* **106**, 12213-12214.

Brook, E. et al., (2008) Potential for abrupt changes in atmospheric methane. In *Abrupt Climate Change. A report by the U.S. Climate Change Science Program and the Subcommittee on Global Change Research*. 360-452 (U.S. Geological Survey).

Canadell, J. G. et al., (2007) Contributions to accelerating atmospheric CO_2 growth from economic activity, carbon intensity, and efficiency of natural sinks. *Proceedings of the National Academy of Sciences* **104**, 18866-18870.

Cavalieri, D. J. & C. L. Parkinson, (2008) Antarctic sea ice variability and trends, 1979-2006. *Journal of Geophysical Research* **113**, C07004.

Cazenave, A. et al., (2009) Sea level budget over 2003-2008: A reevaluation from GRACE space gravimetry, satellite altimetry and ARGO. *Global and Planetary Change* **65**, 83-88.

CCSP, (2008a) Weather and Climate Extremes in a Changing Climate. Regions of Focus: North America, Hawaii, Caribbean, and U.S. Pacific Islands. A Report by the U.S. Climate Change Science Program. (Department of Commerce, NOAA's National Climatic Data Center, Washington, D.C., USA).

CCSP, (2008b) Abrupt Climate Change. A report by the U.S. Climate Change Science Program and the Subcommittee on Global Change Research. (U.S. Geological Survey, Reston VA).

Chang, P. et al., (2008) Oceanic link between abrupt change in the North Atlantic Ocean and the African monsoon. *Nature Geoscience* **1**, 444-448.

Chapman W.L. & J.E. Walsh, (2007) A synthesis of Antarctic temperatures. *Journal of Climate*, **20**, 4096-4117.

Chen, J. et al., (2006) Antarctic mass rates from GRACE. *Geophysical Research Letters* **33**, L11502.

Church, J. A. & N. J. White, (2006) A 20th century acceleration in global sea-level rise. *Geophysical Research Letters* **33**, L01602.

Clark, P. U. et al., (1999) Northern Hemisphere ice-sheet influences on global climate change. *Science* **286**, 1104-1111.

Cogley, J. G., (2009) Geodetic and direct mass-balance measurements: comparison and joint analysis. *Annals of Glaciology* **50**, 96-100.

Comiso, J. C. & F. Nishio, (2009) Trends in the sea ice cover using enhanced and compatible AMSR-E, SSM/I and SMMR data. *Journal of Geophysical Research* **113**, C02S07.

Cook, A. et al., (2005) Retreating glacier-fronts on the Antarctic Peninsula over the last 50 years. *Science* **22**, 541-544.

Cook, K. H. & E. K. Vizy, (2006) Coupled Model Simulations of the West African Monsoon System: Twentieth- and Twenty-First-Century Simulations. *Journal of Climate* **19**, 3681-3703.

Cook, K. H. & E. K. Vizy, (2008) Effects of Twenty-First-Century Climate Change on the Amazon Rain Forest. *Journal of Climate* **21**, 542-560.

Cox, P. M. et al., (2004) Amazonian forest dieback under climate-carbon cycle projections for the 21st century. *Theoretical and Applied Climatology* **78**, 137-156.

Cox, P. M. et al., (2008) Increasing risk of Amazonian drought due to decreasing aerosol pollution. *Nature* **453**, 212-216.

Cox, P. M. & C. D. Jones, (2008) Data from the past illuminates the modern dance of climate and carbon dioxide. *Science* **321**, 1642-1643.

Cruz, F. et al., (2009 in press) Probabilistic simulations of the impact of increasing leaf-level atmospheric carbon dioxide on the global land surface. *Climate Dynamics*, doi:10.1007/s00382-008-0497-0.

Cui, X. & H. F. Graf, (2009) Recent land cover changes on the Tibetan Plateau: a review. *Climatic Change* **94**, 47-61.

Curry, R. et al., (2003) A change in the freshwater balance of the Atlantic Ocean over the past four decades. *Nature* **426**, 826-829.

Dakos, V. et al., (2008) Slowing down as an early warning signal for abrupt climate change. *Proceedings of the National Academy of Sciences* **105**, 14308-14312.

Delworth, T. L. et al., (2008) The potential for abrupt change in the Atlantic Meridional Overturning Circulation. In *Abrupt Climate Change. A report by the U.S. Climate Change Science Program and the Subcommittee on Global Change Research*. 258-359

Dessler, A. E. et al., (2008) Water-vapor climate feedback inferred from climate fluctuations, 2003-2008. *Geophysical Research Letters* **35**, L20704.

Domingues, C. M. et al., (2008) Improved estimates of upper-ocean warming and multi-decadal sea-level rise. *Nature* **453**, 1090-1093.

Dorrepaal, E. et al., (2009) Carbon respiration from subsurface peat accelerated by climate warming in the subarctic. *Nature* **460**, 616-619.

Easterling, D. R. & M. F. Wehner, (2009) Is the climate warming or cooling? *Geophysical Research Letters* **36**, L08706.

Eby, M. et al., (2009) Lifetime of anthropogenic climate change: millennial time scales of potential CO_2 and surface temperature perturbations. *Journal of Climate* **22**, 2501-2511.

Eisenman, I. & J. S. Wettlaufer, (2009) Nonlinear threshold behavior during the loss of Arctic sea ice. *Proceedings of the National Academy of Sciences* **106**, 28-32.

Elsner, J. B. et al., (2008) The increasing intensity of the strongest tropical cyclones. *Nature* **455**, 92-95.

Emanuel, K. et al., (2008) Hurricanes and Global Warming: Results from Downscaling IPCC AR4 Simulations. *Bulletin of the American Meteorological Society* **89**, 347-367.

England, M. H. et al., (2009) Constraining future greenhouse gas emissions by a cumulative target *Proceedings of the National Academy of Sciences* **106**, 16539-16540.

EPICA community members, (2004) Eight glacial cycles from an Antarctic ice core. *Nature* **429**, 623-628.

Esper, J. et al., (2002) Low-frequency signals in long tree-ring chronologies for reconstructing past temperature variability. *Science* **295**, 2250-2253.

Fabry, V. J. et al., (2008) Impacts of ocean acidification on marine fauna and ecosystem processes. *ICES Journal of Marine Science* **65**, 414-432.

Fargione, J. et al., (2008) Land clearing and the biofuel debt. *Science* **319**, 1235-1238.

Fischer, E. M. et al., (2007) Contribution of land-atmosphere coupling to recent European heat waves. *Geophysical Research Letters* **34**, L06707.

Flanner, M. G. et al., (2007) Present-day climate forcing and response from black carbon in snow. *Journal of Geophysical Research* **112**, D11202.

Frame, D. J. et al., (2005) Constraining climate forecasts: The role of prior assumptions *Geophysical Research Letters* **32**, L09702.

Frederick, E. et al., (2004) Greenland Ice Sheet: increased coastal thinning *Geophysical Research Letters* **31**, L24402.

Friedlingstein, P. et al., (2006) Climate-carbon cycle feedback analysis: Results from the C4MIP model intercomparison. *Journal of Climate* **19**, 3337-3353.

Fyke, J. G. & A. J. Weaver, (2006) The effect of potential future climate change on the marine methane hydrate stability zone. *Journal of Climate* **19**, 5903-5916.

Galloway, J. N. et al., (2008) Transformation of the nitrogen cycle: recent trends, questions and potential solutions. *Science* **320**, 889-892.

Ganopolski, A. & D. M. Roche, (2009 in press) On the nature of lead–lag relationships during glacial–interglacial climate transitions. *Quaternary Science Reviews*, doi:10.1016/j.quascirev.2009.09.019.

Goosse, H. et al., (2009) Consistent past half-century trends in the atmosphere, the sea ice and the ocean at high southern latitudes. *Climate Dynamics*, **33**, 999-1016

Gedney, N. et al., (2006) Detection of a direct carbon dioxide effect in continental river runoff records. *Nature* **439**, 835-838.

Gleason, K. L. et al., (2008) A Revised U.S. Climate Extremes Index. *Journal of Climate* **21**, 2124-2137.

Guan, D. et al., (2009) Journey to world top emitter: An analysis of the driving forces of China's recent CO_2 emissions surge. *Geophysical Research Letters* **36**, L04709.

Guttal, V. & C. Jayaprakash, (2008) Changing skewness: an early warning signal of regime shifts in ecosystems. *Ecology Letters* **11**, 450-460.

Guttal, V. & C. Jayaprakash, (2009) Spatial variance and spatial skewness: leading indicators of regime shifts in spatial ecological systems. *Theoretical Ecology* **2**, 3-12.

Hagos, S. M. & K. H. Cook, (2007) Dynamics of the West African Monsoon Jump. *Journal of Climate* **20**, 5264-5284.

Hall, D. K. et al., (2008) Greenland ice sheet surface temperature, melt and mass loss: 2000-06. *Journal of Glaciology* **54**, 81-93.

Hanna, E. et al., (2008) Increased runoff from melt from the Greenland Ice Sheet: a response to global warming. *Journal of Climate* **21**, 331-341.

Hanna, E. et al., (2009) Hydrologic response of the Greenland Ice Sheet: the role of oceanographic forcing. *Hydrological Processes* **23**, 7-30.

Hansen, B. & S. Østerhus, (2007) Faroe Bank Channel overflow 1995 - 2005. *Progress in Oceanography* **75**, 817-856.

Harris, C. et al., (2009) Permafrost and climate in Europe: monitoring and modelling thermal, geomorphological and geotechnical responses. *Earth-Sciecne Review* **92**, 117-171.

Hays, J. D. et al., (1976) Variations in the Earth's orbit: Pacemaker of the ice ages. *Science* **194**, 1121-1132.

Haywood, A. M. et al., (2007) The mid-Pliocene Warm Period: a test-bed for integrating data and models. In *Deep-time perspectives on climate change: marrying the signal from computer models and biological proxies* M. Williams et al. eds 443-458 (The Micropalaeontological Society, Special Publication, The Geological Society, London).

Hock, R. et al., (2009) Mountain glaciers and ice caps around Antarctica make a large sea-level rise contribution. *Geophysical Research Letters* **36**, L07501.

Hofmann, M. & H. J. Schellnhuber, (2009) Oceanic acidification affects marine carbon pump and triggers extended marine oxygen holes. *Proceedings of the National Academy of Sciences* **106**, 3017-3022.

Hofmann, M. & S. Rahmstorf, (2009) On the stability of the Atlantic Meridional Overturning Circulation. *Proceedings of the National Academy of Sciences*. doi:10.1073/pnas.0909146106

Holland, M. M. et al., (2006) Future abrupt reductions in the summer Arctic sea ice. *Geophysical Research Letters* **33**, L23503.

Holland, D. M. et al., (2008) Acceleration of Jakobshavn Isbrae triggered by warm subsurface ocean waters. *Nature Geoscience* **28**, 659-664.

House, J. I. et al., (2008) What do recent advances in quantifying climate and carbon cycle uncertainties mean for climate policy? *Environmental Research Letters* **3**, 044002.

Howat, I. M. et al., (2007) Rapid changes in ice discharge from Greenland outlet glaciers. *Science* **315**, 1559-1561.

Howat, I. M. et al., (2008) Rates of southeast Greenland ice volume loss from combined ICESat and ASTER observations. *Geophysical Research Letters* **35**, L17505.

Hoyos, C.D. et al. (2006) Deconvolution of the Factors Contributing to the Increase in Global Hurricane Intensity, *Science*, **312**, 94-97.

Hyvönen, R. et al., (2007) The likely impact of elevated CO2, nitrogen deposition, increased temperature and management on carbon sequestration in temperate and boreal forest ecosystems: a literature review. *New Phytologist* **173**, 463-483.

IPCC, (2001) *Climate Change 2001: The Scientific Basis. Contribution of Working Group I to the Third Assessment Report of the Intergovernmental Panel on Climate Change (IPCC TAR)*. J. T. Houghton et al. eds (Cambridge University Press, Cambridge, UK and New York, NY, USA).

IPCC, (2007) *Climate Change 2007: The Physical Science Basis. Contribution of Working Group I to the Fourth Assessment Report of the Intergovernmental Panel on Climate Change (AR4)*. S. Solomon et al. eds (Cambridge University Press, Cambridge, UK & New York, NY, USA).

IPCC, (2007) Summary for Policymakers. In *Climate Change 2007: The Physical Science Basis. Contribution of Working Group I to the Fourth Assessment Report of the Intergovernmental Panel on Climate Change (IPCC AR4)* S. Solomon et al. eds (Cambridge University Press).

Jansen, E. et al., (2007) Palaeoclimate. In *Climate Change 2007: The Physical Science Basis. Contribution of Working Group I to the Fourth Assessment Report of the Intergovernmental Panel on Climate Change* S. Solomon et al. eds (Cambridge University Press).

Jin, H.-j. et al., (2008) Changes in permafrost environments along the Qinghai-Tibet engineering corridor induced by anthropogenic activities and climate warming. *Cold Regions Science and Technology* **53**, 317-333.

Johannessen, O. et al., (2005) Recent ice-sheet growth in the interior of Greenland. *Science* **310**, 1013-1016.

Johnson, G. C. & N. Gruber, (2007) Decadal water mass variations along 20°W in the Northeastern Atlantic Ocean. *Progress in Oceanography* **73**, 277-295.

Johnson, G. C. et al., (2008) Reduced Antarctic meridional overturning circulation reaches the North Atlantic Ocean. *Geophysical Research Letters* **35**, L22601.

Johnson, G. C. et al., (2008) Warming and freshening in the abyssal southeastern Indian Ocean. *Journal of Climate* **21**, 5351-5363.

Jones, G. S. et al., (2008) Human contribution to rapidly increasing frequency of very warm Northern Hemisphere summers. *Journal of Geophysical Research* **113**, D02109.

Jones, K. F. & B. Light, (2008) Sunlight, water, and ice: Extreme Arctic sea ice melt during the summer of 2007. *Geophysical Research Letters* **35**, L11501.

Jones, C. et al., (2009) Commited ecosystem change due to climate change. *Nature Geoscience* **2**, 484-487.

Joos, F. & R. Spahni, (2008) Rates of change in natural and anthropogenic radiative forcing over the past 20,000 years. *Proceedings of the National Academy of Sciences* **105**, 1425-1430.

Kaser, G. et al., (2006) Mass balance of glaciers and ice caps: Consensus estimates for 1961-2004. *Geophysical Research Letters* **33**, L19501.

Kaufman, D. S. et al., (2009) Recent Warming Reverses Long-Term Arctic Cooling. *Science* **325**, 1236-1239.

Kharin, V. V. et al., (2007) Changes in temperature and precipitation extremes in the IPCC ensemble of global coupled model simulations. *Journal of Climate* **20**, 1419-1444.

Khvorostyanov, D. V. et al., (2008) Vulnerability of east Siberia's frozen carbon stores to future warming. *Geophysical Research Letters* **35**, L10703.

Khvorostyanov, D. V. et al., (2008) Vulnerability of permafrost carbon to global warming. Part I: model description and the role of heat generated by organic matter decomposition. *Tellus B* **60B**, 250-264.

Knutti, R. & G. C. Hegerl, (2008) The equilibrium sensitivity of the Earth's temperature to radiation changes. *Nature Geoscience* **1**, 735-743.

Krabill, W. et al., (2000) Greenland Ice Sheet: High-Elevation Balance and Peripheral Thinning *Science* **289**, 428-430.

Krabill, W. et al., (2004) Greenland Ice Sheet: Increased coastal thinning. *Geophysical Research Letters* **31**, L24402.

Kriegler, E. et al., (2009) Imprecise probability assessment of tipping points in the climate system. *Proceedings of the National Academy of Sciences* **106**, 5041-5046.

Kürschner, W. M. et al., (1996) Oak leaves as biosensors of late Neogene and early Pleistocene paleoatmospheric CO_2 concentrations. *Marine Micropaleontology* **27**, 299-312.

Kwok, R. & D. A. Rothrock, (2009) Decline in Arctic sea ice thickness from submarine and ICESat records: 1958–2008. *Geophysical Research Letters* **36**, L15501.

Lam, P. et al., (2009) Revising the nitrogen cycle in the Peruvian oxygen minimum zone. *Proceedings of the National Academy of Sciences* **106**, 4752-4757.

Latif, M. & N. S. Keenlyside, (2009) El Niño/Southern Oscillation Response to Global Warming. *Proceedings of the National Academy of Sciences*, doi:10.1073/pnas.0710860105

Lawrence, D. M. & A. G. Slater, (2005) A projection of severe near-surface permafrost degradation during the 21st century. *Geophysical Research Letters* **32**, L24401.

Lawrence, D. M. et al., (2008) Accelerated Arctic land warming and permafrost degradation during rapid sea ice loss. *Geophysical Research Letters* **35**, L11506.

Le Quéré, C. et al., (2007) Saturation of the Southern Ocean CO_2 sink due to recent climate change. *Science* **316**, 1735-1738.

Le Quéré, C. et al., (2009) Trends in the sources and sinks of carbon dioxide. *Nature Geosciences*, **2**, in press.

Lean, J. L. & D. H. Rind, (2008) How natural and anthropogenic influences alter global and regional surface temperatures: 1889 to 2006. *Geophysical Research Letters* **35**, L18701.

Lean, J. L. & D. H. Rind, (2009) How will Earth's surface temperature change in future decades? *Geophysical Research Letters* **36**, L15708.

Lefebvre, W. et al., (2004) Influence of the southern annular mode on the sea-ice-ocean system. *Journal of Geophysical Research* **109**, C090005.

Lemke, P. et al., (2007) Observations: Changes in Snow, Ice and Frozen Ground In *Climate Change 2007: The Physical Science Basis. Contribution of Working Group I to the Fourth Assessment Report of the Intergovernmental Panel on Climate Change* S. Solomon et al. eds (Cambridge University Press).

Lenton, T. M. et al., (2008) Tipping Elements in the Earth's Climate System. *Proceedings of the National Academy of Sciences* **105**, 1786-1793.

Lenton, T. M. et al., (2009) Using GENIE to study a tipping point in the climate system. *Philosophical Transactions of the Royal Society A* **367**, 871-884.

Letenmaier, D. P. & P. C. D. Milly, (2009) Land water and sea level. *Nature Geoscience* **2**, 452-454.

Lindsay, R. W. et al., (2009) Arctic sea ice retreat in 2007 follows thinning trend. *Journal of Climate* **22**, 165-175.

Livina, V. & T. M. Lenton, (2007) A modified method for detecting incipient bifurcations in a dynamical system. *Geophysical Research Letters* **34**, L03712.

Lombard, A. et al., (2006) Perspectives on present-day sea level change. *Ocean Dynamics* **56**, 445-451.

Loulergue, L. et al., (2008) Orbital and millennial-scale features of atmospheric CH_4 over the past 800,000 years. *Nature* **453**, 383-386.

Lovenduski, N. et al., (2008) Toward a mechanistic understanding of the decadal trends in the Southern Ocean carbon sink. *Global Biogeochemical Cycles* **22**, GB3016.

Luthcke, S. B. et al., (2006) Recent Greenland ice mass loss by drainage system from satellite gravity observations. *Science* **314**, 1286-1289.

Lüthi, D. et al., (2008) High-resolution carbon dioxide concentration record 650,000-800,000 years before present. *Nature* **453**, 379-382.

Malhi, Y. et al., (2008) Climate Change, deforestation and the fate of the Amazon. *Science* **319**, 169-172.

Malhi, Y. et al., (2009) Exploring the likelihood and mechanism of a climate-change induced dieback of the Amazon rainforest. *Proceedings of the National Academy of Sciences*, doi:10.1073/pnas.0804619106.

Mann, M. E. et al., (1998) Global-Scale Temperature Patterns and Climate Forcing Over the Past Six Centuries. *Nature* **392**, 779-787.

Mann, M. E. et al., (1999) Northern Hemisphere Temperatures During the Past Millennium: Inferences, Uncertainties, and Limitations. *Geophysical Research Letters* **26**, 759-762.

Mann, M. E. et al., (2008) Proxy-Based Reconstructions of Hemispheric and Global Surface Temperature Variations over the Past Two Millennia. *Proceedings of the National Academy of Sciences* **105**, 13252-13257.

Mann, M. E. et al., (2009) Atlantic hurricanes and climate over the past 1,500 years. *Nature* **460**, 880-883.

Mann, M. E. et al., (in press) Global Signatures and Dynamical Origins of the "Little Ice Age" and "Medieval Climate Anomaly". *Science*.

Marsh, P. T. et al., (2009) Preliminary investigation into the severe thunderstorm environment of Europe simulated by the Community Climate Systems Model 3. *Atmospheric Research* **93**, 607-618.

Matthews, H. D. & K. Caldeira, (2008) Stabilizing climate requires near zero emissions. *Geophysical Research Letters* **35**, L04705.

McIntyre, S. & R. McKitrick, (2003) Corrections to the Mann et al. (1998) proxy database and northern hemispheric average temperature series. *Energy and Environment* **14**, 751-771.

McIntyre, S. & R. McKitrick, (2005) Hockey sticks, principal components, and spurious significance. *Geophysical Research Letters* **32**, L03710.

McIntyre, S. & R. McKitrick, (2005) The M&M critique of the MBH98 Northern Hemisphere climate index: Update and implications. *Energy and Environment* **16**, 69-99.

McNeil, B.I., and R.J. Matear (2007) Climate Change Feedbacks on Oceanic pH. *Tellus-B*, **59B**, 191-198.

McNeil, B. I. & R. J. Matear, (2008) Southern Ocean acidification: A tipping point at 450-ppm atmospheric CO_2. *Proceedings of the National Academy of Sciences* **105**, 18860-18864.

Meehl, G. A. et al., (2004) Combinations of Natural and Anthropogenic Forcings in Twentieth-Century Climate. *Journal of Climate* **19**, 3721-3727.

Meehl, G. A. et al., (2007a) Global Climate Projections. In *Climate Change 2007: The Physical Science Basis. Contribution of Working Group I to the Fourth Assessment Report of the Intergovernmental Panel on Climate Change* S. Solomon et al. eds (Cambridge University Press).

Meehl, G. A. et al., (2007b) Contributions of natural and anthropogenic forcing to changes in temperature extremes over the U.S. *Geophysical Research Letters* **34**, L19709.

Meehl, G. A. et al., (2008) Effects of Black Carbon Aerosols on the Indian Monsoon. *Journal of Climate* **21**, 2869-2882.

Meier, M. F. & M. B. Dyurgerov, (2007) Glaciers dominate eustatic sea-level rise in the 21st century. *Science* **317**, 1064-1067.

Meinshausen, M. et al., (2009) Greenhouse-gas emission targets for limiting global warming to 2°C. *Nature* **458**, 1158-1162.

Mercado, L. M. et al., (2009) Impact of change in diffuse radiation on the global land carbon sink. *Nature* **458**, 1014-1017.

Metzl, N., (2009) Decadal increase of oceanic carbon dioxide in Southern Indian surface ocean waters (1991-2007). *Deep Sea Research Part II: Topical Studies in Oceanography* **56**, 607-619.

Moberg, A. et al., (2005) Highly variable Northern Hemisphere temperatures reconstructed from low- and high-resolution proxy data. *Nature* **433**, 613-617.

Monaghan A. J. et al., (2008) Recent variability and trends of Antarctic near-surface temperature. *Journal of Geophysical Research*, **113**, D04105.

Mote, T. L., (2007) Greenland surface melt trends 1973-2007: Evidence of a large increase in 2007. *Geophysical Research Letters* **34**, L22507.

Moy, A. D. et al., (2009) Reduced calcification in modern Southern Ocean planktonic foraminifera. *Nature Geoscience* **2**, 276-280.

Nakicenovic, N. et al., (2000) IPCC Special Report on Emissions Scenarios. (Cambridge, UK), 599 pp.

NASA Goddard Institute for Space Studies, (2009) *GISS Surface Temperature Analysis. Global Temperature Trends: 2008 Annual Summation.* <http://data.giss.nasa.gov/gistemp/2008/>.

Nghiem, S. V. et al., (2007) Rapid reduction of Arctic perennial sea ice. *Geophysical Research Letters* **34**, L19504.

Nicholls, R. J. et al., (2007) Coastal systems and low-lying areas. In *Climate Change 2007: Impacts, Adaptation and Vulnerability. Contribution of Working Group II to the Fourth Assessment Report of the Intergovernmental Panel on Climate Change* M. L. Parry et al. eds 315-356 (Cambridge University Press).

NOAA, (2009) *State of the Climate, 2009*, <http://www.ncdc.noaa.gov/sotc/ >.

NRC (National Research Council), (2006) *Surface Temperature Reconstructions for the Last 2,000 Years*. (National Academies Press, Washington, DC).

NSDIC - National Snow and Ice Data Center, (2009) <http://nsidc.org/news/press/20091005_minimumpr.html>.

Oerlemans, J. et al., (2007) Reconstructing the glacier contribution to sea-level rise back to 1850. *The Cryosphere* **1**, 59-65.

Oppo, D. W. et al., (2009) 2,000-year-long temperature and hydrology reconstructions from the Indo-Pacific warm pool *Nature* **460**, 1113-1116.

Orr, J. C. et al., (2005) Anthropogenic ocean acidification over the twenty-first century and its impact on calcifying organisms. *Nature* **437**, 681-686.

Orr, J. C. et al., (2009) Amplified acidification of the Arctic Ocean. *IOP Conf. Series: Earth and Environmental Science* **6**, 462009.

Oschlies, A. et al., (2008) Simulated 21st century's increase in oceanic suboxia by CO_2-enhanced biotic carbon export *Global Biogeochemical Cycles* **22**, GB4008.

Pall, P. et al., (2007) Testing the Clausius-Clapeyron constraint on changes in extreme precipitation under CO2 warming. *Climate Dynamics* **28**, 351-363.

Patricola, C. M. & K. H. Cook, (2008) Atmosphere/vegetation feedbacks: A mechanism for abrupt climate change over northern Africa. . *Journal of Geophysical Research (Atmospheres)* **113**, D18102.

Pearson, P. L. & M. R. Palmer, (2000) Middle Eocene Seawater pH and Atmospheric Carbon Dioxide Concentrations. *Science* **284**, 1824-1826.

Pedersen, C. A. et al., (2009) A new sea ice albedo scheme including melt ponds for ECHAM5 general circulation model. *Journal of Geophysical Research* **114**, D08101.

Perovich, D. K. et al., (2007) Increasing solar heating of the Arctic Ocean and adjacent seas, 1979-2005: Attibution and role in the ice-albedo feedback. *Geophysical Research Letters* **34**, L19505.

Petrenko, V. V. et al., (2009) $^{14}CH_4$ measurements in Greenland ice: investigating last glacial termination CH_4 sources. *Science* **324**, 506-508.

Pfeffer, W. T. et al., (2008) Kinematic constraints on glacier contributions to 21st-Century sea-level rise. *Science*, **321**, 1340-1343.

Phillips, O. L. et al., (2009) Drought sensitivity of the Amazon rainforest. *Science* **323**, 1344-1347.

Piao, S. et al., (2007) Changes in climate and land-use have a larger direct impact than rising CO_2 on global river runoff records. *Proceedings of the National Academy of Sciences* **104**, 15242-15247.

Piekle, R. A. et al., (2007) An overview of regional land-use and land-cover impacts on rainfall. *Tellus B* **59**, 587-601.

Pitman, A. J. et al., (2007) The impact of climate change on the risk of forest and grassland fires in Australia. *Climatic Change* **84**, 383-401.

Pitman, A. J. et al., (2009) Uncertainties in climate responses to past land cover change: First results from the LUCID intercomparison study. *Geophysical Research Letters* **36**, L14814.

Pollard, D. & R. M. DeConto, (2009) Modelling West Antarctic ice sheet growth and collapse through the past five million years. *Nature* **458**, 329-332.

Polyakov, I. V. et al., (2004) Variability of the intermediate Atlantic water of the Arctic Ocean over the last 100 years. *Journal of Climate* **17**, 4485-4497.

Portmann, R. W. et al., (2009) Linkages between climate change, extreme temperature and precipitation across the United States. *Proceedings of the National Academy of Sciences* **106**, 7324-7329.

Pritchard, H. D. & D. G. Vaughan, (2007) Widespread acceleration of tidewater glaciers on the Antarctic Peninsula. *Journal of Geophysical Research* **112**, F03S29.

Pritchard, H. D. et al., (2009) Extensive dynamic thinning on the margins of the Greenland and Antarctic ice sheets. *Nature*, **461**, 971-975.

Rahmstorf, S., (2007) A Semi-Empirical Approach to Projecting Future Sea-Level Rise. *Science* **315**, 368-370.

Rahmstorf, S. et al., (2007) Recent climate observations compared to projections. *Science* **316**, 709.

Ramanathan, V. et al., (2005) Atmospheric brown clouds: Impacts on South Asian climate and hydrological cycle. *Proceedings of the National Academy of Sciences* **102**, 5326-5333.

Ramanathan, V. & G. Carmichael, (2008) Global and regional climate changes due to black carbon. *Nature Geoscience* **1**, 221-227.

Raupach, M. R. et al., (2007) Global and regional drivers of accelerating CO_2 emissions. *Proceedings of the National Academy of Sciences* **104**, 10288-10293.

Raymo, M. E. et al., (1996) Mid-Pliocene warmth: stronger greenhouse and stronger conveyor. *Marine Micropaleontology* **27**, 313-326.

Rayner, N. A. et al., (2006) Improved analyses of changes and uncertainties in sea surface temperature measured in situ since the mid-nineteenth century: the HadSST2 data set. *Journal of Climate* **19**, 446-469.

Reichstein, M. et al., (2007) Reduction of ecosystem productivity and respiration during the European summer 2003 climate anomaly: a joint flux tower, remote sensing and modelling analysis. *Global Change Biology* **13**, 634-651.

Repo, M. E. et al., (2009) Large N_2O emissions from cryoturbated peat soil in tundra. *Nature Geoscience* **2**, 189-192.

Richardson, K. et al., (2009) Climate Change: Global Risks, Challenges & Decisions. Synthesis Report of the Copenhagen Climate Congress. (University of Copenhagen).

Riebesell, U. et al., (2009) Sensitivities of marine carbon fluxes to ocean change. *Proceedings of the National Academy of Sciences*.

Rigby, M. et al., (2008) Renewed growth of atmospheric methane. *Geophysical Research Letters* **35**, L22805.

Rignot, E. et al., (2004) Accelerated ice discharge from the Antarctic Peninsula following the collapse of Larsen B ice shelf. *Geophysical Research Letters* **31**, L18401.

Rignot, E., (2006) Changes in ice dynamics and mass balance of the Antarctic ice sheet. *Philosophical Transactions of the Royal Society A* **364**, 1637-1655.

Rignot, E. & P. Kanagaratnam, (2006) Changes in the velocity structure of the Greenland Ice Sheet. *Science* **311**, 986-990.

Rignot, E., (2008a) Changes in West Antarctic ice stream dynamics observed with ALOS PALSAR data. *Geophysical Research Letters* **35**, L12505.

Rignot, E. et al., (2008b) Recent Antarctic ice mass loss from radar interferometry and regional climate modelling. *Nature Geoscience* **1**, 106-110.

Rignot, E. et al., (2008) Mass balance of the Greenland ice sheet from 1958 to 2007. *Geophysical Research Letters* **35**, L20502.

Rintoul, S. R., (2007) Rapid freshening of Antarctic Bottom Water formed in the Indian and Pacific oceans. *Geophysical Research Letters* **34**, L06606.

Rohling, E. J. et al., (2008) High rates of sea-level rise during the last interglacial period. *Nature Geoscience* **1**, 38-42.

Rosa, R. & B. A. Seibel, (2008) Synergistic effects of climate-related variables suggest future physiological impairment in a top oceanic predator. *Proceedings of the National Academy of Sciences* **105**, 20776-20780.

Rotstatyn, L. D. & U. Lohmann, (2002) Tropical Rainfall Trends and the Indirect Aerosol Effect. *Journal of Climate* **15**, 2103-2116.

Rutherford, S. et al., (2005) Proxy-Based Northern Hemisphere Surface Temperature Reconstructions: Sensitivity to Method, Predictor Network, Target Season, and Target Domain. *Journal of Climate* **18**, 2308-2329.

Sabine, C. L. et al., (2004) The Oceanic Sink for Anthropogenic CO_2. *Science* **305**, 367-371.

Salazar, L. F. et al., (2007) Climate change consequences on the biome distribution in tropical South America. *Geophysical Research Letters* **34**, L09708.

Santer, B. D. et al., (2007) Identification of human-induced changes in atmospheric moisture content. *Proceedings of the National Academy of Sciences* **104**, 15248-15253.

Saunders, M. A. & A. S. Lea, (2008) Large contribution of sea surface warming to recent increase in Atlantic hurricane activity. *Nature* **451**, 557-560.

Scambos, T. A. et al., (2004) Glacier acceleration and thinning after ice shelf collapse in the Larsen B embayment, Antarctica. *Geophysical Research Letters* **31**, L18402.

Schellnhuber, H. J., (2009) Tipping elements in the Earth System. *Proceedings of the National Academy of Sciences*.

Scholze, M. et al., (2006) A climate-change risk analysis for world ecosystems. *Proceedings of the National Academy of Sciences* **103**, 13116-13120.

Schuster, U. et al., (2009 in press) Trends in North Atlantic sea surface pCO_2 from 1990 to 2006. *Deep Sea Research Part II: Topical Studies in Oceanography*, doi:10.1016/j.dsr2.2008.12.011.

Schuur, E. A. G. et al., (2008) Vulnerability of permafrost carbon to climate change: Implications for the global carbon cycle. *BioScience* **58**, 701-714.

Shackleton, N. J., (2000) The 100,000-year ice-age cycle identified and found to lag temperature, carbon dioxide, and orbital eccentricity. *Science* **289**, 1897-1902.

Sheffield, J. & E. F. Wood, (2008) Global Trends and Variability in Soil Moisture and Drought Characteristics, 1950–2000, from Observation-Driven Simulations of the Terrestrial Hydrologic Cycle. *Journal of Climate* **21**, 432-458.

Shindell, D. & G. Faluvegi, (2009) Climate response to regional radiative forcing during the twentieth century. *Nature Geoscience* **2**, 294-300.

Siegenthaler, U. et al., (2005) Stable carbon cycle-climate relationship during the late Pleistocene. *Science* **310**, 1313-1317.

Sitch, S. et al., (2007) Indirect raditive forcing due to ozone effects on the land carbon sink. *Nature* **448**, 791-794.

Sokolov, A. P. et al., (2009) Probabilistic forecast for 21st century climate based on uncertainties in emissions (without policy) and climate parameters. *Journal of Climate* **22**, 5175-5204.

Solomon, S. et al., (2009) Irreversible climate change due to carbon dioxide emissions. *Proceedings of the National Academy of Sciences* **106**, 1704-1709.

Soon, W. & S. Baliunas, (2003) Proxy climatic and environmental changes of the past 1000 years. *Climate Research* **23**, 89-110.

Stammerjohn, S. E. et al., (2008) Trends in Antarctic annual sea ice retreat and advance and their relation to El Niño-Southern Oscillation and Southern Annular Mode variability. *Journal of Geophysical Research* **113**, C03S90.

Steffen, K. et al., (2008) Rapid changes in glaciers and ice sheets and their impacts on sea level. In *Abrupt Climate Change: A Report by the U.S. Climate Change Science Program and the Subcommittee on Global Change Research* 60-142 (U.S. Geological Survey).

Steig, E. J. et al., (2009) Warming of the Antarctic ice-sheet surface since the 1957 International Geophysical Year. *Nature* **457**, 459-462.

Stott, P. A. et al., (2008) Detection and attribution of Atlantic salinity changes. *Geophysical Research Letters* **35**, L21702.

Stramma, L. et al., (2008) Expanding oxygen-minimum zones in the tropical oceans. *Science* **320**, 655-658.

Stroeve, J. et al., (2007) Arctic sea ice decline: Faster than forecast. *Geophysical Research Letters* **34**, L09501.

Takahashi, T. et al., (2009) Climatological mean and decadal changes in surface ocean pCO_2, and net sea-air CO_2 flux over the global oceans. *Deep Sea Research Part II: Topical Studies in Oceanography* **56**, 554-577.

Tarnocai, C. et al., (2009) Soil organic carbon pools in the northern circumpolar permafrost region. *Global Biogeochemical Cycles* **23**, GB2023.

Thompson, D. W. J. & S. Solomon, (2002) Interpretation of recent Southern Hemisphere Climate Change *Science* **296**, 895-899.

Thorne, P. W., (2008) The answer is blowing in the wind. *Nature Geoscience* **1**, 347-348.

Trapp, R. J. et al., (2007) Changes in severe thunderstorm environment frequency during the 21st century caused by anthropogenically enhanced global radiative forcing. *Proceedings of the National Academy of Sciences* **104**, 19719-19723.

Trapp, R. J. et al., (2009) Transient response of severe thunderstorm forcing to elevated greenhouse gas concentrations. *Geophysical Research Letters* **36**, L01703.

Tripati, A. K. et al., (2009 in press) Coupling of CO2 and Ice Sheet Stability Over Major Climate Transitions of the Last 20 Million Years. *Science*, doi:10.1126/science.1178296.

Turner, J. et al., (2009) Non-annular atmospheric circulation change induced by stratospheric ozone depletion and its role in the recent increase of Antarctic sea ice extent. *Geophysical Research Letters* **36**, L08502.

van den Broeke, M., (2005) Strong surface melting preceded collapse of Antarctic Peninsula ice shelf. *Geophysical Research Letters* **32**, L12815.

Vecchi, G. A. et al., (2006) Weakening of tropical Pacific atmospheric circulation due to anthropogenic forcing. *Nature* **441**, 73-76.

Vecchi, G. A. et al., (2008) Whither hurricane activity? *Science* **322**, 687-689.

Velicogna, I. & J. Wahr, (2006) Acceleration of Greenland ice mass loss in spring 2004. *Nature* **443**, 329-331.

Velicogna, I., (2009) Increasing rates of ice mass loss from the Greenland and Antarctic ice sheets revealed by GRACE. *Geophysical Research Letters* **36**, L19503.

Vellinga, P. et al., (2008) Exploring high-end climate change scenarios for flood protection of the Netherlands: an international scientific assessment. (KNMI, Wageningen, the Netherlands).

Veron, J. E. N. et al., (2009) The coral reef crisis: the critical importance of <350ppm CO_2. *Marine Pollution Bulletin* **58**, 1428-1437.

Wahl, E. R. et al., (2006) Comment on "Reconstructing past climate from noisy data". *Science* **312**, 529.

Wahl, E. R. & C. M. Ammann, (2007) Robustness of the Mann, Bradley, Hughes reconstruction of Northern Hemisphere surface temperatures: Examination of criticisms based on the nature and processing of proxy climate evidence. *Climatic Change* **85**, 33-69.

Wallack, J. S. & R. Ramanathan, (2009 accepted) Strategies for Hedging Against Rapid Climate Change. *Foreign Affairs*.

WBGU - German Advisory Council on Global Change, (2006) The Future Oceans - Warming Up, Rising High, Turning Sour. (WBGU, Berlin).

WBGU - German Advisory Council on Global Change, (2009) Solving the climate dilemma: The budget approach. (WBGU, Berlin).

Weart, S. & R. T. Pierrehumbert, (2007) *A Saturated Gassy Argument*, <http://www.realclimate.org/index.php/archives/2007/06/a-saturated-gassy-argument/>.

Wentz, F. J. et al., (2007) How much more rain will global warming bring? *Science* **317**, 233-235.

Westerling, A. L. et al., (2006) Warming and Earlier Spring Increase Western U.S. Forest Wildfire Activity. *Science* **313**, 940-943.

Wild, M. et al., (2007) The impact of global dimming and brightening on global warming. *Geophysical Research Letters* **34**, L04702.

Wingham, D. et al., (2006) Mass balance of the Antarctic ice sheet. *Transactions of the Royal Society of London Series A* **364**, 1627-1635.

Wouters, B. et al., (2008) GRACE observes small-scale mass loss in Greenland. *Geophysical Research Letters* **35**, L20501.

Yeh, S.-W. et al., (2009) El Niño in a changing climate. *Nature* **461**, 511-514.

Yin, J. et al., (2009) Model projections of rapid sea-level rise on the northeast coast of the United States. *Nature Geoscience* **2**, 262-266.

Zhang, X. et al., (2007) Detection of human influence on twentieth-century precipitation trends. *Nature* **448**, 461-465.

Zickfeld, K. et al., (2009) Setting cumulative emissions targets to reduce the risk of dangerous climate change. *Proceedings of the National Academy of Sciences* **106**, 16129-16134.

Zimov, S. A. et al., (2006) Permafrost and the Global Carbon Budget. *Science* **312**, 1612-1613.

BIOGRAPHIES

Allison, Ian

Ian Allison is leader of the Ice Ocean Atmosphere and Climate program in the Australian Antarctic Division, a Lead Author of the IPCC Fourth Assessment Report and the President of the International Association of Cryospheric Sciences.

Bindoff, Nathan

Nathan Bindoff is Professor of Physical Oceanography at the University of Tasmania, Australia, and a Coordinating Lead Author of the IPCC Fourth Assessment Report.

Bindschadler, Robert

Robert Bindschadler is Chief Scientist of the Laboratory for Hydrospheric and Biospheric Processes at NASA Goddard Space Flight Center, USA, a Senior Fellow of NASA Goddard, an AGU Fellow and past President of the International Glaciological Society.

Cox, Peter

Peter Cox is Professor and Met Office Chair in Climate System Dynamics at the University of Exeter, UK, and a Lead Author of the IPCC Fourth Assessment Report.

de Noblet, Nathalie

Nathalie de Noblet is a Research Scientist at the Laboratoire des Sciences du Climat et de l'Environnement (LSCE), Gif-sur-Yvette, France.

England, Matthew

Matthew England is an Australian Research Council Federation Fellow, Professor of Physical Oceanography, an IPCC Contributing Author and joint Director of the UNSW Climate Change Research Centre (CCRC) at the University of New South Wales, Australia.

Francis, Jane

Jane Francis is a Senior Lecturer of Earth Sciences at Leeds University, UK, and the Director of the Leeds University Centre for Polar Science.

Gruber, Nicolas

Nicolas Gruber is Professor of Environmental Physics at ETH Zurich, Switzerland, and a contributing author of the IPCC Fourth Assessment Report.

Haywood, Alan

Alan Haywood is Reader in Palaeoclimatology at the School of Earth and Environment, University of Leeds, UK, and a recent recipient of the Philip Leverhulme Prize.

Karoly, David

David Karoly is Professor of Meteorology and an ARC Federation Fellow at the University of Melbourne, Australia, and a Lead Author of the IPCC Third and Fourth Assessment Reports.

Kaser, Georg

Georg Kaser is a glaciologist at the University of Innsbruck, Austria, a Lead Author of the IPCC Fourth Assessment Report and the IPCC Technical Paper on Climate Change and Water, and the Immediate Past President of the International Association of Cryospheric Sciences.

Le Quéré, Corinne

Corinne Le Quéré is Professor of Environmental Science at the University of East Anglia, UK, a researcher at the British Antarctic Survey, co-Chair of the Global Carbon Project and a Lead Author of the IPCC Third and Fourth Assessment Reports.

Lenton, Tim

Tim Lenton is Professor of Earth System Science at the University of East Anglia, UK and the recipient of the Times Higher Education Award for Research Project of the Year 2008 for his work on climate tipping points.

Mann, Michael

Michael E. Mann is a Professor in the Department of Meteorology at Penn State University, USA, Director of the Penn State Earth System Science Center, and a Lead Author of the IPCC Third Assessment Report.

McNeil, Ben

Ben McNeil is an Australian Research Council Queen Elizabeth II Research Fellow at the Climate Change Research Centre at the University of New South Wales, Australia and an expert reviewer of the IPCC Fourth Assessment Report.

Pitman, Andy

Andy Pitman is joint director of the Climate Change Research Centre at the University of New South Wales, Australia, and a Lead Author of the IPCC Third and Fourth Assessment Reports.

Rahmstorf, Stefan

Stefan Rahmstorf is Professor of Physics of the Oceans and department head at the Potsdam Institute for Climate Impact Research in Germany, a Lead Author of the IPCC Fourth Assessment Report and a member of the German government's Advisory Council on Global Change.

Rignot, Eric

Eric Rignot is a glaciologist and Senior Research Scientist at NASA's Jet Propulsion Laboratory, USA, a Professor of Earth System Science at the University of California Irvine, and a Lead Author of the IPCC Fourth Assessment Report.

Schellnhuber, Hans Joachim

Hans Joachim Schellnhuber is Professor for Theoretical Physics and Director of the Potsdam-Institute for Climate Impact Research, Germany, Chair of the German Advisory Council on Global Change (WBGU) and a longstanding member of the Intergovernmental Panel on Climate Change (IPCC).

Schneider, Stephen

Stephen Schneider is the Lane Professor of Interdisciplinary Environmental Studies at Stanford University, an IPCC Lead Author of all four Assessment and two Synthesis Reports, and founder and Editor of the Journal *Climatic Change*.

Sherwood, Steven

Steven Sherwood is a Professor of atmospheric sciences at the Climate Change Research Centre at the University of New South Wales, Australia, and a contributing author to the IPCC Fourth Assessment Report.

Somerville, Richard

Richard C. J. Somerville is Distinguished Professor Emeritus at Scripps Institution of Oceanography, University of California, San Diego, USA and a Coordinating Lead Author of the IPCC Fourth Assessment Report.

Steffen, Konrad

Konrad Steffen is Director of the Cooperative Institute for Research in Environmental Sciences (CIRES) and Professor of Climatology at the University of Colorado in Boulder, USA, and the Chair of the World Climate Research Programme's Climate and Cryosphere (CliC) project.

Steig, Eric

Eric J. Steig is Director of the Quaternary Research Center, and Professor of Earth and Space Sciences at the University of Washington, USA.

Visbeck, Martin

Martin Visbeck is Professor of Physical Oceanography and Deputy Director of the Leibniz Institute of Marine Sciences, IFM-GEOMAR, Germany, Chair of Kiel's multidisciplinary research cluster of excellence "The Future Ocean" and Co-Chair of the World Climate Research Programme's Climate Variability and Predictability (CLIVAR) Project.

Weaver, Andrew

Andrew Weaver is Professor and Canada Research Chair in Climate Modelling and Analysis at the University of Victoria, Canada, a Lead Author of the IPCC Second, Third, and Fourth Assessment Reports and Chief Editor of the *Journal of Climate*.

Climatic Change (2008) 91:249–274
DOI 10.1007/s10584-008-9484-z

EDITORIAL

Reductions of greenhouse gas emissions in Annex I and non-Annex I countries for meeting concentration stabilisation targets

An editorial comment

Michel den Elzen · Niklas Höhne

Received: 20 May 2008 / Accepted: 27 June 2008 / Published online: 11 September 2008

Abstract The IPCC Fourth Assessment Report, Working Group III, summarises in Box 13.7 the required emission reduction ranges in Annex I and non-Annex I countries as a group, to achieve greenhouse gas concentration stabilisation levels between 450 and 650 ppm CO_2-eq. The box summarises the results of the IPCC authors' analysis of the literature on the regional allocation of the emission reductions. The box states that Annex I countries as a group would need to reduce their emissions to below 1990 levels in 2020 by 25% to 40% for 450 ppm, 10% to 30% for 550 ppm and 0% to 25% for 650 ppm CO_2-eq, even if emissions in developing countries deviate substantially from baseline for the low concentration target. In this paper, the IPCC authors of Box 13.7 provide background information and analyse whether new information, obtained after completion of the IPCC report, influences these ranges. The authors concluded that there is no argument for updating the ranges in Box 13.7. The allocation studies, which were published after the writing of the IPCC report, show reductions in line with the reduction ranges in the box. From the studies analysed, this paper specifies the "substantial deviation" or "deviation from baseline" in the box: emissions of non-Annex I countries as a group have to be below the baseline roughly between 15% to 30% for 450 ppm CO_2-eq, 0% to 20% for 550 ppm CO_2-eq and from 10% above to 10% below the baseline for 650 ppm CO_2-eq, in 2020. These ranges apply to the whole group of non-Annex I countries and may differ substantially per country. The most important factor influencing these ranges above, for non-Annex I countries, and in the box, for Annex I countries, is new information on higher baseline emissions (e.g. that of Sheehan, Climatic Change, 2008, this issue). Other factors are the assumed global emission level in 2020 and assumptions on

M. den Elzen (✉)
Netherlands Environmental Assessment Agency, P.O. Box 303,
3720 AH Bilthoven, The Netherlands
e-mail: Michel.den.Elzen@mnp.nl

N. Höhne
Ecofys Germany GmbH, Cologne, Germany

EXHIBIT 23

land-use change and forestry emissions. The current, slow pace in climate policy and the steady increase in global emissions, make it almost unfeasible to reach relatively low global emission levels in 2020 needed to meet 450 ppm CO_2-eq, as was first assumed feasible by some studies, 5 years ago.

1 Introduction

The level of ambition for reductions by developed countries (Annex I countries) and developing countries (non-Annex I countries), in a future international agreement on climate change, is one very important element in the current climate negotiations. The Ad-Hoc Working Group on Further Commitments for Annex I countries under the Kyoto Protocol (AWG-KP), agreed on the wording of the level of its ambition. At a preparatory meeting in August 2007, it noted the usefulness of the contribution of Working Group III to the Fourth Assessment Report (AR4) of the Intergovernmental Panel on Climate Change (IPCC), which states that emissions need to peak within the next 10 to 15 years and that emissions must be reduced to well below half of the 2000 level by the middle of the twenty-first century, in order to stabilise their concentrations in the atmosphere at the lowest level assessed by the IPCC. In addition, AWG-KP recognised that Annex I countries need to reduce their emissions within a range of 25% to 40% below 1990 levels in 2020, in order to reach the lowest stabilisation levels assessed by the IPCC. The reduction range of −25% to −40% refers to Box 13.7 of the Working Group III report of the IPCC AR4 (Table 1) (Gupta et al. 2007). Agreement on this formulation was possible under the Kyoto Protocol because (1) it is only a recognition of this range and not a decision on it and (2) the USA did not take part in this agreement, as it has not ratified the Kyoto Protocol.

At the Conference of the Parties (COP) 13 in Bali in December 2007, the issue of the reduction range for the Annex I was discussed again, this time with all countries, including the USA. Initial drafts by the EU called for the same wording as already agreed to under the Kyoto Protocol. The Box 13.7 of the IPCC report received large attention, including by the media. But in the end, agreement could not be reached on the reduction percentages in the negotiations under the Convention and, instead, it called for "deep cuts in global emissions" and a reference to the IPCC AR4 was included in a footnote.

The conference also agreed to complete the negotiation process on comparable mitigation commitments or actions by all developed countries and nationally appropriate mitigation actions by developing countries by the end of 2009.

In this paper the authors of Box 13.7 provide more details on the studies that were used to prepare the ranges and they analyse whether new information, obtained after completion of the IPCC report, influences these ranges. A first question is how the ranges were derived and whether new allocation studies would change the results (Section 2). A second question concerns the possibility of quantifying what is termed as "substantial deviation from the baseline" for non-Annex I countries and what the important determinants are. One important assumption is the reductions by the Annex I countries, but an even more important assumption is the baseline that was chosen (Section 3). Different baselines were tested, including those with rapid growth in emissions, in particular in the developing countries, as presented by

Table 1 IPCC Box 13.7: The range of the difference between emissions in 1990 and emission allowances in 2020/2050 for various GHG concentration levels for Annex I and non-Annex I countries as a group

Scenario category	Region	2020	2050
A—450 ppm CO_2-eq[a]	Annex I	−25% to −40%	−80% to −95%
	Non-Annex I	Substantial deviation from baseline in Latin America, Middle East, East Asia and Centrally-Planned Asia	Substantial deviation from baseline in all regions
B—550 ppm CO_2-eq	Annex I	−10% to −30%	−40% to −90%
	Non-Annex I	Deviation from baseline in Latin America and Middle East, East Asia	Deviation from baseline in most regions, especially in Latin America and Middle East
C—650 ppm CO_2-eq	Annex I	0% to−25%	−30% to −80%
	Non-Annex I	Baseline	Deviation from baseline in Latin America, Middle East, and East Asia

Source: Gupta et al. (2007, Section 13.3.3.3). The aggregate range is based on multiple approaches to apportion emissions between regions (contraction and convergence, Multi-Stage, Triptych and intensity targets, among others). Each approach makes different assumptions about the pathway, specific national efforts and other variables. Additional extreme cases—in which Annex I or non-Annex I undertake all reductions—are not included. The ranges presented here do not imply political feasibility, nor do the results reflect cost variances.

[a]Only the studies aiming at stabilisation at 450 ppm CO_2-eq assume a (temporary) overshoot of about 50 ppm (see den Elzen and Meinshausen 2006b).

Sheehan (2008). Also important are assumptions on the required global emission level and on CO_2 emissions from land use, land-use change and forestry (LULUCF).

2 Main assumptions underlying the studies quoted in the IPCC report

Several studies have analysed the level of commitment of different regions and countries and the timing of participation, which are required to ensure meeting the long-term concentration stabilisation targets, using different post-2012 regimes for differentiation of future commitments (allocation schemes). This has been summarised in Box 13.7 by IPCC AR4 (Gupta et al. 2007). Table 2 presents the main assumptions of the sixteen studies used and quoted in the IPCC analysis and two additional unquoted studies (i.e. Höhne et al. 2003; Leimbach 2003), which influence the results:

- *Allocation calculations for CO_2 only or all greenhouse gases (GHGs):* Some calculations were based on all GHGs and some only on CO_2. The share of non-CO_2 gases is usually higher in developing counties
- *Baseline:* The baseline emissions are a major determinant for the results, as more reductions are necessary if baseline emissions are higher
- *Kyoto implementation:* For the short term it is important whether studies have assumed that the Kyoto protocol targets are implemented or not.

Table 2 Main assumptions of the studies quoted by the IPCC and more recent studies (in chronological order) underlying Box 13.7

	Allocation calculations	Baseline scenario[a]	Assumptions on meeting Kyoto targets in 2008–2012	Allocation schemes covered[b]	Global emission target (excl. LULUCF CO_2) in 2020/2050 (%-compared to 1990 levels), for CO_2-eq concentration (ppm), IPCC categories		
					A—450	B—550	C—650
Studies used quoted in IPCC report							
Berk and den Elzen (2001)	CO_2	IPCC* A1	Annex I incl. USA	MS, CC, HR	+10/−20		
Blanchard et al. (2002)	CO_2	IPCC** A1	Annex I excl. USA; FSU BAU[c]	CC, HR, EI			+50/NI
Winkler et al. (2002)	CO_2	IPCC B1	Not considered; base-year 2000	HR, AP, EI	0		
Criqui et al. (2003)	CO_2-eq	CPI 2003	Annex I excl. USA & Australia	MS, CC		+35/−20	+50/+35
Höhne et al. (2003) *(not quoted)*	CO_2-eq	IPCC A2	Annex I incl. USA; FSU BAU[c]	MS, CC, EI, TY, other		+27/NI	
Leimbach (2003) *(not quoted)*	CO_2	Own	Not included; base-year 2000	CC			[40; 75]/+25
WBGU (2003)	CO_2	IPCC**	Annex I incl. USA	CC	+20/−60	+30/+5	
Bollen et al. (2004)	CO_2	IPCC A1	Annex I excl. USA & Australia	CC		+30/NI	+50/NI
Groenenberg et al. (2004)	CO_2	IPCC A1	Not included; base-year 1995	TY	+15/NI	[20; 30]/+5	[35; 60]/+50
Böhringer and Löschel (2005)	CO_2	DOE ref.	Annex I excl. USA & Australia	Other			+50
den Elzen and Lucas (2005)	CO_2-eq	CPI 2003	Annex I excl. USA & Australia	MS, CC, EI, TY, other		+35/−20	+50/+35
den Elzen et al. (2005b)	CO_2-eq	CPI 2003	Annex I excl. USA & Australia	MS, CC, HR		+35/−20	+50/+35
Höhne et al. (2005) (Höhne 2005)	CO_2-eq	IPCC all*	Annex I incl. USA; FSU BAU[c]	MS, CC, EI, TY, other	+10/−40	+30/−10	+50/+45
Michaelowa et al. (2005)	CO_2	Own	Annex I excl. USA & Australia	MS			+30[d]/NI
Böhringer and Welsch (2006)	CO_2	IPCC** A1	Not included; base-year 2000	CC		[30; 35]/−15	

den Elzen and Meinshausen (2006a, b)[e]	CO_2-eq	CPI 2003	Annex I excl. USA & Australia	MS, CC	[20; 30]/ [−30;−50]	+40/[−10; 10]	
Persson et al. (2006)	CO_2	IPCC A1	Annex I excl. USA	CC		+36	
Studies published after IPCC AR4							
den Elzen et al. (2007a)[e,f]	CO_2-eq	CPI 2003	Annex I excl. USA & Australia	Other	[20; 30]/ [−30;−50]	+40/[−10; 10]	
den Elzen et al. (2008b)[e]	CO_2-eq	IPCC B2***	Annex I excl. USA & Australia	MS, CC	+20/−35	+35/−5	
den Elzen et al. (2008a)[e]	CO_2-eq	IPCC B2***	Annex I excl. USA & Australia	TY	+20/−35	+35/−5	
Höhne et al. (2006)[f]	CO_2-eq	IPCC* all	Annex I excl. USA; FSU BAU[c]	Other, CC		+35/−25	+50/+35
Vaillancourt and Waaub (2006)	CO_2	Own	Not included; base-year 2000	Other			+57/+65
Höhne et al. (2007)[f]	CO_2-eq	IPCC* all	Annex I excl. USA; FSU BAU[c]	MS, CC, HR, TY, other	+10/−40	+30/−10	+50/+45
Baer et al. (2008)	CO_2	WEO 2007[g]	Annex I excl. USA	Other	+10/−80		
Timilsina (2008)	CO_2	Own	Annex I excl. USA; FSU BAU[c]	EI			+46/NI
Number of studies					11	16	14

NI Not included

[a]Own: scenario based on own assumptions; IPCC*: IMAGE implementation of IPCC SRES 2001 scenarios (IMAGE-team 2001); IPCC**: IIASA (1998) implementation; CPI: common POLES-IMAGE baseline (van Vuuren et al. 2003, 2006); DOE reference scenario (DOE 2003); Update IPCC B2***: updated IMAGE/TIMER implementation of the IPCC-SRES B2 scenario (van Vuuren et al. 2007), which roughly follows the reference scenario of the World Energy Outlook (WEO) 2004 (IEA 2004)

[b]The abbreviations of the schemes are given in Table 3

[c]The emissions of the former Soviet Union (FSU) and Eastern European countries are assumed to equal the baseline or business-as-usual (BAU) emissions (which are far below their Kyoto targets)

[d]For the period 2013–2017

[e]Assuming a (temporary) overshoot of about 50 ppm

[f]Uncertainty ranges presented in this study also include uncertainties in scenarios, but this effect is limited, and not included in Fig. 1

[g]Reference scenario of the WEO 2007 (IEA 2007)

- *The assumed allocation scheme covered:* Some studies in Table 2 focus on one scheme, whereas others include a wide range of about ten schemes (see for example, den Elzen and Lucas 2005).
- *Global emission limits:* Many global emission pathways can lead to the same long-term concentration stabilisation level. Pathways with higher emissions in the earlier part of the century have lower emissions in the later part of the century. Therefore, it is important which global emission level in 2020 and 2050 was chosen from a possible range that represents one long-term stabilisation level (i.e. 450, 550 and 650 ppm CO_2-eq).

Table 2 (bottom part) also shows the seven new allocation studies that became available after the finalisation of the IPCC report. In fact, the first four of these studies were already included in the calculations of the presented reduction ranges, but at the last moment of publication of the IPCC AR4 report, their citations were excluded, as these studies were still unpublished, at the time.

Figure 1 presents the resulting emission reduction targets for the Annex I and non-Annex I countries as a group, which are mainly based on information provided by the authors of the studies or, for some studies, are derived from detailed information in the papers themselves. The figure also presents the adopted IPCC AR4 reduction ranges (Gupta et al. 2007). The IPCC AR4 based these ranges on the outcomes of all studies mentioned in Table 2 (except for Leimbach 2003; Vaillancourt and Waaub 2006; Höhne et al. 2007; Baer et al. 2008; Timilsina 2008). We listed all studies that were available to us. Outliers that provide substantially different results compared to other studies were excluded and more weight was given to the more recent multi-gas studies. We did not make judgements on the way the studies allocated emission reductions across regions and countries.

A brief overview of the studies is given below.

The study by Berk and den Elzen (2001) is one of the first, quantifying post-2012 CO_2 emission allocations for meeting long-term concentration stabilisation targets, based on three regimes, i.e. Multi-Stage, Contraction & Convergence (C&C) and Berk and den Elzen's implementation of the Brazilian proposal (see Table 3). The study assumed that all Annex I countries would meet their Kyoto targets (the USA had not rejected ratification), a low global emission target of only 10% above 1990 levels, by 2020, and 20% below 1990 levels, by 2050. Based on its low short-term emission this study is clustered under the lowest IPCC 450 ppm CO_2-eq category (Table 2).The Annex I countries, as a group, need to reduce their emissions from about 30% to 45% below 1990 levels, which is at the lower end of the IPCC AR4 range (see Fig. 1). The reductions for the non-Annex I countries, as a group, range from 15% to 35% below the baseline emissions. Later, den Elzen (2002) also included Triptych regime calculations and an extensive sensitivity analysis. Similar work has been done by Blanchard (2002), focussing on stabilisation at 550 ppm CO_2 concentration (about 650 ppm CO_2-eq). Winkler et al. (2002) also calculated the CO_2 emission allowances of the key developing countries, using three allocation schemes, and assuming global CO_2 emissions returning to 1990 levels by 2020, and using the lowest IPCC SRES B1 scenario.

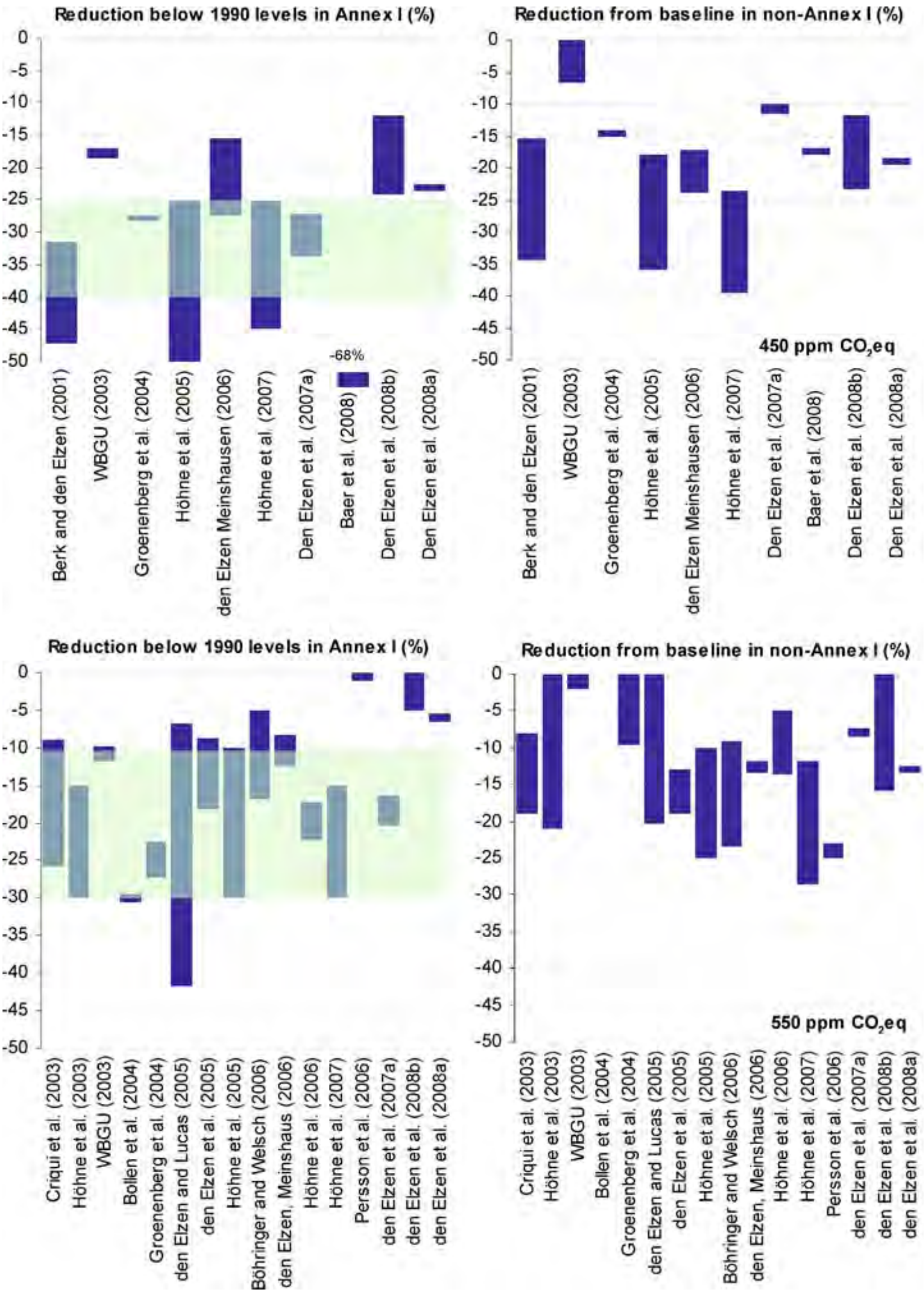

Fig. 1 Reductions in Annex I (below 1990 level) and non-Annex I countries (below baseline) as a group in 2020 for the studies quoted by the IPCC and more recent studies. Uncertainty ranges indicated here, are based on the outcomes of different post-2012 regimes. The figure also depicts the reduction ranges for Annex I countries as reported in IPCC Box 13.7

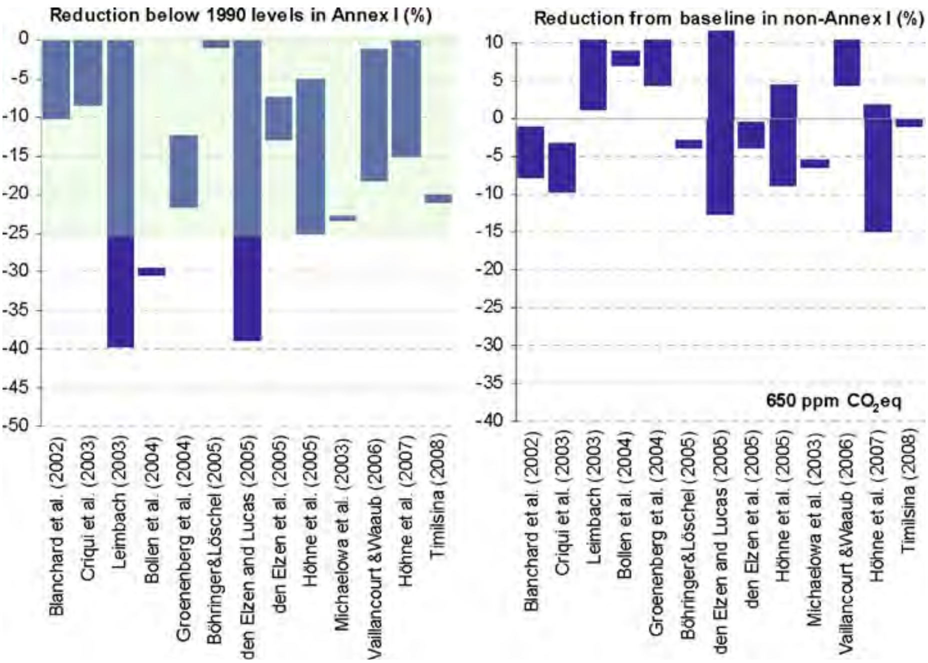

Fig. 1 (continued)

Most studies in Table 2 focussed on CO_2 only, instead of all GHGs. Criqui et al. (2003) and Höhne et al. (2003) were among the first to calculate emission allowances for all GHGs, i.e. CO_2-equivalent emissions, including the anthropogenic emissions of six Kyoto greenhouse gases (fossil CO_2, CH_4, N_2O, HFCs, PFCs and SF_6 (using the 100-year GWPs of IPCC 2001)). These studies, as did all earlier studies, excluded LULUCF CO_2 emissions, as these were too uncertain. Criqui et al. (2003) presented reduction targets for two C&C variants (convergence years 2050 and 2100) and three Multi-Stage variants for regions, and focused on stabilising GHG concentration targets at 550 and 650 ppm CO_2-eq (see also den Elzen et al. 2006). Den Elzen and Lucas (2005) extended this analysis, using ten very different emission allocation schemes, varying from grandfathering to a convergence in per capita emissions before 2015, leading to a wide range of reductions in Annex I countries, below 1990 levels. Another follow-up study, den Elzen et al. (2005b), focused on less regimes, but also presented abatement costs.

Höhne et al. (2003) focussed on a wide range of post-2012 regimes (all variants of those mentioned in Table 3) for a global emission target in 2020 (roughly corresponding with 550 ppm CO_2-eq), and was the first to present the reduction targets for individual countries.[1] The reductions for Annex I countries in 2020 are, in general, more stringent than those in Criqui et al. (2003), due to their assumed lower

[1]They used baseline scenarios for population, GDP and emissions at the level of countries, based on applying the regional downscaling method for the IPCC SRES emission scenarios from the four IPCC SRES regions to countries.

Table 3 Short description of the various post-2012 regimes for differentiation of future commitments (allocation schemes)

Approach	Abbreviation	Operational rule for allocation of emission allowances
Multi-Stage approach	MS	An incremental but rule-based approach, which assumes a gradual increase in the number of parties taking on mitigation commitments and in their level of commitment as they move through several stages according to participation and differentiation rules (Berk and den Elzen 2001; den Elzen 2002).
Historical responsibility (Brazilian Proposal)	HR	Reduction targets based on countries' contribution to temperature increase (UNFCCC 1997; den Elzen et al. 2005a).
Ability to Pay	AP	Emission reduction allocation and participation based on per capita income thresholds (Jacoby et al. 1999).
Contraction & Convergence (C&C)	CC	Emission targets based on a convergence of per capita emission levels of all countries under a contraction of the global emission profile (Meyer 2000).
Emission Intensity	EI	Emission reductions related to improvements in the emission per unit GDP output (Baumert et al. 1999).
Triptych	TY	Emission allowances based on various differentiation rules to different sectors for all Parties (Phylipsen et al. 1998).

2010 emissions in Annex I countries (the starting point of the calculations), from stronger Kyoto reduction assumptions. Höhne et al. (2003) assumed that all Annex I countries (including USA) implement the Kyoto targets, except for the former Soviet Union (FSU) and Eastern European States, which start from their baseline emissions (far below the Kyoto target). Criqui et al. (2003), however, assumed that all Annex I countries meet the Kyoto targets (this is for FSU and Eastern European States well above their baseline), except for the USA, which are assumed to meet their national target (about 25% above 1990 levels in stead of −7% below 1990 emissions under Kyoto in 2010).

Besides these studies, there are also CO_2-only studies with macro-economic or energy-system models, which focus primarily on the C&C regime for global CO_2-only emissions targets, as was done by Bollen et al. (2004), Leimbach (2003), Persson et al. (2006) and WBGU (2003). These studies mainly vary the convergence year between 2025 and 2100, showing stringent reductions for Annex I countries for an early convergence. WBGU (2003) (identical to Nakicenovic and Riahi 2003) focuses on C&C 2050 and 2100 for 400 ppm CO_2 concentration stabilisation under the IPCC B1 and B2 baseline scenarios, and 450 ppm CO_2 under the IPCC A1T scenario. The first group of 400 ppm CO_2,corresponding with the lowest 450 ppm CO_2-eq target, and the lower baseline scenarios (B1 and B2), in particular, lead to low reductions targets for Annex I and non-Annex I countries (well above the IPCC AR4 range) (Fig. 1). Bollen et al. (2004) and Leimbach (2003) focus on global emission targets, in 2020, as high as 50–75% above 1990 levels (within 650 ppm CO_2-eq) and show high reduction targets for Annex I countries (30% to 40% below 1990 levels)—well below the IPCC AR4 range. In contrast, they have surplus emission allowances (emissions above the baseline) for non-Annex I countries. Compared to the other results, these studies seem outliers. Böhringer and Welsch (2006) used emission allocations from current emissions, based on equal-per-capita emission.

Groenenberg et al. (2004) has extended the Triptych approach for all GHGs and also presented an extensive sensitivity analysis, showing a wide range of reduction targets for Annex I and non-Annex I countries in 2020. As Kyoto targets were not considered, the reduction targets are somewhat higher, but still within the IPCC AR4 ranges. Den Elzen et al. (2008a) further improved the Triptych approach by, for example, a differentiated participation for developing countries that, together with accounting for the Kyoto targets (excluding the USA), lead to reduction targets which are somewhat lower than the IPCC AR4 reductions.

Böhringer and Löschel (2005) use another approach that differs from the rule-based allocation schemes used in all previous studies. They interviewed experts about their judgment on four key aspects of a possible Post-Kyoto scenario, until 2020: the targeted global emission reduction, USA participation, the inclusion of developing countries, and the allocation rule for abatement duties. In general, this approach leads to a high global emission limit by 2020 and rather low reduction targets for the Annex I and non-Annex I countries (Table 1 and Fig. 1).

Vaillancourt and Waaub (2006) proposed a dynamical multi-criterion method to compare various alternative allocation rules and found a compromise solution, although this led to global emissions as high as 50% above 1990 levels in 2020.

Höhne et al. (2005) updated the calculations of in their study of 2003, again for a wide range of regimes. For the lowest concentration category, a non-overshoot 400 ppm CO_2 concentration stabilisation (about 450 ppm CO_2-eq) is assumed. This, combined with the stronger Kyoto reduction assumptions (all Annex I countries including the USA implement Kyoto), leads to emission reductions in Annex I countries, up to 45% below 1990 levels in 2020, for 450 ppm CO_2-eq. In general, their reduction range exceeds the IPCC AR4 range on the lower end. Höhne et al. (2007) further updated the analysis with very similar reduction ranges, although they now assumed that the USA follows its national target, leading to a less ambitious range for Annex I countries. In Höhne et al. (2006) a variant of the per capita convergence (‘common but differentiated convergence’) is presented, in which the per capita emissions of all countries converge to a low level. The per capita emissions in non-Annex countries, however, start to converge later, but end up at the same level. This leads to slightly more ambitious 2020 I reduction targets for Annex I countries.

Den Elzen and Meinshausen (2006b) focused on Multi-Stage and C&C, and GHG concentration targets 400–550 ppm CO_2-eq. For 400 and 450 ppm CO_2-eq they assumed an overshoot in the concentration targets. This overshoot, combined with a lower baseline and less stringent Kyoto reduction assumption (all Annex I countries, except for the USA and Australia, implement their Kyoto targets by 2010), lead to less ambitious reduction targets for Annex I countries. Similar assumptions have been made in den Elzen et al. (2008b), presenting in detail the required abatement options and costs. As they excluded the 400 ppm scenario and used a lower baseline (update of IPCC B2), the reductions for Annex I and non-Annex I countries were less ambitious, although the USA still has to return to its 1990 levels by 2020. In den Elzen et al. (2007a) a variant of the Multi-Stage type regime, i.e. the 'South–North Dialogue' Proposal (Ott et al. 2004) was analysed. This proposal is based on the criteria of responsibility, capability and potential to mitigate, and include deep cuts in industrialised (Annex I) countries and differentiated mitigation commitments for developing countries.

Another very recent allocation study came from Baer et al. (2008), called the Greenhouse Development Rights Framework. This framework calculates national shares of the global mitigation requirement based on an indicator that combines capacity (per capita income over a $7,500 threshold) and responsibility (cumulative per capita emissions since 1990) in a way that is sensitive to intra-national income distribution. National allocations are then calculated by subtracting each country's share of the global mitigation requirement from its national baseline emissions trajectory. This approach leads to very high Annex I emission reductions of about −70% below 1990 levels in 2020.

The following findings can be drawn from Table 2 and Fig. 1:

- A wide range of studies cover the different stabilisation levels; most have studied 550 ppm CO_2-eq.
- The number of multi-gas studies that analysed the lowest concentration category, published at the time of writing the IPCC AR4, was limited, i.e. den Elzen and Meinshausen (2006b) and Höhne et al. (2005), but about four of these studies were in press at the time of writing the IPCC AR4 (see Table 1). In general, the studies of Höhne assume a lower global emission limit in 2020 (10%, 30% and 50% above 1990 levels for stabilisation at 450, 550 and 650 ppm CO_2-eq) and stronger Kyoto reduction assumptions (the USA follows Kyoto and FSU starts in 2010 with baseline emissions), whereas the studies of den Elzen assume a higher global emission limit (25%, 40% and 50% for stabilisation at 450, 550 and 650 ppm CO_2-eq by 2020) and lower Kyoto reduction targets (the USA follows national policy by 2010, and FSU starts in 2010 at their Kyoto targets). Therefore, the studies of Höhne et al. lead to more stringent reduction targets in the presented ranges for 2020, whereas those by den Elzen et al. lead to less stringent reduction targets for 2020. However, less stringent reductions in the short term require more stringent reductions in the long term, to reach the same long-term stabilisation level. Hence, the targets presented by Höhne for the long term, are less stringent than those presented by den Elzen.
- There is no argument for updating the ranges in Box 13.7 of the IPCC report based on the new studies published after its completion, as all studies show reductions that are in line with the reduction ranges in the box.
- As has been explained in the IPCC report, the reductions in Annex I and non-Annex I countries in the Box largely depend on the regime assumptions, the

global emissions target (and related to the concentration stabilisation target) and depend on the assumptions on the initial 2010 emission levels. This issue is also further analysed in the next chapter.

- As was also concluded by Sheehan, most of these studies use baseline emission scenarios, mostly the IPCC SRES scenarios, that are developed before 2003 and do not account for the recent rapid growth in emissions. More specifically, in all studies the reference cases are within the SRES marker scenario range, and hence subject to the critique outlined in Sheehan (2008). The impact of new baseline scenarios will be discussed in the next section.
- The studies that were analysed show that emissions in the group of non-Annex I countries deviate from the baseline roughly between 15% to 30% for 450 ppm CO_2-eq, between 0% to 20% for 550 ppm CO_2-eq and from 10% above to 10% below the baseline for 650 ppm CO_2-eq, in 2020. Quantitative estimates per regional group for non-Annex I countries are not possible, as all studies used different regional groupings.

3 Assessing the emission reductions in Annex I and non-Annex I

One particular issue of interest is: if Annex I countries reduce their domestic emissions to a certain extent, then how far do the emissions in non-Annex I countries have to be reduced, to achieve the stabilisation of the climate at a certain level? In the previous sections it is described which Annex I reductions have been calculated by the different studies, as well as what these studies assumed to be a “substantial deviation from the baseline” for non-Annex I countries. This section further analyses which factors are important in this trade-off and it assesses their influence, using simple calculations to quantify this influence. The analysis concentrates on 2020 as this is the timeframe of major interest in the negotiations. The most important factors in the reductions of greenhouse gas emissions in Annex I and non-Annex I countries, in order of descending influence, are:

1. *Baseline emissions*: These are particularly uncertain for non-Annex I countries, but so is the historical emission trend, which is not always the same in the models.
2. *The assumed global emission level in 2020 for a long-term concentration stabilisation target*: As the long-term concentration stabilisation level depends also on the cumulative emissions, a certain stabilisation level can only be translated into an emission *range* in 2020. This range is particularly large if one assumes that concentrations may temporarily overshoot the desired level.
3. *Land-use CO_2 emission projections*: Current land-use related CO_2 emissions and projections are particularly uncertain and, mostly, they are not or only indirectly considered in the studies cited above.

Below, a brief description is given of the assumptions for the first two points, followed by an analysis of each of these points, in Section 3.3.

3.1 Baseline

Current and historical emission levels vary by a few percentage points, depending on the data source, but all data sources report an increase in global emissions. Table 4

Table 4 GHG emissions (excluding LULUCF CO_2 and international transport emissions) for the Annex I and non-Annex I countries as a group and the world, for the period 1990–2006 (upper) and 2020 projection (lower)

	Emission (million tonnes CO_2-eq)			Change compared to 1990 levels		
	Annex I	Non-Annex I	World	Annex I (%)	Non-Annex I (%)	World (%)
1990	18,531	12,847	31,378	0	0	0
1995	18,123	14,294	32,417	−2	11	3
2000	17,986	16,866	34,852	−3	31	11
2005	18,414	20,609	39,023	−1	60	24
2006	18,460	21,548	40,008	0	68	25
2020 scenario[a]						
IPCC A1 2001	23,558	34,732	57,616	27	170	84
IPCC A2 2001	23,110	29,752	52,434	25	132	67
IPCC B1 2001	19,334	28,435	47,222	4	121	50
IPCC B2 2001	20,520	31,234	51,114	11	143	63
IPCC A1F 2001	24,066	35,126	58,521	30	173	87
IPCC A1T 2001	33,408	23,034	55,812	24	160	78
CPI 2003	21,108	31,779	52,243	14	147	66
Update IPCC B2	22,345	27,530	49,370	21	114	57
Sheehan (2008)[b]	22,215	40,575	61,726	20	216	97

Source: GHG emissions for the period 1990–2005: IEA (2008); CO_2 emissions in 2006: BP (2007) and non-$CO_2$and process CO_2 emissions in 2006: using the trend of 2004–2005.

[a]IPCC: IMAGE implementation of IPCC SRES 2001 scenarios (IMAGE-team 2001); CPI: common POLES-IMAGE baseline (van Vuuren et al. 2003, 2006); Update IPCC B2: updated IMAGE/TIMER implementation of the IPCC-SRES B2 scenario (van Vuuren et al. 2007)

[b]As the Sheehan baseline does not include the non-CO_2 GHG emissions, we have estimated these based on the IMAGE IPCC SRES A1b scenario.

gives the historical trend in the global GHG emissions (excluding land-use related CO_2 emissions and international transport emissions) for one very recent data source. In 2005, global CO_2-eq emissions were about 24% above 1990 emission levels (IEA 2008). The 2006 figures are based on a preliminary estimate by the Netherlands Environmental Assessment Agency, using recently published BP [British Petroleum (BP 2007)] energy data and cement production data. From 2005 to 2006, global CO_2 emissions from fossil fuel use increased by about 2.6%, which is less than the 3.3% increase the year before.[2] The 2.6% increase is mainly due to a 4.5% increase in global coal consumption. In the 1990–2006 period, global fossil-fuel related CO_2 emissions increased over 35%, which is an increase of 25% for the overall GHG emissions (excluding LULUCF CO_2 emissions), assuming an ongoing linear trend over the past 5 years, for the non-CO_2 GHG emissions in 2006.

Even if the Kyoto Protocol is implemented by those countries that have ratified it, it is very likely that global emissions will continue to rise until 2012, when a new international climate agreement can start to be effective. The approximate stabilisation of emissions by Annex I countries will be more than counterbalanced by an ongoing and strong rise in emissions in non-Annex I countries.

[2]http://www.mnp.nl/en/dossiers/Climatechange/moreinfo/Chinanowno1inCO2emissionsUSAinsecondposition.html.

Table 4 also shows the projections of future emissions from various sources. The standard set of emission scenarios, IMAGE implementation (IMAGE-team 2001) of the IPCC special report on emission scenarios (Nakicenovic et al. 2000) was prepared already in 2001 and, therefore, does not reflect the recent changes in emissions.[3] Still, its large range covers most of the scenarios that were produced afterwards. Already in 2020, the spread will be high: global emissions could be as low as 50% below, or as high as 92% above 1990 level, according to the recent projection of Sheehan (2008) (for a discussion of this scenario, see van Vuuren and Riahi 2008). The impact of the various baselines on the reductions in Annex I and non-Annex I countries, will be analysed in Section 3.3.

3.2 Global emission level in 2020 necessary for a long-term concentration stabilisation target

A second, very important assumption is the global emission level in 2020, necessary for a long-term concentration stabilisation target. The long-term stabilisation level depends also on the cumulative emissions. A long-term stabilisation level can only be translated into an emission *range* in 2020. This range is particularly large if one assumes that concentrations may temporarily overshoot the desired level. In earlier studies, this emission level is lower, as they assumed that reductions would start earlier and would not be postponed, in the way they are in the current trends.

Höhne et al. (2005) were rather optimistic about the Kyoto implementation and early action by developing countries and did not allow for overshooting. They, therefore, used very low global emission levels of 10% and 30%, compared to 1990 levels in 2020, for 450 and also 550 ppm CO_2-eq, based on stabilisation paths from various sources that were available at that time. Given that today's global GHG emission level (excluding LULUCF CO_2) is already 25% above 1990, and that it will further increase until 2010, the chosen values are very ambitious and reaching +10% may have become unrealistic.

Den Elzen and Meinshausen (2006a, b) also presented emission pathways to stabilise CO_2-eq concentrations at 550 and 450 ppm. The 450 ppm pathway allows overshooting, i.e., concentrations peak before stabilising at lower levels, rising to 500 ppm CO_2-eq, before dropping to the 450 ppm CO_2-eq, later on. Allowing an overshoot also relaxes the global emission targets in the short term (2020), but increases the necessary effort afterwards (up to 2050 and beyond), shifting the burden into the future. The GHG emissions (excluding LULUCF CO_2) may increase to 30%, compared to 1990 levels in 2020, for 450 ppm CO_2-eq.

To illustrate the impact of the first three elements (baseline, 2020 global emission level and land-use CO_2 emissions) on the emission reduction in Annex I and non-Annex I, we use the global emission targets of den Elzen et al. (2007b), presenting the global GHG emission pathways for the three concentration stabilisation levels, and their ranges (see Table 5). The numbers of this study are in line with den Elzen and Meinshausen (2006b) and another study of Meinshausen et al. (2006), using the EQW methodology, and are within the 2020 and 2050 ranges of the IPCC AR4 (Fisher

[3]The IMAGE IPCC SRES scenarios are used here, as this set is used by many allocation studies in Table 2, for reasons of consistency (one single model is used for all scenarios) and regional detailed information.

Table 5 Assumptions for global emission target (excl. LULUCF CO_2) in 2020 and 2050 (%-compared to 1990 emission levels) for the different multi-gas pathways for stabilising at 450, 550 and 650 ppm CO_2-eq concentration of this study and Höhne et al

CO_2-equivalent concentration	This study (based on den Elzen et al. 2007b) Central estimate (%)	Range[a] (%)	Höhne et al. (2005) (%)
2020			
450 ppm (no overshoot)			+10
450 ppm (overshoot)	+25	[+15; +30]	
550 ppm	+40	[+30; +45]	+30
650 ppm	+50	[+40; +60]	+50
2050			
450 ppm (no overshoot)			−40
450 ppm (overshoot)	−35	[−45;−25]	
550 ppm	−5	[−10; 0]	−10
650 ppm	+35	[+20; +60]	+45

Numbers are rounded off to the nearest decimal or half-decimal.

[a]The uncertainty range presented here needs to be considered carefully in the context of the envelope. Choosing lower reductions in the beginning needs to be compensated by higher reductions later on and vice versa.

et al. 2007). These estimates do not account for possible higher carbon releases from the terrestrial biosphere (such as carbon cycle feedbacks, or continuing high deforestation).

3.3 Analysis

Figure 2 shows the trade-off between deviations from baseline in non-Annex I countries in 2020 (left to right) and the change in GHG emissions for Annex I countries, compared to 1990 (top to bottom) for the stabilisation levels, as shown in Table 5 for den Elzen et al. (2007b). The Annex I reduction range of the AWG of −25% to −40% is also shown.

Note that these reductions are assumed to occur independently by domestic reductions in Annex I and non-Annex I countries. If Annex I countries decide to achieve some of these reductions outside of the group (through CDM or any other future mechanisms), additional reductions have to occur in developing countries.

The calculations behind these figures are very straightforward. First, a simple calculation can be made of the total overall global allowable emissions to meet the various concentration stabilisation targets, by combining the global GHG emission targets of Table 5 with the global GHG emissions of Table 4. In the second step, the allowable emissions of the Annex I countries can be calculated, by combing the allowable emissions of the non-Annex I countries (calculated as the reduction from their baseline emissions, see Table 4) and the global allowable emissions of step 1.

Figure 2 provides the average outcome over separate calculations for each of the six IMAGE IPCC SRES scenarios (IMAGE-team 2001) (A1B, A1Fl, A1T, A2, B1, B2) (*the IPCC SRES average*), for 2020 and 2050 to capture a wide spread of possible future baseline emission developments.

To exemplify the figure, an example is given for the average over the six IPCC SRES scenarios. Figure 2a shows that the emission reductions for Annex I countries, as a group, of 25% relative to 1990 in 2020 (top range of the green shaded area),

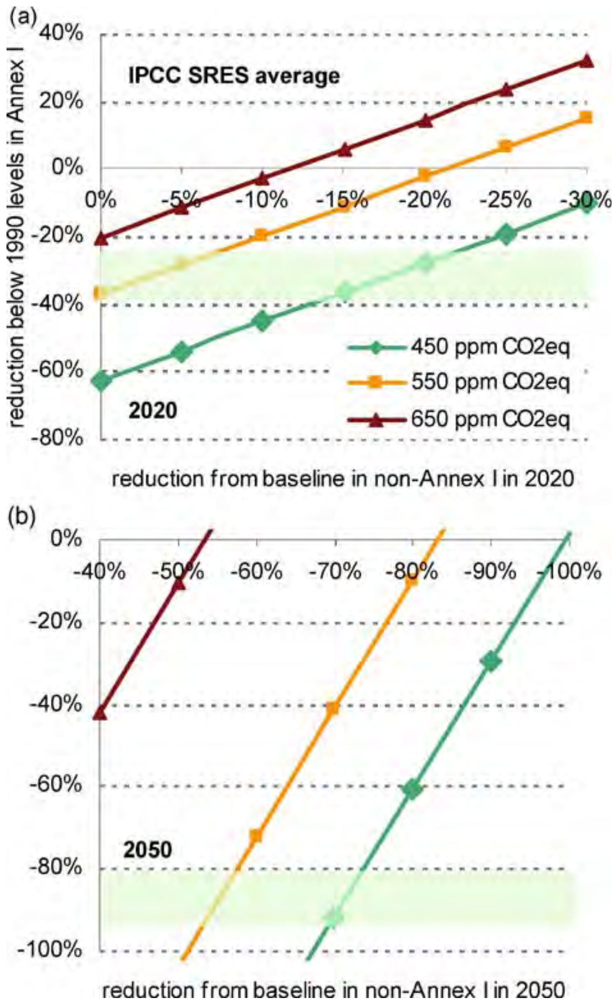

Fig. 2 The trade-off in reductions in 2020 (**a**) and 2050 (**b**), in Annex I and non-Annex I countries as a group, for three concentration stabilisation levels. The *numbers* represent the averaged outcome over separate calculations for each of the six IPCC SRES baselines (IPCC SRES average). The figure also depicts the reduction ranges for Annex I countries for 450 ppm CO_2-eq as reported in IPCC Box 13.7

and deviation from the baseline by non-Annex I countries, as a group, of around 7% is consistent with a 550 ppm CO_2-eq stabilisation level (intersection of the middle yellow line for 550 ppm with the top range of the green shaded area). For meeting 450 ppm CO_2-eq stabilisation, the non-Annex I countries' deviation, compared to the baseline, becomes around 22% (intersection of the bottom green line for 450 ppm with the top range of the green shaded area). If non-Annex I countries do not deviate from the baseline, then even if Annex I countries cut their emissions by about 40% in 2020, stabilisation of only slightly less than 550 ppm CO_2-eq is possible. Figure 2b also shows the results for 2050, for example, showing that for 550 ppm CO_2-eq a 80% emission reduction in Annex I countries corresponds with about 55% reduction from the baseline for non-Annex I countries. Note that this is viable only for the average of the IPCC SRES baseline scenarios. The outcome for individual IPCC SRES scenarios is different (see below).

3.3.1 Baseline emissions

The outcomes of the calculations heavily depend on the assumed baseline scenario (see also Section 3.1), as can be seen in Fig. 3. It shows the same picture for only one stabilisation level at a time (using the central estimate as shown in Table 5), but for various baseline scenarios (the IPCC scenarios and their updates as mentioned in Table 2 and the baseline of Sheehan), i.e. the average of the IPCC SRES baseline, as well as the minimum and maximum outcome, the common POLES-IMAGE (CPI) baseline (van Vuuren et al. 2003, 2006) and the update of IPCC B2 (van Vuuren et al. 2007). The figure shows that if Annex I countries as a group reduces with 30% below 1990 level, non-Annex I need to reduce about 10–25% below baseline for meeting 450 ppm CO_2-eq under the IPCC SRES emission scenarios. For the baseline of Sheehan (2008), which reports much higher growth in emissions in non-Annex I countries compared to the growth under the IPCC scenarios, the reduction becomes as high as 35% for non-Annex I (Table 4).

For all stabilisation levels, the choice of the baseline has significant implications for the required reductions in Annex I and non-Annex I countries. For example, 450 ppm CO_2-eq and 40% reduction of emissions in Annex I countries (top left figure, lower border of the green shaded area) would not require any deviation from the lowest baseline (minimum of the IPCC SRES), but a 20% deviation from the highest baseline for developing countries (maximum of the IPCC SRES). For the baseline of Sheehan this would even mean a deviation as high as 30%. In this scenario, the very high emission growth in non-Annex I countries, leads to much higher reductions in the Annex I and non-Annex I countries as the figure shows. Much less emission space is left for the Annex I countries when we fix the reduction below baseline in non-Annex I, or much higher deviation from the baseline in the non-Annex I countries is necessary when we fix the reduction for the Annex I countries.

3.3.2 The assumed global emission level in 2020 for a long-term concentration stabilisation target

So far, the central estimates have been assumed for the global emission limits in 2020. The uncertainty ranges of the global emission limits of 2020 have been used (see Table 5), and the effects of using the minimum and maximum have been analysed (see Fig. 4). For example, the figure shows that for 450 ppm CO_2-eq and a 40% emission reduction for Annex I countries would require a 7% to 22% deviation from the baseline, for a maximum and minimum global emission limit, compared to a 12% deviation for the default global limit.

3.3.3 Land-use CO_2 emission projections

The next important factor is the assumption of emissions from land use, land-use change and forestry (LULUCF).

The allocation studies by Höhne assume that CO_2 emissions from LULUCF need to decline at the same speed as emissions from all other sectors. However, while most baseline scenarios assume an increase in emissions in other sectors (in particular in the developing countries with the highest LULUCF emissions), all baseline scenarios assume that these emissions will decline over the course of the century. This is due

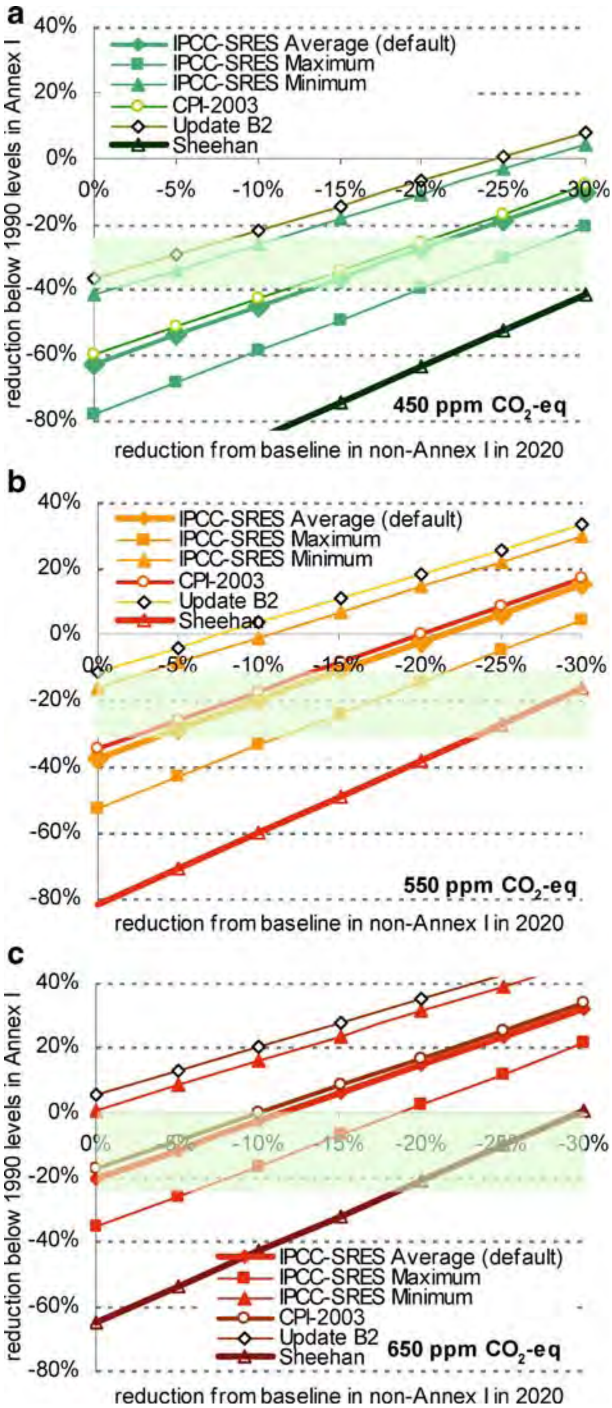

Fig. 3 The trade-off in reductions in 2020, in Annex I and non-Annex I countries as a group, for various baseline emissions (incl. baseline of Sheehan), for concentration stabilisation at 450 (**a**), 550 (**b**) and 650 (**c**) ppm CO_2-eq**.** The figure also depicts the reduction ranges for Annex I countries for the concentration stabilisation levels as reported in IPCC Box 13.7

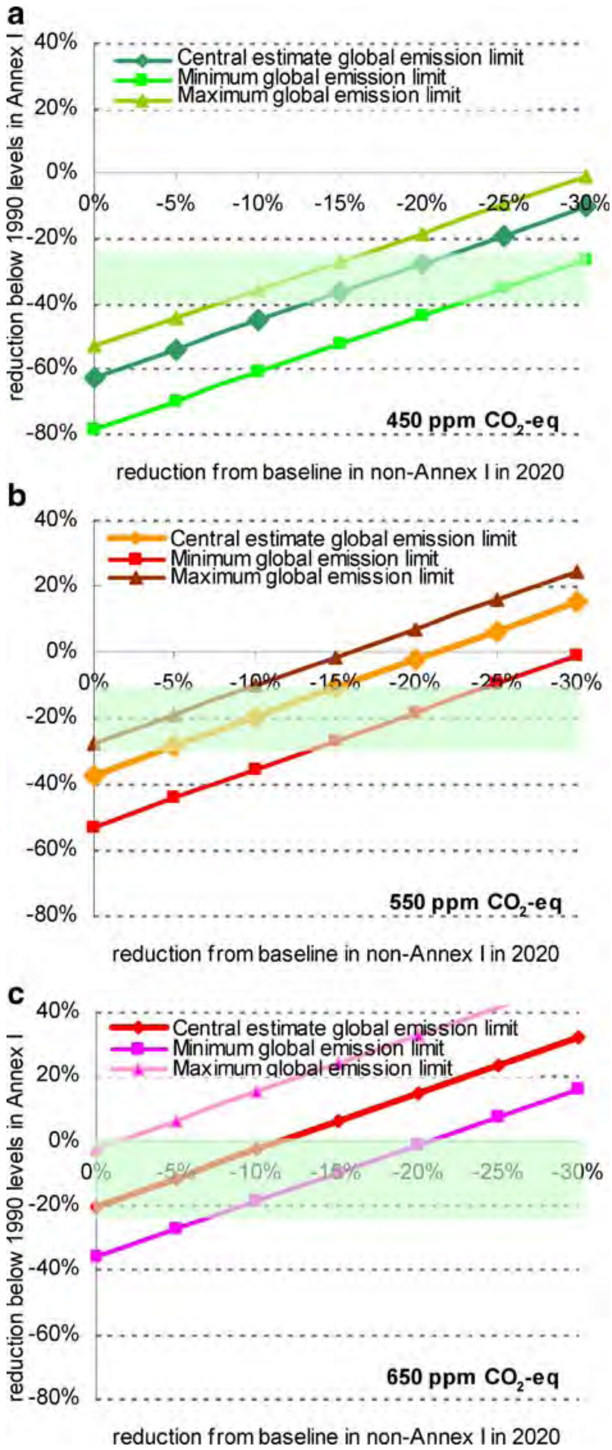

Fig. 4 The trade-off in reductions in 2020, in Annex I and non-Annex I countries as a group, for various global emission limits in 2020, for concentration stabilisation at 450 (**a**), 550 (**b**) and 650 (**c**) ppm CO_2-eq**.** The *numbers* represent the averaged outcome over separate calculations for each of the six IPCC SRES baselines. The figure also depicts the reduction ranges for Annex I countries for the concentration stabilisation levels as reported in IPCC Box 13.7

Table 6 Assumptions for global emission target (excl. LULUCF CO_2) in 2020 (%-compared to 1990 emission levels) for the different multi-gas pathways for stabilising at 450, 550 and 650 ppm CO_2-eq concentration for various assumptions on avoiding deforestation (affecting the LULUCF CO_2 emissions)

CO_2-equivalent concentration	Baseline deforestation (this study)	Avoiding deforestation 2020 (%)	Avoiding deforestation 2030 (%)
	Central estimate (%)		
2020			
450 ppm	25	35	30
550 ppm	40	50	45
650 ppm	50	55	52

to the fact that, at a certain point, all forest is depleted (stopping the emission) and reforestation occurs (increasing the terrestrial carbon uptake).

The allocation studies by den Elzen assume that CO_2 emissions from LULUCF follow the baseline, so there will be no policy intervention against deforestation, and emissions will be ongoing until at least 2020, after which they will decline. This is also assumed in the calculations presented in the figures of this paper. The other allocation studies in Table 2 are not very clear about what they have assumed for the LULUCF emissions.

Separate policy interventions are currently discussed under the UNFCCC to avoid deforestation as early as possible. One could, therefore, assume that emissions from LULUCF, due to policy interventions against deforestation, are declining much faster than all other emissions. This means, in turn, that all other emissions could decrease slightly slower. To illustrate this influence of different intervention policies against deforestation, two cases have been tested (see Table 6). The first case is assuming a strong policy to avoid deforestation on the short-term, leading to zero emission by 2020, in the second case a medium policy is assumed, which leads to zero emission by 2030. The latter roughly corresponds with reducing the baseline LULUCF CO_2 emissions by 50% in 2020. Consequently, global emission levels of *all other sectors* could be higher (higher values in Table 6 compared to the central case).

Note that, again, the reductions in the sectors are treated independently, so they are not linked with the carbon market. If the avoiding of deforestation should be induced by the carbon market through a new emission credits transfer mechanism, then reduction targets of Annex I countries (buyers) would have to be more stringent.

Figure 5 shows the results in terms of reductions in Annex I countries below 1990 (top to bottom) and in non-Annex I countries below the baseline (left to right). Avoiding deforestation by 2020 eases the efforts of developing countries in all other sectors from −22% to −12% below baseline in 2020 for the 450 ppm CO_2-eq case.

3.3.4 Influence of all factors

What does the “substantial deviation from baseline” mean for non-Annex I countries in box 13.7? The answer depends on a number of factors, which are summarised in Fig. 6. It is assumed (a priori) that the group of Annex I countries reduce emissions

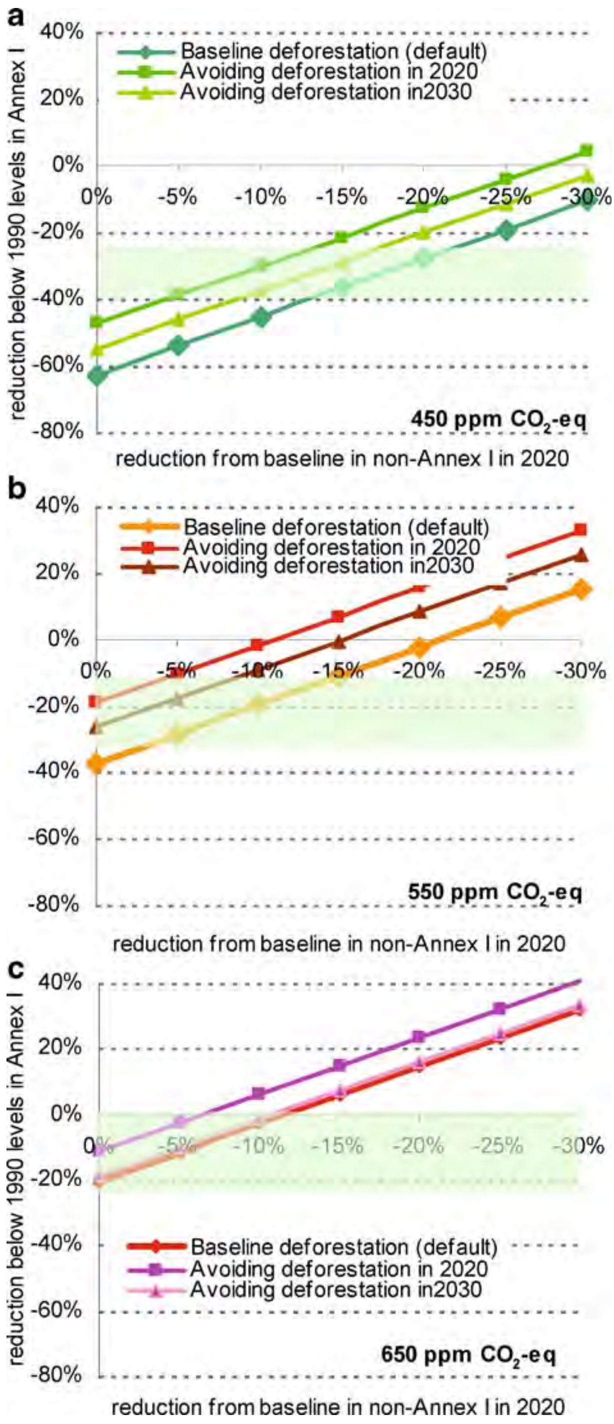

Fig. 5 The trade-off in reductions in 2020, in Annex I and non-Annex I countries as a group, for various assumptions on avoiding deforestation, for concentration stabilisation at 450 (**a**), 550 (**b**) and 650 (**c**) ppm CO_2-eq**.** The *numbers* represent the averaged outcome over separate calculations for each of the six IPCC SRES baselines. The figure also depicts the reduction ranges for Annex I countries for the concentration stabilisation levels as reported in IPCC Box 13.7

Fig. 6 The impact in the reduction from the baseline in non-Annex I countries as a group in 2020 of all factors assuming a 30% reduction in Annex I countries, below 1990 levels (default)

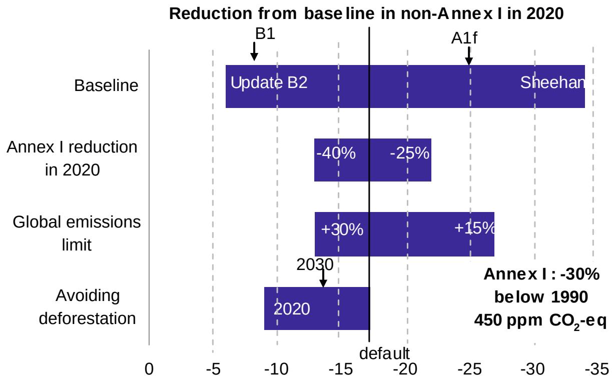

by a certain percentage and then analyse which reductions from baseline will be required in the non-Annex I countries. In this case, a 30% emission reduction below the 1990 emissions level in the Annex I countries was assumed, as this is roughly in the middle of the AWG reduction range of 25% to 40%. The substantial deviation for reaching 450 ppm CO_2-eq is very roughly around 17% below the baseline, in 2020.

The most important factor is the assumption on the baseline. Varying the baseline and keeping all other parameters constant, the reduction in the non-Annex I countries is between −5% and −35% below the baseline, in 2020. The baseline by Sheehan is the most ambitious, because it assumes the largest growth in non-Annex I emissions. Varying the assumed reductions in Annex I countries, means that the reduction in the non-Annex I countries could vary between −13% and −22%. Varying the global emission level in 2020 to still be consistent with 450 ppm CO_2 eq, the reduction in non-Annex I countries could vary between −13% to −27%. Varying assumptions on avoiding deforestation, means that the reduction in the non-Annex I countries could vary between −9% and −17%.

4 Conclusions

This paper provides background information on Box 13.7 of the IPCC Forth Assessment Report, Working Group III, which shows reduction ranges for Annex I and non-Annex I countries, for 2020 and 2050, consistent with stabilising the climate at various levels. In this paper, the authors of the box give more details on the studies used to prepare the ranges and analyse whether new information, obtained after completion of the IPCC report, influences these ranges. This analysis includes all studies that were available to us. We did not make judgements on the way the studies allocated emission reductions across regions and countries.

A first question was how the ranges were derived and whether these new allocation studies would change the results.

The conclusion is that there is no argument for updating the ranges in Box 13.7 of the IPCC report. The new studies that were published after the publication of the IPCC report show reductions that are in line with the reduction ranges in the box. The more recent allocation studies, published after the IPCC report came out, were accounted for in the calculations of the presented reduction ranges. However, the studies themselves were not referred to in the IPCC report, due to the fact that they were still in press or submitted at the time of its publication.

The ranges given in the box and in this paper are assumed to be achieved domestically by both groups of countries. If Annex I countries plan to achieve a part of their emission targets outside of their territory, through credit transfer mechanisms such as the CDM, then first the ranges presented in the box and in this paper would have to be achieved and the credit transfers would have to occur in addition.

From the studies analysed, this paper specifies "substantial deviation" and "deviation" from baseline in the Box: emissions in the group of non-Annex I countries may deviate from the baseline roughly between 15% to 30% for 450 ppm CO_2-eq, 0% to 20% for 550 ppm CO_2-eq and from 10% above to 10% below the baseline for 650 ppm CO_2-eq, in 2020, in addition to the stated reductions for Annex I countries. Quantitative estimates per regional group for non-Annex I countries are not possible, as all studies used different regional groupings.

A second question is what are the important determinants for the "substantial deviation from the baseline" in non-Annex I countries. Simple and transparent calculations were used to illustrate the impact of different assumptions.

The substantial deviation from baseline in the non-Annex I countries for reaching 450 ppm CO_2 eq for the default settings in our calculations is around 17% below the baseline, in 2020. The most important factor for this value is the assumption on the baseline. The reduction in non-Annex I countries is between −5% and −35% below the baseline, in 2020, with the baseline of Sheehan lying leading to the lower end of this range. When the assumed reductions in Annex I countries vary, then the reduction in non-Annex I countries could vary between −13% and −22%. With varying the global emission levels in 2020, the reduction in non-Annex I countries could vary between −13% to −27%. Varying assumptions on avoiding deforestation, means that the reduction in non-Annex I countries could vary between −9% and −17%.

As was also concluded by Sheehan, most of the allocation studies use baseline emission scenarios, mostly the IPCC SRES scenarios, which were developed before 2003, and do not account for the recent rapid growth in emissions. This paper shows that if higher baselines are used, such as the one of Sheehan, then reductions in Annex I and/or non-Annex I countries have to be more ambitious.

The analysis by this paper reconfirms that stabilising the climate at safe levels is a serious challenge. The current slow pace in climate policy and steadily increasing global emissions mean that it is almost unfeasible to reach relatively low global emission levels, in 2020, as was assumed to be possible by some studies of 5 years ago (e.g. +10% above 1990 level compared to +26% today). Newer studies assume higher global emission levels in the short term, but also assume more stringent emission reductions in the longer term, to reach the same stabilisation levels. Amplified efforts are needed to be able to turn around the trend in global greenhouse gas emissions.

Acknowledgements The authors thank Leo Meyer, Annemieke Righart, Jos Olivier and Joop Oude Lohuis of the Netherlands Environmental Assessment Agency, Marcel Berk of the Netherlands Ministry of Housing, Spatial Planning, and the Environment (VROM), Sara Moltmann of Ecofys Germany, Stephen Cornelius of the United Kingdom Department for Environment, Food and Rural Affairs (DEFRA) and Tom van Ierland and Martin Weiss of the European Commission DG Environment for their input and comments. Also thanks to the authors of the studies underlying

Box 13.7 of the IPCC AR4, i.e. Paul Baer, Chris Böhringer, Marian Leimbach, Malte Meinshausen, Tobias Persson and Kathleen Vaillancourt, who provided us with more detailed data.

References

Baer P, Athanasiou T, Kartha S (2008) The right to development in a climate constrained world: the greenhouse development rights framework, 2nd edn, October 2008. Heinrich Böll Foundation, Berlin, Germany. www.ecoequity.org/docs/TheGDRsFramework.pdf

Baumert KA, Bhandari R, Kete N (1999) What might a developing country climate commitment look like? World Resources Institute, Washington

Berk MM, den Elzen MGJ (2001) Options for differentiation of future commitments in climate policy: how to realise timely participation to meet stringent climate goals? Clim Pol 1(4): 465–480

Blanchard O (2002) Scenarios for differentiating commitments. In: Baumert KA, Blanchard O, Llose, Perkaus JF (eds) Options for protecting the climate. WRI, Washington, pp 203–222

Böhringer C, Löschel A (2005) Climate policy beyond Kyoto: Quo Vadis? A computable general equilibrium analysis based on expert judgments. KYKLOS 58(4):467–493

Böhringer C, Welsch H (2006) Burden sharing in a greenhouse: egalitarianism and sovereignty reconciled. Appl Econ 38:981–996

Bollen JC, Manders AJG, Veenendaal PJJ (2004) How much does a 30% emission reduction cost? Macroeconomic effects of post-Kyoto climate policy in 2020. CPB Document no 64, Netherlands Bureau for Economic Policy Analysis, The Hague

BP: (2007) Statistical review of World Energy 2007. British Petroleum. http://www.bp.com/productlanding.do?categoryId=6848&contentId=7033471

Criqui P, Kitous A, Berk MM, et al (2003) Greenhouse gas reduction pathways in the UNFCCC Process up to 2025—Technical Report. B4-3040/2001/325703/MAR/E.1 for the DG Environment, CNRS-IEPE, Grenoble, France

den Elzen MGJ (2002) Exploring climate regimes for differentiation of future commitments to stabilise greenhouse gas concentrations. Integrated Assessment 3(4):343–359

den Elzen MGJ, Lucas P (2005) The FAIR model: a tool to analyse environmental and costs implications of climate regimes. Environ Model Assess 10(2):115–134

den Elzen MGJ, Meinshausen M (2006a) Meeting the EU 2°C climate target: global and regional emission implications. Clim Pol 6(5):545–564

den Elzen MGJ, Meinshausen M (2006b) Multi-gas emission pathways for meeting the EU 2°C climate target. In: Schellnhuber HJ, Cramer W, Nakicenovic N, Wigley T, Yohe G (eds) Avoiding dangerous climate change. Cambridge University Press, Cambridge, UK, pp. 299–310

den Elzen MGJ, Fuglestvedt JS, Höhne N et al (2005a) Analysing countries' contribution to climate change: scientific uncertainties and methodological choices. Environ Sci Policy 8(6):614–636

den Elzen MGJ, Lucas P, van Vuuren DP (2005b) Abatement costs of post-Kyoto climate regimes. Energ Pol 33(16):2138–2151

den Elzen MGJ, Berk MM, Lucas P, Criqui C, Kitous A (2006) Multi-Stage: a rule-based evolution of future commitments under the Climate Change Convention. International Environmental Agreements: Politics, Law and Economics 6(1):1–28

den Elzen MGJ, Höhne N, Brouns B, Winkler H, Ott HE (2007a) Differentiation of countries' post-2012 mitigation commitments under the "South–North Dialogue" Proposal. Environ Sci Policy 10(3):185–203

den Elzen MGJ, Meinshausen M, van Vuuren DP (2007b) Multi-gas emission envelopes to meet greenhouse gas concentration targets: costs versus certainty of limiting temperature increase. Glob Environ Change 17(2):260–280

den Elzen MGJ, Höhne N, Moltmann S (2008a) The Triptych approach revisited: a staged sectoral approach for climate mitigation. Energ Pol 36(3):1107–1124 den Elzen MGJ, Lucas P, van Vuuren DP (2008b) Regional abatement action and costs under allocation schemes for emission allowances for achieving low CO2-equivalent concentrations. Climate Change, in press. http://dx.doi.org/10.1007/s10584-008-9466-1

DOE (2003) International Energy Outlook 2003. www.eia.doe.gov/. Department of Energy (DOE), Energy Information Administration, Washington, DC

Fisher BS, Nakicenovic N, Alfsen K et al (2007) Issues related to mitigation in the long term context. In: Metz B, Davidson OR, Bosch PR, Dave R, Meyer LA (eds) Climate change 2007: mitigation. Contribution of working group III to the fourth assessment report of the intergovernmental panel on climate change. Cambridge University Press, Cambridge, UK

Groenenberg H, Blok K, van der Sluijs JP (2004) Global Triptych: a bottom-up approach for the differentiation of commitments under the Climate Convention. Clim Pol 4:153–175

Gupta S, Tirpak DA, Burger N et al (2007) Policies, instruments and co-operative arrangements. In: Metz B, Davidson OR, Bosch PR, Dave R, Meyer LA (eds) Climate Change 2007: Mitigation. Contribution of Working Group III to the Fourth Assessment Report of the Intergovernmental Panel on Climate Change. Cambridge University Press, Cambridge, UK

Höhne N (2005) What is next after the Kyoto Protocol. Assessment of options for international climate policy post 2012. University of Utrecht, PhD thesis, Utrecht, the Netherlands

Höhne N, Galleguillos C, Blok K, Harnisch J, Phylipsen D (2003) Evolution of commitments under the UNFCCC: involving newly industrialized countries and developing countries. Research-report 20141255, UBA-FB 000412, ECOFYS Gmbh, Berlin, Germany

Höhne N, Phylipsen D, Ullrich S, Blok K (2005) Options for the second commitment period of the Kyoto Protocol, research report for the German Federal Environmental Agency. Climate Change 02/05, ISSN 1611-8855, ECOFYS Gmbh. Available at www.umweltbundesamt.de, Berlin, Germany

Höhne N, den Elzen MGJ, Weiss M (2006) Common but differentiated convergence (CDC), a new conceptual approach to long-term climate policy. Clim Pol 6(2):181–199

Höhne N, Phylipsen D, Moltmann S (2007) Factors underpinning future action. Reporrt PECSDE061439, commissioned by Department for Environment Food and Rural Affairs (DEFRA), ECOFYS Gmbh. Available at: http://www.post-kyoto.com/data/fufa2.pdf, Cologne, Germany

IEA (2004) World Energy Outlook 2004. International Energy Agency, Paris

IEA (2007) World Energy Outlook 2007. International Energy Agency, Paris

IEA (2008) CO2 emissions form fuel combustion—1971–2005, 2007 edn. International Energy Agency (IEA), Paris

IIASA (1998) IIASA/WEC Global Energy Perspectives, Available at: http://www.iiasa.ac.at/cgi-bin/ecs/book_dyn/bookcnt.pyAustria. Laxenburg

IMAGE-team (2001) The IMAGE 2.2 implementation of the SRES scenarios. A comprehensive analysis of emissions, climate change and impacts in the 21st century. CD-ROM publication 481508018, Netherlands Environmental Assessment Agency (MNP), Bilthoven, the Netherlands

IPCC (2001) Climate Change 2001.The science of climate change. IPCC Assessment Reports. Cambridge University Press, Cambridge, UK, pp. 1–18

Jacoby HD, Schmalensee R, Wing IS (1999) Toward a useful architecture for climate change negotiations. Report No 49, MIT, Cambridge, MA

Leimbach M (2003) Equity and carbon emissions trading: a model analysis. Energ Pol 31(10):1033–1044

Meinshausen M, Hare WL, Wigley TML et al (2006) Multi-gas emission pathways to meet climate targets. Climate Change 75(1–2):151–194

Meyer A (2000) Contraction & Convergence. The global solution to climate change. Schumacher Briefings, 5. Green Books, Bristol, UK

Michaelowa A, Butzengeiger S, Jung M (2005) Graduation and deepening: an ambitious post-2012 climate policy scenario. International Environmental Agreements: Politics, Law and Economics 5:25–46

Nakicenovic N, Riahi K (2003) Model runs with MESSAGE in the Context of the Further Development of the Kyoto-Protocol, WBGU—German Advisory Council on Global Change. WBGU website, http://www.wbgu.de/. Berlin, Germany

Nakicenovic N, Alcamo J, Davis G et al (2000) Special report on emissions scenarios. IPCC Special Reports. Cambridge University Press, Cambridge, UK

Ott HE, Winkler H, Brouns B et al (2004) South–North dialogue on equity in the greenhouse. A proposal for an adequate and equitable global climate agreements. Eschborn, Gesellschaft für Technische Zusammenarbeit, www.erc.uct.ac.za/recentpub.htm or www.south-north-dialogue.net

Persson TA, Azar C, Lindgren K (2006) Allocation of CO2 emission permits—economic incentives for emission reductions in developing countries. Energ Pol 34:1889–1899
Phylipsen GJM, Bode JW, Blok K, Merkus H, Metz B (1998) A Triptych sectoral approach to burden differentiation; GHG emissions in the European bubble. Energ Pol 26(12):929–943
Sheehan P (2008) Responsibility for past and future global warming: uncertainties in attributing anthropogenic climate change. Climatic Change. doi:10.1007/s10584-008-9415-z
Timilsina GR (2008) Atmospheric stabilization of CO2 emissions: near-term reductions and absolute versus intensity-based targets. Energ Pol 36:1927–1936
UNFCCC (1997) Paper no. 1: Brazil; Proposed Elements of a Protocol to the United Nations Framework Convention on Climate Change. UNFCCC/AGBM/1997/MISC.1/Add.3 GE.97, Bonn
Vaillancourt K, Waaub JP (2006) A decision aid tool for equity issues analysis in emission permit allocations. Clim Pol 5(5):487–501
van Vuuren DP, Riahi K (2008) Do recent emission trends imply higher emissions for ever? Climatic Change. doi:10.1007/s10584-008-9485-y
van Vuuren DP, den Elzen MGJ, Berk MM et al (2003) Regional costs and benefits of alternative post-Kyoto climate regimes. RIVM-report 728001025. www.mnp.nl/en, Netherlands Environmental Assessment Agency (MNP), Bilthoven, the Netherlands
van Vuuren DP, Eickhout B, Lucas PL, den Elzen MGJ (2006) Long-term multi-gas scenarios to stabilise radiative forcing. Energy Journal, Multi-Greenhouse Gas Mitigation and Climate Policy (Special Issue #3):201–234
van Vuuren DP, den Elzen MGJ, Eickhout B et al (2007) Stabilizing greenhouse gas concentrations at low levels: an assessment of reduction strategies and costs. Climatic Change 81(2):119–159
WBGU (2003) Climate protection strategies for the 21st century. Kyoto and beyond. German Advisory Council on Global Change, Berlin
Winkler H, Spalding-Fecher R, Tyani L (2002) Comparing developing countries under potential carbon allocation schemes. Clim Pol 9:1–16

Environ. Res. Lett. **4** (2009) 024001 (7pp) doi:10.1088/1748-9326/4/2/024001

Proper accounting for time increases crop-based biofuels' greenhouse gas deficit versus petroleum

M O'Hare[1], R J Plevin[2], J I Martin[3], A D Jones[2], A Kendall[4] and E Hopson[3]

[1] Goldman School of Public Policy, University of California, Berkeley, CA 94720, USA
[2] Energy and Resources Group, University of California, Berkeley, CA 94720, USA
[3] Union of Concerned Scientists, 2 Brattle Square, Cambridge, MA 02238-9105, USA
[4] Department of Civil and Environmental Engineering, University of California, Davis, CA 95616, USA

E-mail: ohare@berkeley.edu

Received 11 February 2009
Accepted for publication 30 March 2009
Published 7 April 2009
Online at stacks.iop.org/ERL/4/024001

Abstract
The global warming intensities of crop-based biofuels and fossil fuels differ not only in amount but also in their discharge patterns over time. Early discharges, for example, from market-mediated land use change, will have created more global warming by any time in the future than later discharges, owing to the slow decay of atmospheric CO_2. A spreadsheet model of this process, BTIME, captures this important time pattern effect using the Bern CO_2 decay model to allow fuels to be compared for policy decisions on the basis of their real warming effects with a variety of user-supplied parameter values. The model also allows economic discounting of climate effects extended far into the future. Compared to approaches that simply sum greenhouse gas emissions over time, recognizing the physics of atmospheric CO_2 decay significantly increases the deficit relative to fossil fuel of any biofuel causing land use change.

Keywords: biofuels, greenhouse gas emissions, life cycle assessment, land use change

1. Introduction

Performance-based regulations under development in several jurisdictions promote transportation fuels with lower life cycle greenhouse gas (GHG) emissions than petroleum-based fuels. For this comparison, they use a performance metric that aggregates each fuel's direct and indirect GHG emissions into a global warming intensity (GWI). Recent studies of the effects of expanding biofuel feedstock production find large GHG emissions from land use change (LUC) for biofuels that compete for land with other uses such as the production of food. Changes in land use are transmitted across global markets linked by commodity substitutability and competition for land. These market-mediated LUC emissions are not only separated from the biofuel production process by several economic links and physical distance, but also follow a time profile very different from the direct emissions from fossil and biofuel use, being released quickly upon expansion of biofuel production [19].

To obtain a GWI, previous analysts average the total indirect emissions over the total fuel produced during a predicted production period and add these to the direct emissions, implicitly treating a unit GHG emission released today as though it has the same consequences as one released decades in the future. This 'straight-line amortization', for example, is proposed for the California Air Resources Board's implementation of that state's Low Carbon Fuel Standard [3]. Economic discounting can in principle be used to compare costs and benefits over time, but annual GHG flows are, in general, a poor proxy for economic costs: most GW costs are imposed by GHG *stocks* in the atmosphere. Furthermore, consideration of long time frames requires realistic predictions

EXHIBIT 24

about technological innovation and land use changes over that timeframe, including post-cultivation changes in land use.

We define a framework to aggregate GHG emissions and other radiative forcing effects that occur over a significant span of time into a GWI metric that better represents the climate effects of fuel substitution, applicable to any estimate of discharges that are not uniform over time. Our framework accommodates changes in the duration of the production period and post-production LUC, and converts physical effects to economic damages that can properly be discounted. These corrections to previous practice increase the relative importance of early emissions, and in turn the GWI of biofuels that cause LUC.

1.1. Treatment of time in life cycle assessment

In life cycle assessment (LCA), emissions of pollutants are typically summed without regard for when or where these emissions occur [10]. For well-mixed greenhouse gases, it is appropriate to ignore the location of the emissions, as these are global pollutants. However, for long-lived pollutants, summing emissions over time masks potentially important differences among processes, especially if effects are measured at a fixed target date. In these situations, early emissions are in the environment longer relative to the target date, and thus cause greater environmental damage.

In the case of greenhouse gases (GHGs), global warming effects are usually aggregated by summing emissions of three gases (CO_2, CH_4, and N_2O) weighted by their respective global warming potentials (GWP). GWP is the measure of the cumulative radiative forcing (CRF) over a fixed time horizon (e.g., 20 or 100 years) of a pulse of some gas compared to the CRF of an equal mass of CO_2 over the same period [7]. Most LCAs use the 100 year GWPs published by the IPCC [7].

In an LCA, it is appropriate to sum GWP-weighted GHG emissions for a process whose emissions are largely coincident with production and use. Summing GWP-weighted GHG emissions also makes sense in a national emissions inventory for a single year, because over the standard 100 year time horizon the specific release date *within* the inventory year is inconsequential to the total CRF. In both of these cases, emissions are implicitly summed or compared using a consistent integration period.

Since LCAs are defined in terms of a functional unit (e.g., emissions per MJ of fuel) [14], emissions from preparatory processes, such facility construction, must be allocated over the assumed lifetime of the facility to place these emissions in terms of the functional unit [1]. In practice, these amortized emissions are generally assumed negligible and ignored in LCA, resulting in a well-recognized 'truncation error' [9].

However, when considering indirect LUC caused by land-competitive biofuels, the assumptions that (i) emissions are largely coincident with production and use, or (ii) that preparatory emissions are negligible, no longer hold. The up-front iLUC emissions from land-competitive biofuels must be allocated over (that is, causally linked to) a quantity of fuel produced over decades, and the biofuel must be compared with a petroleum fuel with relatively small up-front emissions. When we compare processes with very different emission profiles over decades, the simple summation approach is no longer valid because it incorrectly sums the CRF of releases measured over overlapping, but distinct, integration periods. This is not the same as summing the CRF of these releases over a consistent, short time horizon during which all emissions occur. Discounting emission flows, as some have proposed, only compounds the error, since GWPs apply no discounting within their defined time horizon, and 100% discounting beyond the time horizon.

We recognize that GWPs represent an imperfect compromise in their treatment of time, but this compromise has been broadly accepted. Comparing the CRF as implemented in our model of two processes with different emission profiles, over a single time horizon, is consistent with the use of GWPs in national inventories, and therefore it is an appropriate approach for use with policies intended to mitigate climate change.

1.2. Time horizons

Estimating LUC GW effects for biofuels requires careful distinction of three characteristic time periods often confused in political discourse. The first of these is the *analytic horizon*, the period over which consequences are 'counted' in analysis. This may be one hundred years or more. The second is the *production period*, the time during which the analysis assumes a biofuel will be produced and displace fossil fuel. The appropriate production period is no longer than the time until the biofuel will be economically displaced by other fuels or cease production for other reasons. This value is very important for GWI estimation because it affects how long biofuel production has to 'pay back' its initial LUC emissions [8, 6], and because it determines when post-production LUC must be considered.

The third important period runs from the present to a *policy target date*. For example, the California low carbon fuel standard (LCFS) requires a 10% reduction in transportation fuels' average GWI by 2020, and the US Energy Independence and Security Act of 2007 (EISA) requires 21 billion gallons (80 GL) of 'advanced renewable fuels', that achieve a 50% GWI reduction compared to their petroleum counterparts, to be used by 2022 [4, 2]. However, neither policy specifies the date at which measurement of the GWI should be taken. The standard approach used in life cycle assessment, summing GHG emissions weighted by their global warming potential (GWP) regardless of when they occur in time [10], is incoherent (as noted earlier) and it underestimates the climate effects of LUC. A flawed protocol for calculating fuel GWI could inadvertently drive a wedge between the policy and its larger purposes, causing increased global warming rather than less. Our analysis focuses on assuring that GWI calculations implementing a biofuels policy will advance the goal of mitigating climate change.

2. Conceptual framework

To determine whether substituting a particular biofuel for petroleum increases or decreases global warming requires decisions about the analytic and production timeframes, and whether only physical quantities, or their costs and benefits in social and economic terms, are to be assessed. Our analysis proceeds first from discharges to warming consequences, and then (prospectively) to improved benefit/cost assessment.

2.1. Physical approach

Fuel production and use increases climatic warming not only via the release of GHGs but also by direct perturbation of the earth's energy balance through land use changes that alter biophysical land surface properties such as albedo and evapotranspiration. These effects can be aggregated into a time-dependent annual radiative forcing term attributable to fuel i's use, $\mathrm{RF}_i(t)$.

$$\mathrm{RF}_i(t) = \sum_j a_j G_{ij}(t) + B_i(t) \tag{1}$$

$G_{ij}(t)$ is the additional atmospheric abundance of GHG j at time t attributable to the use of fuel i, a_j is the radiative efficiency of GHG j. Given the projected time profile of discharges for fuel i and GHG j, the time-dependent abundance, $G_{ji}(t)$, is obtained using models such as the Bern carbon cycle model [15, 7]. $B_i(t)$ represents all non-GHG radiative forcing effects of fuel i at time t.

Integrating the radiative forcing term over the analytic timeframe, $0 < t < t_\mathrm{a}$, gives the cumulative radiative forcing:

$$\mathrm{CRF}_i = \mathrm{CRF}_i(t_\mathrm{a}) = \int_0^{t_\mathrm{a}} \mathrm{RF}_i(t)\,\mathrm{d}t \tag{2}$$

a physically plausible proxy for the total damage to the planet from the CO_2 emissions stream up to a particular analytic horizon t_a. The ratio of the CRF for the biofuel b to that of the reference fuel g, provides a physical *fuel warming potential*, or $\mathrm{FWP_p}$,

$$\mathrm{FWP_p} \equiv \frac{\mathrm{CRF}_b}{\mathrm{CRF}_g}. \tag{3}$$

This $\mathrm{FWP_p}$ (generally a function of t_a) is a more meaningful physical quantity on which to evaluate biofuel lifecycle emissions than the aggregated emissions over time. Moreover, $\mathrm{FWP_p}$ follows the approach of the Global Warming Potential metric, or GWP, used to convert emissions from non-CO_2 GHGs into their CO_2 equivalencies, an approach well established in policy and science [7].

2.2. Benefit–cost analysis

Uniformly allocating the initial emission from LUC across the production period treats a unit of GHG discharge now as though it is equally costly as a unit emitted twenty years from now. Specifically, it means that two fuels differing only in that one has, say, 10% of its total discharge at the end of an analytic horizon of 50 years while the other discharges 10% right away, with the remaining 90% in each case distributed uniformly over the period, would be scored as equals and treated as equally costly or beneficial on a GW basis. Policy analysis conventionally recognizes discounting as the tool with which to make distinctions like this. A discounted model counts the *net present value* (NPV) of benefits of B (also costs) t years in the future as

$$\mathrm{NPV}(B) = \left[\frac{1}{1+r}\right]^t B \tag{4}$$

where r is an annual discount rate. For example, if one knows a capital asset will wear out in about twenty years, one does not count that as the present cost of its replacement, but a smaller number, namely the amount that would have to be deposited in some sort of interest-bearing investment to attain the price of the asset twenty years from now. Discounting may also measure a pure delay effect, wherein something of value is simply worth less to us if received at a time in the future than it would be if received now. The effect on global warming decisions of economic discounting can be very large because the time spans analyzed are usually long: the present value of \$1 received twenty years in the future is only about 50c at $r = 3\%$. A current debate about the appropriate discount rate for global warming policy analysis focuses on the extremely low discount rate used in the *Stern Review* and the rapid commitment of expensive resources it implies [20, 18, 17, 22]. The controversy does *not* concern *whether* economic costs and benefits occurring over time should be discounted when calculating costs and benefits for action (though the discount rate apparently used in Stern is so low as to be nearly zero).

However, the intellectual and behavioral basis of this kind of discounting and the debate around it applies only to economic goods, in a world in which market mechanisms (like banks and contracts) exist by which goods in the future and the present can actually be traded against each other: the discounting model applies to costs and benefits, not to physical phenomena that generate them, *unless* their economic value is otherwise stable over time. Consider a simple example: let the *economic value* of a gallon of water on January 1 be W, and assume that a gallon of water will also sell for W on July 1. The net present value on January 1, by conventional discounting, of 10 gallons of water *for delivery on July 1* is then

$$\left[\frac{1}{1+0.06}\right]^{0.5} W \tag{5}$$

at 6%, or about 0.97 W.

It is tempting also to say, in January, that a *gallon* of water on July 15 is worth[5] 0.97 *gallons* of water now, but if the use of the water is known and it is not available for purchase whenever desired, this easy approximation can be entirely misleading. For example, if the water is intended for a garden that would not be planted until May, it is much *more* valuable in July than in January. And if it is to be applied to a house that is on fire on January 1, delaying delivery to July makes it pretty much worthless. In both cases, conventionally discounting a physical quantity produces absurd results for reasons more fundamental than an incorrect choice of r. If the money values of water at each time under each assumption (garden later or fire now) are

[5] The phrase *A is worth xB* in the present context does not denote a theoretical philosophical judgment, but the precise normative behavioral claim that society should be willing to actually give up A for x units of B indifferently. Policy choice is an act of exchange.

calculated, these may be appropriately discounted in the usual way, but discounting the physical quantity will not indicate these differential values for many cases, including the present one of iLUC GW estimation.

The purely physical assessment of radiative forcing can be amended to incorporate social preferences typically included in policy analyses, the simplest being the preference to have benefits sooner rather than later as reflected by computing a net present value (NPV) using a discount rate r. However, discounting is correctly applied only to economic rather than physical quantities, so before such economic analysis can be meaningfully pursued the relationship between physical and economic quantities must be established. This relationship can be described in a *damage function*, $D(\mathrm{RF}_f(t), t)$. A complete and realistic damage function is beyond the scope of this paper. However, among the relevant physical quantities discussed above, the radiative forcing $\mathrm{RF}(t)$ is the most appropriate starting point, since this is the most straightforward measurement of the extra heat absorbed by the planet as a result of biofuel use, and it is this heat that drives many of the damages caused by climate change [7, p 210]. A highly simplified approximate damage function, $D(t)$, treats economic damage as directly proportional to $\mathrm{RF}(t)$ with a proportionality constant that is invariant in time such that:

$$D(t) \cong d\mathrm{RF}(t) \tag{6}$$

where d is the damage proportionality constant[6]. Using this damage function, an especially appropriate approximation for the small increments and decrements in GHG emission associated with fuel policies, and an appropriate discount rate allow computation of a net present value (NPV):

$$\mathrm{NPV} = \int_0^{t_a} \frac{d\mathrm{RF}(t)}{(1+r)^t}\,\mathrm{d}t. \tag{7}$$

We emphasize that discounting a stream of *emissions* with long residence times is not a satisfactory approximation. Comparing the NPV of the biofuel case b and reference gasoline case g over the analytic time horizon allows for the computation of an *economic* $\mathrm{FWP_e}$

$$\mathrm{FWP_e} \equiv \frac{\mathrm{NPV_b}}{\mathrm{NPV_g}}. \tag{8}$$

For the simple cost function discussed above, the damage proportionality constant d cancels out of the $\mathrm{FWP_e}$ calculation. For the limiting case $r = 0$, $\mathrm{FWP_e} = \mathrm{FWP_p}$.

For use in regulations based on ratings measured in g CO_2e $\mathrm{MJ^{-1}}$, either FWP can be scaled by the GWI of the baseline petroleum fuel to produce a commensurate biofuel *fuel warming intensity* (FWI):

$$\mathrm{FWI}_x = \mathrm{FWP}_x \times \mathrm{GWI_{baseline}} \tag{9}$$

where x is either p or e to specify a physical or economic fuel warming intensity.

[6] The authors do not suggest that the true damage is adequately captured by such a simple expression, especially the implication that the damage constant is constant over time. Reductions in radiative forcing that occur after irreversible calamities—such as the failure of the Gulf Stream, or the Greenland ice cap melting or sliding into the sea—may be described with time-dependent damage functions more complex than ours.

3. Methods

To demonstrate the importance of the differences between biofuel and petroleum-based GHG discharge profiles, we have developed the *Biofuels Time Integrated Model of Emissions* (BTIME)[7]. BTIME can be easily parameterized by users with values corresponding to different LUC model results. We present it here with parameters distilled from iLUC modeling results based on the GTAP model [12, 11] and ecosystem carbon data from Woods Hole Research Center [19, supporting online materials] to generate a CO_2 emissions scenario for maize ethanol and gasoline[8].

Emissions over time are estimated for the following streams:

(1) Immediate loss of above-ground biomass carbon.
(2) Loss of 25% of below-ground carbon in the top 1 m of soil. Of this 25%, 80% (20% of the total) is lost in the first 5 years, and 20% (5% of the total) is lost over the subsequent 20 years [5]. The model can be adjusted to reflect other emission profiles for below-ground carbon.
(3) Foregone sequestration. Following Searchinger *et al* [19], we assume that the conversion of forest to cropping results not only in loss of sequestered carbon, but in the loss of future sequestration that *would have* occurred had the forest been left standing. These are treated as 'emissions' occurring over a variable number of years, depending on model parameters.

BTIME tracks the accumulation of CO_2 in the atmosphere for maize ethanol capacity brought on-line in 2010, and the gasoline it displaces. To track how much of the released CO_2 remains in the atmosphere we use the revised version of the Bern Carbon cycle model, assuming a background CO_2 concentration of 378 ppm [13, 15]. Specifically, the decay of a pulse of CO_2 at time t is given by

$$a_0 + \sum_{k=1}^{3} a_k \mathrm{e}^{\left(\frac{-t}{\tau_k}\right)} \tag{10}$$

where $a_0 = 0.217$, $a_1 = 0.259$, $a_3 = 0.338$, $\tau_1 = 172.9$ years, $\tau_2 = 18.51$ years, and $\tau_3 = 1.186$ years[9].

3.1. Model limitations

In the model, we make several simplifications that could be corrected in a more elaborate version:

(1) The decay rate for atmospheric CO_2 assumes a constant background concentration in the atmosphere.

[7] The BTIME model is described further in the supporting materials, and can be downloaded from http://rael.berkeley.edu/BTIME.

[8] BTIME does not purport to be a complete model of the climate effects of increased biofuels production. The model does not include the full range of indirect effects (e.g., changes in methane emissions from rice and livestock production or changes in fossil fuel use), nor does it include changes in biogeophysical phenomena (e.g., albedo, surface roughness, and latent heat flux) or non-GHG emissions (e.g., black carbon, aerosols, and ozone precursors). More research is required in all of these areas. The general framework presented can accommodate these factors within the globally averaged radiative forcing term once estimates exist.

[9] BTIME tracks the decay of each term in the sum separately.

(2) We assume that the radiative efficiency of the GHG is constant.
(3) We treat iLUC and ongoing emissions as if they were entirely CO_2.
(4) We neglect non-GHG radiative forcing effects.

The radiative forcing of a pulse of a particular GHG depends both on its radiative efficiency and the quantity of gas remaining in the atmosphere. Radiative efficiency for a marginal unit of CO_2 decreases non-linearly as the background concentration of CO_2 in the atmosphere increases, while for methane and N_2O the relationship is approximately linear [7]. At the same time as radiative efficiency decreases, CO_2's residence time in the atmosphere will *increase* owing to a slowing of CO_2 removal from the atmosphere. Decreasing marginal radiative efficiency for CO_2 and a slowing decay rate for atmospheric CO_2 partially balance out [16]. Indeed, the IPCC's GWPs ignore the effect of changing background concentration as well. Both corrections are absent in our model. A more complete analysis should include both of these corrections, and should also account for GHGs other than CO_2.

The relevant non-CO_2 GHGs in the biofuels life cycle are N_2O and CH_4. N_2O releases are affected by yield intensification of crops, especially crops fertilized with nitrogen compounds, and CH_4 is especially affected by livestock production changes. Both of these changes occur as a result of market signals associated with increased or decreased production of any biofuels that compete with food for land. The current model simply converts all GHG emissions to CO_2e using GWPs from the IPCC's Fourth Assessment Report [7]. This treatment does not reflect the actual behavior of the gases in the atmosphere especially with respect to CH_4, where it underestimates effects over shorter time horizons. CH_4 has a much shorter lifetime in the atmosphere than CO_2, which partly explains the falling standard GWP value for CH_4 as the time horizon of analysis grows (75 for a 20 year time horizon versus 25 for a 100 year time horizon) [7, table 2.14]. However, according to the GREET 1.8b model, CH_4 emissions make up less than 5% of total CO_2e emissions in the maize ethanol life cycle and even less in the gasoline life cycle, so we do not expect omitting its proper treatment in the current model to significantly influence the outcome [21]. N_2O emissions, however, constitute about 25% of CO_2e emissions for maize ethanol and only 1% for gasoline [21], so its current treatment in BTIME requires explanation. The mean lifetime of N_2O in the atmosphere is approximately 114 years, not too different from the average life time of CO_2, and its GWP only changes by 3% between a 20 and 100 year time horizon [7, p 212]. Thus, while our treatment of N_2O in a CO_2e form is imperfect, the outcome would not change significantly from its correct treatment since its relative behavior compared to CO_2 does not vary significantly over the time horizons used in our model.

4. Results

We emphasize that this paper is concerned with the methodology embodied in BTIME, and not any particular estimate of LUC emissions for any particular biofuel. To

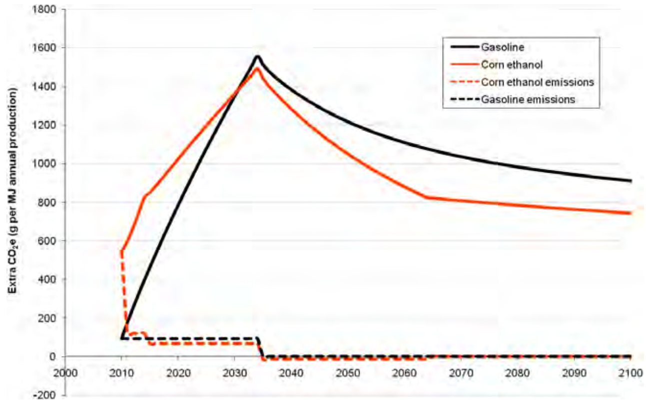

Figure 1. CO_2 emissions and resulting atmospheric abundance for gasoline (25 years at 94 g CO_2e MJ^{-1}) and maize ethanol (25 years at 60 g CO_2e MJ^{-1} plus iLUC discharge of 776 g CO_2 MJ^{-1} and foregone sequestration totaling 102 g CO_2 MJ^{-1}; post-cultivation recovery of 50% of the lost biomass carbon over 30 years).

illustrate the importance of this methodology, we report the effect of applying it to LUC estimates from our GTAP work [12] (which are much lower than Searchinger's). Assuming that maize ethanol is produced for 25 years starting in 2010 with direct life cycle emissions of 60 g CO_2 MJ^{-1} versus 94 for gasoline, and that the converted ecosystems revert over 30 years to hold 50% of the carbon held before cultivation, we project the annual emissions streams for maize ethanol and gasoline shown in figure 1 with dashed lines. Using the Bern carbon cycle model [7] we compute the increased abundance of CO_2 in the atmosphere over time, (solid lines).

The maize ethanol emissions stream depicted by the dashed orange line begins with a large release as land is cleared (directly or indirectly) for biofuels feedstock cultivation, followed by five years in which soil carbon is released rapidly and twenty years of slower release [5]. After the ethanol production ceases in 2035 we assume a small annual carbon sequestration through 2065 as land reverts in part to its original condition (other ways to handle post-cultivation LUC are discussed further in SOM). The emissions profile of gasoline displaced MJ-for-MJ has no initial release and fixed production/use emissions over the time in which biofuel is being produced. The solid lines show the abundance of extra CO_2 in the atmosphere for the two cases, which is the sum of new releases subject to gradual reduction through the functioning of the carbon cycle. The implicit policy choice is between obtaining the same amount of fuel energy by following the black or orange paths.

For the first 15 years of production the maize ethanol case leads to higher CO_2 abundance, and after that gasoline's is higher. This crossover should not be interpreted as a 'break-even' point, because at this crossover, the planet has been warmer for the preceding 15 years in the maize ethanol case, leading to damage that remains at the crossover point manifested in higher sea levels, more ecosystem damage, and retained heat in reservoirs like the ocean.

A physical 'break-even' occurs with equal *cumulative warming*, as is captured in the FWP and FWI metrics described below. We assume that after 25 years, the maize ethanol

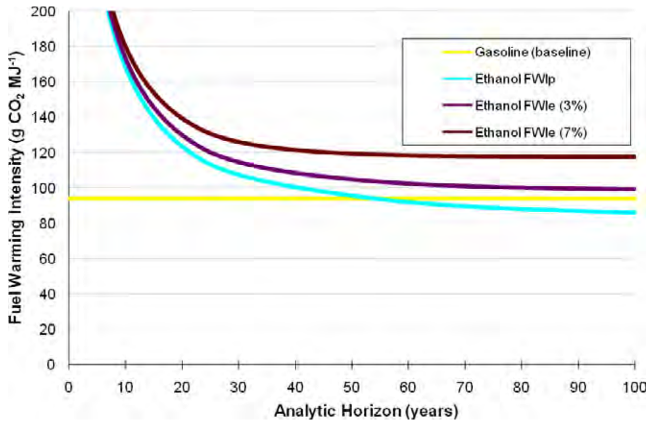

Figure 2. Fuel warming intensity (g CO_2 MJ^{-1}) versus analytic horizon.

production and the displaced gasoline emissions cease. The post-cultivation period has some recovery sequestration for ethanol and significant reductions in CO_2 abundance for both species as the carbon cycle absorbs some of the atmospheric carbon.

Figure 2 illustrates the difference between the physical and economic metrics, and the effect of discount rate on the result. In this figure, the y axis indicates the relative performance of maize ethanol to gasoline and the x-axis reflects different analytical horizons.

The FWI_p for maize ethanol (light blue line) shows that using this biofuel results in greater warming than does using gasoline over analytic horizons of less than 50 years. For a 30 year analytic horizon the ethanol's FWI_p is 15% higher than gasoline's. To compare this result to earlier work, note that the parameters used in our model would show biofuel emissions 5% *lower* than gasoline's if the annual emissions were simply averaged, even over 30 production years [19]. Over a 100 year analytic horizon, biofuel production shows an 8% benefit versus gasoline, and this result is highly dependent upon the assumption that the land reverts toward a natural state following biofuel production. The extent of ecosystem recovery after biofuel production ceases decades from now is unknowable, therefore crediting a biofuel with this regrowth may be inappropriate. Excluding this credit results in the FWI_p of the modeled ethanol being 4% greater than that of gasoline after 100 years.

Non-zero discount rates further degrade the benefits of projected future fuel production and reduce sensitivity to assumptions regarding post-production regrowth. With a 3% discount rate and 100 year analytic horizon, the FWI_e of ethanol is 3% greater than that of gasoline; with a 7% discount rate ethanol's FWI_e is 16% greater. Excluding land reversion increases these spreads to 11% and 20%, respectively.

5. Conclusion

5.1. Summary

We developed a model of the cumulative radiative forcing caused by the production and use of biofuels and gasoline, including emissions from biofuels-induced land use change (LUC). Our model aggregates GHG emissions that occur over a significant span of time into a global warming intensity metric that better represents the climate effects of fuel substitution.

Properly treating emissions and decay over time increases the importance of near-term emissions since the cumulative warming and associated damages from those emissions, for any finite analytic horizon, are more severe. Compared to approaches that simply sum GHG emissions over time, we show that recognizing the physics of atmospheric CO_2 decay and radiative forcing significantly increases the estimated climate effects relative to fossil fuel for any biofuel causing LUC. We also show that economic discounting is only applicable to costs and benefits, not to physical phenomena that generate them, *unless* their economic value is stable over time. Cumulative radiative forcing is a better proxy for economic damages than the sum of GHG flows, and as such is a more appropriate quantity to which to apply discounting.

We propose a new measure of the climate performance of biofuels, *fuel warming potential* (FWP), defined as the ratio of the cumulative radiative forcing caused by the life cycle GHG emissions from a biofuel relative to that of its fossil substitute. Where discounting is desired, we propose an 'economic' version of the FWP, defined as the ratio of the net present values of the cumulative radiative forcing from the two fuels. Any positive discount rate magnifies the importance of early emissions.

We also define a metric called fuel warming intensity (FWI), which simply multiplies either version of FWP by the global warming intensity of direct emissions (in units of g CO_2e MJ^{-1}) of the fossil fuel (e.g., gasoline) to produce a quantity with suitable units for use in fuel regulations.

Finally, we note that large initial GHG discharges are not unique to crop-based biofuels. Analysis of any GHG-reducing technology with large up-front capital investments (nuclear, tidal, wind, photovoltaics) should similarly account for up-front GHG discharges (for example, from cement manufacture) as we do here.

5.2. Policy considerations

To achieve real climate benefits, 'low carbon' biofuel policy must recognize the importance of early emissions, and climate policies should use performance metrics that reflect cumulative warming rather than GHG flows.

Operationalizing the approach recommended herein forces the regulator to choose values for several influential model parameters, particularly the analytic horizon. An analytic horizon extending into decades requires predictions about the expected cultivation period and post-cultivation LUC, decisions on how post-cultivation LUC emissions should be credited, and assessment of the time-value of benefits and costs. Benefit–cost analysis brings with it the need to settle on a reasonable damage function and an appropriate discount rate as well. Policymakers may find it appropriate to focus on more certain, near-term climate impacts, in which case a short horizon physical FWI is sufficient. For short analytic horizons, discounting has little effect and post-cultivation LUC occurs beyond the system boundary.

Acknowledgments

This research was supported by a contract with the California Air Resources Board, a National Science Foundation Graduate Research Fellowship (RJP), and an Environmental Protection Agency STAR fellowship (ADJ). This paper does not necessarily represent the views of the ARB, NSF, EPA or the Union of Concerned Scientists. The authors especially appreciate comments from Mark Delucchi on earlier drafts.

References

[1] Canals L M I, Muller-Wenk R, Bauer C, Depestele J, Dubreuil A, Knuchel R F, Gaillard G, Michelsen O and Rydgren B 2007 Key elements in a framework for land use impact assessment within LCA *Int. J. Life Cycle Assess.* **12** 2–4
[2] CARB 2008 *The California Low Carbon Fuel Standard Regulation-Draft* ed California Air Resources Board
[3] CARB 2009 Proposed regulation to implement the low carbon fuel standard *Staff Report: Initial Statement of Reasons* vol II (Sacramento, CA: California Air Resources Board) p 332
[4] Congress U S 2007 *Energy Independence and Security Act*
[5] Davidson E and Ackerman I 1993 Changes in soil carbon inventories following cultivation of previously untilled soils *Biogeochemistry* **20** 161–93
[6] Fargione J, Hill J, Tilman D, Polasky S and Hawthorne P 2008 Land clearing and the biofuel carbon debt *Science* **319** 1235–8
[7] Forster P *et al* 2007 *Climate Change 2007-The Physical Science Basis. Contribution of Working Group I to the Fourth Assessment Report of the Intergovernmental Panel on Climate Change* ed S Solomon *et al* (New York: Cambridge University Press)
[8] Gibbs H K, Johnston M, Foley J A, Holloway T, Monfreda C, Ramankutty N and Zaks D 2008 Carbon payback times for crop-based biofuel expansion in the tropics: the effects of changing yield and technology *Environ. Res. Lett.* **3** 034001
[9] Guinee J B, van Oers L, de Koning A and Tamis W 2006 *Life Cycle Approaches for Conservation Agriculture* Department of Industrial Ecology and Department of Environmental, Leiden University, p 156 http://www.leidenuniv.nl/cml/bieb_internet/publications/cml_rapporten/cml%20report%20171_life_cycle_approaches_conservation_agriculture_2parts.pdf
[10] Hellweg S, Hofstetter T B and Hungerbuhler K 2003 Discounting and the environment—should current impacts be weighted differently than impacts harming future generations? *Int. J. Life Cycle Assess.* **8** 8–18
[11] Hertel T W 1997 *Global Trade Analysis: Modeling and Applications* (Cambridge: Cambridge University Press)
[12] Hertel T W, Golub A, Jones A D, O'Hare M, Plevin R J and Kammen D M 2009 Global commodity trade analysis identifies significant land-use change and greenhouse gas emissions linked to US corn ethanol production, forthcoming
[13] IPCC 2007 *Climate Change 2007—The Physical Science Basis* ed S Solomon *et al* (Cambridge: Cambridge University Press)
[14] ISO 2006 *ISO 14040: Environmental Management—Life Cycle Assessment—Principles and Framework* (Geneva: International Standards Organization)
[15] Joos F, Prentice I C, Sitch S, Meyer R, Hooss G, Plattner G K, Gerber S and Hasselmann K 2001 Global warming feedbacks on terrestrial carbon uptake under the Intergovernmental Panel on Climate Change (IPCC) emission scenarios *Glob. Biogeochem. Cycles* **15** 891–907
[16] Moura Costa P and Wilson C 2000 An equivalence factor between CO_2 avoided emissions and sequestration—description and applications in forestry *Mitig. Adapt. Strateg. Glob. Change* **5** 51–60
[17] Nordhaus W 2007 Critical assumptions in the stern review on climate change *Science* **317** 201–2
[18] Nordhaus W 2007 The stern review on the economics of climate change *J. Econ. Lit.* **45** 686–702
[19] Searchinger T, Heimlich R, Houghton R A, Dong F, Elobeid A, Fabiosa J, Tokgoz S, Hayes D and Yu T-H 2008 Use of US croplands for biofuels increases greenhouse gases through emissions from land use change *Science* **319** 1238–40
[20] Stern N 2007 *The Economics of Climate Change* (Cambridge: Cambridge University Press)
[21] Wang M Q 2008 *GREET 1.8b Spreadsheet Model* Center for Transportation Research, Energy Systems Division, Argonne National Laboratory
[22] Weitzman M L 2007 A review of the stern review on the economics of climate change *J. Econ. Lit.* **45** 703–24

Technical Highlights

EPA Lifecycle Analysis of Greenhouse Gas Emissions from Renewable Fuels

As part of proposed revisions to the National Renewable Fuel Standard program (commonly known as the RFS program), EPA analyzed lifecycle greenhouse gas (GHG) emissions from increased renewable fuels use. The Energy Independence and Security Act of 2007 (EISA) establishes new renewable fuel categories and eligibility requirements. EISA sets the first U.S. mandatory lifecycle GHG reduction thresholds for renewable fuel categories, as compared to those of average petroleum fuels used in 2005. The regulatory purpose of the lifecycle greenhouse gas emissions analysis is to determine whether renewable fuels meet the GHG thresholds for the different categories of renewable fuel.

Lifecycle GHG emissions are the aggregate quantity of GHGs related to the full fuel cycle, including all stages of fuel and feedstock production and distribution, from feedstock generation and extraction through distribution and delivery and use of the finished fuel. The lifecycle GHG emissions of the renewable fuel are compared to the lifecycle GHG emissions for gasoline or diesel (whichever is being replaced by the renewable fuel) sold or distributed as transportation fuel in 2005.

EISA established specific greenhouse gas emission thresholds for each of four types of renewable fuels, requiring a percentage improvement compared to a baseline of the gasoline and diesel. EISA required a 20% reduction in lifecycle GHG emissions for any renewable fuel produced at new facilities (those constructed after enactment), a 50% reduction in order to be classified as biomass-based diesel or advanced biofuel, and a 60% reduction in order to be classified as cellulosic biofuel. EISA provides some limited flexibility for EPA to adjust these GHG percentage thresholds downward by up to 10 percent under certain circumstances. EPA is proposing to exercise this flexibility for the advanced biofuels category in this proposal.

EPA United States Environmental Protection Agency

Office of Transportation and Air Quality
EPA-420-F-09-024
May 2009

EXHIBIT 25

EPA must conduct a lifecycle analysis to determine whether or not renewable fuels produced under varying conditions will meet the greenhouse gas (GHG) thresholds for the different fuel types for which EISA establishes mandates. While these thresholds do not constitute a control on greenhouse gases for transportation fuels (such as a low carbon fuel standard), they do require that the volume mandates be met through the use of renewable fuels that meet certain lifecycle GHG reduction thresholds when compared to the baseline lifecycle emissions of petroleum fuel. Determining compliance with the thresholds requires a comprehensive evaluation of renewable fuels, as well as of gasoline and diesel, on the basis of their lifecycle emissions. EISA defines lifecycle GHG emissions as follows:

> The term 'lifecycle greenhouse gas emissions' means the aggregate quantity of greenhouse gas emissions (including direct emissions and significant indirect emissions such as significant emissions from land use changes), as determined by the Administrator, related to the full fuel lifecycle, including all stages of fuel and feedstock production and distribution, from feedstock generation or extraction through the distribution and delivery and use of the finished fuel to the ultimate consumer, where the mass values for all greenhouse gases are adjusted to account for their relative global warming potential.[1]

As mandated by EISA, the greenhouse gas emission assessments must evaluate the full lifecycle emission impacts of fuel production including both direct and indirect emissions, including significant emissions from land use changes. We recognize the significance of using lifecycle greenhouse gas emission assessments that include indirect impacts such as emission impacts of indirect land use changes. Therefore, in our proposal we have been transparent in breaking out the various sources of GHG emissions to enable the reader to readily detect the impact of including international land use impacts.

EPA has analyzed the lifecycle GHG impacts of the range of biofuels currently expected to contribute significantly to meeting the volume mandates of EISA through 2022, including those from domestic and international sources. In these analyses we have used the best science available. Our analysis relies on peer reviewed models and the best estimate of important trends in agricultural practices and fuel production technologies as these may impact our prediction of individual biofuel GHG performance through 2022. We have identified and highlighted assumptions and model inputs that particularly influence our assessment and seek comment on these assumptions, the models we have used and our overall methodology so as to assure the most robust assessment of lifecycle GHG performance for the final rule.

The GHG lifecycle analysis combines a suite of peer-reviewed process models and peer-reviewed economic models of the domestic and international agricultural sectors to determine direct and significant indirect emissions, respectively (see Figure 1). As required by EISA, the broad system boundaries of our analysis encompass all significant secondary agricultural sector GHG impacts, not only impacts from land use change. The analysis uses economic models to determine the area and location of land converted into cropland in each country as a result of the RFS

[1] Clean Air Act Section 211(o)(1)

Technical Highlights

program. Satellite data are used to predict the types of land that would be converted into cropland (e.g. forest, grassland).

EPA's draft results suggest that biofuel-induced land use change can produce significant near-term GHG emissions; however, displacement of petroleum by biofuels over subsequent years can "pay back" earlier land conversion impacts. Therefore, the time horizon over which emissions are analyzed and the application of a discount rate to value near-term versus longer-term emissions are critical factors. We highlight two options. One option assumes a 30 year time period for assessing future GHG emissions impacts and values equally all emission impacts, regardless of time of emission impact (i.e., 0% discount rate). The second option assesses emissions impacts over a 100 year time period and discounts future emissions at 2% annually. Several other variations of time period and discount rate are also discussed in the proposed rule. Table 1 provides draft GHG emission reductions that result under two time horizon/discount rate approaches for a sample of fuel pathways evaluated in the proposed rulemaking. Figures 1 and 2 break out emissions for each of these pathways by lifecycle component (e.g. fuel production, domestic and international and use change, domestic and international agricultural inputs) for the two time horizon/discount rate approaches.

Table 1. Draft Lifecycle GHG Emission Reduction Results For Different Time Horizon And Discount Rate Approaches.

Fuel Pathway	100 year, 2% Discount Rate	30 year, 0% Discount Rate
Corn Ethanol (Natural Gas Dry Mill)	-16%	+5%
Corn Ethanol (Best Case Natural Gas Dry Mill)[2]	-39%	-18%
Corn Ethanol (Coal Dry Mill)	+13%	+34%
Corn Ethanol (Biomass Dry Mill)	-39%	-18%
Corn Ethanol (Biomass Dry Mill with Combined Heat and Power)	-47%	-26%
Soy-Based Biodiesel	-22%	+4%
Waste Grease Biodiesel	-80%	-80%
Sugarcane Ethanol	-44%	-26%
Switchgrass Ethanol	-128%	-124%
Corn Stover Ethanol	-115%	-116%

[2] Best case plants produce wet distillers grain co-product and include the following technologies: combined heat and power (CHP), fractionation, membrane separation and raw starch hydrolysis

Figure 1. Net Lifecycle Greenhouse Gas Emissions By Lifecycle Component With 100 Year Time Horizon And 2% Discount Rate.

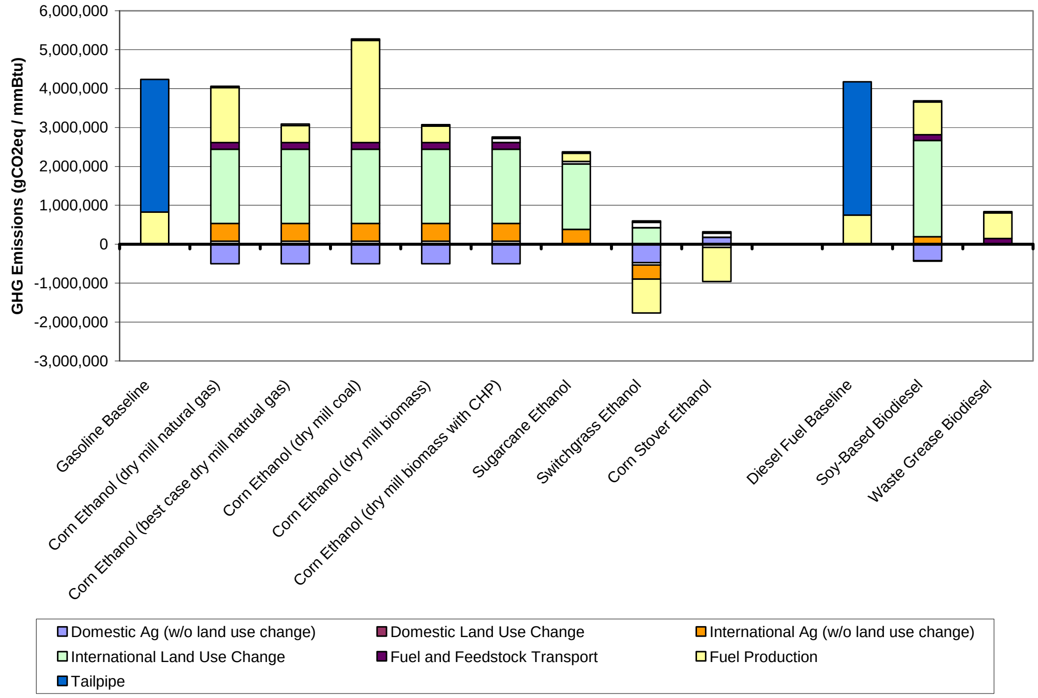

Figure 2. Net Lifecycle Greenhouse Gas Emissions By Lifecycle Component With 30 Year Time Horizon And 0% Discount Rate.

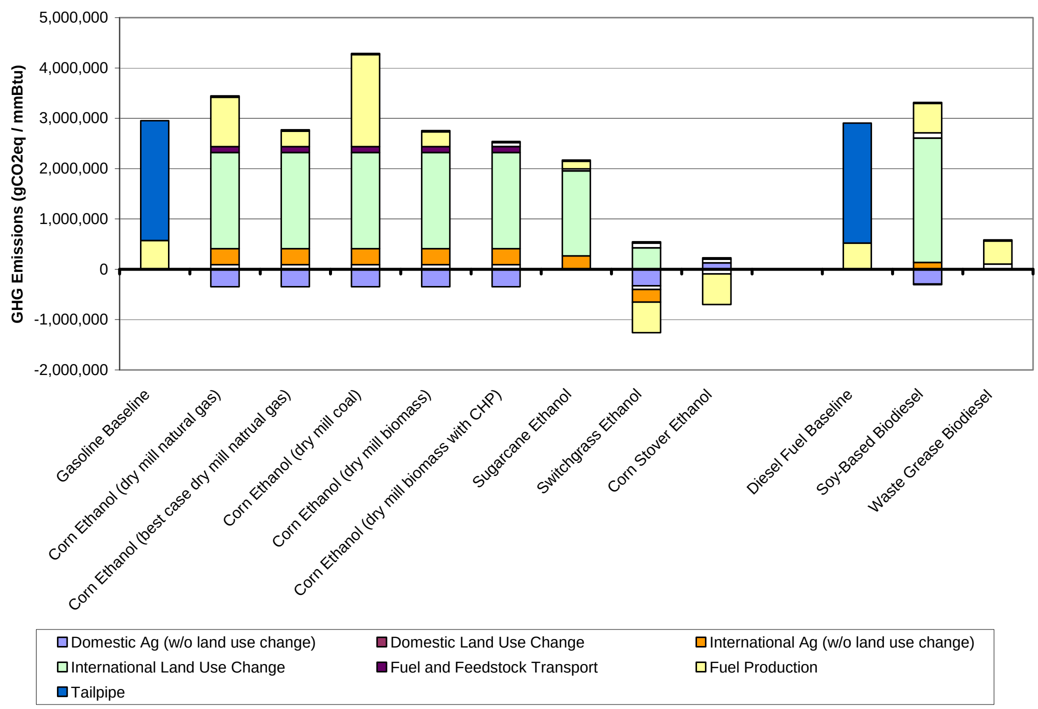

We believe that our lifecycle analysis is based on the best available science, and recognize that in some aspects it represents a cutting edge approach to addressing lifecycle GHG emissions. Because of the varying degrees of uncertainty in the different aspects of our analysis, we conducted a number of sensitivity analyses which focus on key parameters and demonstrate how our assessments might change under alternative assumptions. By focusing attention on these key parameters, the comments we receive as well as additional investigation and analysis by EPA will allow narrowing of uncertainty concerns for the final rule. In addition to this sensitivity analysis approach, we will also explore options for more formal uncertainty analyses for the final rule to the extent possible.

Because lifecycle analysis is a new part of the RFS program, in addition to the formal comment period on the proposed rule, EPA is making multiple efforts to solicit public and expert feedback on our proposed approach. EPA plans to hold a public workshop focused specifically on lifecycle analysis during the comment period to assure full understanding of the analyses conducted, the issues addressed and the options that are discussed. We expect that this workshop will help ensure that we receive submission of the most thoughtful and useful comments to this proposal and that the best methodology and assumptions are used for calculating GHG emissions impacts of fuels for the final rule. Additionally, between this proposal and the final rule, we will conduct peer-reviews of key components of our analysis. As explained in more detail in the section VI of the proposal, EPA is specifically seeking peer review of: our use of satellite data to project future the type of land use changes; the land conversion GHG emissions factors estimates we have used for different types of land use; our estimates of GHG emissions from foreign crop production; methods to account for the variable timing of GHG emissions; and how the several models we have relied upon are used together to provide overall lifecycle GHG estimates.

Each component of our analysis is discussed in detail in the preamble and the Draft Regulatory Impact Analysis that accompany the Notice of Proposed Rulemaking. The proposed rule is an important opportunity to seek public comment on EPA's entire lifecycle GHG analysis, including questions about land use modeling, and the choice of which time horizon and discount rate is most appropriate for this analysis.

For More Information

For more information on this proposal, please contact EPA's Office of Transportation and Air Quality, Assessment and Standards Division information line at:

U.S. Environmental Protection Agency
Office of Transportation and Air Quality
2000 Traverwood Drive
Ann Arbor, MI 48105

Voicemail: (734) 214-4636
E-mail: asdinfo@epa.gov

Or visit: www.epa.gov/otaq/renewablefuels/index.htm

ENVIRONMENTAL WORKING GROUP



Clearcut Disaster: Carbon Loophole Threatens U.S. Forests

By Mary S. Booth PhD

with

Richard Wiles

Senior Vice President

Environmental Working Group

June 2010

www.ewg.org

EXHIBIT 26

Table of Contents

EXECUTIVE SUMMARY 1
- Projecting the Impact of the House Climate Change Bill 4
- Conclusions and Recommendations 5

FULL REPORT
- I. Biomass Power: Forests to Fuel 6
- II.Promoting "Renewable" Energy: Surprising Consequences 8
  - Biomass burning will increase greenhouse gas emissions 9
  - Millions of forest acres would be logged 10
- III. Why Current Calculations Omit Carbon Dioxide from Biomass 11
- IV. Current and Proposed Policies Create Powerful Incentives for Tree Cutting 12
  - Trees will be the biomass fuel of choice 13
  - The impact of a federal renewable energy standard 15
- V. Why Burning Trees is Worse than Burning Coal 18
- VI. Demand for Bioenergy Will Put More Pressure on Forests 20
- VII. Biomass Power Development Will Cost Taxpayers Billions 22
- VIII. State Policies Are Creating Biomass Power Hotspots 24
  - Maine – furthest down the road 24
  - Massachusetts – thinking twice about biopower 26
  - Florida and Georgia – headlong into biopower 28
  - Ohio – using biopower to consolidate a commitment to coal 29
- IX. Conclusions and Recommendations 31
  - Environmental Working Group recommends 32

Appendix A: Biomass provisions in the American Clean Energy and Security Act 33
Appendix B: Analysis and methodology 34
- From BTUs to Acres Cut 41

Figures and Tables
- Figure 1. Biomass burning increases with federal renewables incentives 2, 8
- Figure 2. Counting biomass emissions eliminates projected emissions reductions 9
- Figure 3. Forest cutting will increase dramatically under climate bill 10
- Figure 4. Forest regrowth takes decades 19
- Figure 5. Wood demand for projects in the pipeline is already increasing 21
- Figure 6. Clear-cutting for biomass energy in Maine 26
- Table 1. Non-tree biomass supplies are limited 17
- Table 2. Proposed biomass power plants and pellet plants, Florida and Georgia 29

Executive Summary

House and Senate climate legislation, as well as federal and state policies designed to promote the use of biomass fuels for electricity generation, will sharply increase cutting of U.S. forests by the year 2025 while pouring huge amounts of carbon into the atmosphere, an extensive analysis by Environmental Working Group (EWG) shows.

biomass-fueled electricity generation will produce billions of tons of uncounted CO_2 emissions over the next 15 years while wiping out millions of acres of woodlands

Reaching these goals – generating 25 percent of US electricity from renewable sources by 2025 – will require the equivalent of clear-cutting between 18 and 30 million acres of forests over the next 15 years; 30 million acres is 46,291 square miles, an area larger than the entire state of Pennsylvania. By 2030, the equivalent of up to 50 million acres could be clear-cut as utilities become dependent on biomass to meet their renewables targets. Less intensive harvesting merely means that more acres that will be cut.

This perverse outcome of pending climate and energy bills and existing state and federal renewable energy incentives results from a glaring flaw in carbon accounting practices, which falsely assumes that burning biomass fuels, including trees, produces zero net carbon emissions. Close examination shows that the reverse is true: logging and burning trees will produce a near-term surge in carbon releases – greater than from burning coal – while eroding for decades the forests' ability to recapture those emissions.

This Enron-style accounting system, embedded in virtually all climate policies worldwide, hides massive carbon emissions that will result from burning biomass to generate electricity. EWG's analysis of government projections predicts that over the next 15 years about 4.7 billion tons of carbon will be generated from burning biomass, most of it from whole trees and all of it "off the books." This massive pulse of uncounted carbon dioxide will effectively erase 80% of the reduction in CO_2 emissions from the power sector that is at the heart of federal climate legislation.

Adding insult to injury, this destruction and pollution will be heavily subsidized by U.S. taxpayers. The Congressional Budget Office estimates that under the American Clean Energy and Security Act (ACESA), the treasury would forfeit about $10.5 billion in tax revenues over the next 15 years as we subsidize the construction of biomass-burning power plants, most of them burning whole trees. Because biomass emissions are not counted, facilities generating power from biomass would avoid purchasing carbon allowances worth a staggering $129 billion by 2025 under the carbon cap.

EWG's analysis examined two scenarios using data and projections from the Energy Information Administration (EIA) of the U.S. Department of Energy. We analyzed the impact on forests of EIA's basic scenario, which projects the impact of the House-passed climate bill (ACESA) if enacted as written, and second ACESA scenario that achieves maximum carbon reductions. Our analysis indicates that meeting the demand for biomass fuel under EIA's basic ACESA scenario would require the equivalent of cutting between 18 and 30 million acres by 2025, and up to 50 million acres by 2030. The fuel requirement for the even faster ramp-up of biomass power envisioned under the optimal scenario would require the equivalent of cutting up to 59 million acres by 2025. Legislation proposed in the Senate would produce essentially the same results.

Over the past decade, many states have adopted renewables portfolio standards (RPS)[1] under which a certain proportion of power must be produced from renewable sources. One potentially disastrous outcome of these policies, even prior to enactment of a federal RPS, has been an explosion of proposals to construct wood-burning power plants and to burn wood at coal-fired plants (co-firing). Some existing coal plants are proposing to switch to burning wood entirely, which under current policy would allow them to declare that their carbon dioxide emissions have gone to zero, when in reality they would have increased substantially.

Figure 1. Biomass burning will increase dramatically under federal renewables incentives

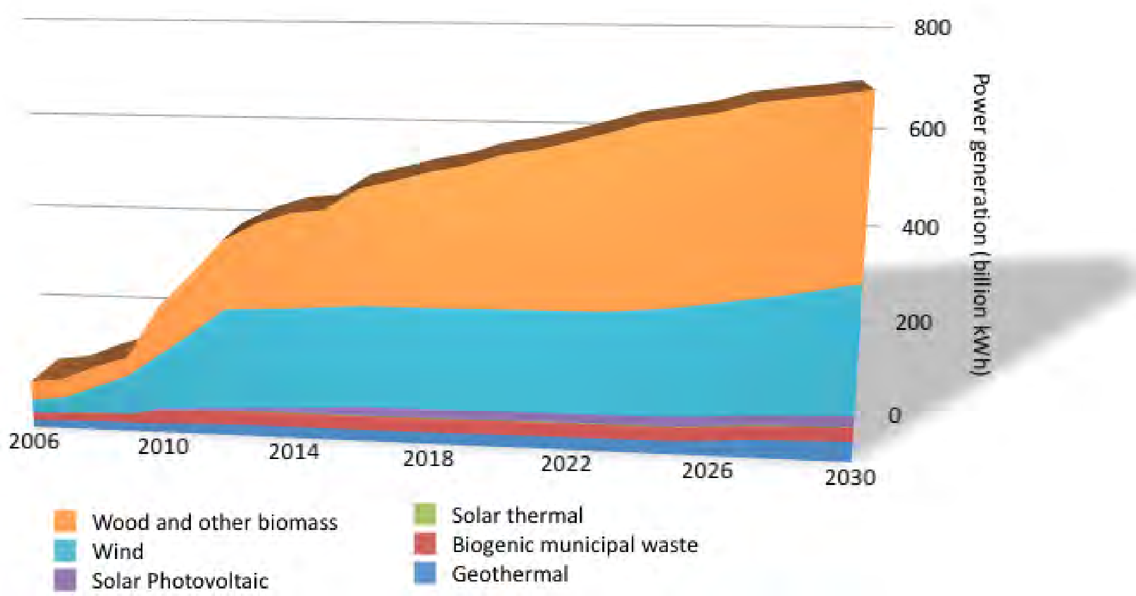

Trees and other biomass fuels account for 55 percent of renewable power by 2025 under the basic ACESA scenario (includes end-use generation and excludes conventional hydropower). Under current policies, all carbon emissions from biomass burning are off the books. (Source: EIA National Energy Modeling System Run HR2454CAP.D072909A)

At least 118 new biomass power plant and co-firing proposals that would use wood as fuel are currently in various stages of permitting or approval in at least 30 states, with capacity increasing at an exponential rate.

1 Also known as renewable electricity standards (RES)

"Hardly a day passes in the Southern U.S. without an announcement of a new bioenergy facility or expansion of an existing one… What is increasingly obvious is that the amount of truly available logging residues will be nowhere near enough to supply the current and announced bioenergy processors in the Southern U.S…"

Biomass Magazine
August 2009

A typical 50-megawatt biomass plant burns more than a ton of wood a minute. Two wood-burning plants recently proposed in Massachusetts would generate a combined 97 MW and require the equivalent of cutting 12,000 acres of forest annually, more wood than is currently harvested in the entire state each year, while providing just 0.7 percent of the power generated in the state. Permitting documents reveal that whole-tree harvesting would provide one-half to two-thirds of the fuel for at least one of the plants.

In response to objections by citizens and environmental groups, Massachusetts recently suspended the eligibility of biomass for the state's renewables portfolio standard pending a complete review. In Ohio, multiple proposals to co-fire biomass in coal plants have been proposed. Plant operators admit that whole trees, specifically white, interior trunk wood, are the only biomass fuel that will meet emissions requirements. The 1,125 megawatt Beckjord plant in Ohio has proposed to replace up to 100 percent of its coal consumption with biomass. Where will this fuel come from?

"The most likely initial fuel will be woody biomass produced by whole tree chipping" from a 50-mile radius of a coal loading terminal on the Big Sandy River.

Beckjord application to the
Ohio Public Utilities Commission - 2009

Many co-firing proposals rely on processed wood pellets for biomass fuel, which require massive energy and wood inputs to produce.

The assumption that burning biomass, including trees, produces zero carbon emissions is the cornerstone of current state-level renewables electricity standards, pending energy legislation in the US Senate and the House-passed climate bill. The erroneous classification of biomass power as carbon neutral has allowed biomass power to emerge as a significant potential source of "renewable" power, even as the overwhelming experience to date indicates that the primary source of biomass will be whole trees.

Without the biomass accounting loophole, many of the carbon reduction goals in federal climate and energy legislation are simply not attainable. Given the massive ramp-up in biomass power that is already occurring, and that 2025 emissions reductions targets must be met in only 15 years, it is urgent to correct this carbon accounting flaw.

Projecting the impact of congressional climate change bills.

A central goal of congressional climate initiatives is to provide up to 25 percent of the nation's power from renewable sources by 2025 and to cut carbon emissions to 17 percent below 2005 levels by 2020.

To do this, the House-passed ACESA bill relies on dramatic increases in renewable energy sources, more than half of which will be biomass. The bill defines biomass renewable fuels, among other things, as "trees, logging residue, thinnings, cull trees and brush..." [Title I, Section 101(b)(16)(H)(i)]

The American Power Act, proposed in the Senate, defines renewable biomass as "renewable plant material, including … other plants and trees" and defines "excess biomass" as including "trees or tree waste on public land." [American Power Act, S. xx, 111th Cong., § 2002 (2010) (amending Title VII of the Clean Air Act (42 U.S.C. 7401 et seq.) as added by American Power Act § 2001, by adding § 700 (44)]

As discussed throughout this report, heavy reliance on biomass will translate into millions of acres of forests being cut to fuel electric power plants. Burning trees generates more carbon pollution than coal, but under EPA's flawed carbon accounting system, the carbon emissions from this cutting and burning of America's forests will count as zero. As a result, the 2020 emissions targets will be met only on paper, not in reality.

In its projections of the impact of the ACESA, the Energy Information Administration (EIA) includes several alternative policy scenarios. We analyzed two EIA scenarios in writing this report.

EIA's "basic" scenario projects emissions reductions if ACESA is enacted into law as passed. Under this scenario, biomass power would constitute 55 percent of renewable power, excluding hydropower, and about 8 percent of total power generation in 2025. Our analysis shows that 18 million acres of forests would be cut to meet the biomass targets projected by EIA in this scenario. Carbon emissions from the power sector would be 17 percent higher than projected because the government assumes that burning trees releases no carbon dioxide into the atmosphere.

Uncounted carbon emissions would be even higher under the second scenario that disallows international carbon offsets, a distinct possibility given the increasingly tenuous credibility of these projects. This scenario forces power plants to reduce carbon emissions directly, producing significant reductions by 2025, but this is accomplished in part through an immediate and massive ramp-up in biomass co-firing (burning trees) at coal plants. The other notable carbon reduction assumption in this scenario is a 230 percent increase in nuclear power by 2030.

Under this scenario, biomass would provide 11 percent of all power generation and 46 percent of renewable power in 2025. About 30 million acres of forest would need to be cut to fill this demand. When the pollution from burning trees is put back on the books, cumulative carbon emissions from the power sector by 2025 are 35 percent higher than EIA projects.[2]

---

2 EIA's emissions projections for the power sector include the assumed effect of carbon capture and storage technology (CCS), which is assumed to be operational starting in 2016 (Source: EIA National Energy Modeling System runs HR2454CAP.D072909A, HR2454NOINT.D072909A). To estimate the proportion of total power sector emissions that biomass power would contribute, we estimate biomass emissions relative to total power sector emissions with CCS emissions added back in.

Conclusions and Recommendations

Federal and state carbon tracking systems do not accurately account for carbon emitted by biomass power or place any restrictions on burning whole trees. The rush is on to capitalize on this lucrative loophole, with drastic consequences for forests.

Forests are a major force pulling carbon out of the atmosphere. The annual aboveground growth alone in US forests counteracts about 14 percent of all emissions from power generation each year. Cutting them down to burn in power plants will not only inject massive amounts of stored carbon into the atmosphere, it will also destroy our best defense against the buildup of atmospheric carbon.

To avert this potentially devastating outcome, carbon accounting needs to be reformed, and renewable fuels and greenhouse gas reduction policies need to be aligned accordingly. Specifically:

Pass a strong climate bill.

Congress must enact strong climate legislation that eliminates the biomass carbon accounting loophole. Carbon accounting practices must be corrected to include the full and immediate impact of cutting down forests to burn in biomass power plants. Biomass burning must not be permitted unless each specific proposal can unequivocally demonstrate that it will not increase greenhouse gas emissions, even in the short term. These reforms must be incorporated into all federal and state energy and climate policies.

Require biomass power plants to purchase emission allowances.

Biomass plants should be added to the list of "covered entities" required to purchase carbon emission allowances under federal and regional cap-and-trade programs. To the extent that biomass emissions are demonstrably re-sequestered in a short period of time, exceptions could be made.

Eliminate federal and state incentives for biomass power.

The federal production tax credit for biomass systems that burn whole trees, meaning chipped or pelletized whole trees, must be eliminated. The tax credit provides a massive federal subsidy for forest exploitation. Likewise, the Biomass Crop Assistance Program (BCAP) program providing matching funds to biomass suppliers should be revised to exclude funding of any facilities or operations that encourage forest cutting.

Exclude utility-scale biomass and co-fired coal plants from renewables portfolio standards.

Only high efficiency, small-scale, combined heat-and-power plants that extract maximum energy value from "additional" biomass should be considered to sell Renewable Energy Credits, and such projects should also undergo rigorous lifecycle analysis to determine their carbon footprints. "Additional" biomass should be defined as sustainably generated biomass containing carbon that would not otherwise remain stored, or become stored, or be meaningfully used for purposes other than energy production.

FULL REPORT

I. Biomass Power: Forests to Fuel

More than 50 percent, perhaps far more, of the renewable power generation promoted by federal programs and legislation now under consideration by Congress will come from burning trees and other "biomass" materials.[3]

Biomass power is considered a renewable and carbon-neutral form of electricity generation because it is assumed to utilize the non-marketable parts of trees (like the tops and branches generated by logging) and the non-food portions of agricultural crops (like the stalks of corn and wheat plants). Because these "residues" left after harvesting emit carbon dioxide during decomposition, burning them is considered to produce no more carbon dioxide than would be emitted if they were left in place.

In theory, regrowth then locks up as much atmospheric carbon dioxide into new biomass as was released by combustion. Once this cycle is completed, the power generated by burning biomass is considered to be effectively "carbon neutral,"[4] since the fossil fuel emissions associated with biomass harvesting and transport are generally disregarded.

Until recently, this theory had been widely accepted, and most carbon accounting schemes do not count or regulate emissions from biomass power.[5] This convention has made biomass power an attractive option for meeting state-level "Renewables Portfolio Standards" (RPS)[6] as well as the proposed renewables standard at the heart of federal climate legislation, including the American Clean Energy and Security Act (ACESA) passed by the House of Representatives in 2009.

---

3 Many forms of material can be defined as biomass, including old tires, chicken waste, and chicken carcasses. Much of the power generated at existing biomass plants comes from "wood liquors," by-products of the pulp and paper industry, as well as sawmill and other wood-processing waste. However, most new biomass plants utilize wood as fuel. Woody biomass fuels are derived from non-marketable whole trees as well as: leftover branches and tops cut during forestry operations; sawmill waste; urban tree trimming; trees and stumps dug out of the ground during land clearing; and construction and demolition waste. These materials are in limited supply, however, meaning that forest cutting will increase in response to new demand.

4 The Environmental Protection Agency grants biomass energy special status not only as a renewable but also as a "green power source," defined as a power source that produces electricity "with an environmental profile superior to conventional power technologies [that] produce[s] no anthropogenic (human caused) greenhouse gas emissions." (http://www.epa.gov/greenpower/gpmarket/index.htm). The Agency acknowledges that biomass produces biogenic emissions but states that these are "balanced by the natural uptake of CO_2 by growing vegetation, resulting in a net zero contribution of CO_2 emissions to the atmosphere." The Agency's new rules on emissions reporting require that biogenic carbon emissions be reported separately from other emissions. (Environmental Protection Agency, 2009. Mandatory reporting of greenhouse gases; final rule. 40 CFR 86,87,89 et al. Federal Register, October 30, 2009.)

5 See below for an explanation of how the "accounting error" that ignores biomass emissions originated.

6 Currently, 42 States and the District of Columbia have enacted an RPS or similar renewable energy requirement (http://www.dsireusa.org/summarytables/rrpre.cfm)

biomass-fueled electricity generation would produce billions of tons of uncounted emissions while wiping out millions of acres of woodlands

A closer examination of data and projections by the U.S. Department of Energy's own Energy Information Administration (EIA)[7] reveals that this analysis is profoundly flawed. Environmental Working Group (EWG) studied this publicly available but largely unexamined data, and our research reveals that policies based on these assumptions would have drastic consequences. EWG's analysis, based on the government's own data, shows that most biomass-fueled electricity generation would produce billions of tons of uncounted emissions over the next 15 years while wiping out millions of acres of woodlands and eroding for decades the ability of existing forests to sequester atmospheric carbon.

This outcome requires a thorough rethinking of all legislation and proposals that promote biomass-based renewable fuels as a means to achieve energy independence and combat global warming.

ACESA seeks to increase the market share of renewable electricity generation to 25 percent by 2025, although the actual percentage may be as low as 17 percent when exemptions are taken into account.[8] EIA projects that biomass will generate 55 percent of all renewable electricity in 2025.[9]

entire forests can be cut to provide biomass fuel and still be considered "carbon neutral."

Biomass power is simply not carbon neutral. Even where existing logging residues are the sole source of fuel, the assumption that burning these materials emits no more carbon dioxide than natural decomposition fails to acknowledge that decomposition, like regrowth, is a slow, even decadal process, while burning releases greenhouse gases instantaneously. Even more significantly, biomass power is considered equally "climate friendly" whether whole trees or logging residues are used for fuel; in other words, an entire forest can be clear-cut to provide biomass fuel and still be considered "carbon neutral."[10]

---

7 The Energy Information Administration, a division of the Department of Energy, uses the National Energy Modeling System (NEMS) to project power sector development under various legislative scenarios. Modeling to describe the growth of both renewable and conventional power generation under ACESA was published in 2009.

8 According to documentation from the Energy Information Administration, "The level of renewables required to comply with the RES (renewable electricity standard) will be lower than the nominal target because of the exemptions and baseline adjustments. While the nominal share in 2025 is 25 percent, exempting the small retailers lowers the effective target to 22 percent of total electricity sales. The effective target is lowered further to 21 percent when the generation from hydroelectric power and municipal solid waste is removed from the sales baseline. The effective target will be lowered still further by the degree to which qualifying energy efficiency credits are used. If States are able to take full advantage of the energy efficiency credits, using them to meet up to 20 percent of the RES requirement, the effective share of renewables required could drop to approximately 17 percent of total electricity sales." (Energy Information Administration. Impacts of a 25-percent renewable electricity standard as proposed in the American Clean Energy and Security Act Discussion Draft. SR/OIAF/2009-04. April, 2009. Washington, DC.)

9 This figure includes end use generation, power generated on site by commercial and industrial users.

10 Johnson, E. 2008. Goodbye to carbon neutral: getting biomass footprints right. Environ Impact Asses Rev, doi:10.1016/j.eiar.2008.11.002; Searchinger, T., et al. 2009. Fixing a critical climate accounting error. Science 326: 527 - 528.

II. Promoting "Renewable" Energy: Surprising Consequences

Modeling by the Energy Information Administration projects that under a federal Renewables Portfolio Standard, renewables-based generation will constitute an increasing percentage of total power generation, with a goal of reaching 25 percent by 2025, although exemptions from RPS rules will lower the actual share to about 17–to-19 percent under the various scenarios modeled by EIA.[11] EIA's "basic" scenario, which projects the impacts of ACESA if it were implemented as written, predicts that biomass power will provide about 8 percent of total power generation and about 55 percent of all renewables-based generation,[12] excluding hydropower, by 2030.

Figure 1. Biomass burning will increase dramatically under a federal renewables standard

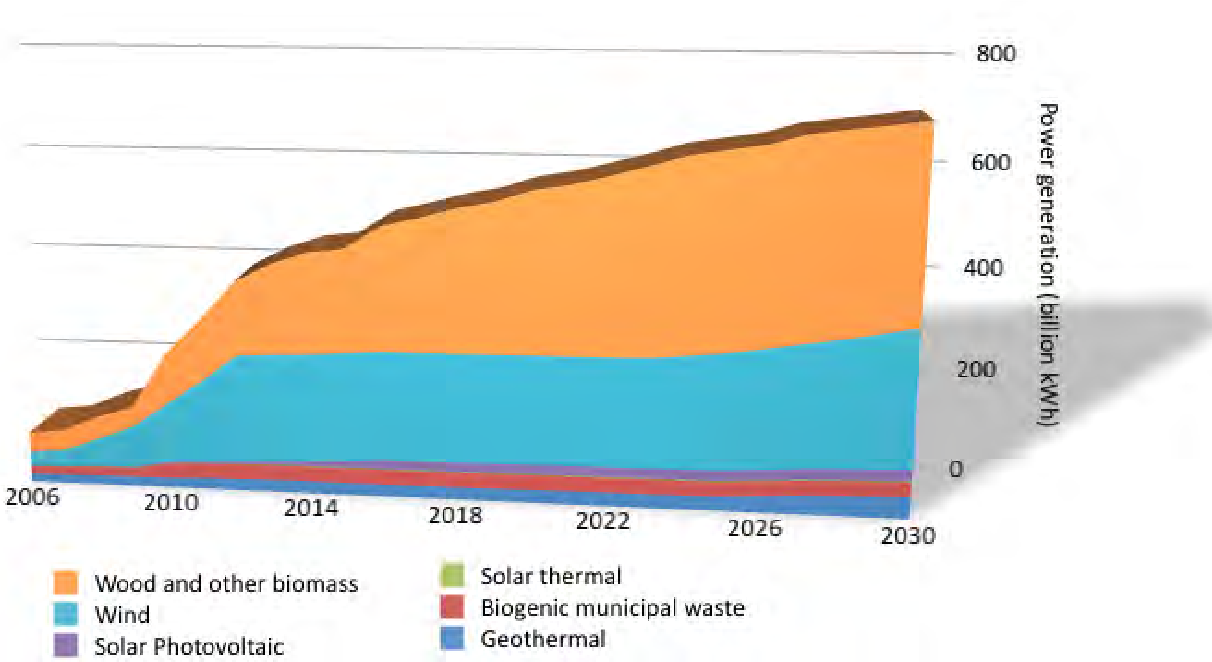

Projected development (in billion kilowatt-hours), excluding conventional hydropower, in EIA's "basic" scenario for renewable power deployment under ACESA. Scenario includes end use generation

11 See footnote 9 for an explanation.

12 Energy Information Administration. 1990 – 2008 Net generation by state by type of producer by energy source (EIA 906) (available at http://www.eia.doe.gov/cneaf/electricity/page/capacity/capacity.html). "Renewable" power sources defined as wind, solar, and geothermal. The second largest source of renewable power under the EIA scenario is wind power. Deployment of wind power is constrained by a number of factors, including wind speed, limitations on development in reserved and inaccessible areas, and transmission costs. In fact, EIA projects that enactment of federal RPS will do little to incentivize wind power development beyond what is predicted to occur as a result of incentives included in the 2009 American Recovery and Reinvestment Act (ARRA). (Energy Information Administration. Impacts of a 25-percent renewable electricity standard as proposed in the American Clean Energy and Security Act Discussion Draft. SR/OIAF/2009-04. April, 2009. Washington, DC)

Biomass burning will increase greenhouse gas emissions

Between 2010 and 2025, EIA predicts greenhouse gas emissions from the power sector will decline significantly, in part due to a reduction in the amount of power generated by coal. But this decline also depends on the assumption that biomass produces no net carbon emissions, as well as on carbon capture and sequestration, which is assumed to become operational around 2016. When true biomass emissions are counted, it turns out that the majority of greenhouse gas reductions are an artifact of the carbon accounting loophole (Figure 2).[13] The relatively small amount of power produced from biomass has a disproportionate effect on carbon emissions because biomass power produces much more carbon dioxide "at the stack" per unit of energy than coal or natural gas.[14]

Figure 2. Counting biomass emissions eliminates projected emissions reductions

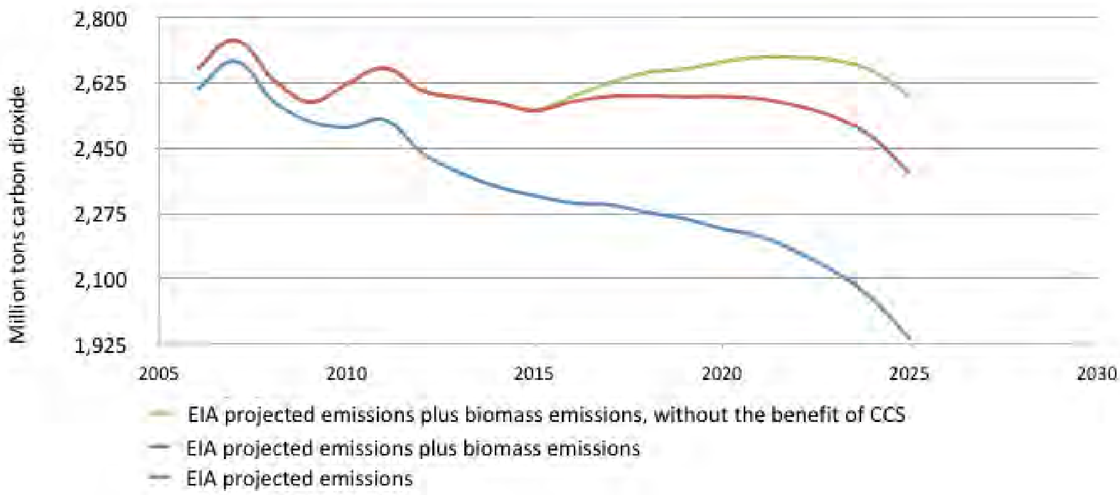

Power sector emissions (million tons carbon dioxide) for the United States, 2006 to 2030. EIA's totals (blue line) do not include biomass emissions but assume that carbon capture and storage (CCS) can start in 2016, reducing emissions by 26 percent from 2006 levels. Adding projected biomass emissions to emissions totals (red line) results in a decline of only 11 percent. Adding biomass emissions and emissions assumed to have been sequestered using CCS (green line) results in a decline of just 3 percent. Stack emissions from biomass are only part of the story, as they do not include emissions from harvest and transport, soil emissions following harvesting disturbance or lost forest carbon uptake. (Source for EIA projection: EIA National Energy Modeling System run HR2454CAP. D072909A).

13 Biomass power stack emissions were calculated by estimating the amount of fuel required to meet EIA's projections of biomass power generation, using EIA's conversion factors for BTUs in biomass to kilowatt-hours of power. Carbon content was assumed to be 50 percent for wood and 45 percent for agricultural residues, following the convention used by Oak Ridge National Laboratory (http://bioenergy.ornl.gov/papers/misc/energy_conv.html). Our approach to estimating CO_2 emissions from biomass is identical to that used by EPA (Environmental Protection Agency, 2009. Mandatory reporting of greenhouse gases; final rule. 40 CFR 86,87,89 et al. Federal Register, October 30, 2009.)

14 Stack emissions are only part of the lifecycle emissions of forest harvesting, which include fossil fuels used for harvest and transport, lost carbon sequestration and soil disturbance following logging. A recent study suggests soil carbon losses following harvesting can be substantial, comprising on average 8 percent of soil carbon, which itself comprises about two-thirds of forest carbon (Nave et al, 2010. Harvest impacts on soil carbon storage in temperate forests.Forest Ecology and Management, 259:857 – 866.)

In addition, EIA's estimates do not take into account fossil fuels consumed during biomass harvesting and processing. Wood chips are a bulky material for the energy they deliver. By 2025, transport of biomass will require up to 1.1 billion miles of travel per year by delivery trucks, consuming a cumulative 2 billion gallons of diesel fuel by 2025. Carbon dioxide emissions from use of fuel during transport will be more than 23 million tons by 2025.[15] These numbers do not take into account fossil fuel use during harvest and processing of biomass fuels.

Millions of forest acres would be logged to provide fuel for biomass plants

As the amount of biomass power ramps up, so will forest cutting. The US currently cuts about 2.1 percent of its forests per year, or about 11 million acres. About 39 percent are clear-cut, with all trees removed.[16] EWG estimated the number of additional acres that would need to be logged to meet projected energy demand under two EIA scenarios for biomass buildout and two scenarios for availability of existing biomass fuels.

Figure 3. Forest cutting will increase dramatically under climate bill; clearcut equivalent in acres

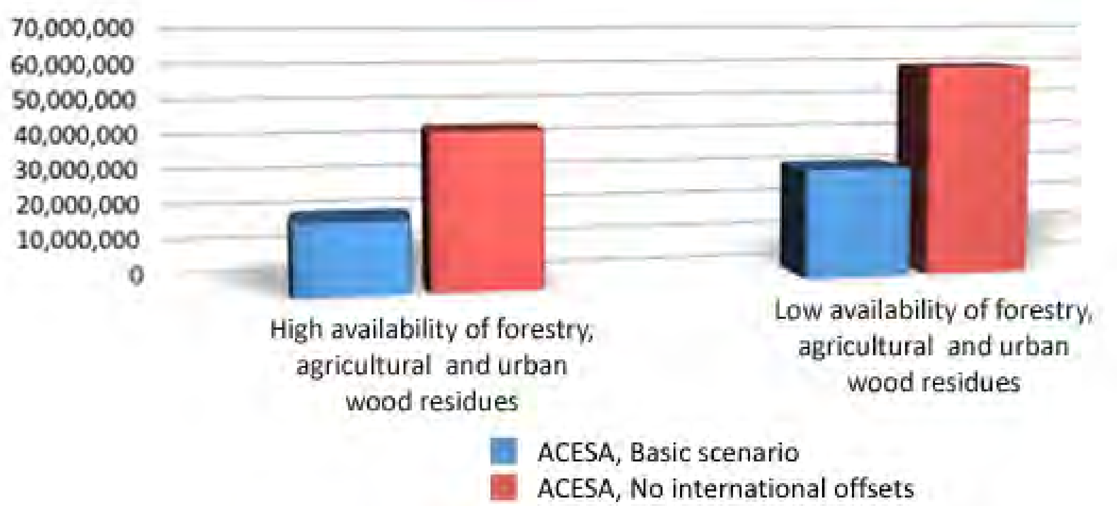

Equivalent acres that would need to be cut to meet biomass fuel needs by 2025 under EIA's basic and "no international offsets" scenarios for the House-passed climate bill (American Clean Energy and Security Act).

15 The EIA NEMS model assumes that 50 miles is the maximum distance over which most biomass residues can be transported economically and that the cost of transport within a 50-mile radius is $12/ton. Urban wood waste is assumed to be economically transported over distances of up to 100 miles. (Energy Information Administration, Office of Integrated Analysis and Forecasting. Model documentation: Renewable fuels module of the National Energy Modeling System. DOE/EIA-M069 (2009). July, 2009. Washington, DC.) Our estimate of transport costs also assumed that 50 miles is the maximum distance that biomass would be transported, but this is clearly a dramatic underestimate of even current transport distances, which can be much higher. In addition to domestic transport, the growing international demand for biomass means that wood from the United States is currently being shipped to Europe.

16 Smith, W.B., et al. 2007. Forest Resources of the United States, 2007. United States Forest Service, Gen.Tech Report WO-78. December, 2008.

The acres of cutting that would be required to meet biomass fuel needs are calculated after taking into account "existing" biomass fuel that could be provided by forestry residues, agricultural residues, and urban wood. "High" and "Low" scenarios for availability of these existing fuels were estimated using realistic assumptions as described below.

Harvesting large amounts of forest biomass in a cost-efficient manner requires large, specialized harvesting equipment that swiftly harvests all trees in the target zone. Removal of 50-to-100 percent of trees is typical. We present our results in terms of equivalent wood from clearcutting for the sake of simplicity, since the assumption of removing half the trees for biomass fuel simply requires doubling the number of acres.

For EIA's basic ACESA scenario, assuming *high availability* of existing biomass fuels (crop residues, construction debris, energy crops, and logging residues generated by existing logging operations), about 39 percent of the biomass fuel requirement would have to be met by new forest harvesting by 2025. In this case, cumulative biomass fuel needs by 2025 would require the equivalent of cutting 17.7 million acres. To make up this fuel deficit with energy crops would require harvesting 14.9 million acres of dedicated land each year (see Appendix B for details on how we made these calculations).

Assuming *low availability* of biomass fuel, about 60 percent of the fuel needs would be met by new forest cutting. In this case, biomass fuel needs would require the equivalent of clear-cutting 29.6 million acres by 2025. Meeting this need with energy crops would require 23 million acres to be harvested each year.

III. Why Current Calculations Omit Carbon Dioxide from Biomass Burning

A 2009 paper by Timothy Searchinger et al. in the journal Science called attention to the urgency of fixing a "critical accounting error" that has allowed biomass power to be treated as if it were carbon neutral. The authors concluded that "harvesting existing forests for electricity adds net carbon to the air. That remains true even if limited harvest rates leave the carbon stocks of regrowing forests unchanged, because those stocks would otherwise increase and contribute to the terrestrial carbon sink."[17] The only biomass fuels that do not add net carbon to the air are residues that would otherwise decompose quickly and fuels that result from additional carbon having been previously sequestered beyond what would have been sequestered in the normal course of business.

Forests play an important role in sequestering current carbon emissions from fossil fuel burning. From 2002 to 2007, forests of the continental United States tied up the equivalent of nearly 14 percent of carbon dioxide emissions from the power sector into new above ground growth alone.[18]

[17] Searchinger, T., et al. 2009. Fixing a critical climate accounting error. Science 326: 527 - 5 28.

[18] Carbon dioxide sequestered into new forest growth was estimated by calculating the growth increment of forests between 2002 and 2007, using Forest Service data.

Far from providing a carbon neutral fuel source, harvesting standing forests for biomass degrades this critical forest function.

The "accounting error" that assumes carbon neutrality for biomass power is based on a misreading of internationally accepted carbon accounting standards promulgated by the Intergovernmental Panel on Climate Change (IPCC). These rules count any harvesting of wood as a direct and immediate emission of carbon dioxide to the atmosphere *at the time of harvesting*.[19] These emissions are only considered to be re-sequestered following the slow, often multi-decade regrowth of cut forests. Emissions released when biomass power plants actually burn this fuel are *not* counted under IPCC rules in order to avoid double counting.

The U.S. Environmental Protection Agency (EPA) and other institutions that track carbon emissions have misinterpreted this accounting rule. The EPA does not count stack emissions when biomass is burned for power generation, but it also does not account for emissions at the time of harvesting.[20] *The result is that emissions from biomass power are never counted.*

the EPA does not count stack emissions when biomass is burned for power generation, but it also does not account for emissions at the time of harvesting *the result is that emissions from biomass power are never counted*

This feawed accounting system is at the core of US renewable energy policy, including all state and federal renewables portfolios and the House and Senate energy and climate bills.

IV. Current and Proposed Policies Create Powerful Incentives for Tree Cutting

The version of ACESA passed by the House requires large power plants to show emissions reductions (relative to 2005) of 17 percent by 2020, 42 percent by 2030 and 83 percent by 2050.[21] As the electricity generation sector comes under increasing pressure to reduce carbon dioxide emissions, the pressure on forests to provide "carbon neutral" biomass fuel will also increase. Here's why:

Coal-fired power plants are the largest source of electricity generation in the United States, providing more than 50 percent of the national total,[22] and coal is by far the greatest source of carbon dioxide

---

19 Intergovernmental Panel on Climate Change, 2006. IPCC Guidelines for National Greenhouse Gas Inventories. Volume 4: Agriculture, Forestry, and Other Land Use. Chapter 4: Forest Lands.

20 Searchinger et al, 2009.

21 Energy Information Administration. Energy Market and Economic Impacts of H.R. 2454, the American Clean Energy and Security Act of 2009. SR/OIAF/2009-05. July 2009. Washington, DC.

22 Testimony of Dr. Richard Newell, Administrator, Energy Information Administration, U.S. Department of Energy, before the Committee on Energy and Natural Resources, United States Senate. October 14, 2009.

from the sector. Because prospects for large-scale carbon capture and sequestration remain a distant illusion, co-firing (replacing some coal with biomass) or "re-powering" (complete conversion to burn only biomass[23]) provide the only real opportunity for the coal power industry to claim it is reducing carbon emissions.[24]

there are also significant financial benefits to replacing coal with biomass

There are also significant financial benefits to replacing coal with biomass. Beyond benefiting from tax incentives and other federal programs designed to promote biomass use, power plants receive renewable energy credits based on the proportion of power they generate using biomass, eliminating the need to buy credits elsewhere. In addition, under regional carbon cap-and-trade schemes such as the Regional Greenhouse Gas Initiative (RGGI) in the Northeast, power plants do not have to purchase emission allowances for the carbon dioxide they emit from burning biomass, an exemption that would also apply at the federal level if a national cap and trade program is enacted. Many coal plants already have the capability to co-fire biomass,[25] and proposals for co-firing and re-powering have increased dramatically.

Trees will be the biomass fuel of choice

There are four primary categories of biomass fuel: "urban wood" (primarily construction and demolition waste, but EIA also includes urban tree trimmings and mill residues); agricultural residues (corn stover, wheat straw, and materials from "a number of other major agricultural crops"[26]); energy crops (such as switchgrass and willows); and forestry residues.

EIA uses price-supply curves to estimate the availability of various biomass fuels. At maximum availability for all categories, EIA estimates that 4.1 percent of the fuel supply would come from urban wood and mill residues, 16.5 percent from agricultural residues, 24.2 percent from forest wood and 55.1 percent from energy crops.

---

23 Interestingly, as noted on the website for Mississippi Power, "Re-powering an existing plant typically results in the loss of about 50 percent of the current generating capacity due to the low heating value of biomass compared to natural gas or coal." (http://www.mississippipower.com/topic_renewable/biomass.asp).

24 The idea that biomass co-firing can reduce carbon dioxide emissions at coal plants appears in Congressional testimony from the Acting Administrator of EIA in February 2009. "The impact on carbon dioxide emissions, which are not currently constrained by a cap-and-trade system or otherwise regulated at the Federal level, largely depends on the fuels and generators being displaced -- carbon dioxide reductions are significantly larger when coal is displaced than when natural gas is displaced. Certain renewables, such as biomass co-firing at existing plants, directly displace coal use." (Testimony of Dr. Howard Gruenspecht, Acting Administrator, Energy Information Administration, before the Subcommittee on Energy and Environment, Committee on Energy and Commerce, U.S. House of Representatives, February 26, 2009.)

25 Energy Information Administration, 2009. Form EIA-860 Database: 2007 Annual Electric Generator Report.

26 Energy Information Administration. Model documentation: Renewable fuels module of the National Energy Modeling System. DOE/EIA-M069 (2009), July 2009. Washington, DC. Additional documentation of some of the assumptions behind NEMS modeling is available at http://www.eia.doe.gov/oiaf/aeo/assumption/renewable.html.

EIA assumes no social or environmental constraints on any fuel source, no conflicting demands on resources (such as competition for agricultural residues between biomass power and biofuels production),[27] and the availability of significant amounts of land to grow biomass energy crops as well as the technology and infrastructure to harvest and transport them.

energy crops do not currently exist; to grow the amounts needed for biomass power would require putting millions of acres under cultivation

These estimates are significantly too optimistic. Urban wood, consisting primarily of construction and demolition waste, must be sorted to remove pressure-treated lumber and other contaminants, a requirement that raises costs. Mill residues are already allocated to existing uses; only about 1.5 percent of the supply is currently unused and available for power generation.[28] Collection and processing of agricultural residues into forms useable as biomass fuel requires specialized infrastructure that does not currently exist and may not be cost-effective. Additionally, if technology for generating ethanol from cellulosic sources becomes widespread, the nation's ethanol mandate will likely absorb most existing supplies of agricultural residues. Energy crops do not currently exist; to grow the amounts needed for biomass power would require putting millions of acres under cultivation. (Some of these caveats are acknowledged in EIA's documentation: see Appendix B for a detailed explanation of the constraints on fuel availability.)

The amount of "forestry residues" considered available by EIA is also a large overestimate. EIA's estimate includes "logging residues" as defined by the Forest Service.[29] These are unmarketable low-diameter materials and "cull" (unmarketable) trees cut in the course of harvesting that, if left to decompose, will emit carbon dioxide equivalent to the amount produced by burning them. However, as defined for the EIA biomass modeling inputs dataset,[30] the forest residues category also includes part of the massive national inventory of *standing* cull trees, as well as standing inventories of "excess small pole trees."[31] Because the Forest Service inventory includes standing cull trees on potentially

---

27 EIA model documentation states that significant uncertainty exists regarding the true availability of agricultural residues, due both to potential competition with the biofuels industry and because the infrastructure for collection and processing of these materials does not currently exist (Energy Information Administration. Model documentation: Renewable fuels module of the National Energy Modeling System. DOE/EIA-M069 (2009), July, 2009.)

28 Smith et al, 2007.

29 The category of logging residues as defined by the Forest Service data includes virtually anything "sound enough to chip" other than the commercial roundwood removed by harvesting. It includes "growing–stock volume cut or knocked down during harvest but left at the harvest site" and "wood volume other than growing stock cut or knocked down during harvest but left on the ground. This volume is net of wet rot or advanced dry rot and excludes old punky logs; consists of material sound enough to chip; includes downed dead and cull trees, tops above the 4–inch growing–stock top, and smaller than 5 inches d.b.h. (diameter at breast height); excludes stumps and limbs." Cull trees are unmarketable because of rot, roughness, or species (Smith et al, 2007).

30 Walsh, M., et al. 2000. Biomass feedstock availability in the United States: 1999 state level analysis. Prepared for EIA; available at http://bioenergy.ornl.gov/resourcedata/index.html

31 The term "excess small pole trees" does not occur in the glossary of terms included with the Forest Service forest

harvestable forest land, whether or not this land is likely to be logged, the estimated supply of potentially harvestable cull and pole trees vastly exceeds the amount of true logging residues that are actually generated each year. [32]

The Energy Information Administration's definition of forestry residues – hidden in plain sight in government documents – is congruent with the wording of ACESA, which defines whole trees, along with logging residues, as "renewable biomass." (see Appendix A for the relevant sections of legislation). It should be emphasized that EIA's expansion of the pool of available "residues" to include standing timber contravenes the standard approach taken in a National Renewable Energy Laboratory report on biomass availability,[33] which excluded increased harvesting of standing timber from the available forest biomass pool.

Because it includes a portion of the standing cull and pole tree inventories, the EIA estimate of potentially available forest wood is about three times greater than the supply of currently generated logging residues alone. Thus, *the majority of forest biomass supply in the EIA model consists of trees that would be cut specifically for power generation*. This will dramatically increase logging above current levels and significantly increase greenhouse gas emissions from the "renewable" power sector. By employing more realistic assumptions about the availability of existing biomass fuels, EWG's analysis determined that even more forest cutting would be required than EIA projects.

The impact of a federal renewable energy standard

To determine how increased deployment of biomass power will increase forest cutting and carbon dioxide emissions, EWG analyzed EIA's scenarios for biomass power development under a federal renewables portfolio standard for electricity. We also examined the impacts of currently proposed biomass power, biofuels and wood pellet facilities.

---

inventory dataset but presumably refers to some portion of the standing stock of poletimber, which is defined as "live trees at least 5.0 inches in d.b.h but smaller than sawtimber trees" and which, along with seedling-sapling stands, comprise the "core of the merchantable forests of the mid-21st century" (Smith et al., 2007)

32 Documentation for the ACESA scenarios, available at http://www.eia.doe.gov/oiaf/aeo/assumption/renewable.html, makes it clear that new logging will be required to provide biomass fuel: "Fuel supply schedules are a composite of four fuel types: forestry materials, wood residues, agricultural residues and energy crops. Energy crop data are presented in yearly schedules from 2010 to 2030 in combination with the other material types for each region. The forestry materials component is made up of logging residues, rough rotten salvageable dead wood, and excess small pole trees. The wood residue component consists of primary mill residues, silvicultural trimmings and urban wood such as pallets, construction waste, and demolition debris that are not otherwise used. Agricultural residues are wheat straw, corn stover and a number of other major agricultural crops. Energy crop data are for hybrid poplar, willow, and switchgrass grown on crop land, pasture land, or on Conservation Reserve Program lands."

33 Milbrandt, A. A geographic perspective on the current biomass resource availability in the United States. National Renewable Energy LaboratoryTechnical Report NREL/TP-560-39181. December, 2005. Golden, CO.

EIA modeled total electricity sector development as it would occur under the RPS specified in the House-passed ACESA, which anticipates a significant ramp-up in renewable power generation. EWG analyzed two sets of projections from EIA – one that models the effect of ACESA if enacted as written, and one that achieves the maximum reduction in greenhouse gas emissions by 2025. This is achieved with the assumption that no international carbon sequestration projects will be permitted as "offsets" for domestic emissions, thus forcing greater emissions reductions in the U.S. These reductions would be achieved in part by a substantial increase in biomass co-firing at coal plants, and in the longer term with an 84 percent increase in nuclear power generation by 2025 and a 230 percent increase by 2030 (even under the "basic" case, the EIA projects at 44 percent increase in nuclear power by 2025 and a 91 percent increase by 2030[34]).

EIA's projection include projected impacts of the 2009 American Recovery and Reinvestment Act, as well as other energy laws

EIA measures the potential effects of ACESA against a reference case. Although this "business-as-usual" scenario is EIA's projection of power sector development in the absence of a federal RPS, it does include projected impacts of the 2009 American Recovery and Reinvestment Act (ARRA) as well as other significant energy laws, including the Energy Improvement and Extension Act of 2008, the Energy Independence and Security Act of 2007 and the Energy Policy Act of 2005[35]. All these pieces of legislation promote renewable energy development to some extent.

EIA's estimate of biomass availability already depends on increasing whole-tree harvesting. But EIA appears to dramatically overestimate the availability of other kinds of biomass fuels as well, assuming no social or environmental constraints, no conflicting demands on resources (such as competition for agricultural residues between biomass power and biofuels feedstock)[36] and availability of significant amounts of land to grow biomass energy crops. If these assumptions are incorrect, it is extremely likely that more forests will be cut for biomass fuel than are currently projected, as only forest biomass can fill the gap between projections and reality.

EWG's analysis introduced constraints on EIA's assumptions about biomass availability, describing a likely range for each fuel category by specifying a "high" and "low" availability factor that modifies the amount of biomass in the basic dataset. We then estimated what these constraints would mean for the demand for forest wood to serve as biomass fuel (where availability of biomass is low, demand for new forest cutting will be high). Our assumptions were as follows (for a detailed explanation of how we arrived at these values, see Appendix B):

---

34 Projections from EIA's AEO2009 National Energy Modeling System run hr2454noint.d072909 and AEO2009 National Energy Modeling System run hr2454cap.d072909a.

35 Testimony of Dr. Richard Newell, Administrator, Energy Information Administration, U.S. Department of Energy, before the Committee on Energy and Natural Resources, United States Senate. October 14, 2009.

36 EIA model documentation states that significant uncertainty exists regarding the true availability of agricultural residues, due both to potential competition with the biofuels industry, and also because the infrastructure for collection and processing of these materials does not currently exist (Energy Information Administration. Model documentation: Renewable fuels module of the National Energy Modeling System. DOE/EIA-M069 (2009), July, 2009.)

Table 1. Non-tree Biomass Supplies Are Limited

Biomass is sought for other uses. Percentage of each source available as fuel for power plants is shown for two scenarios, assuming either high or low availability.

	Low availability	High availability
Urban wood	25%	75%
Mill waste	42%	42%
Agricultural residues	25%	50%
Logging residues	24%	24%

Percentage of EIA's estimates of existing wood and agricultural residues that the EWG re-analysis assumes are actually available. The estimate of logging residue availability is based on the Forest Service estimate of currently generated logging residues, and not EIA's estimate, which includes whole-tree harvesting along with currently generated residues. Under a "high availability" scenario, there is less need for additional forest cutting to meet fuel needs. Bracketing the extremes of low and high fuel availability defines the limits to EWG's estimates (see Appendix B for details).

For its analysis, EIA combined logging residues and increased whole-tree harvesting of cull trees and "excess pole trees" into a single estimate of forest biomass availability. In order to determine the amount of whole-tree harvesting that would be required above current cutting levels, EWG assumed that the forest wood category includes just true logging residues as defined by the Forest Service – that is, the amount of low diameter material and unmarketable trees currently cut each year. This allowed us to calculate the size of the fuel deficit that would be met by increased whole-tree harvesting.

Our approach assumes that currently generated logging residues are the only source of forestry wood that can be used for biomass fuel without significantly increasing carbon dioxide emissions, because their use does not generate greenhouse gas emissions beyond what would be generated if these materials were left to decompose on the forest floor. However, we do not assume that logging residues are "carbon neutral" in any meaningful sense, since burning them emits an instantaneous pulse of carbon dioxide, while natural decomposition would occur over a matter of years while maintaining soil nutrient status and building soil carbon.[37]

37 Advocates of using logging residues for biomass fuel sometimes claim that allowing logging residues to decompose in the forest actually produces more greenhouse gas emissions than collecting and burning them, because decomposition can involve bacterial methane production, and methane is a more powerful greenhouse gas than carbon dioxide. To the extent that this occurs, however, the phenomenon has likely been significantly overstated. In fact, bacterial methane production during decomposition occurs under low oxygen conditions that occur mostly in wetland soils, and not in the well-aerated conditions of uplands where most logging residues are found. Additionally, another group of bacteria consumes methane produced in forest soils, so that some soils actually act as net sinks for methane, consuming more than is produced locally. Bacterial methane production in upland environments is not even considered important enough to be included in EPA's listing of methane sources (http://epa.gov/methane/sources.html), which focuses on methane production in wetlands. Methane production from termites can occur in upland areas, but again, bacterial consumption of methane also occurs. In all, net methane flux to the atmosphere from decomposition of logging residues is poorly characterized, and the "methane myth" that decomposition of forest residues emits more greenhouse gases than combustion of those residues is not backed up by credible science.

Because every state with a renewable electricity mandate includes biomass power as an eligible technology, and many incentives for biomass power development already exist, biopower proposals have already increased dramatically. To assess the emerging demand for wood fuel at bioenergy facilities, EWG used commercially available data to analyze current proposals for biomass power, wood pellet and liquid biofuels plants that plan to use wood as feedstock.

V. Why Burning Trees is Worse than Burning Coal

Unfortunately, cutting and burning trees for power actually emits *more* carbon than burning fossil fuels per unit of energy generated. Because wood and other biomass materials have a very low energy density, and because biomass power plants are significantly less efficient than gas and even coal plants, carbon dioxide emissions from biomass per unit of energy generated are about 1.5 times higher than from coal and three to four times greater than from natural gas.

Biomass plants are extremely inefficient. Large-scale biomass power plants typically operate at less than 25 percent efficiency, meaning that for every four tons of wood burned, one ton is converted into electric power -- but all four tons emit carbon dioxide. The more forest biomass is used to replace fossil fuels, the more greenhouse gas emissions will increase.

Cutting forests to burn trees in power plants is actually a global warming double whammy. An intact forest sequesters atmospheric carbon dioxide into new growth each year. Following logging, it takes decades to rebuild the lost biomass. This results in a net increase in atmospheric carbon dioxide levels, just as biomass burning does. The double impact of wood burning for energy, both from smokestack emissions and reduction of the forest carbon "sink" for atmospheric carbon, is occurring just when reducing carbon emissions is most urgent.

Figure 4: Forest regrowth takes decades

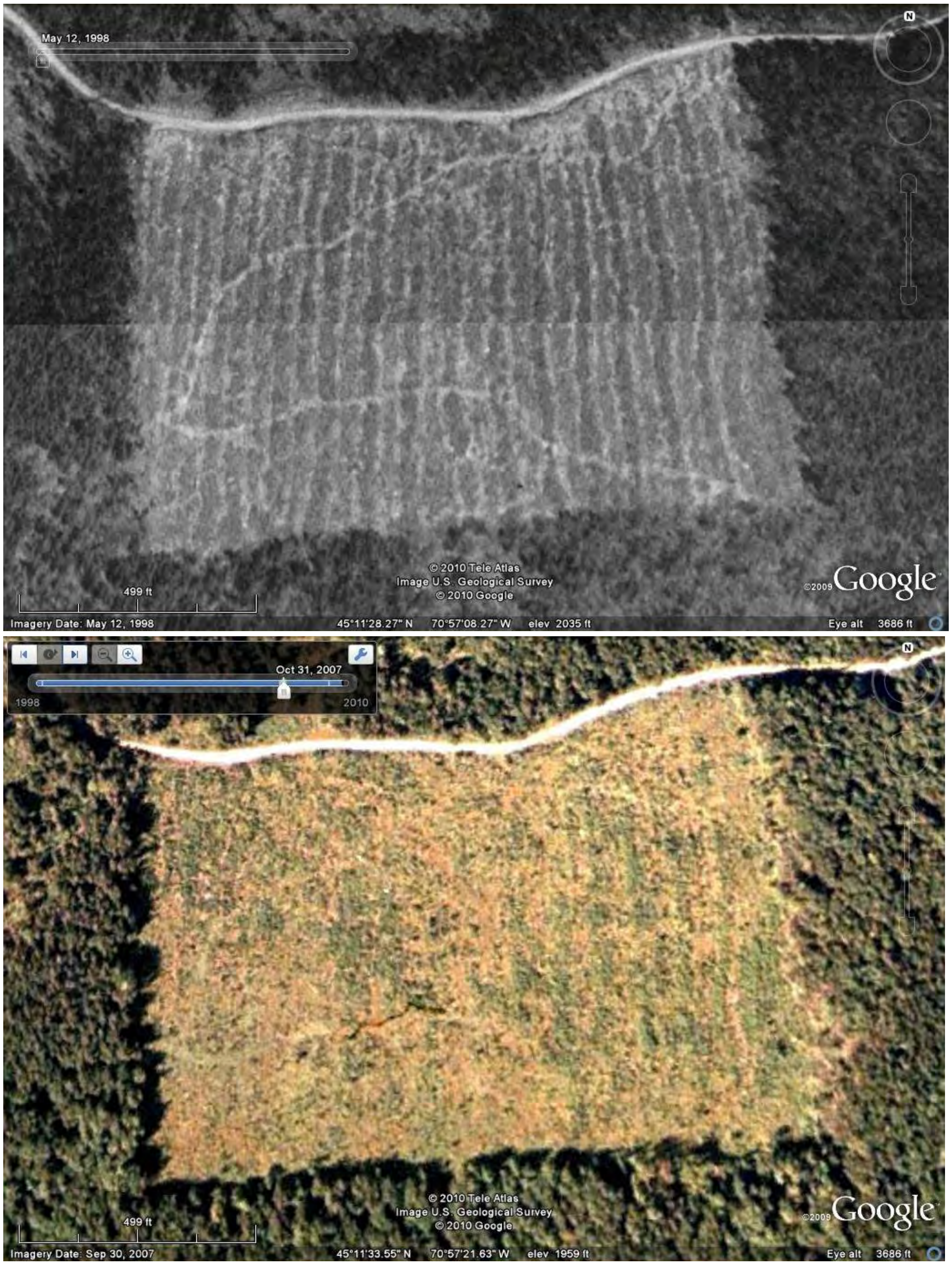

Satellite images of Maine's Boundary Mountains region show that in this tract, logged sometime before 1998, trees had not yet returned after 10 years to take up carbon released by logging. According to Forest Service data (Smith et al, 2007), the trees from this 25-acre clear-cut would be sufficient to fuel one 50 megawatt biomass plant for only about 21 hours. Source: Google Earth images, 1998 and 2007.

VI. Demand for Bioenergy Will Put More Pressure on Forests

A surge in proposals for biomass power, wood pellet and biofuels plants that use wood for feedstock is already underway in the United States, spurred by state renewable electricity standards and existing federal tax policies even in the absence of a federal renewables standard or climate legislation. At least 118 new wood-burning facilities[38] and biomass co-firing operations are currently proposed, representing about 5,830 MW of capacity.[39] Total proposed capacity is thus almost double existing capacity.[40] The average size of proposed direct-fired biomass plants is 39 MW, about a third larger than the average capacity of existing plants. Total wood demand for this amount of biopower will be about 71 million green tons per year.

The market for wood pellets is also expanding dramatically, both domestically, where use is primarily in the residential heating market, and internationally, where biomass is in demand for power generation.[41] About 60 new wood pellet plants are currently proposed or under construction in the United States, with a combined wood demand of about 21 million green tons per year.[42] Wood pellets are mostly produced from mill residues or whole-tree harvesting, not logging residues.[43] Some coal plants that are proposing to co-fire biomass have found that in order to meet emissions requirements, they can only burn pellets or chips made with white, interior bolewood of trees that does not include any bark or low-diameter material.[44]

Due to their composition and cost of production, wood pellets typically sell for around ten times the cost of unprocessed woodchips.[45] Nonetheless, international demand is exploding. In Great Britain alone, proposals for 3,070 MW in direct-fired biomass projects represent an order of magnitude increase over current generation, a figure that does not include power generated from biomass co-

---

38 Development costs for proposed direct-fired plants will total about $12.5 billion.

39 Some biomass co-firing proposals do not yet specify the percentage coal that will be replaced. We estimated 10 percent co-firing in these cases.

40 As of 2008, there were 151 operating facilities representing 2,910 MW of biomass power in the United States whose primary fuel is "wood solids," and another 153 facilities, representing 4,263 MW, where wood liquors from pulp and paper manufacturing are the primary fuel. Of these, 80 facilities, representing 2,305 MW of generation, use wood solids as a secondary fuel. (Energy Information Administration. Existing electric generating units by energy source, 2008)

41 Under a European Union directive that member states must generate 20 percent of their electricity from renewable sources by 2020, Great Britain and Europe plan a massive ramp-up of biomass power.

42 RISI Wood Products Database, 2010.

43 Many pellet companies utilize only stemwood for pellets, finding that bark and residue material produce too much ash when pellets are combusted. (Grard, L.. Pellet-producing plants going strong. *Kennebec Journal*, November 1, 2009.)

44 Notes from Ohio Solid Biomass Work Group meeting, March 12, 2010. Representatives of First Energy, which owns the Burger coal plant, stated that burning significant amounts of agricultural residues or any wood other than white interior wood would make it difficult to meet emissions requirements.

45 http://www.woodpelletprice.com

firing. Most new biomass plants will be located near deep-water ports that can accommodate marine shipments of fuel from remote locations. Green Circle Energy of Georgia, which at a production capacity of 560,000 tons per year is the largest pellet plant in the nation, ships exclusively to Europe.

Proposals for biofuels plants will also place new demands on forests. Currently, there are eight plants proposed in the United States that would use wood for feedstock, with a combined wood demand of about 3.6 million tons, but the projected demand for cellulosic biofuels feedstock is increasing. The total projected wood demand for biopower, pellet, and biofuels proposals is about 92 million green tons.

Figure 5. Wood demand for projects in the pipeline is already increasing

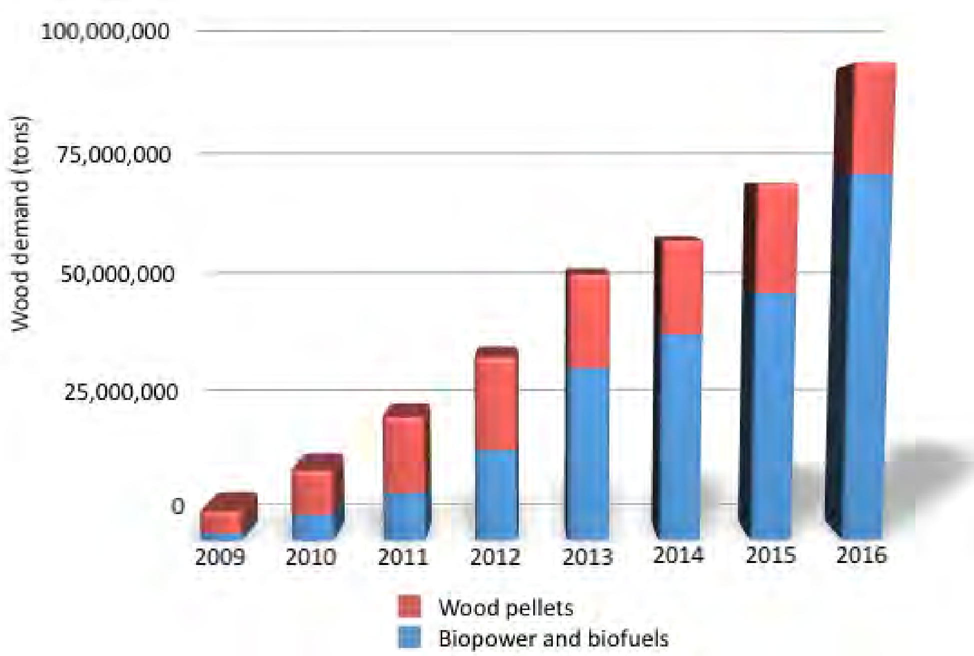

Cumulative wood demand for proposed biomass power, biofuels and wood pellet projects. Projects without firm start dates were classified as starting in 2015 and 2016 for purposes of this illustration. To the extent that biopower facilities use wood pellets from new capacity, demand projections may be overstated. However, the international market and the residential and commercial heating markets for pellets are also expanding rapidly. (Source: RISI Wood Products database; EWG research).

VII. Biomass Power Development Will Cost Taxpayers Billions of Dollars

Biomass power is eligible for tax credits and direct subsidies from the federal government.[46] Currently, the federal renewable energy production tax credit (PTC) for biomass power[47] is set at 1.1 cents per kilowatt-hour, a rate that reduces the tax burden of a typical 50 MW plant by about $4.4 million,[48] or about $96,360 for every megawatt of biomass at a coal plant or a direct-fired plant. Facilities can receive the PTC for a period of five years.[49] The Congressional Budget Office estimated that lost tax revenues from the biomass PTC at $1.5 billion for 2009 – 2013 under a business-as-usual scenario; if biomass power development accelerated as envisioned by EIA's ACESA scenario, the total cost of the biomass PTC over the next five years would be about $3.5 billion, and about $10.5 billion over the next fifteen years.

Instead of taking the production tax credit, biomass developers can elect to take an investment tax credit created under the 2009 American Reinvestment and Recovery Act (ARRA), which reimburses 30 percent of plant development costs if the plant begins operation within a certain period. Many of the plants currently proposed are eager to begin construction as soon as possible to qualify within the eligibility window for this program, which will yield a $30 million to $75 million savings for a typical utility-scale biomass plant.[50]

Besides avoiding tax payments, direct-fired and co-fired biomass plants also avoid the expense of purchasing carbon emission allowances. Existing cap-and-trade schemes such as the Regional Greenhouse Gas Initiative (RGGI) in the Northeast and the proposed federal cap-and-trade program require facilities to pay for every ton of carbon dioxide they emit, funds that are returned to the states under the regional programs to support energy efficiency and renewable power initiatives. Biomass emissions are exempted from regulation due to the assumption of carbon neutrality, resulting in substantial savings to the industry; for instance, a typical 50 MW biomass power plant would avoid payments of $58 million over the initial five-year period of a federal carbon pricing scheme starting in 2012, a savings that would increase to $110 million for the 2021 – 2025 period.[51]

besides avoiding tax payments, direct-fired and co-fired biomass plants also avoid the expense of purchasing carbon emission allowances

46 The incentives for biomass power development at the state level are too numerous to mention in this report, but the DSIRE database (http://www.dsireusa.org/) provides a comprehensive listing.
47 Rate for open-loop biomass
48 Kotrba, R. The Power of Association. *Biomass Magazine*, June, 2008.
49 The biomass industry is currently lobbying to have this period extended.
50 Our survey of plants under development determined that typical development costs for utility-scale plants are $100 million to $250 million, although some proposals are significantly higher.
51 EIA includes carbon allowance pricing in its modeled projections. Under the basic scenario, of the allowance price

Regulating biomass emissions would increase cumulative covered emissions by up to 17 percent by 2025 and would represent a staggering $129 billion in carbon allowance value, although the total would be somewhat smaller to the extent that emissions from some plants are probably lower than EPA's proposed threshold value for regulation and thus would not be covered under the cap.[52] Allowance payments from biomass facilities could potentially be refunded to the extent that facilities were able to demonstrate that they were not adding net carbon to the atmosphere. Currently, funds from purchase of allowances under regional cap and trade programs like RGGI are returned to the states, and the revenue lost by not regulating biomass emissions is an increasing proportion of total potential revenues.

biomass power facilities and fuel suppliers also benefit from direct payments

Biomass power facilities and fuel suppliers also benefit from direct payments. Facilities burning biomass can generate Renewable Energy Credits (RECs),[53] selling them or using them to meet their own renewable power purchase requirements. At recent REC prices, which have been volatile, a typical 50 MW plant generates about $3 million to $20 million in credits per year. Assuming a rate of $0.05 per kWh, facilities burning biomass would receive about $47.2 billion in revenue from RECs from 2014 – 2018 under the basic ACESA scenario.

Biomass suppliers are also eligible for the Biomass Crop Assistance Program, a federal program administered by the U.S. Department of Agriculture that matches what facilities pay for fuel, paying suppliers up to $45 per dry ton (about $25 per green ton). The program has been extremely popular; $517 million of taxpayer money was allocated for the first quarter of 2010.[54]

---

for a ton of carbon dioxide will rise from $16 in 2012 to $41 in 2025. Projections from EIA's AEO2009 National Energy Modeling System run hr2454cap.d072909a.

52 EPA's proposed rules for carbon regulation would exempt new facilities emitting less than 100,000 tons of carbon a year.

53 Purchase of Renewable Energy Credits or Certificates (RECs) from renewable power producers allows buyers to claim avoidance of the environmental impacts of their electricity, since the REC represents a specific amount of avoided greenhouse gas emissions. The price of RECs is partially tied to the difference between the cost of production at a renewable energy facility and the price offered for power sold to the grid. The RECs can be sold separately from the power itself, which is fed into the grid and becomes indistinguishable from power generated from conventional sources. RECs thus essentially serve as a demonstration that a certain amount of power has been generated from renewable sources. Every megawatt-hour of electricity generated from a renewable source is assigned a REC with a tracking number, allowing transfers between buyers and sellers to be monitored. Once a final owner makes a claim, the REC is retired. Regional tracking systems across the United States allow RECs generated in one part of the country to be purchased in another.

54 Wood Resources International LLC. Forest products market update, January 2010. www.woodprices.com.

VIII. State Policies are Creating Biomass Power Hotspots

Biomass power development at the state level is not waiting for a federal renewables portfolio standard. Currently, 37 states and the District of Columbia have some form of Renewable Electricity Standard or renewable generation goal,[55] and all include biomass as an eligible technology. In 2007, 45 states in the continental United States generated some power from renewable sources (including wood and wood-derived fuels,[56] wind, solar and geothermal). Of these, 24 depended on wood and wood-derived power to provide at least 50 percent of that renewable power.[57] What follows is a closer look at five forested states where biomass power is at various stages of development. Given the "substantial and sustained net loss of forest cover"[58] that has occurred in eastern forests over the last three decades, further forest loss should be taken very seriously.

Maine – furthest down the biopower road

Biomass power is already a major component of Maine's electricity supply, providing about 24 percent of the state's power in 2007[59], a pace well ahead of EIA's modeling estimate that approximately 16 percent of Maine's power would come from biomass by 2030.[60] This commitment has profound implications for Maine's greenhouse gas emissions.

On paper, greenhouse gas emissions from Maine's electricity generation sector[61] are relatively low, for several reasons: Emissions from biomass burning are not counted, and the state generates about 23 percent of its electricity from hydropower, which has no stack emissions. Maine gets another 41 percent of its power from natural gas, which has the lowest emissions per unit energy of any fossil fuel. Maine's total reported emissions from power generation were 5.57 million tons of carbon dioxide in 2007.[62]

But these figures are misleading. If stack emissions from biomass power generation were counted, it would more than double total emissions from the power sector, contributing an additional 7.9

55 Database of State Incentives for Renewables and Efficiency; http://www.dsireusa.org
56 Includes "wood liquors" used as fuel, by-products of the paper and pulp industry
57 Energy Information Administration. 1990 – 2008 Net generation by state by type of producer by energy source (EIA 906) (available at http://www.eia.doe.gov/cneaf/electricity/page/capacity/capacity.html).
58 Drummond, M. and Loveland, T. 2010. Land-use pressure and a transition to forest-cover loss in the Eastern United States. Bioscience 60:286-298.
59 Ibid. For 2007, Maine had about 615 MW of biomass power operating, which provided 3.85 billion kWhrs of electricity.
60 This goal is approximate, and is based on EIA's modeling for the New England region, in which Maine is located.
61 Energy Information Administration. 1990 – 2008 U.S. electric power industry estimated emissions by state (EIA-767 and EIA-906).
62 Ibid.

million tons of carbon dioxide each year.[63] Total lifecycle emissions, including the reduced carbon sequestration capacity of logged forests, would be even higher.

Maine's commitment to wood-fueled power is not surprising, given the importance of the forest products industry to the state. Some basic math shows that even in Maine, the biomass power industry does not run just on logging residues but relies also on whole tree fuel. Shortages of wood and favorable economics have also led the state to permit importation and burning of construction and demolition waste from other states. Neither whole tree fuel or construction and demolition waste can be considered carbon neutral.

if stack emissions from biomass power generation were counted, it would more than double total emissions from the power sector

The amount of mill residues and logging residues generated in Maine in 2006 was almost exactly equal to the total amount of wood from all sources burned in biomass plants in 2007, meaning that it would take 100 percent utilization of all potentially available of sources of residues to provide the biomass fuel needed in the state. But 100 percent utilization is impossible, since mill residues have greater economic value and are used in other applications,[64] and logging residues are not completely collectable. The shortage has to be made up with whole tree fuel.

Evidence on the ground supports this conclusion. As is the case for the proposed federal energy legislation (see Appendix A), Maine does not distinguish between biomass fuel from logging residues and whole tree fuel. The state's forest cutting practices allow clear cuts of up to 250 acres for "forest products," the definition of which includes biomass fuel.[65] The result is not only whole-tree but also "whole forest" removal, with the biomass industry providing a market for as much material as can be removed from a site. Cutting is also increasing to provide material to the state's growing wood pellet industry, which currently supplies the domestic home heating market and is growing, partially in response to increasing European demand.[66] Current and proposed pellet mills in the state will require at least 840,000 green tons by the end of 2010.[67]

As recently as 2002, Maine was cutting about 10 percent more timber than it was growing, and

---

63 We took the total number of MWhrs reported by EIA as having been generated from woody fuels in Maine in 2007, and converted this to fuel use by assuming 8600 BTU/lb wood (bone dry; EIA's estimate). We assumed wood is 50 percent carbon.

64 Canfield, C. Mill, Waste No Longer Just Dust in the Wind. Associated Press, April 3, 2008. This article reports that the price of sawdust to dairy farmers who use it as bedding had gone from $800 to upwards of $1400 for a trailer load between 2007 and 2008.

65 Maine Department of Conservation. 1999. Forest regeneration and clearcutting standards. Available at http://www.maine.gov/doc/mfs/pubs/htm/fpafnl.htm#SECTION 5.

66 Spelter, H. and Toth, D. 2009. North America's wood pellet sector. United States Forest Service Forest Products Laboratory, FPL-RP-656.

67 RISI Wood Products Database, 2010.

removals plus mortality were 165 percent of net growth,[68] meaning the state's forests as a whole were serving as a net carbon source, not a carbon sink. As of the 2007 forest inventory, cutting had slowed somewhat but removals were still 84 percent of net growth, and removals plus mortality were 130 percent of net growth.[69] Increasing demand for bioenergy wood may drive Maine forests even further into the red.

Figure 6. Clear-cutting for biomass energy in Maine

Biomass clear-cut in the Moosehead Lake region, Maine, 2009. (credit. James Wallace)

Massachusetts – thinking twice about biopower

With only one utility-scale (17 MW) biomass plant, as well as a few small plants primarily operated for thermal power, Massachusetts has not been a hotspot of biopower until recently. However, the simultaneous consideration of four large-scale wood-powered projects – two biomass plants that would burn forest wood, one that would burn about 80 percent construction and demolition debris, and a proposal to repower the 120 MW Somerset coal plant with construction and demolition debris – caught the attention of citizens concerned about forest cutting, carbon emissions and air pollution.

68 Smith et al, 2007.
69 Ibid.

The combined generation of the four proposals would be 255 MW, or about 1.9 percent of the state's total generating capacity. Excluding the power that would be generated by burning construction and demolition waste, the amount of power to be fueled by forest biomass would be about 105 MW.

Only about 106,000 tons of total forest residues were generated in the state in 2007, enough to fuel about 8 MW of biomass power, so additional biomass to fuel these plants would likely come from increased forest cutting. Expert testimony submitted to the state suggested that fuel demand from these large plants would require the equivalent of heavily logging every eligible forest acre in the state within less than 20 years, and that fuel demand from even one of the plants would require doubling the rate of forest cutting in the state.

fuel demand from these large plants would require the equivalent of heavily logging every eligible forest acre in the state within less than 20 years

In response to objections from citizens and environmental groups, the state commissioned a sustainability study of biomass power and suspended biomass' eligibility for the state's Renewables Portfolio Standard pending its completion.

Massachusetts also provides insight into the limitations of burning so-called urban wood (primarily construction and demolition waste) for power generation. In 2009, citizens protested potential pollutant emissions from burning construction and demolition debris at a plant proposed in the city of Springfield, which has environmental justice[70] concerns over high asthma levels and high incidence of elevated blood lead levels in children.[71]

In response to objections raised by environmental groups, citizens and the Massachusetts Bureau of Environmental Health, the state suspended permitting of facilities that would burn construction and demolition debris pending completion of a statewide environmental and health impacts study. Lending its voice to the issue, the Massachusetts Medical Society passed a resolution opposing large-scale biomass plants on the grounds that they would increase air pollution[72] and present an unacceptable risk to public health.

---

70 Lower-income and minority communities suffer from a disproportionately high share of environmental burdens and at the same time lack environmental assets in their neighborhoods. The State of Massachusetts defines an environmental justice community as a neighborhood where median annual household income is at or below 65% of the statewide median income; 25% or more of the residents are a minority; 25% or more of the residents are foreign born; or 25% or more of the residents are lacking English language proficiency. http://www.mass.gov/envir/smart_growth_toolkit/pages/mod-ej.html

71 Letter from Suzanne Condon, Director, Massachusetts Bureau of Environmental Health, to Daniel Hall, Executive Office of Energy and Environmental Affairs, November 19, 2009.

72 Massachusetts Medical Society adopts policy opposing biomass power plants. Press release, Massachusetts Medical Society, December 9, 2009.

Florida and Georgia – headlong into biopower

Florida and Georgia are in the heart of the Southeastern wood products industry and are home to a number of existing biopower facilities that utilize byproducts of pulp and papermaking to generate heat and power. Both states are also seeing a dramatic increase in proposals for utility-scale biomass power plants and wood pellet plants.

Table 2. Proposed biomass power plants and pellet plants, Florida and Georgia

	Florida	Georgia
Existing biopower[73] (MW)	382	643
Biopower proposals (number of facilities)	9	14
Biopower proposals (MW)	679	846
Wood demand, new biopower (million green tons)	8.2	10.3
New pellet plant proposals, number of facilities	1	7
Pellet plant wood demand (million green tons)	1.1	6.6
Total new wood demand (million green tons)	9.4	15.4
Available logging residues (million green tons)	2.7	7.5

The biomass industry is fully aware that the amount of wood currently being cut is not sufficient to provide fuel for all the proposed biomass plants. In August 2009, Biomass Magazine reported that, "Hardly a day passes in the Southern U.S. without an announcement of a new bioenergy facility or expansion of an existing one… What is increasingly obvious is that the amount of truly available logging residues will be nowhere near enough to supply the current and announced bioenergy processors in the Southern U.S… The increasing scale of forestry biomass for bioenergy will only be possible with developments in forest bioenergy plantations as there will be insufficient feedstock from logging residuals for all announced and planned facilities."[74]

the minimum time for resequestration of the carbon released by burning trees for power is more than 25 years

More than 34 percent of Florida's forests and 30 percent of Georgia's forests already consist of intensively managed plantations.[75] Creation of new "energy wood" plantations will likely further reduce native forests, as the amount of agricultural land available for afforestation is increasingly limited, and a more lucrative market for energy crops grown on agricultural lands is emerging.

73 According to EIA data, the large majority of existing biopower facilities in Georgia and Florida use wood liquors as their primary fuel, not wood solids.
74 Gonzales, R., et al. Filling a Need: Forest Plantations for Bioenergy in the Southern US. *Biomass Magazine*. August 2009.
75 Smith et al, 2007.

Wood from even fast-growing plantations cannot be considered a low carbon fuel. Typical Southern pine plantations are usually thinned at 15 years and are harvested completely at around 25 years.[76] Even under such tight harvest cycles, the minimum time for resequestration of the carbon released by burning trees for power is thus more than 25 years,[77] not even accounting for the loss in overall carbon storage involved in conversion of native forests to pine plantations, which can be significant.[78] The proposed increase in biomass power in the Southeast will therefore represent a significant increase in carbon emissions.

Ohio – using biopower to consolidate a commitment to coal

despite claims that various fuels could be employed, including agricultural residues, it is clear that wood will constitute the lion's share

Ohio generates more than 85 percent of its electric power from coal and has more coal-fired generation any state but Texas.[79] It also has the second highest power sector greenhouse gas emissions. To help meet an ambitious goal of producing 25 percent of its power from renewable resources by 2025, Ohio is choosing to co-fire biomass at coal plants. The state has created further incentives for co-firing by granting extra renewable energy credits for power generated at facilities above 75 MW that "primarily" use biomass.[80]

Ohio's Public Utilities Commission is currently considering proposals for renewable energy certification from seven coal plants that plan to co-fire biomass at varying percentages, as well as from one direct-fired biomass plant. Depending on the percentage of co-firing, the proposals would provide up to 1,318MW of biomass capacity. Despite claims that various fuels could be employed, including agricultural residues, it is clear that wood will constitute the lion's share, with potentially massive effects on the state's forests. Even taking into account the somewhat greater efficiency of coal plants than direct-fired biomass plants,[81] the combined demand by these facilities for wood would be more than seven times the total amount of logging residues currently generated in Ohio, about 1.8 million green tons per year.[82] Use of wood pellets would increase wood demand further,

---

76 Gonzales et al, 2009.

77 The totality of lifecycle emissions of fuel from forest plantations is significantly higher than just emissions from burning, because these tree "crops" require intensive management and chemical inputs.

78 Replacement of native forests by plantations represents a substantial reduction in the amount of carbon held in forest biomass, as dense long-lived hardwoods are replaced by fast-growing softwoods. Sohngen, B., and Brown, S. 2005. The influence of conversion of forest types on carbon sequestration and other ecosystem services in the South Central United States. Ecological Economics 57:698-708.

79 Energy Information Administration.. 1990 – 2008 Net generation by state by type of producer by energy source (EIA 906) (available at http://www.eia.doe.gov/cneaf/electricity/page/capacity/capacity.html).

80 This provision is interpreted by the utilities to mean that at least 51 percent of power must be fueled by biomass.

81 EIA assumes coal plants have efficiencies around 35 percent; direct-fired biomass plants have efficiencies around 20 – 24 percent.

82 Smith et al, 2007.

since their production requires about two tons of wood to produce one ton of pellets. Where torrefaction (pre-combusting fuel to improve its usability) is used, the impacts of fuel preparation on wood demand and greenhouse gas emissions are even higher.

Utilities and other biomass developers in Ohio have been vague regarding their fuel sources, admitting that they do not know what the final mix will be. The proposed 200 MW South Point biomass plant says that about 45 percent of its fuel supply of about 2.4 million green tons a year will come from utility right-of-way clearing, but that it will need contracts with 30-to-40 contractors to provide the rest. Some will come from land clearing for coal mine expansion. In its application to the Public Utilities Commission, the coal-fired Conesville Generating Station wrote that it will use "solid biomass fuel, including but not limited to torrefied biomass, raw wood chips, sawdust, wood pellets, herbaceous crops, agricultural waste [that] will be co-fired with coal and/or natural gas in proportions up to 100% of total heat input."[83]

The 1,125MW Beckjord plant, which plans to co-fire up to 100 percent with biomass, says that, "the most likely initial fuel will be woody biomass produced by whole tree chipping" from a 50-mile radius of a coal-loading terminal on the Big Sandy River. The 350 MW Burger coal plant in Shadyside, Ohio, proposes to co-fire 60 percent or more of its capacity with biomass. However, in a March 2010 meeting on biomass fuel availability,[84] an official from the plant admitted that to meet emissions requirements, only white interior wood can be used, with no limbs, bark or leaves, and that due to emissions and fuel feeding considerations, the plant would only be able to supply 10–to-20 percent of its biomass fuel with agricultural residues. The inescapable conclusion of these restrictions is that the three million tons of biomass required by the Burger plant would mostly come from whole-tree harvesting.

Several groups[85] have filed motions with the Public Utilities Commission of Ohio to intervene in proceedings that would grant "renewable energy" status to these facilities, expressing concerns about the viability of the fuel supply and impacts on forests. The Ohio Consumers' Council, which has intervened on all co-firing applications, said of the Beckjord plant:

"In order to replace the coal with biomass for up to 100% of the total heat supplied, the Applicant will need a massive amount of biomass material. The Applicant does not identify its source of

---

83 The application goes on to explain that the torrefaction process, which partially pre-combusts woody biomass, "decreases the amount of moisture and volatile matter in the fuel. Raw or green biomass is more volatile than coal and its dust. Because of this, there is a risk of explosion given ignition source. If raw or green biomass is integrated into the fuel supply, significant investment in materials handling and fire protection and detection would be required." (Application for certification as an eligible Ohio renewable energy resource generating facility from the Southern Company for Conesville Generating Station Unit 3, to the Public Utilities Commission of Ohio)

84 Buckeye Forest Council, Ohio Solid Biomass Work Group Meeting notes, March 12, 2010.

85 These include the Ohio Consumers Council, the Ohio Chapter of the Sierra Club, the American Wind Energy Association, Ohio Advanced Energy, the Environmental Law and Policy Center, and the Buckeye Forest Council.

biomass material. If the Commission grants this Applicant a certificate for a renewable source, the Applicant may commence with costly modifications on the six generating units identified in its application. If the Applicant is unable to obtain the huge supply of biomass materials it claims it will employ to produce power in these plants, any potential retrofits will not provide the benefits intended and consumers should not bear costs associated with these potential retrofits or modifications. In order to prevent such a wasteful project, the Applicant should be required to identify its source of biomass materials before receiving certification."[86]

IX: Conclusion and Recommendations

Biomass power is at the core of federal and state renewables portfolio standards and congressional climate change legislation and is expected to deliver the lion's share of "renewable" power in the United States over the next 15 years. Unless bogus carbon accounting schemes are reformed, this headlong rush to biomass fuels will produce several perverse and potentially devastating outcomes that are currently being overlooked by the Congress, the EPA and state policy makers.

Cutting of US forests will sharply increase, and when this wood is burned in power plants, it will produce a huge surge in carbon emissions that will be kept off the books and, even worse, will be counted as an emissions reduction. As a result we will seriously erode the power of standing forests to pull carbon out of the atmosphere, allow coal plants to continue operating by co-firing and fuel-switching, and stymie real progress toward true alternative power sources.

This unacceptable outcome results from the glaring but largely unrecognized flaw in carbon accounting practices, which falsely assume that burning biomass fuels, including trees, produces zero net carbon emissions.

The biomass industry has no shortage of talking points contending that logging improves forest health and that "sustainable" harvesting can provide a carbon-neutral fuel source. But no argument can avoid the fact that burning forests for energy transfers carbon stocks from standing forest into the atmosphere and degrades the forest carbon sink. Despite this, billions of dollars in subsidies and tax breaks, as well as and higher electricity rates for consumers who pay extra to purchase "green" energy, are creating powerful incentives for biomass power generation. And although the assumption of carbon neutrality for biomass energy lies at the heart of every state and federal incentive, neither EPA nor any other agency has critically examined this concept, even though lifecycle greenhouse gas analysis is now mandated by law for biofuels.

86 Motion to intervene and comments by the Office of the Ohio Consumers' Counsel. In the matter of the application of Duke Energy Ohio – Walter C. Beckjord Generating Station for certification as an eligible Ohio renewable resource generating facility. Case No. 09-1023-EL-REN, Public Utilities Commission of Ohio.

Environmental Working Group recommends:

Pass a strong climate bill.

Congress must enact strong climate legislation that eliminates the biomass carbon accounting loophole. Carbon accounting practices must be corrected to include the full and immediate impact of cutting down forests to burn in biomass power plants. Biomass burning must not be permitted unless each specific proposal can unequivocally demonstrate that it will not increase greenhouse gas emissions, even in the short term. These reforms must be incorporated into all federal and state energy and climate policies.

Require biomass power plants to purchase emission allowances.

Biomass plants should be added to the list of "covered entities" required to purchase carbon emission allowances under federal and regional cap-and-trade programs. To the extent that biomass emissions are demonstrably re-sequestered in a short period of time, exceptions could be made.

Eliminate federal and state incentives for biomass power.

The federal production tax credit for biomass systems that burn whole trees, meaning chipped or pelletized whole trees, must be eliminated. This provides a massive federal subsidy for forest exploitation. Likewise, the Biomass Crop Assistance Program (BCAP) program providing matching funds to biomass suppliers should be revised to exclude funding of any facilities or operations that encourage forest cutting.

Exclude utility-scale biomass and co-fired coal plants from renewables portfolio standards.

Only high efficiency, small-scale, combined heat-and-power plants that extract maximum energy value from "additional" biomass should be considered to sell Renewable Energy Credits, and such projects should also undergo rigorous lifecycle analysis to determine their carbon footprints. "Additional" biomass should be defined as sustainably generated biomass containing carbon that would not otherwise remain stored, or become stored, or be meaningfully used for purposes other than energy production.

Appendix A: Biomass provisions in proposed climate and energy legislation

Biomass provisions in the House-passed ACESA and other federal legislation place few restrictions on forest cutting for biomass fuel. In ACESA, the definition of "renewable fuel" at Title I, Sec. 101(a)(16)(H)(ii) includes:

- Trees, logging residue, thinnings, cull trees, pulpwood, and brush removed from naturally re-generated forests or other non-plantation forests
- Dead or severely damaged trees removed within 5 years of fire, blowdown, or other natural disaster, and badly infested trees.
- Materials, pre-commercial thinnings, or removed invasive species from National Forest System land and public lands… and that are –

    (i) not from components of the National Wilderness Preservation System, Wilderness Study Areas, Inventoried Roadless Areas, old growth or mature forest stands, components of the National Landscape Conservation System, National Monuments, National Conservation Areas, Designated Primitive Areas; or Wild and Scenic Rivers corridors;
    (ii) harvested in environmentally sustainable quantities, as determined by the appropriate Federal land manager; and
    (iii) are harvested in accordance with federal and state law, and applicable land management plans.

The American Power Act, as proposed in the Senate, contains a definition of renewable biomass to be inserted in the Clean Air Act, which includes:

- "Materials, pre-commercial thinnings, or removed invasive species from National Forest System land and public lands …
- ...including those that are byproducts of preventive treatments (such as trees, wood, brush, thinnings, chips, and slash)…
- any organic matter that is available on a renewable or recurring basis from non-Federal land… including

    (i) renewable plant material, including
    (I) feed grains;
    (II) other agricultural commodities;
    (III) other plants and trees"

One source of feedstock for the 60 biochar facilities proposed in the bill is identified as "excess biomass." It is defined to include:

(i) trees or tree waste on public land;
(ii) wood and wood wastes and residues; and
(iii) weedy plants and grasses (including aquatic, noxious, or invasive plants).

[American Power Act, S. xx, 111th Cong., § 2002 (2010) (amending Title VII of the Clean Air Act (42 U.S.C. 7401 et seq.) as added by American Power Act § 2001, by adding § 700 (44)]

Appendix B: Analysis and Methodology

We analyzed output from the NEMS model, using publicly available projections from EIA that forecast how the energy sector would likely develop if ACESA were enacted. EIA power development projections are reported for each of the 13 North American Electric Reliability Council (NERC) regions in the continental United States. We examined EIA's data on total generation, coal-fired generation and biomass power generation, as well as carbon dioxide emissions from the power sector.

EIA reports the gigawatts of capacity to be built, which refers to direct-fired plants, and the total kilowatt-hours of biomass power to be generated, which refers to both direct-fired and co-fired biomass power. EIA also models GW of capacity and kWh of generation for end-use facilities. We converted the proposed GW of direct-fired plants to be built to express the number of kWh of power that would be generated at direct-fired plants. We then subtracted that number from EIA's own estimate of the total number of kWh of power generated from biomass to estimate how much of that total generation would come from co-firing biomass in coal plants in each NERC region. We checked the summed totals from all the NERC regions against EIA's own reported values for co-firing and direct generation that are reported for the country as a whole. End use generation data was used as reported, in kilowatt-hours. We converted kilowatt-hours of power generated to BTUs using conversion factors provided by EIA.

Our analysis of biomass availability used the same basic input datasets as used by EIA. The data come from a 1999 Oak Ridge National Laboratory (ORNL) dataset on urban wood, mill residues, agricultural residues and forestry residues. EIA uses these raw data on supply availability to generate price/supply curves that take various factors into consideration, including transportation costs. We did not adjust the availability of residues on a cost basis, using the simplified assumption that residues are equivalently available within the region where they are needed, which likely overstates their actual availability. This is a conservative assumption in the context of our analysis because to the extent that we overstate the availability of non-forest sources of biomass, we understate the amount of forest biomass that will be needed to meet fuel demand.

EIA's final supply curves for forestry residues include not only logging residues as included in the ORNL dataset, but also a significant portion of the standing "cull" tree biomass from the Forest Service inventory. We confined our estimate of forest biomass availability to logging residues as defined by the Forest Service, only. While EIA's estimate of forest biomass is based on 1999 data, we instead used 2006 Forest Service data on logging residues that are on average 26 percent higher than the ORNL values from 1999 that EIA used. This analysis is conservative in the context of our analysis because the estimates of logging residues that we used are larger than EIA's estimates.

To estimate the amount of new forest cutting that would be needed to meet biomass fuel demand after other sources of biomass (including logging residues) were exhausted, we converted biomass power generation from kWh to BTUs, using EIA's own assumptions about fuel energy content and plant efficiency. We then estimated the amount of BTUs available from existing sources of biomass based on the limitations we imposed. The BTU "deficit" was then presumed to be made up by new forest cutting. We calculated the number of acres that would need to be cut by converting the BTU deficit to tons of wood, and then divided this value by the aboveground biomass per acre for forests of each NERC region, using Forest Service data on aboveground biomass.[87]

Fossil fuel use and CO_2 emissions from biomass transport

This analysis was conducted using a number of conservative assumptions. Fuel use during transport was calculated using numbers from a typical 50 MW plant. Fuel use depends on various factors, but we assumed that trucks carry about 25 tons each of wood chips and are primarily in the HDDV8B class (>60,000 lbs). We assumed an average round-trip fuel transport distance of 100 miles and that trucks get 6.2 mpg.[88]

Analysis of EIA's assumptions concerning biomass fuel availability

A number of assumptions are built into EIA's estimates of fuel availability and the configuration of NEMS. Our analysis identifies a range for potential availability of existing fuels.

"Urban wood" (Construction and demolition debris)

We used EIA's input data for urban wood availability, although the category is so broadly defined as to probably overstate actual availability. The data documentation itself expresses little confidence in the accuracy of the data: "Urban wood wastes include yard trimmings, site clearing wastes, pallets, wood packaging, and other miscellaneous commercial and household wood wastes that are generally disposed of at municipal solid waste (MSW) landfills, and demolition and construction wastes that are generally disposed of in construction/demolition (C/D) landfills. Data regarding quantities of these wood wastes is difficult to find and price information is even rarer."[89]

---

87 Smith, et al 2007.

88 Texas Transportation Institute. 2007. A modal comparison of domestic freight transportation effects on the general public. December 2007; Amended March 2009. Houston, TX

89 Walsh, M., et al. 2000. Biomass feedstock availability in the United States: 1999 state level analysis. Prepared for EIA; available at http://bioenergy.ornl.gov/resourcedata/index.html. The document further adds, "Additionally, both the quantity and price of urban wastes are highly speculative. The analysis is based solely on one national study and regional averages taken from two additional surveys. There is no indication of the quality of the material present (i.e., whether the wood is contaminated with chemicals, etc.). Because of the ways in which the surveys were conducted, there may be double counting of some quantities (i.e., MSW may contain yard trimmings and C/D wastes as well). Additionally, the analysis assumes that the majority of this urban wood is available for a minimal fee, with much of the cost resulting from transportation. Other industries have discovered that once a market is established, these "waste materials" become more valuable and are no longer available at minimal price. This situation could also happen with urban wastes used for energy if a steady customer becomes available. It should also be noted however, that some studies indicate that greater

The modeling also likely overstates the usability of the urban wood stream because it assumes that a high percentage of urban wood is burnable but does not take into account the expense and difficulty of sorting this wood supply to remove pressure-treated lumber, which contains arsenic and chromium, as well as sources of contamination, such as painted wood, that can contain lead and other toxins. The analysis also does not take into account that sophisticated and expensive emissions control equipment may be required to control metals and dioxin emissions. Public opposition to combustion of this material can also be strong.[90] Because of these considerations, our analysis considered urban wood availability to be lower than that assumed by EIA. Our high level of availability was 75 percent of the EIA figure, approximately matching the proportion of "high grade" plus painted and stained wood found in a Massachusetts study of construction and demolition debris (this fuel stream would thus exclude most pressure-treated lumber, which contains chromium and arsenic, although fuel sorting studies demonstrate it is impossible to reduce the amount of this material in the fuel stream to zero).

Characterization of construction and demolition waste as a "renewable" or "carbon neutral" fuel is also objectionable,[91] particularly given that actual recycling and re-use of processed wood is a far "greener" use that actually saves the greenhouse gas costs of producing new materials.[92] Our low value for an availability factor for urban wood is thus 25 percent of EIA projections, which factors in public opposition to the use of this material as fuel.

---

quantities of urban wastes are available, and are available at lower prices, than are assumed in this analysis. Given the high level of uncertainty surrounding the quantity and price estimates of urban wastes and mill residues, and the fact that these wastes are estimated to be the least cost feedstock available, they should be viewed with caution until a more detailed analysis is completed."

90 In response to concerns raised by citizens and the State Department of Public Health, Massachusetts declared a moratorium in December 11, 2009 on permitting for proposals to burn construction and demolition waste for power, pending a full environmental and health review. A week earlier, the Massachusetts Medical Society passed a resolution expressing the organization's opposition to large-scale biomass plants proposed in Massachusetts due to their "unacceptable public health risk", and encouraged the state to promote zero-pollutant emissions renewable energy technologies.

91 A memo from the Massachusetts Department of Environmental Protection regarding the recent application by the Somerset coal plant in Somerset, MA to repower the plant with construction and demolition waste states "MassDEP believes it is highly unlikely that Somerset Power could make an acceptable demonstration that construction and demolition is a source of carbon neutral fuel. It would be difficult, if not impossible, to have the information necessary to provide a reliable carbon neutral life-cycle analysis that includes consideration of material source, harvesting practices, transportation, impact of any coatings or treatments applied, and land use changes. At this time, it is unclear how such an analysis would even be done and evaluated." (Memo to Alicia McDevitt, Executive Office of Energy and Environmental Affairs, from David Johnston, Acting Regional Director, Southeast Regional Office/MassDEP. Sept. 22, 2009).

92 United States Environmental Protection Agency. Opportunities to reduce greenhouse gas emissions through materials and land management practices. Washington, DC. September 2009.

Mill residues

Mill residues include bark, coarse residues (chunks and slabs), and fine residues (shavings and sawdust). EIA uses data on mill residues and assumptions on end-use from 1997. For our re-analysis, we acquired mill residues data from 2006. According to the Forest Service,[93] only about 1.5 percent of current mill residues go unused, suggesting this is a negligible source of fuel for new biomass power capacity. We do not discount this source of material, however. Forest Service data estimate that about 42 percent of mill residues are currently used for power generation, therefore we include this material in our re-analysis of EIA data, acknowledging that it is mostly allocated to existing, end-use biomass power generation. We assume 42 percent availability for mill residues in both our low and high fuel availability scenarios.

Agricultural residues

The NEMS model assumes that about 150 million tons[94] of agricultural residues (primarily corn stover and wheat straw, but including other crop residues) are potentially available annually for biomass fuel, a number that assumes about 40 percent of material is collected[95] and 60 percent is left on the field to maintain soil fertility (earlier versions of EIA's model assumed that between 30 and 40 percent of agricultural residues should be left on the field[96]).

However, as documentation for the NEMS model itself states, the estimate of availability of agricultural residues is possibly a significant overestimate. Aside from the lack of equipment for collecting and processing agricultural residues for use as fuel, the goal of generating 36 billion gallons of biofuels by 2021 includes a mandate to produce 16 billion gallons from cellulosic sources, an end-use that directly competes with the allocation of agricultural residues for power generation. Recent projections by the EIA of actual production estimate that cellulose-based ethanol production will reach 5.11 billion gallons by 2035, with an additional 12.5 billion gallons of "liquids from biomass".[97] At a conversion efficiency of about 50 gallons ethanol per ton of material, the demand for cellulosic feedstock would be about 102 million tons, or about 68 percent of all the agricultural residues that EIA states are available.

Use of agricultural residues as biomass fuel is also limited by the amount of processing they require before they can be burned, particularly in coal plants where the fuel feeding apparatus cannot handle

93 Smith et al, 2007.

94 The Union of Concerned Scientists used a similar estimate of agricultural residue availability of 158 million tons, which they state takes into account the need to leave some residues in the field to maintain soil fertility. Information from Union of Concerned Scientists, Climate Blueprint 2030, Appendix G, Biomass Energy Supply and Land-use Assumptions.

95 http://bioenergy.ornl.gov/papers/misc/resource_estimates.html

96 Haq, Z. 2002. Biomass for electricity generation. Energy Information Administration.

97 Voegele, E. 2009. EIA: Biofuels production to grow significantly, but short of RFS mandates. Biomass Magazine, December, 2009.

materials beyond a certain size and consistency. Further, the cost of processing and delivering these materials may be prohibitively high for their use as fuel without significant subsidies. A recent study[98] found that the cost of collecting, processing and delivering corn stover for energy was about $77 per ton, equating to more than the $50 price threshold for fuels modeled by NEMS on the basis of the 1987 dollar value. Our high availability scenario therefore is generous in assuming the availability of agricultural residues as biomass fuel could be 50 percent of the EIA estimate. Our low estimate assumed availability was 25 percent of the EIA estimate, reflecting the numerous constraints on use of these materials for biopower.

Logging residues

EIA's estimate of forest biomass availability not only overstates the actual supply that is available, but also depends on increased tree cutting, a trend that will increase greenhouse gas emissions. We confined our estimate of available forest biomass to logging residues generated by current forestry operations, which is the definition that the Forest Service uses. The presumption of carbon neutrality is based on the idea that having been cut, this material will decompose anyway, ultimately producing greenhouse gas emissions equivalent to those released if it is burned for energy, although the time scales of these two processes differ.

As defined by the U.S. Forest Service, forest residues include tree, tops, and unmarketable "cull" trees that are removed at current harvesting levels.[99] We used 2006 data on logging residues availability, which sums to about 56 million dry tons (EIA's estimates were based on 1999 data). Unlike EIA, we did not include standing "cull" trees or "excess small pole trees" in our estimate of forestry residues, since increased harvesting of this material would represent a new source of greenhouse gas emissions and does not fit under the assumption of carbon neutrality described above. We assumed that forest harvesting will remain relatively constant into the future and thus the supply of logging residues will be relatively constant.

Many forests of the United States are important sources of fuel wood for commercial and domestic heating, and about two thirds of the fuel wood used in the United States comes from sources that include cull trees cut during timber harvesting, and wood cut during land-clearing.[100] Thus, although some biomass fuel studies, such as that published by the National Renewable Energy Laboratory,[101] include wood from "cultural operations" (pre-commercial thinning for timber stand improvement)

---

98 Morey, V., et al. A biomass supply logistics system. Submitted for publication.

99 These data are presented in units of cubic feet. We converted volume to mass using the same conversion factor used in the National Renewable Energy Laboratory report on biomass availability (Milbrandt, 2005.)

100 Smith et al, 2007. "Other sources" is defined as "Sources of roundwood products that are nongrowing stock. These include salvable dead trees, rough and rotten trees, trees of noncommercial species, trees less than 5.0 inches d.b.h., tops, and roundwood harvested from nonforest land (e.g., fence rows)." This category of data is also included in EIA's estimates of biomass fuel for biopower applications.

101 Milbrandt, .2005.

and land clearing in their estimates of biomass availability, we confined our estimate to logging residues only, because wood from land-clearing appears to be already allocated to various uses, including fuel wood. In fact, the amount of fuel wood harvested annually in the United States[102] is about 77 percent of the amount of wood that is removed by cultural operations and land clearing. However, just as importantly, wood from permanent land clearing should not be considered a "renewable" biomass fuel, since re-growth and thus re-sequestration of carbon can never occur on permanently cleared land.

Other estimates of wood supply, such as that published in the joint report by the U.S. Department of Energy and the U.S. Department of Agriculture[103] assume that significant quantities of wood from "fuel reduction thinning" of forests of the western United States will also be available as biomass fuel. Reference is also sometimes made to the large amount of pine beetle-killed trees that exist in some regions of the West. We do not include these wood sources in our estimate of biomass availability. These removal programs are geographically limited, as yet largely speculative and would cause no less of a sudden pulse of carbon emissions than any other program of new tree harvesting would. Cutting of "overstocked" and beetle-killed wood for biomass fuel on the assumption that these trees may burn in the future ensures a 100 percent probability of near-term carbon emissions from these sources. Further, while all the biomass fed into a burner is combusted, recent research suggests that forest fire emissions are actually significantly less than had been assumed because so much standing timber remains after most fires.[104]

Earlier estimates from EIA assumed that 100 percent of logging residues generated by current logging is recoverable,[105] an assumption that not only overstates availability in terms of practical considerations, but also is an actual threat to forest sustainability. There are many constraints on the collection of logging residues for biomass fuel, including limited availability of the specialized equipment required for dragging material to a central chipping site, chipping and transport; accessibility of the land to this equipment; and collection and transport costs (green biomass chips are a low-value material and their removal is not cost-effective at many remote sites).

Retention of logging residues on site is also vital for maintaining forest health and sustainability. The tops and branches of trees are where the majority of nutrients reside; removing these from the site can lead to soil nutrient depletion, as well as leaving freshly logged areas open to erosion. Even the very optimistic joint U.S. Department of Agriculture/Department of Energy report on biomass

---

102 Smith et al, 2007.

103 Perlack, et al. 2005. Biomass as feedstock for a bioenergy and bioproducts industry: the technical feasibility of a billion-ton annual supply. U.S. Department of Energy, DOE/GO-102995-2135, ORNL/TM-2005/66. Oak Ridge National Laboratory, Oak Ridge, TN.

104 C Meigs, G.W., et al. 2009. Forest Fire Impacts on Carbon Uptake, Storage, and Emission: The Role of Burn Severity in the Eastern Cascades, Oregon. Ecosystems 12: 1246–1267.

105 Walsh, M., et al. 2000.

availability informally known as the "Billion Ton Vision"[106] asserts that "not all of this material should be recovered. Some portion of this material, especially the leaves and part of tree crown mass, should be left on site to replenish nutrients and maintain soil productivity."

EIA's estimates of agricultural residue availability acknowledge that 40-to-60 percent of residues should be maintained on farm fields to maintain soil productivity, but no such guidelines have been stated for logging residues. Yet retaining these materials is just as important in forested systems, where fertilizer is not added to make up for nutrient losses in harvest, as in agricultural systems, where fertilizer can be used.

Due to the logistical constraints outlined above, we assume that the number of acres where biomass is collected will be smaller than the number logged and could range from 50-to-75 percent of logged acres, with a generous estimate being 60 percent.[107] We further assume that in those areas where logging residues *are* collected, a minimum of 60 percent of material should be left in place (allowing 40 percent to be removed) to retain nutrient stocks (this number matches the guideline for agricultural soil but is nonetheless only a hypothetical scenario, since it is too low to be properly protective of soil nutrient stocks in many soils). Thus, our estimate for availability of logging residues is calculated as 60 percent of harvested areas times 40 percent of residues collected, equaling 24 percent.

This estimate of logging residues availability does not even take into consideration the considerable competing demands for wood that may be presented by the pellet industry, which is already shipping pellets internationally, or for wood used in cellulosic ethanol production. As observed in a research brief by Resources for the Future, wood is likely to be used for meeting mandated production levels of cellulosic ethanol, for "while grasses and other crops could prove to be a feasible long-term alternative, in the near term the onus of meeting the mandated targets would probably fall on wood because large inventories of wood and an infrastructure currently exist for harvest and transport; these are not available for grasses… It is clear that the timber harvest levels needed to supply both the conventional forest products industry and the new biofuel industry would be huge. For example, given commonly used conversion factors for wood to ethanol, the wood required for the targeted 2022 biofuel feedstock would need to equal to 348 million cubic meters (m^3) or 71 percent of the 2005 harvest of 489 million m^3." [108]

---

106 Perlack, et al. 2005.
107 According to the Forest Service, 39 percent of forest harvesting is clearcutting. We assume that up to 75 percent of this land could be available for residue collection. The remaining 61 percent of harvested lands are likely less accessible, thus we assume 50 percent accessibility. The weighted accessibility value is thus 60 percent.
108 Sedjo, R.A. and Sohngen, B. The implications of increased use of wood for biofuel production. Issue Brief # 09-04, June 2009. Resources for the Future, Washington, DC.

Energy crops

EIA assumes energy crops can be grown to meet biomass power needs. Some energy crops would displace crops currently grown on agricultural land, and some would be grown on currently idled land and Conservation Reserve lands. However, production costs for energy crops may prove to be prohibitive to their use as biomass fuel. A recent five-year study of farmers growing switchgrass found that on average, production costs were nearly $60/ton dry matter. For a typical 50 MW biomass plant, the production cost of the fuel prior to any transport or further processing (such as pelletizing) would thus be more than $19 million, two to three times the cost of wood chips. Given these costs, energy crops may provide a better financial return as biofuel feedstock, especially given the mandate for cellulosic ethanol production.

Virtually no energy crops of significance are being grown today, and our analysis does not attempt to modify EIA assumptions about fuel available from this resource. Instead, by estimating the gap between projected biomass power fuel needs and fuel availability, we calculate both the number of forest acres that would need to be harvested to make up the gap, and also the number of acres that would need to be planted with energy crops if the fuel deficit were to be made up that way. We use switchgrass as a "model" energy crop, assuming yields of 7 tons per acre, a generous estimate given previous estimates of switchgrass yields at 5 tons per acre.[109]

How did we translate BTUs of biomass energy into acres of forest cut?

Example calculation

EIA projects that under a federal renewables standard, the United States will generate 227 billion kWh of power from biomass in 2015.

Taking into account average power plant efficiencies for direct-fired biomass plants, coal plants where biomass is co-fired, and end-use generators, the 227 billion kWh translates into a need to generate 3,338,858,691 MMBTUs (million British thermal units) from biomass in 2015.

How many MMBTUs could be available from various sources of biomass in 2015?

Tons of urban wood available 9,211,654 — (158,440,449 MMBTUs)
Tons of mill waste available 37,975,560 — (653,179,632 MMBTUs)
Tons of agricultural waste available 37,662,851 — (580,007,905 MMBTUs)
Tons of logging residues available 13,549,180 — (233,045,896 MMBTUs)

Total: 1,624,673,882 BTUs can be generated from sources of biomass that are presumed available,

109 Natural Resources Defense Council, 2004. Growing Energy: how biofuels can help end America's oil dependence. Washington, DC.

leaving a deficit of 1,714,184,809 MMBTUs that could be made up with new forest cutting, or energy crops.

BTUs per ton of forest biomass: 17,200,000
BTUs per ton of switchgrass: 15,400,000

Therefore, 1,714,184,809 MMBTUs could be generated by harvesting and burning 99,661,907 tons of dry wood, or 111,310,702 tons of an energy crop like switchgrass.

Tons of dry forest biomass per acre: 45
Tons of switchgrass per acre: 7

Burning 99,661,907 tons of dry wood would require the equivalent of clearcutting 2,214,709 acres of forest. Burning 111,310,702 tons of an energy crop such as switchgrass would require harvesting 15,901,529 acres.

Other assumptions of EIA modeling

The EIA modeling assumes that available biomass fuels are consumed in the order of least expensive to most expensive, so that "urban wood" (primarily construction and demolition wood, or C&D) and mill waste are used first, agricultural residues are next, then forestry residues, and finally energy crops.

This may make sense from a modeling point of view, but it is not the case in reality. The plants that are currently permitted to burn construction and demolition waste wood are mostly in Maine and have had difficulty meeting emissions standards, as all were originally designed to burn only forest wood and only later began burning C&D as forest wood supplies tightened. Permitting for a direct-fired biomass plant that was proposed in Massachusetts to burn 80 percent C&D waste and 20 percent forest biomass, and also for a proposal to repower a coal plant using up to 100 percent C&D waste, was suspended by the state pending completion of a state-wide environmental and health study. The C&D burning biomass plant proposed to install more sophisticated and expensive emissions control equipment than generally used on such plants, but still would have had unacceptably high emissions of arsenic, chromium, and dioxins,[110] as well as criteria air pollutants. The Massachusetts Bureau of Environmental Health became involved, expressing concerns about placement of a combustion power source in the environmental justice community of Springfield, Mass.[111]

110 Letter on Palmer Renewable Energy proposed Beneficial Use Determination from Massachusetts Environmental Energy Alliance to Massachusetts Department of Environmental Protection, November 18, 2009. Available at www.massenvironmentalenegy.org.

111 Letter from Suzanne Condon, Director, Massachusetts Bureau of Environmental Health, to Daniel Hall, Executive Office of Energy and Environmental Affairs, November 19, 2009. Available at www.massenvironmentalenergy.org.

Relevant to emissions of carbon dioxide, EIA modeling with NEMS also assumes that all direct-fired biomass plants built in the future will use gasification technology,[112] rather than direct combustion, and that plant efficiency at both biomass plants and coal plants will increase over time. The assumption that gasification technology will be used decreases projected fuel needs relative to conventional boilers. However, as EIA model documentation acknowledges, relatively few gasification plants exist, and capital costs for this technology are highly uncertain.[113] A review of recently proposed biomass co-firing and direct-fired proposals finds a minority of projects plan to use gasification. The result is that EIA's estimates of the conversion efficiency of biomass to power are likely overestimated, and that fuel needs are thus underestimated. For utility scale direct-fired plants, we assumed an efficiency of 30 percent, which is on the high end of the range for direct-fired plants that use conventional combustion technology,[114] the technology that will constitute the overwhelming majority of biomass power plants for years to come. For end-use generators, such as paper mills that generate power with waste materials, we assumed 25 percent efficiency. For biomass co-fired at coal plants, we assumed an average efficiency for the coal fleet of 33 percent. To the extent that we have overestimated efficiency, we have underestimated biomass fuel needs and potential impacts.

---

112 Online documentation for the NEMS model states, "The conversion technology represented, upon which the costs in Table 8.3 in the EMM chapter are based, is an advanced gasification-combined cycle plant that is similar to a coal-fired gasifier" (from http://www.eia.doe.gov/oiaf/aeo/assumption/renewable.html). Other documentation states, "Finally, EIA assumes the use of biomass gasification technology for dedicated biomass generation plants. Based on current estimates, these plants trade off somewhat higher capital costs for significantly improved efficiency compared to direct-combustion technology, thus reducing operating costs. However, few commercial biomass gasification operations currently exist, and capital costs for this technology are highly uncertain." Energy Information Administration, Office of Integrated Analysis and Forecasting. Model documentation: Renewable fuels module of the National Energy Modeling System. DOE/EIA-M069(2009). July, 2009. Washington, DC.

113 Energy Information Administration. Impacts of a 25-percent renewable electricity standard as proposed in the American Clean Energy and Security Act Discussion Draft. SR/OIAF/2009-04. April, 2009. Washington, DC.

114 For instance, review of specifications for the proposed 50 MW Russell Biomass plant in Massachusetts reveal that the plant will operate at 24 percent efficiency, far below the average efficiency factor of 30 percent that we have estimated for biomass power plants.

CALIFORNIA ENERGY COMMISSION

CALIFORNIA ENERGY DEMAND 2010-2020 ADOPTED FORECAST

COMMISSION REPORT

December 2009

CEC-200-2009-012-CMF

Arnold Schwarzenegger, *Governor*

EXHIBIT 27

Executive Summary

Introduction

The *California Energy Demand 2010-2020 Adopted Forecast* (*CED 2009 Adopted*) is an Energy Commission report[1] presenting forecasts of electricity and end-user natural gas consumption and peak electricity demand for California as a whole and for each major utility planning area within the state for 2010-2020. *CED 2009 Adopted* supports the analysis and recommendations in the *2007 Integrated Energy Policy Report (2007 IEPR)* and *2008 Integrated Energy Policy Report Update (2008 IEPR Update)*, including electricity and natural gas system assessments, and the analysis of progress toward increased energy efficiency. As a result of a major effort to improve the measurement and attribution of efficiency impacts within the energy demand forecast, *CED 2009 Adopted* provides more detail on the impacts of energy efficiency programs and standards than in the past.

Summary of Changes to Forecast

The long-run forecast used in the 2007 IEPR cycle, the *California Energy Demand 2008-2018 Staff Revised Forecast*[2] *(CED 2007*), was based on 2006 peak demand and energy. For the current electricity and end-user natural gas consumption forecasts, staff added 2007 and 2008 energy consumption data to the historical series used for forecasting, while the peak demand forecast incorporates recent analysis of 2008 temperatures and peak demand at the planning area level.

As in the *California Energy Demand 2010-2020 Staff Draft Forecast*[3] (*CED 2009 Draft* or *Draft Forecast*), residential lighting was broken out as a separate end use in the *CED 2009 Draft* to better capture the impacts of residential lighting efficiency programs. For self-generation, staff refined its methods to track various technologies and individual programs. Unlike *CED 2007* and *CED 2009 Draft*, *CED 2009 Adopted* includes a forecast of electricity use by dedicated electric and plug-in hybrid vehicles, provided by the Energy Commission's Fuels Office.

CED 2007 assumed constant electricity rates throughout the forecast period and increasing (by around 30 percent) natural gas rates. *CED 2009 Adopted* assumes rates for electricity and natural gas increase by 15 and 10 percent, respectively, between 2010 and 2020. This corresponds to the "mid-rate" scenario forecast in *CED 2009 Draft*.

---

[1] *California Energy Demand 2010-2020, Staff Revised Forecast, Second Edition*, November 2009, CEC-200-2009-012-SF-REV, plus errata for inclusion in Chapter 8, p. 236, before the subheading "Statewide Results," were adopted at the California Energy Commission's business meeting held December 2, 2009. *CED 2009 Adopted* combines the two into one report.

[2] California Energy Commission, *California Energy Demand 2008–2018 Revised Forecast*, November 2007, CEC-200-2007-015-SF2.

[3] California Energy Commission, *California Energy Demand 2010–2020 Staff Draft Forecast*, June 2009, CEC-200-2009-012-SD.

The increased effort to capture the effects of energy efficiency programs, along with including the expected effects of 2010-2012 investor-owned utility (IOU) programs, results in reduced forecasted energy demand in California relative to *CED 2007*. *CED 2009 Adopted* provides details on staff work related to efficiency program measurement and attribution for this forecast.

Electricity Forecast Results

Table 1 compares *CED 2007* with *CED 2009 Adopted* and *CED 2009 Draft* forecasts for select years. For the draft forecast, the table shows results for the mid-rate case scenario, the same set of rates used in *CED 2009 Adopted*. *CED 2007* assumed constant rates throughout the forecast period. Both the energy consumption and non-coincident[4] peak forecasts are lower in *CED 2009 Adopted* than in *CED 2007* over the entire forecast period, primarily due to worsening short-term economic conditions. Electricity consumption in *CED 2009 Adopted* is down by more than 5 percent and peak demand by almost 4 percent by 2018 compared to *CED 2007*. However, consumption and peak demand are projected to be higher in *CED 2009 Adopted* than in the draft, since predictions for economic growth are slightly more optimistic compared to a few months ago. Electricity consumption is projected to grow at a rate of 1.2 percent per year from 2010-2018, the same rate as in *CED 2007*, versus 0.7 percent per year in the draft forecast. Peak demand also grows at the same rate for 2010-2018 as in *CED 2007*, 1.3 percent annually, compared to 1.0 percent in the draft forecast.

The revised statewide forecast of electricity consumption is lower than in *CED 2007* over the entire forecast period, beginning with a dip in 2009 (**Figure 1**). This difference reflects current economic conditions, which affect the forecast through lower personal income growth, lower employment, lower industrial output, and fewer additions to commercial floor space. Most of the remaining difference between *CED 2009 Adopted* and *CED 2007* comes from increased efficiency program impacts assumed in this forecast. Slightly more optimistic economic projections compared to those used in *CED 2009 Draft* along with the inclusion of an electric vehicle forecast lead to projected consumption by 2018 almost 5 percent higher in *CED 2009 Adopted* than in the draft.

Figure 2 compares *CED 2009 Draft* and *CED 2009 Adopted* forecasts of statewide non-coincident peak demand with *CED 2007*. As with electricity consumption, current economic conditions have a major effect in the short-term in both the draft and revised forecasts. Both forecasts show a significant reduction in peak relative to the 2007 forecast for 2010. In the longer term, beyond 2010, the growth rate in the *CED 2009 Adopted* is close to that in *CED 2007*, but levels remain around 3.7 percent lower by 2018. More optimistic recent economic

[4] Statewide peaks are non-coincident; that is, they are the sum of the individual coincident peak demands for each planning area in California. These individual peaks often occur at different hours of the day. Peak demands provided in this report for individual planning areas are coincident peaks.

projections push the *CED 2009 Adopted* forecast peak 2.5 percent higher than in the draft by the end of the forecast period. **Figure 2** also shows the load factor for the state as a whole.

Table 1: Comparison of *CED 2007*, *CED 2009 Draft*, and *CED 2009 Adopted* Statewide Electricity Forecasts

Consumption					
	CED 2007 (Oct. 2007)	*CED 2009 Draft* Mid-Rate Case (June 2009)	*CED 2009 Adopted* (Dec. 2009)	Difference, *CED 2009 Adopted* and *CED 2007*	Difference, *CED 2009 Adopted* and *CED 2009 Draft*
1990	229,868	228,473	228,473	-0.61%	0.00%
2000	265,769	264,233	264,233	-0.58%	0.00%
2008	288,976	280,184	286,771	-0.76%	2.35%
2010	297,062	278,043	280,843	-5.46%	1.01%
2015	316,575	289,493	299,471	-5.40%	3.45%
2018	327,085	294,895	309,561	-5.36%	4.97%
Average Annual Growth Rates					
1990-2000	1.46%	1.46%	1.46%		
2000-2008	1.01%	0.94%	1.03%		
2008-2010	1.39%	-0.38%	-1.04%		
2010-2018	1.21%	0.74%	1.22%		
Non-Coincident Peak					
	CED 2007 (Oct. 2007)	*CED 2009 Draft* Mid-Rate Case (June 2009)	*CED 2009 Adopted* (Dec. 2009)	Difference, *CED 2009* Adopted and *CED 2007*	Difference, *CED 2009 Adopted* and *CED 2009 Draft*
1990	47,308	47,241	47,530	0.47%	0.61%
2000	53,669	53,708	53,709	0.08%	0.00%
2008	62,946	62,948	61,825	-1.78%	-1.78%
2010	64,760	62,520	62,452	-3.55%	-0.10%
2015	69,302	65,968	66,772	-3.62%	1.25%
2018	71,889	67,873	69,240	-3.68%	2.01%
Average Annual Growth Rates					
1990-2000	1.27%	1.29%	1.23%		
2000-2008	2.01%	2.00%	1.78%		
2008-2010	1.43%	-0.34%	0.51%		
2010-2018	1.31%	1.03%	1.30%		
Historical values are shaded					
GWH = gigawatt hour					
MW = megawatt					

Source: California Energy Commission, 2009

Figure 1: Statewide Electricity Consumption

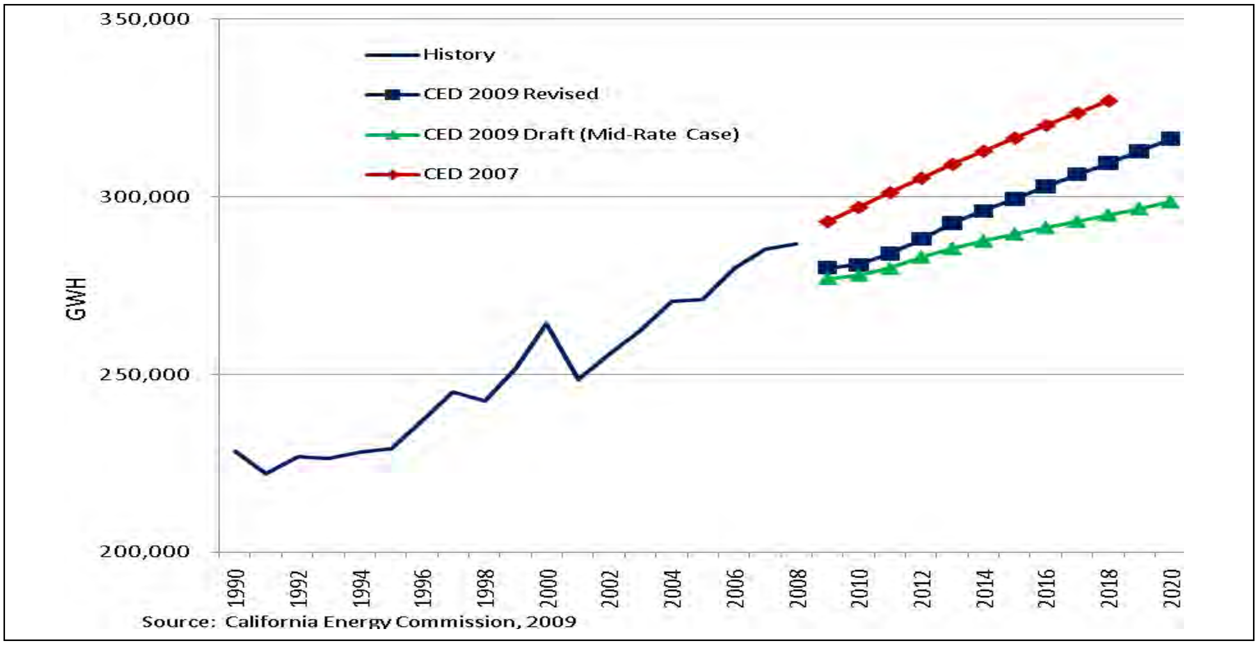

Source: California Energy Commission, 2009

Figure 2: Statewide Non-Coincident Peak Demand

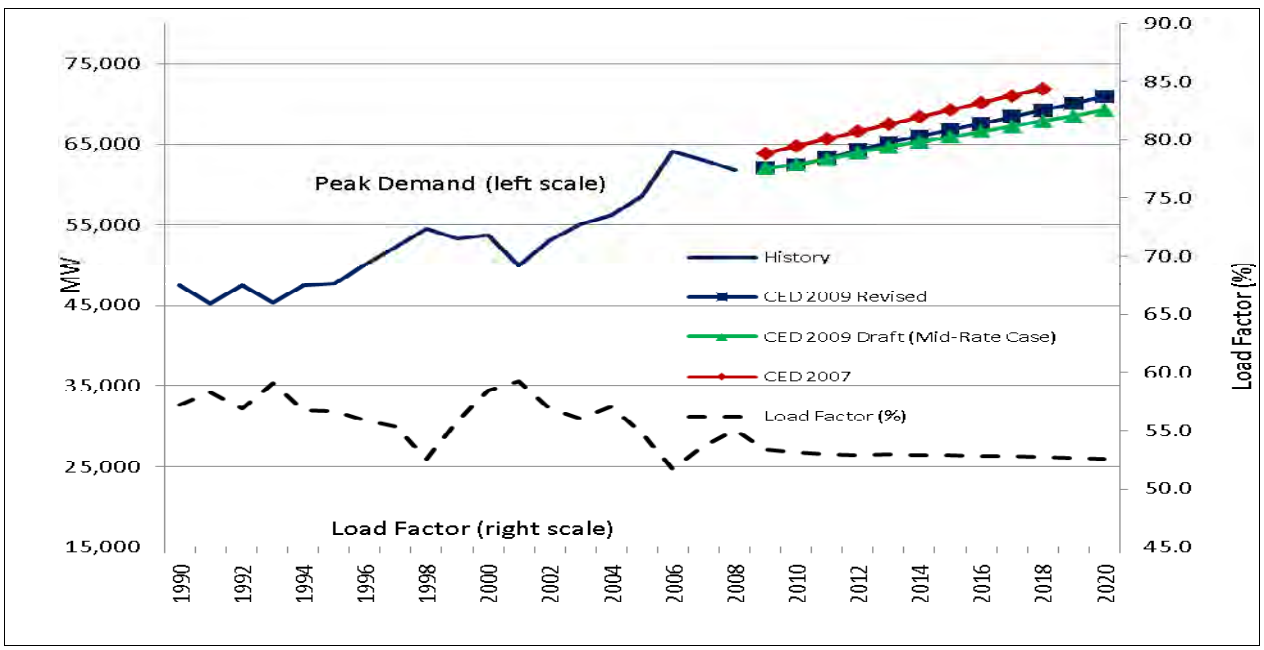

Source: California Energy Commission, 2009

The load factor represents the relationship between average energy demand and peak: the smaller the load factor, the greater the difference between peak and average hourly demand. The load factor varies with temperature; in extremely hot years (for example, 1998 and 2006) demand is *peakier*. The general decline in the load factor over the last 20 years indicates a greater proportion of homes and businesses with central air conditioning. This trend is projected to continue over the forecast period. Energy efficiency measures, such as more efficient lighting, can also contribute to the declining load factor by reducing overall energy use while having an insignificant effect on peak demand.

End-User Natural Gas Forecast Results

CED 2009 Adopted and *CED 2009 Draft* natural gas forecasts are compared with *CED 2007* for selected years (**Table 2**). These forecasts do not include natural gas used for generating electricity. As in the case of electricity, the set of rates used in the *CED 2009 Adopted* forecast corresponds to the mid-rate scenario in the draft forecast; thus the comparison is made to the draft mid-rate case. *CED 2007* used slightly higher rates, roughly equivalent to those in the draft high-rate scenario.

Reported 2008 natural gas consumption for the *CED 2009 Adopted* forecast is below that predicted in the draft forecast and *CED 2007*. This difference, along with a projected consumption reduction from 2008-2010 in the industrial and mining sectors, leads to a lower forecast through 2020. However, as the economy recovers beyond 2010, the growth rate exceeds those of the two previous forecasts.

Table 2: Statewide End-User Natural Gas Consumption

End-User Consumption (MM Therms)					
	CED 2007 (Oct. 2007)	*CED 2009 Draft* Mid-Rate Case (June 2009)	*CED 2009 Adopted* (Dec. 2009)	Difference, *CED 2009 Adopted* and *CED 2007*	Difference, *CED 2009 Adopted* and *CED 2009 Draft*
1990	12,893	12,893	12,893	0.00%	0.00%
2000	13,913	13,913	13,913	0.00%	0.00%
2008	13,445	12,941	12,494	-7.07%	-3.46%
2010	13,616	12,992	12,162	-10.68%	-6.48%
2015	13,932	13,218	12,751	-8.48%	-3.54%
2018	14,058	13,319	12,894	-8.28%	-3.20%
Average Annual Growth Rates					
1990-2000	0.76%	0.76%	0.76%		
2000-2008	-0.55%	-0.73%	-1.11%		
2008-2010	0.63%	0.19%	-1.34%		
2010-2018	0.40%	0.31%	0.73%		
Historical values are shaded					
End-user consumption excludes natural gas used to generate electricity					

Source: California Energy Commission, 2009

Economic Scenarios

The results presented above rely on economic inputs from a *base case* economic scenario provided by Moody's Economy.com (Economy.com). Staff also examined the effects of two alternative economic scenarios for California electricity demand: an *optimistic* case provided by IHS Global Insight and an Economy.com *pessimistic* case. For this analysis, staff developed econometric models for the three largest sectors (residential, commercial, and industrial plus mining) at the planning area level, using historical data for electricity consumption, electricity rates, weather, and various economic and demographic variables. Electricity consumption for the remaining sectors was held constant (*CED 2009 Adopted* levels) in the alternative scenarios. **Figure 3** shows the projected impacts of the optimistic and pessimistic scenarios on statewide consumption. Peak demand was developed by applying projected load factors from the *CED 2009 Adopted* forecast at the planning area and sector level to the consumption results for each scenario. Projected peak impacts are shown in **Figure 4**.

Electricity consumption is projected to be 2.3 percent higher in the optimistic economic case than in the *CED 2009 Adopted* forecast by 2020 and 1.9 percent lower in the pessimistic scenario. The peak demand forecast increases by 2.3 percent under the optimistic scenario by 2020 and falls by 2.2 percent in the pessimistic case. The percentage of peak reduction is more than consumption in the pessimistic case because the relative decrease in consumption is projected to be higher for the residential and commercial sectors than for the industrial, which has a higher load factor (is less *peaky*). Annual growth rates from 2010-2020 for electricity consumption and peak demand increase from 1.2 percent and 1.3 percent, respectively, to 1.3 percent and 1.4 percent in the optimistic case, and fall to 1.1 percent each under the pessimistic scenario.

Figure 3: Projected Statewide Electricity Consumption, *CED 2009 Adopted* and Alternative Economic Scenarios

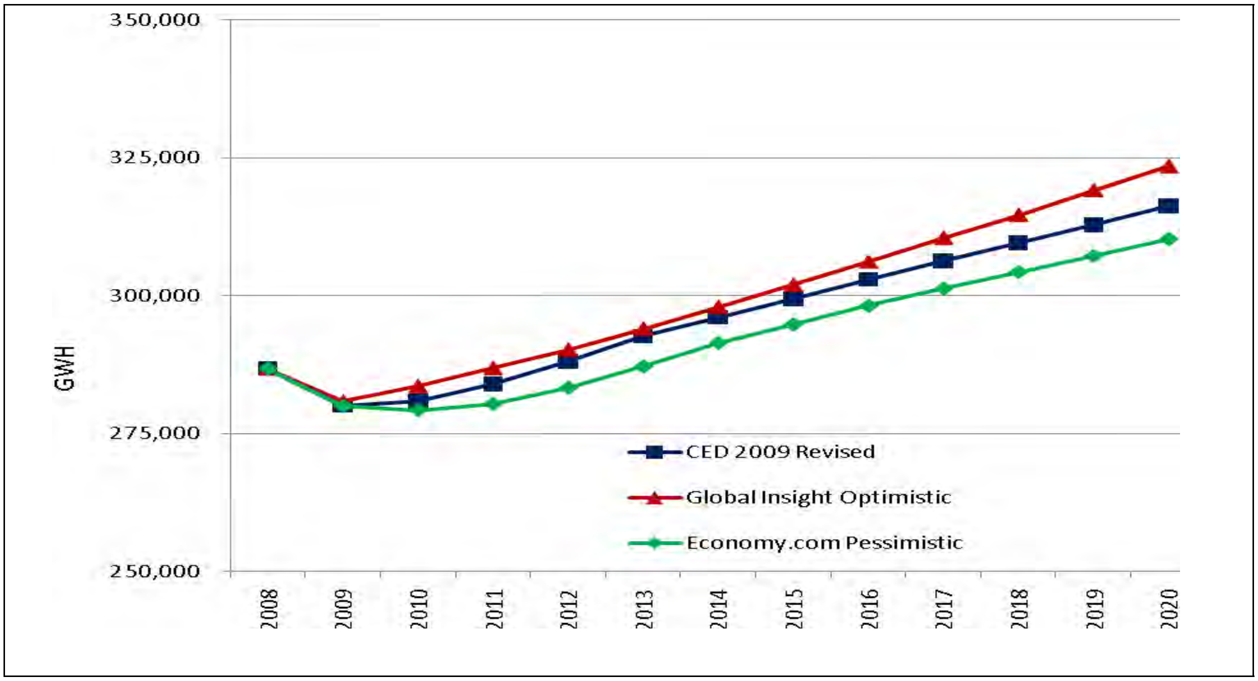

Source: California Energy Commission, 2009

Figure 4: Projected Statewide Peak Demand, *CED 2009 Adopted* and Alternative Economic Scenarios

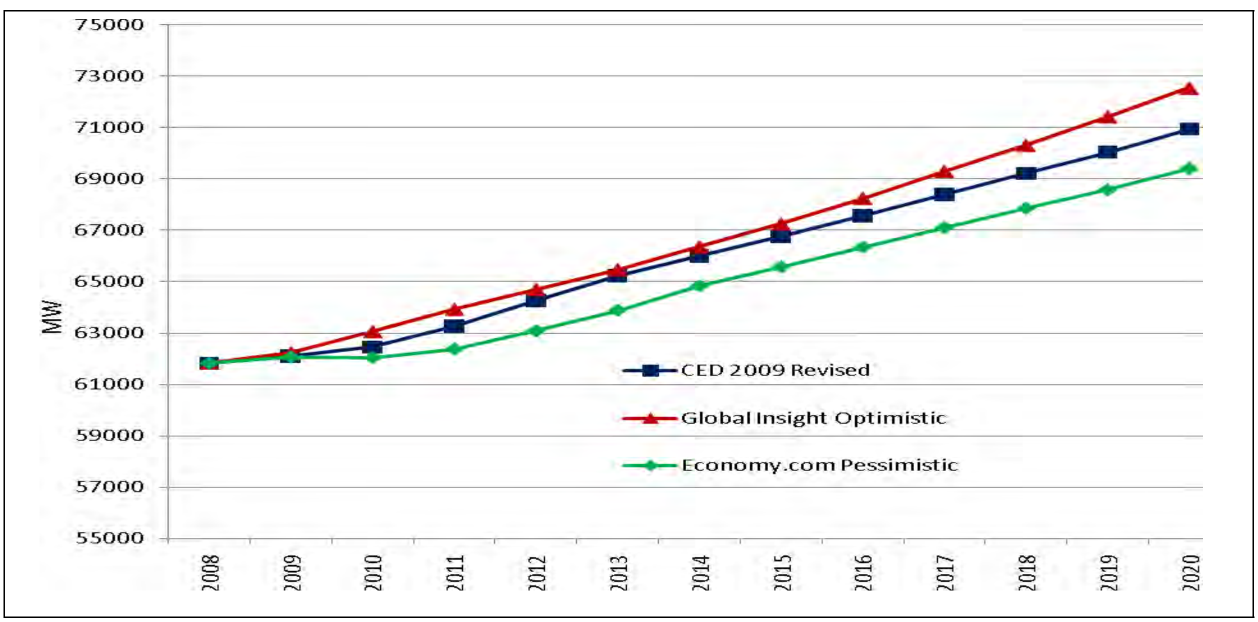

Source: California Energy Commission, 2009

Conservation/Efficiency

With the state's adoption of the first *Energy Action Plan (EAP)* in 2003, energy efficiency became the resource of first choice for meeting the state's future energy needs. Assembly Bill 2021 (Levine, Chapter 734, Statutes of 2006) set a statewide goal of reducing total forecasted electricity consumption by 10 percent over the next 10 years. Under AB 2021, the Energy Commission, in consultation with the California Public Utilities Commission (CPUC), is responsible for setting annual statewide efficiency targets in a public process using the most recent investor-owned and publicly owned utility targets. These targets, combined with California's greenhouse gas emission reduction goals, make it essential for the Energy Commission to properly account for energy efficiency impacts when forecasting future electricity and natural gas demand.

Much time and effort was put into refining the staff's forecasting methods to account for energy efficiency and conservation impacts while preparing this forecast, particularly for utility efficiency programs. **Figure 5** shows electricity consumption savings estimates incorporated in *CED 2009 Adopted* for building and appliance standards, utility and public agency programs, and *naturally occurring* savings, or savings associated with rate changes and market trends not directly related to programs or standards.

Figure 5: Efficiency/Conservation Consumption Savings by Source

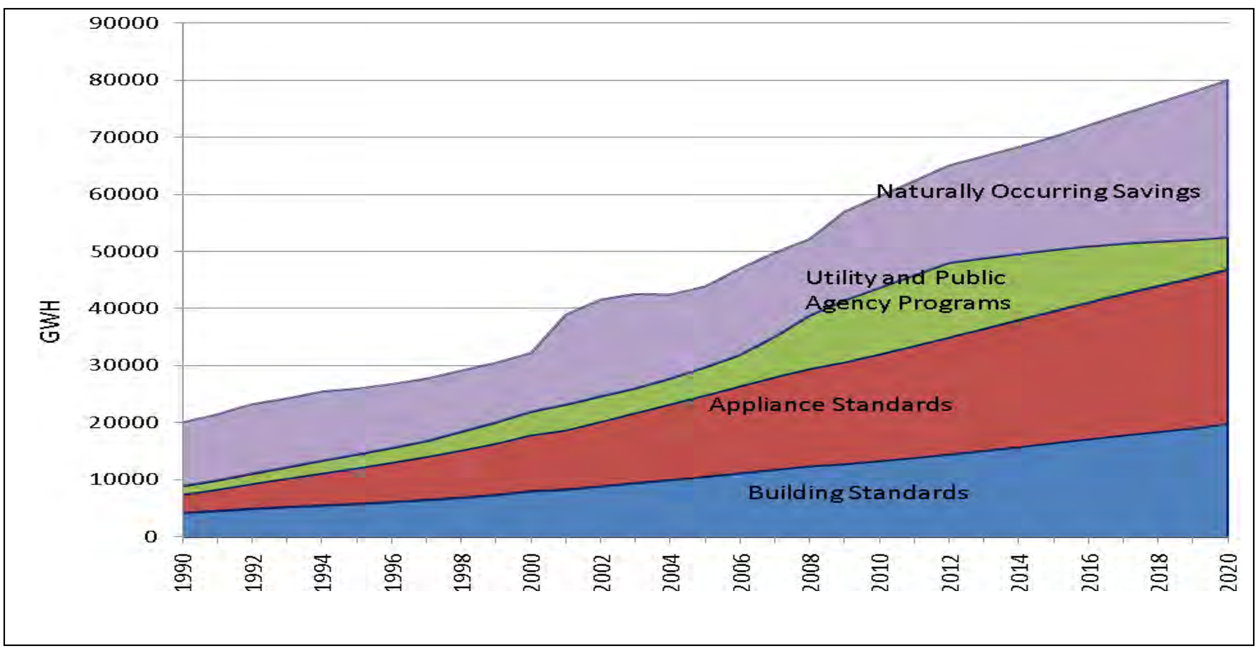

Source: California Energy Commission, 2009

Sierra Pacific Industries
P.O. Box 496028 • Redding, CA 96049-6028 • (530) 378-8000

For Immediate Release **Contact:** **Mark Pawlicki**
August 20, 2010 **530-378-8000**

Sierra Pacific Industries to Close its Loyalton, CA Power Plant

Anderson, CA – Sierra Pacific Industries (SPI) today announced that it has sent a notice to NV Energy in Nevada stating that SPI will suspend operations at its Loyalton, CA power plant immediately. The plant's fifteen power plant operators who will be directly affected by this announcement were notified today.

Numerous government decisions, including decisions not to implement laws passed by Congress, have cut off SPI from feasible fuel supplies and otherwise made it impossible to operate. Additionally, Nevada Energy recently lowered the rates it pays to SPI for electricity generated from the Loyalton plant. The combination of uncertain fuel supplies and reduced energy rates made the facility uneconomic to run.

The circumstances forcing the shutdown include: First, the United States Forest Service failed to carry out its legally mandated timber sales under the 1998 Herger-Feinstein Quincy Library Group Forest Recovery Act ("QLG Act") (the act mandates unequivocally certain timber sales on Federal Land in the vicinity of the power plant). SPI rebuilt its sawmill in Loyalton relying on the QLG Act, only to have to close it about two years later when the timber supply failed to materialize. Second, litigation filed by environmental groups has blocked certain attempts by the government to offer timber sales that would have produced in-woods biomass from federal land surrounding Loyalton.

As a result of these events, beyond SPI's control, SPI has been unable to procure sufficient supplies of suitable fuel to operate its power plant in compliance with legal requirements of federal, state, and local law.

Notwithstanding these events, Sierra Pacific Industries is exploring opportunities that might allow it to reopen the facility.

EXHIBIT 28

Ecosystems (2009) 12: 1246–1267
DOI: 10.1007/s10021-009-9285-x

ECOSYSTEMS

Forest Fire Impacts on Carbon Uptake, Storage, and Emission: The Role of Burn Severity in the Eastern Cascades, Oregon

Garrett W. Meigs,[1]* Daniel C. Donato,[2] John L. Campbell,[1] Jonathan G. Martin,[1] and Beverly E. Law[1]

[1]*Department of Forest Ecosystems and Society, Oregon State University, Corvallis, Oregon 97331, USA;* [2]*USDA Forest Service, Pacific Southwest Research Station, Institute of Pacific Islands Forestry, Hilo, Hawaii 96720, USA*

Abstract

This study quantifies the short-term effects of low-, moderate-, and high-severity fire on carbon pools and fluxes in the Eastern Cascades of Oregon. We surveyed 64 forest stands across four fires that burned 41,000 ha (35%) of the Metolius Watershed in 2002 and 2003, stratifying the landscape by burn severity (overstory tree mortality), forest type (ponderosa pine [PP] and mixed-conifer [MC]), and prefire biomass. Stand-scale C combustion ranged from 13 to 35% of prefire aboveground C pools (area − weighted mean = 22%). Across the sampled landscape, total estimated pyrogenic C emissions were equivalent to 2.5% of statewide anthropogenic CO_2 emissions from fossil fuel combustion and industrial processes for the same 2-year period. From low- to moderate- to high-severity ponderosa pine stands, average tree basal area mortality was 14, 49, and 100%, with parallel patterns in mixed-conifer stands (29, 58, 96%). Despite this decline in live aboveground C, total net primary productivity (NPP) was only 40% lower in high- versus low-severity stands, suggesting strong compensatory effects of non-tree vegetation on C uptake. Dead wood respiratory losses were small relative to total NPP (range: 10–35%), reflecting decomposition lags in this seasonally arid system. Although soil C, soil respiration, and fine root NPP were conserved across severity classes, net ecosystem production (NEP) declined with increasing severity, driven by trends in aboveground NPP. The high variability of C responses across this study underscores the need to account for landscape patterns of burn severity, particularly in regions such as the Pacific Northwest, where non-stand-replacement fire represents a large proportion of annual burned area.

Key words: carbon balance; Cascade Range; disturbance; fire emissions; heterotrophic respiration; mixed-severity fire regime; net ecosystem production; net primary productivity; *Pinus ponderosa*; wildfire.

Received 22 April 2009; accepted 10 August 2009;
published online 30 October 2009

Author Contributions: G.M. contributed to the study design, conducted field work and data analysis, and wrote the manuscript. D.D., J.C., and J.M. contributed to the study design, field work, data analysis, and writing. B.L. conceived the study, guided design and methods, and contributed to data analysis and writing.

**Corresponding author; e-mail:* gmeigs@gmail.com

Introduction

Forest ecosystems play a vital role in the global carbon (C) cycle, and spatiotemporal variability due to disturbance remains an active frontier in C research (Goward and others 2008; Running 2008).

EXHIBIT 29

With increasing focus on forests in the context of climate change and potential mitigation strategies for anthropogenic C emissions (Birdsey and others 2007; IPCC 2007), it is important to quantify the impacts associated with anthropogenic and natural disturbance regimes, particularly wildfire. Although numerous studies have investigated the effects of fire on C dynamics, very few to date have analyzed the full gradient of burn severity and quantified pyrogenic C emission, C pools, and postfire C balance across multiple forest types in the first few years following disturbance.

Fire's role in the terrestrial C cycle has been studied extensively in the boreal zone (for example, Amiro and others 2001; Hicke and others 2003; Kurz and others 2008) and, to a lesser extent, in temperate forests (for example, Kashian and others 2006; Gough and others 2007; Irvine and others 2007), but many uncertainties remain. Like other disturbances (insects, pathogens, large storms), fire alters the distribution of live and dead C pools and associated C fluxes through mortality and regeneration, but fire also causes direct pyrogenic C emission through combustion (Amiro and others 2001; Campbell and others 2007; Bormann and others 2008). Depending on burn severity (defined here as overstory tree mortality), C transfer to the atmosphere, and from live to dead pools, can vary substantially. In some cases the amount of C released from necromass decomposition over decades can exceed the one-time emission from combustion (Wirth and others 2002; Hicke and others 2003). One key uncertainty is the magnitude of pyrogenic C emission and the relative combustion of different C pools (Campbell and others 2007). Another important uncertainty is the rate at which postfire vegetation net primary productivity (NPP) offsets the lagged decomposition of necromass pools and their effects on net C uptake (that is, net ecosystem production [NEP]; Wirth and others 2002; Chapin and others 2006). A third uncertainty is the dynamics of heterotrophic respiration (R_h) and soil C over the first few years postfire. Although fire might increase R_h or facilitate soil C loss, recent studies in Oregon and California have shown that both can be remarkably conserved following disturbance, buffering potential negative spikes in postfire NEP (that is, C source to atmosphere; Campbell and others 2004, 2009; Irvine and others 2007). A final uncertainty is the distribution and abundance of understory vegetation—shrubs, herbs, and regenerating trees—which influence both short-term NPP trends and C balance through succession. All of these ecosystem responses and uncertainties might diverge radically in high- versus low-severity stands, but most fire-carbon studies have been limited to stand-replacement events. For example, regional and continental C models typically ignore low-severity fire, largely due to remote-sensing detection limitations and assumed minor C impacts (Turner and others 2007), despite the inherent heterogeneity of fire effects across forest landscapes.

The area burned by wildfire has increased in recent decades across western North America due to an interaction of time since previous fire, forest management, and climate (Westerling and others 2006; Keane and others 2008). Recent fires have also exhibited increasing severity, but low- and moderate-severity fire effects remain an important component of nearly all large wildfires (Schwind 2008; Miller and others 2009). The mixed-severity fire regime, defined by a wide range and high variability of fire frequencies and effects (that is, high pyrodiversity; Martin and Sapsis 1991), is characteristic of many forest types (Schoennagel and others 2004; Lentile and others 2005; Hessburg and others 2007) and may represent a new fire regime in other types that historically burned with lower severity (Monsanto and Agee 2008). The widespread increase in burned area, combined with the intrinsic variability of mixed-severity fire regimes, represents a potentially dramatic and unpredictable shift in terrestrial C cycle processes. In addition, historically uncharacteristic fires in some systems, including ponderosa pine (*Pinus ponderosa* Douglas ex P. Lawson & C. Lawson) forests, can push vegetation into fundamentally different successional pathways and disturbance feedbacks (Savage and Mast 2005), which may lead to long-term reductions in terrestrial C storage (Dore and others 2008).

Since 2002, wildfires have burned approximately 65,000 ha in and around the Metolius River Watershed in the Eastern Cascades of Oregon (Figure 1). These fires generated a complex burn severity mosaic across multiple forest types and a wide range of prefire conditions. The extent and variability of these fires, coupled with robust existing datasets on C dynamics in unburned forests in the Metolius area (for example, Law and others 2001a, 2003), presented a unique opportunity to investigate wildfire impacts on the terrestrial C cycle. In this study, we measured forest ecosystem responses across four levels of burn severity and two forest types 4–5 years following fire. Our research objective was to quantify the effects of burn severity on:

1. Pyrogenic carbon emission (combustion);
2. Carbon pools (mortality, storage, and vegetation response);

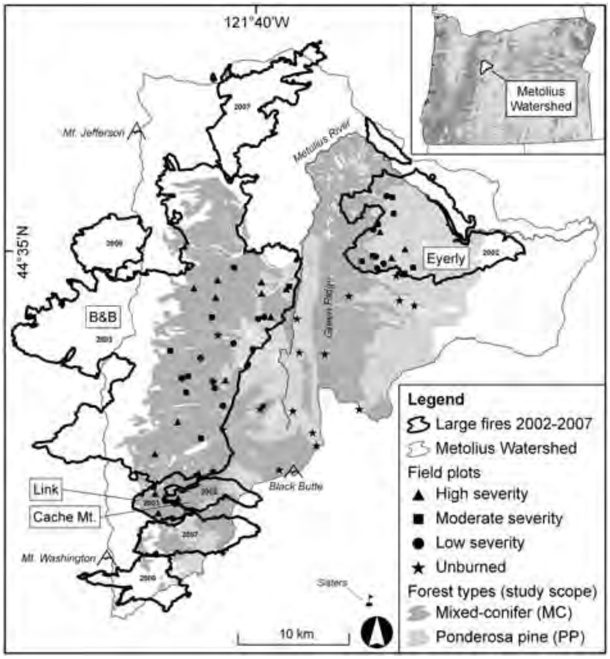

Figure 1. Metolius fire study area on the east slope of the Oregon Cascades. Point symbols denote survey plots ($n = 64$), labeled fires are the four surveyed (Table 2), and *shaded areas* are the sampled forest types. Other fires are outside the study scope and are labeled by fire year only. Forest type layer clipped to study scope: two types (MC and PP) on the Deschutes National Forest (DNF) within the Metolius Watershed. Other types (*unshaded area* within fires) include subalpine forests on the western margin, *Juniperus* woodlands to the east, riparian zones, and non-forest. Inset map shows study area location within Oregon elevation gradients. Fire perimeter and forest type GIS data from DNF. Other GIS data from archives at Oregon State University. Projection: UTM NAD 83.

3. Postfire carbon balance (biogenic C fluxes and NEP).

Here, we describe these three related response variables to elucidate the short-term fate of C pools and fluxes in the context of a highly heterogeneous postfire landscape.

Methods

Study Area

The Metolius Watershed is located NW of Sisters, OR, on the east slope of the Cascade Range (Figure 1). The postfire landscape is shaped by three important environmental gradients: forest type associated with climate, prefire biomass associated with past disturbance and management, and burn severity (overstory tree mortality) from recent fires.

Forest Type and Climate

The east slope is defined by one of the steepest precipitation gradients in western North America (Daly and others 2002; PRISM Group, Oregon St. Univ., http://prism.oregonstate.edu/). Within 25 km, vegetation transitions from subalpine forests (cool, wet) to *Juniperus* woodlands (warm, dry) and encompasses an unusual diversity of conifer species (Swedberg 1973). We focus on the two most prominent forest types—ponderosa pine (PP) and mixed-conifer (MC)—described by Franklin and Dyrness (1973) as the *Pinus ponderosa* and *Abies grandis* zones of Eastern Oregon. In general, the higher the elevation, mesic MC forest is more productive. Across the study area, ponderosa pine, grand fir (*Abies grandis* [Douglas ex D. Don] Lindl.), and Douglas-fir (*Pseudotsuga menziesii* [Mirb.] Franco) are the dominant tree species, and incense-cedar (*Calocedrus decurrens* [Torr.] Florin), western larch (*Larix occidentalis* Nutt.), and lodgepole pine (*Pinus contorta* Douglas ex Louden) are also abundant. Characteristic understory species include shrubs greenleaf manzanita (*Arctostaphylos patula* Greene), snowbrush (*Ceanothus velutinus* Douglas ex Hook.), and bitterbrush (*Purshia tridentata* [Pursh] DC.); forbs fireweed (*Epilobium angustifolium* L.), bracken fern (*Pteridium aquilinum* [L.] Kuhn), and American vetch (*Vicia americanum* Muhl. ex Willd.); and graminoids pinegrass (*Calamagrostis rubescens* Buckley), squirreltail grass (*Elymus elymoides* [Raf.] Swezey), and Idaho fescue (*Festuca idahoensis* Elmer). Study area elevation ranges from 600 to 2000 m, and slopes are generally gradual and east-facing. Mean annual precipitation ranges from 400 mm in eastern parts of the PP type to 2150 mm at high points in the MC type (Thornton and others 1997; DAYMET 2009). Summers are warm and dry; most precipitation falls as snow between October and June (Law and others 2001a). From W to E across the study area, average minimum January temperature ranges from −6 to −3.5°C and average maximum July temperature from 22 to 30°C (DAYMET 2009). Soils are volcanic in origin (vitricryands and vitrixerands), well-drained sandy loams/loamy sands. Additional study area characteristics are summarized in Table 1, and characteristic postfire stands are shown in Figure 2.

Historic Disturbance and Prefire Biomass

Historic fire return intervals ranged from 3 to 38 years in PP forests (Weaver 1959; Soeriaatmadhe 1966; Bork 1985; Fitzgerald 2005), from 9 to 53 years in the MC forest type (Bork 1985; Simon

Table 1. Metolius Watershed Study Area Characteristics

Forest type[1] Burn severity[2]	Number of plots	Burned area (ha) within study scope	Burned area %	Elevation (m) (mean, range)	Slope (°) (mean, range)	Total tree basal area (mean m^{-2} ha^{-1}, SE)[3]	Total tree density (mean trees ha^{-1}, SE)[3]	Tree % mortality (mean, SE)[4]
Mixed-conifer (MC)[1]	32	21,952	74	1160 (910–1558)	8.4 (1–22)	36 (3)	874 (103)	*61 (6)*
Unburned	8	na	na	1139 (910–1558)	4.9 (1–22)	35 (7)	911 (255)	13 (3)
Low severity	8	7236	25	1045 (972–1128)	6.8 (2–14)	40 (5)	1041 (252)	*29 (4)*
Moderate severity	8	4810	16	1155 (1068–1291)	10.5 (5–22)	35 (4)	1068 (142)	*58 (4)*
High severity	8	9906	33	1300 (1136–1479)	11.6 (8–14)	33 (7)	477 (81)	*96 (2)*
Ponderosa pine (PP)[1]	32	7821	26	1004 (862–1247)	5.2 (1–22)	21 (2)	643 (91)	*54 (8)*
Unburned	8	na	na	1035 (862–1247)	5.5 (1–17)	24 (4)	1020 (247)	6 (2)
Low severity	8	2371	8	977 (910–1074)	5.5 (1–22)	27 (5)	515 (122)	*14 (4)*
Moderate severity	8	2827	9	1046 (921–1092)	4.1 (1–7)	14 (3)	461 (122)	*49 (7)*
High severity	8	2623	9	957 (902–1063)	5.8 (1–15)	18 (5)	578 (168)	*100 (0)*
Overall	64	29,773	100	1082 (862–1558)	6.8 (1–22)	28 (2)	759 (70)	*58 (5)*

*Notes: Study scope was the area available for field sampling: Deschutes National Forest (DNF) non-wilderness land at least 50 m from roads, non-forest, and riparian areas. These area estimates also used for landscape scaling of pyrogenic C emission (Table 3). Note the uneven distribution of severity*type treatments across the sampled landscape.*

[1]Determined from DNF plant association group GIS data. Forest type rows describe sum or mean values as applicable.

[2]Determined from DNF BARC burn severity GIS data.

[3]Mean basal area and density of all trees with DBH more than 1 cm, including live and dead. SE in parentheses.

[4]Mean% basal area mortality due to fire for burned stands (indicated by italics), mean% dead tree basal area for unburned plots. SE in parentheses.

Figure 2. Characteristic forest stands across the Metolius Watershed study gradients. Clockwise from top-left: **A** unburned MC, **B** low-severity PP, **C** moderate-severity MC, **D** high-severity PP. Unburned stands contain heavy fuel accumulations and high tree and understory vegetation density; low-severity stands show partial bole scorching, high tree survivorship, and rapid recovery of surface litter; moderate-severity stands show increased bole scorch heights and overstory mortality; high-severity stands show near 100% tree mortality and generally thick understory vegetation (shrubs and herbs). Note that almost all fire-killed trees remain standing 4–5 years postfire.

1991), and up to 168 years in subalpine forests (Simon 1991). Given abundant lightning ignitions (Rorig and Ferguson 1999), it is likely that historic fires burned multiple forest types and exhibited the high spatiotemporal variability in fire behavior characteristic of mixed-severity fire regimes. During the twentieth century, fire suppression, grazing, timber harvest, and road construction resulted in fire exclusion. Dispersed patch clearcutting was the primary disturbance in recent decades, and most low biomass areas were young plantations (Deschutes National Forest [DNF] silvicultural GIS data). Anomalously dry, warm years (1985–1994, 2000–2005), contributed to regional drought stress (Figure 3; Thomas and others 2009). Beginning in 1986, an outbreak of western spruce budworm (*Choristoneura occidentalis*) and bark beetles (Family *Scolytidae*) killed trees across mid-to-high elevation MC forests (Franklin and others 1995). These interacting factors—time since previous fire, forest management, drought, and insect outbreaks—created fuel conditions conducive to large-scale wildfire.

Recent Large Wildfires

Since 2002, multiple large (>1000 ha) wildfires have affected half of the forested area in the watershed, burning across multiple forest types, land ownerships, and a wide range of fuel, weather, and topographic conditions. Surface, torching, and active crown fire behavior yielded a heterogeneous spatial pattern of burn severity (overstory tree mortality) at stand- and landscape-scales. This study focused on 4 major fires that burned approximately 35% of the watershed in 2002–2003 (Table 2, Figure 1).

Sampling Design and Scope

We measured postfire C pools and fluxes at 64 independent plots across the Metolius Watershed (Figure 1), sampling burned stands in 2007 (4–5 years postfire) and unburned stands in 2008. We employed a stratified random factorial sampling design with two factors—forest type and burn severity—and included prefire biomass as a covariate. We mapped forest type and burn severity

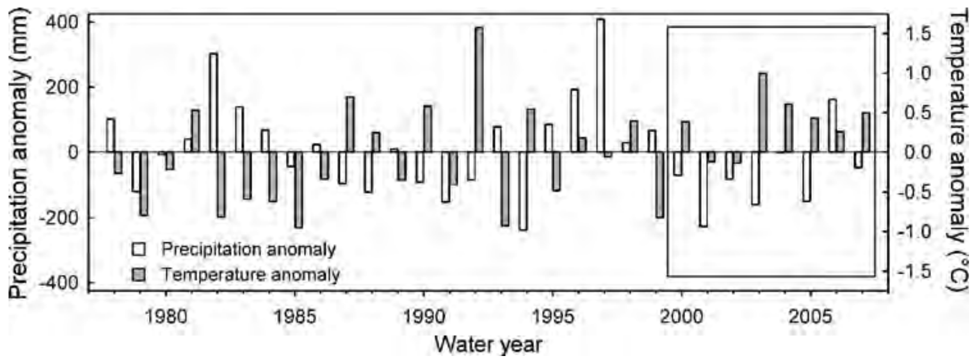

Figure 3. Climate anomalies in the Metolius Watershed. Anomalies in precipitation (mm) and temperature (°C) are in reference to the 30 year mean (1978-2007) from PRISM data (http://prism.oregonstate.edu/) extracted at a central location in the watershed (described by Thomas and others [2009]). Water year is defined as the 12-month period from October–September. The 2000 water year marked the beginning of an anomalously warm and dry period, coincident with a positive phase of the Pacific Decadal Oscillation (Thomas and others 2009). These anomalies contributed to drought stress and set the stage for wildfires and potentially harsh conifer regeneration conditions.

Table 2. Four Large Fires in the Metolius Watershed

Fire name	Fire size (ha) within watershed	Fire year	Ignition source
B&B Complex[1]	28,640	2003	Lightning
Eyerly Complex	9362	2002	Lightning
Link	1453	2003	Human
Cache Mt.	1376	2002	Lightning
Fire total	40,831		
Fire within MC and PP forest types (scope)	29,773		
Metolius Watershed area	115,869		

Note: [1]Booth and Bear Butte Complex: two large fires that merged into one.

classes from DNF GIS data. For forest type, we used a plant association group layer and combined wet and dry PP into one type and wet and dry MC into another. For burn severity, we used maps derived from the differenced normalized burn ratio (dNBR; Key and Benson 2006) classified as unburned, low, moderate, and high by DNF technicians following field assessment. Although the remotely sensed dNBR index has both known and unknown limitations (Roy and others 2006; French and others 2008), it is highly correlated with fire effects on vegetation and soil and has been used widely in conifer forests (Key and Benson 2006; Thompson and others 2007; Miller and others 2009). We defined plot-level burn severity as overstory tree basal area mortality (%), verified that plot-level mortality was consistent with the dNBR severity classes, and used the severity classes as a categorical variable (factor) in statistical analyses (described below). We used GIS to establish eight randomized survey plots within each combination of forest type and burn severity (hereafter 'type*severity treatment'; n = 64; Table 1, Figure 1). All plots were on DNF non-wilderness land at least 50 m from roads, non-forest, salvage-logged, and riparian areas. In addition, we used a live, aboveground biomass map from 2001 to sample the full range of prefire biomass and to ensure comparability among type*severity treatments. This biomass map was derived from regression tree analysis of Landsat spectral data and biophysical predictors (S. Powell, Univ. Montana, unpublished manuscript).

We used standard biometric methods described previously (Law and others 2001a, 2003; Campbell and others 2004; Irvine and others 2007). Below, we summarize these methods and provide specifics regarding postfire measurements, which are described in further detail by Meigs (2009). Each plot encompassed a 1 ha stand of structurally homogenous forest, which we sampled with a plot design similar to the USDA Forest Inventory and Analysis protocol (USDA 2003) enhanced for C budget measurements including tree increment, forest floor, fine and coarse woody detritus, and soil CO_2 effluxes (protocols in Law and others 2008). We scaled all measurements to slope-corrected areal units for comparison across study treatments.

Like other fire studies, this natural experiment lacked experimental control and detailed prefire data, but remotely sensed prefire biomass, GIS data, and plot attributes allowed us to account for preexisting differences. Because the forest type, burn severity, and prefire biomass were not randomly assigned, we limited statistical inference and interpretations to the sampled forest types. To minimize potential confounding effects of spatial and temporal autocorrelation, we located plots at least 500 m apart, maximized interspersion within study area gradients, and sampled multiple fires from two different years. The experimental unit was the 1 ha plot.

Ecosystem Measurements

Aboveground C Pools, Productivity, and Heterotrophic Respiration

At each plot, we quantified aboveground C pools in four circular subplots (overstory trees, stumps, understory vegetation, forest floor) and along transects (coarse woody detritus [CWD], fine woody detritus [FWD]). We sampled overstory trees at various scales to account for different stem densities (10 m default subplot radius for trees 10.0–69.9 cm diameter at breast height [DBH; 1.37 m]). For all trees with DBH at least 1 cm, we recorded species, DBH, height, % bark and wood char, decay class (1–5; Maser and others 1979; Cline and others 1980), and whether or not trees were broken and/or dead prior to burning. We estimated CWD and FWD volume using line intercepts (Van Wagner 1968; Brown 1974; Harmon and Sexton 1996; Law and others 2008), recording diameter, decay class, and char class on four 75 m transects per plot. We sampled CWD (all pieces ≥7.62 cm diameter) along the full 300 m and FWD less than 0.64, 0.65–2.54, and 2.55–7.62 cm along 20, 60, and 120 m, respectively.

We sampled understory vegetation (tree seedlings [DBH < 1 cm], shrubs, forbs, graminoids), and ground cover in four 5 m radius subplots nested within overstory tree subplots. For tree seedlings, we recorded species, age, height, and live/dead status and identified seedlings established before fire. Based on seedling age and DNF GIS replanting data, we determined if seedlings were planted and excluded these from natural regeneration analyses. We calculated shrub volume from estimates of live shrub % cover in three height classes (0–0.5, 0.5–1.0, 1.0–2.0 m) and dead shrub stem number, length, and diameter. We estimated the % cover of forbs, graminoids, litter, woody detritus, cryptogams, rocks, and mineral soil.

We computed biomass with an allometry database of species-, ecoregion-, and decay class-specific volume equations and densities (Hudiburg 2008; Hudiburg and others 2009), adjusting tree, CWD, and FWD biomass estimates for char reduction (Donato and others 2009a), broken status, and severity-specific estimates of bark, wood, and foliage combustion after Campbell and others (2007). We used species-specific allometric equations to convert live shrub volume to mass and converted dead shrub volume to mass using the mean decay class 1 wood density of three locally abundant genera (*Acer*, *Alnus*, *Castanopsis*). We converted herbaceous cover to biomass using 0.25 m^2 clip plots of dominant species sampled across the study area. We assumed that the C content of all pools was 0.51 except for forest floor (assumed to be 0.40; Campbell and others 2007). We sampled forest floor (litter and duff) to mineral soil with 10.2 cm diameter pvc corers at 16 randomized locations per plot and oven-dried samples at 60°C for more than 72 h to determine mass.

We determined NPP and heterotrophic respiration (R_h) at the 48 burned plots. We estimated bolewood NPP from radial increment measurements of current and previous live tree biomass (Van Tuyl and others 2005; Hudiburg and others 2009), collecting increment cores at breast height from 20 representative live trees in each low- and moderate-severity plot. Although researchers typically average radial increment from the previous 5-10 y to account for climatic variability (for example, Law and others 2003), we used the last full year of radial growth (2006) to estimate bolewood NPP because we could not assume a steady state 4–5 years postfire. For live trees in high-severity stands (<0.5% of inventoried trees, $n = 23$ at 3 of 16 stands), we applied forest type averages of increment data from low- and moderate-severity stands. We calculated foliage NPP as the product of specific leaf mass per unit area (SLA), leaf retention time (LRT), and plot-level leaf area index (LAI). We estimated SLA and LRT from representative canopy shoots with full retention and measured LAI optically using a Sunfleck ceptometer (Decagon Devices, Inc., Pullman, WA) after Law and others (2001b) and Pierce and Running (1988). Because moderate- and high-severity fire substantially altered tree crowns through combustion and mortality, we scaled LAI measurements from low-severity plots using a regression of the positive relationship between LAI and live tree basal area ($LAI = 3.85 * [1 - e^{(-0.0311 * \text{live basal area})}]$, adj. $R^2 = 0.54$, $n = 16$; fitted using the exponential rise to maximum statistical program in SigmaPlot [Version 11.0, SPSS Science, IL]). We computed shrub wood and foliage NPP from annual radial increment and LRT (Law and Waring 1994; Hudiburg and others 2009). We assumed that herbaceous mass equaled annual NPP and that annual mass loss was 50% (Irvine and others 2007).

We computed aboveground R_h of dead woody pools (R_{hWD}) as the product of necromass and decomposition constants from a regional CWD database (Harmon and others 2005). Because snags decay much more slowly than CWD in this seasonally moisture-limited system, we assumed that snag decomposition was 10% of CWD decomposition (Irvine and others 2007), but we used CWD decomposition rates for stumps, for which microbial decay processes are less moisture-limited (M. Harmon, Oregon St. Univ., 2009, personal communication). We estimated FWD decomposition after McIver and Ottmar (2007).

Belowground C Pools, Productivity, and Heterotrophic Soil Respiration

At the 48 burned plots, we collected soil and fine roots (FR: <2 mm diameter) at 16 randomized locations per plot using 7.3 cm diameter augers. Default sampling depth was 20 cm with one core up to 100 cm per plot. We used linear regression to scale C, N, and FR to 100 cm. We assumed that 49% (SD = 14) of soil C, 48% (SD = 17) of soil N, and 62% (SD = 20) of FR were in the top 20 cm, within the variation of the FR correction factor reported by Law and others (2003). All samples were sorted through 2 mm sieves, bench-dried, mixed by subplot, and analyzed for mass fraction of C and N (LECO CNS 2000 analyzer, Leco Corp., St. Joseph, MI), texture (hydrometer method), and pH (Oregon St. Univ. Central Analytical Laboratory). We calculated bulk density via stone displacement and separated FR and other organic matter. We combusted a representative FR subsample in a muffle furnace at 550°C for 5 h to determine organic content (74.24%), which we applied to all FR samples to estimate total organic matter. Based on published estimates of regional FR decomposition (Chen and others 2002) and mortality (Andersen and others 2008), we assumed that less than 40% of fire-killed FR remained when sampled, that far fewer were retained by 2 mm sieves, and that the vast majority of sampled FR was newly recruited postfire. We estimated that live roots were 61% of total FR mass in PP stands (Irvine and others 2007) and 87% of FR mass in MC stands (P. Schwarz, Oregon St. Univ., unpublished data). We computed FR NPP as the product of total organic FR mass and a root turnover index from rhizotron measurements in a nearby unburned PP forest (Andersen and others 2008). We estimated live and dead coarse root (CR: > 10 mm diameter) mass from the tree, snag, and stump surveys as a function of DBH (Santantonio and others 1977) and computed CR NPP from modeled current and previous live tree diameters (from increment cores). Because the median stump height was 30 cm, we applied a correction factor of 0.9 to account for bole taper to 1.37 m for stump CR estimates (adapted from D. Donato, unpublished data).

We measured soil CO_2 efflux and adjacent soil temperature at burned plots during the peak flux period (12 randomized locations; one set of manual measurements per plot in late June) using a Li-6400 infrared gas analyzer with Li-6000-9 soil chamber (Li-Cor Biosciences, Lincoln, NE) and established protocols (Law and others 1999; Campbell and Law 2005; Irvine and others 2007, 2008). We estimated annual soil respiration (R_{soil}) by matching plot measurements with concurrent, hourly, automated soil respiration measurements at a nearby unburned AmeriFlux PP tower site (Irvine and others 2008). The automated record consisted of hourly measurements spanning early May to mid November and was gap-filled using 16 cm soil temperature and 0–30 cm integrated soil moisture (see Irvine and others 2008 for model specifics). We scaled plot measurements to the annual dataset using plot-specific correction factors based on the ratio of mean soil respiration for a given plot divided by the concurrent automated rate. Correction factors ranged from 0.47 to 1.60 (range of type*severity means: 0.87–1.02). This approach sampled the spatial variability of R_{soil} within each plot to determine base rates and leveraged the long-term, intensive measurements of temperature- and moisture-driven variability. Similar automated measurements were made in 2002–2003 in a MC stand that subsequently burned in the B&B fire. A comparison of MC and PP continuous respiration datasets during the overlapping measurement period indicated near identical diel amplitudes and seasonal patterns between the two sites (data not shown). Given this similarity, we concluded that annual, plot-specific R_{soil} estimates based on the PP automated soil respiration would adequately represent the spatial and temporal variation within and among plots. We computed the heterotrophic fraction of soil respiration (R_{hsoil}) based on previous measurements at vegetation-excluded automated chambers at high-severity and unburned AmeriFlux tower sites within the study area (Irvine and others 2007).

Net Ecosystem Production

We estimated net ecosystem production (NEP: the difference between gross primary production and ecosystem respiration; Chapin and others 2006) using the mass balance approach (Law and others 2003; Campbell and others 2004; Irvine and others 2007):

$$NEP = (NPP_A - R_{hWD}) + (NPP_B - R_{hsoil}) \quad (1)$$

where NPP_A is aboveground NPP, R_{hWD} is heterotrophic respiration of aboveground woody detritus, NPP_B is belowground NPP, and R_{hsoil} is heterotrophic soil surface CO_2 efflux (includes forest floor). NEP is the appropriate metric of C balance and uptake at the spatiotemporal scale of our measurements, whereas net ecosystem carbon balance (that is, net biome production) describes landscape- to regional-scale C balance and longer-term effects of fire and other fluxes (for example, erosion, leaching, timber harvest; Chapin and others 2006). Here, we assume these other fluxes to be negligible during the sampling period, and we account for combustion losses independently of NEP.

Pyrogenic C Emission from Combustion

Before-after measurement of C pools is the most certain method to measure pyrogenic C emission (Campbell and others 2007), but in this study, co-located prefire measurements were not available, and it was not possible to establish a paired plot for every burned condition across the study gradients. We estimated C loss from combustion using a standard simulation program (Consume 3.0; Prichard and others 2006), augmented with field estimates of tree consumption. Consume predicts aboveground fuel consumption, C emission, and heat release based on weather data, fuel moisture, and fuelbed inputs from the Fuel Characteristic Classification System (FCCS 2.0; Ottmar and others 2007); both models available at: www.fs.fed.us/pnw/fera/. We selected representative FCCS fuelbeds for PP and MC stands (Table 3) using GIS and modified these to develop custom fuelbeds based on field measurements at the 16 unburned plots. We simulated low-, moderate-, and high-severity fire by adjusting percent canopy consumption and fuel moisture content for woody fuels and duff (R. Ottmar, US Forest Service, 2009, personal communication). Because Consume 3.0 does not account for consumption of live tree stems and bark, we used field measurements to calculate the changes in mass and density due to charring (Donato and others 2009a). We assessed combustion at the stand-scale and scaled combustion to the sampled landscape with forest type and burn severity GIS data.

Statistical and Uncertainty Analysis

We used multiple linear regression and analysis of covariance to compare response variables across the study gradients. Because one- and two-way ANOVA (forest type and burn severity tested separately and combined) revealed a significant difference in prefire biomass between the two forest types ($P < 0.001$) but no significant prefire difference among burn severities within either forest type ($P > 0.5$), we conducted analyses separately by forest type. We derived test statistics (coefficients and standard errors) from a multiple linear regression model of the response variable as a function of prefire biomass (continuous) and burn severity (categorical) within a given forest type. Regression analysis showed no significant interactions among explanatory variables; coefficient estimates were calculated from additive models with an assumption of parallel lines among type*severity treatments. We log-transformed data when necessary to satisfy model assumptions. We accounted for multiple comparisons and reported statistical significance as the highest significant or lowest non-significant Tukey-adjusted P value ($\alpha = 0.05$) common to all groups (for example, severity classes) in a given comparison (PROC GLM lsmeans multiple comparisons; SAS 9.1, SAS Institute, Inc., Cary, NC).

We take a pragmatic view of uncertainty analysis after Irvine and others (2007). Many scaling assumptions are necessary to estimate plot-level metrics from components sampled at varying spatiotemporal scales. Further, given the wide range of sampled prefire biomass and variability across the postfire landscape, it is possible to commit Type II statistical errors when important differences exist but are confounded by additional factors. We thus focus on the trends and proportions across type*severity treatments rather than absolute magnitudes. To estimate NEP uncertainty, we used a Monte Carlo procedure with the four major fluxes described in equation (1) for each type*severity treatment (NEP uncertainty expressed as ±1 SE after 10000 iterations based on the standard normal distribution with mean, standard deviation, and between-flux covariance in R [R Development Core Team 2009]).

Table 3. Pyrogenic C Emission (PE) from Consume 3.0 Simulations and Field Measurements of Consumption

FCCS fuelbed[1]	Forest type / Burn severity[2]	Stand scale				Landscape scale	
		Total aboveground C (Mg C ha^{-1})[3]	Stand-scale PE (Mg C ha^{-1})[4]	% Consumption, aboveground C[5]	% Consumption, live tree stems[6]	Total PE (Tg C)[7]	Landscape % of total PE[7]
Grand fir–Douglas fir forest (fire suppression) (SAF 213)	Mixed-conifer						
	Unburned	132.6					
	Low severity		16.6	13	0.23	0.120	16
	Mod severity		25.3	19	0.71	0.122	16
	High severity		32.3	24	2.01	0.320	42
Pacific ponderosa pine forest (fire suppression) (SAF 237)	Ponderosa pine						
	Unburned	87.2					
	Low severity		19.7	23	0.27	0.047	6
	Mod severity		25.6	29	1.43	0.072	10
	High severity		30.2	35	2.77	0.079	10
Across sampled burn area (29,773 ha)			**25.5**[8]	**22**[8]	**1.24**[8]	**0.760**	100

Notes: [1]*Fuel Characteristic Classification System (FCCS) fuelbeds determined using GIS data and descriptions from US Forest Service FERA group: www.fs.fed.us/pnw/fera/. SAF codes are Society of American Foresters cover types (Eyre 1980).*
[2]*Severity classes derived by adjusting surface fuel moisture and canopy consumption (R. Ottmar, US Forest Service, 2009, personal communication).*
[3]*Total aboveground C from unburned stands, used for parameterizing FCCS fuelbed inputs for Consume modeling. Multiply by 2 for Mg ha^{-1} mass or by 100 for g C m^{-2}.*
[4]*Pyrogenic C emission (PE) computed from simulated biomass combustion in Consume and field measurements of bark and bole charring calculated after Donato and others (2009a) and Campbell and others (2007).*
[5]*% of unburned plot aboveground C (4th column).*
[6]*% of live tree bark and bole bark mass estimated from charring (mean, weighted by tree mass).*
[7]*Stand-scale PE scaled to the sampled landscape based on area of type*severity treatments (Table 1).*
[8]*Mean, weighted by area of type*severity treatments (Table 1).*

Results and Discussion

Pyrogenic C Emission (Combustion)

Simulated mean pyrogenic C emission (PE) was 25.5 Mg C ha^{-1} (range: 16.6–32.3 Mg C ha^{-1}) and was similar between forest types. The % consumed in PP stands was substantially higher (range: 23–35 vs. 13–24% for PP versus MC stands, respectively, Table 3). Stand-scale PE from low-severity fire was 51% and 65% of high-severity PE in MC and PP stands, respectively, indicating that the largest proportion of emissions was from combustion of surface and ground fuels. This result is consistent with Campbell and others (2007), who determined that greater than 60% of total combustion was from litter, foliage, and small downed wood, and that these high surface area:volume ratio pools were readily consumed ($>$50% combusted) in all burn severities in SW Oregon mixed-conifer forests. Our field-based estimate of live tree stem consumption was on average 1.24% (range: 0.23–2.77%) of live bark and bole mass, a trivial amount compared to other PE uncertainties. The largest remaining uncertainty is that the Consume 3.0 model does not account for belowground C loss due to combustion, erosion, or other fire effects, which can be substantial in some cases (Bormann and others 2008). Without detailed prefire measurements, we were unable to address this issue directly, but our soil C surveys did not show any significant C declines in high-severity stands (described below).

Scaled to the sampled landscape (approximately 30,000 ha of burned area), simulated total PE was 0.76 Tg C (Table 3). High-severity MC stands, with the largest per unit area emissions and landscape area, contributed a disproportionate amount of PE (42% of the total), whereas all PP forests combined released 26% of total PE. These proportions underscore the importance of incorporating landscape patterns of vegetation and fire effects (that is, the severity mosaic) into modeling and policy analyses. On a per unit area basis, PE from these fires was 33% higher than from the 200,000 ha Biscuit Fire (25.5 vs. 19 Mg C ha^{-1}; Campbell and others 2007). This C transfer represents a substantial pulse to the atmosphere relative to annual net C fluxes from unburned forest in the Metolius area (mean annual net C uptake at a mature PP site: 4.7 ± 0.4 Mg C ha^{-1} y^{-1}; Thomas and others 2009). Conversely, 0.76 Tg C is approximately 2.5% of Oregon statewide anthropogenic CO_2 emissions from fossil fuel combustion and industrial processes for the 2-year period 2002–2003 (30.62 Tg C equivalent; http://oregon.gov/energy/gblwrm/docs/ccigreport08web.pdf). It is important to note that the study scope burned area is less than half of the area burned in and around the Metolius Watershed since 2002 ($>$65,000 ha, 35,000 ha beyond this study scope) and that these were large fire years regionally. Thus, our study area represents a relatively small proportion of total wildfire PE. Although further refinements are possible, the current analysis provides a reasonable constraint for regional modeling efforts.

Carbon Pools (Mortality, Storage, and Vegetation Response)

Because large C pools (that is, live tree boles) were largely unaffected by combustion in all severities, fire-induced mortality was the most important overall C transformation, larger in magnitude than combustion. The distribution of live and dead C pools changed predictably with burn severity, dominated by the shift from live trees to dead wood mass (Table 4). Aboveground live tree and dead wood mass (g C m^{-2}) both exhibited wide ranges (live tree range: 0–9302, PP high severity to MC low severity; dead wood range: 924–6252, PP low severity to MC high severity), the latter range encompassing dead wood estimates from Washington East Cascades high-severity stands (approximately 3000; Monsanto and Agee 2008). Mean basal area mortality increased with burn severity classes, ranging from 14% in low-severity PP stands to 49% in moderate-severity and 100% in high-severity PP stands, with parallel patterns in MC stands (29, 58, 96%, respectively; Table 1, Figure 4A). Across both forest types, this mortality resulted in a significant reduction in live aboveground C in high- versus low-severity stands ($P < 0.005$), coupled with a near tripling of dead wood aboveground C (Table 4). In both forest types, forest floor mass showed the largest absolute and relative difference between burned and unburned stands (mean: 1588 and 232 g C m^{-2}, respectively), consistent with near-complete combustion of these pools. Whereas the difference between burned and unburned forest floor mass was highly significant (85% reduction; $P < 0.001$), there were no significant differences among low-, moderate-, and high-severity stands in either forest type ($P > 0.850$). Because of the decline in forest floor and high tree survival, low-severity stands exhibited lower aboveground necromass than unburned stands (Table 4).

Total aboveground C and total ecosystem C declined with increasing burn severity in both forest

Table 4. Carbon Pools of Forest Stands in the Metolius Watershed

Forest type[1] Burn severity	Aboveground					Belowground			
	Live tree mass	Non-tree live mass[2]	Dead wood mass[3]	FWD[4]	Forest floor[5]	Coarse root[6]	Fine root[7]	Soil C[8]	Ecosystem C[9]
Mixed-conifer[1]	5153 (807)	156 (12)	4080 (537)	171 (15)	610 (135)	3115 (232)	*185 (34)*	*6556 (348)*	***18,648*** *(1213)*
Unburned	$_{ab}$9302 (1146)	$_{ab}$140 (22)	2884 (1008)	205 (31)	$_{a}$1610 (180)	3588 (480)	na (na)	na (na)	**na** (na)
Low severity	$_{abc}$7268 (1147)	$_{a}$105 (22)	2813 (1009)	166 (31)	$_{b}$374 (180)	3162 (481)	172 (62)	5960 (611)	**20,414** (2189)
Mod severity	$_{bcd}$3071 (1140)	$_{ab}$181 (22)	4371 (1003)	162 (30)	$_{b}$289 (179)	2931 (478)	211 (61)	6434 (604)	**17,884** (2163)
High severity	$_{cd}$972 (1141)	$_{b}$200 (22)	6252 (1003)	153 (30)	$_{b}$169 (179)	2780 (478)	172 (61)	7225 (604)	**17,727** (2166)
Ponderosa pine[1]	3178 (538)	104 (9)	1898 (300)	112 (16)	531 (151)	1713 (142)	*135 (10)*	*5903 (195)*	***12,677*** *(648)*
Unburned	$_{w}$5110 (714)	$_{wxy}$78 (14)	$_{wx}$1517 (543)	$_{w}$179 (29)	$_{w}$1566 (219)	1842 (276)	na (na)	na (na)	**na** (na)
Low severity	$_{w}$5576 (716)	$_{wx}$67 (14)	$_{w}$924 (544)	$_{wx}$75 (29)	$_{x}$234 (219)	2131 (276)	128 (18)	6034 (353)	**$_{w}$15,244** (922)
Mod severity	$_{x}$2098 (724)	$_{xyz}$126 (14)	$_{wx}$1934 (551)	$_{wx}$130 (30)	$_{x}$258 (222)	1563 (280)	141 (18)	5899 (359)	**$_{wx}$12,089** (937)
High severity	$_{x}$0 (0)	$_{yz}$146 (14)	$_{x}$3218 (542)	$_{x}$64 (29)	$_{x}$67 (218)	1317 (275)	137 (18)	5775 (351)	**$_{x}$10,677** (918)

Notes: Values: mean C pools (g C m^{-2}). SE from ANCOVA in parentheses. Subscript letters indicate pairwise significant differences (Tukey-adjusted $P < 0.05$) between severities within each forest type. To convert values to Mg biomass ha^{-1}, divide by 50.

[1]Forest type row: non-italics denote all stands (unburned and burned, n = 32); italics denote burned stands only (n = 24, unburned stands not surveyed [na]).

[2]Other live pools: shrubs, seedlings, graminoids, forbs.

[3]Dead wood mass: sum of snags, stumps, and CWD (dead down wood ≥ 7.63 cm diameter).

[4]FWD: all woody fuels less than 7.63 cm diameter.

[5]Forest floor: sum of litter and duff.

[6]Coarse roots at least 10 mm diameter (modeled from diameter of live and dead trees and stumps).

[7]Fine roots less than 2 mm diameter (live and dead), scaled from 20 cm depth (62% [SD = 20] of fine roots assumed in top 20 cm).

[8]Soil C to 100 cm depth, scaled from 20 cm depth (49% [SD = 14] of soil C assumed in top 20 cm).

[9]Ecosystem C: sum of all C pools. Includes dead shrubs (not included in other columns).

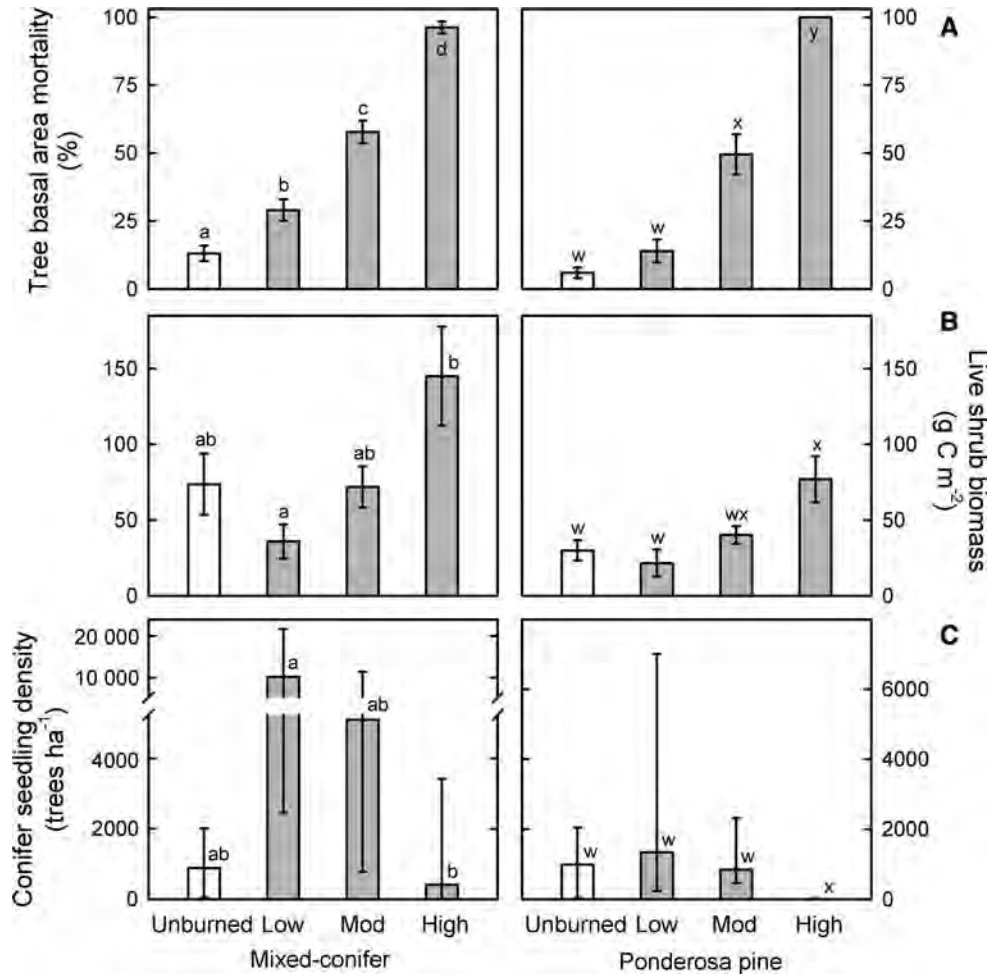

Figure 4. **A** Tree basal area (BA) mortality, **B** live shrub biomass, and **C** conifer seedling regeneration 4–5 years postfire by forest type and burn severity in the Metolius Watershed. Bars in **A** and **B** denote means; error bars denote ±1 SE from 8 plots in each forest type*burn severity treatment. Due to skewness, bars in **C** denote medians and error bars denote 25 and 75th percentile. Note the different scales between forest types above y-axis break in **C**. Tree mortality in **A** is % BA mortality due to fire in burned stands and total % dead BA in unburned stands. Lowercase letters denote statistically significant differences (Tukey-adjusted $P < 0.05$) among severities. Statistical tests for **A** used total % BA mortality, a metric common to all treatments. Statistical tests for **C** used $\log_e$-transformed data. **A** and **C** excluded the prefire biomass covariate. Seedlings are live, non-planted trees from the postfire time period only. Note that high-severity PP stands included 100% tree mortality in all 8 plots and a median seedling density of zero.

types (Table 4), although total ecosystem C was not significantly different among severities in MC forests ($P > 0.670$). In both types, fine root mass and soil C to 20 cm depth were not significantly different among severities ($P > 0.330$). Scaled to 100 cm, mean soil C stocks (±1 SE from regression) were 6556 ± 348 and 5903 ± 195 g C m^{-2} for burned MC and PP stands, respectively (Table 4). These values are similar to nearby unburned stands (7057 g C m^{-2}) and substantially lower than soil C in more mesic Oregon forests (14,244 and 36,174 g C m^{-2} in the West Cascades and Coast Range, respectively; Sun and others 2004). The lack of significant differences among severities furthers the evidence that soil C can be conserved with disturbance (Campbell and others 2009), including high-severity fire (Irvine and others 2007). Without site-specific prefire data we were unable to directly measure changes in soil C, and in applying a fixed-depth approach, a limitation of most postfire studies, we could not fully preclude the possibility of fire-induced soil C loss due to combustion, plume transport, or erosion (Bormann and others 2008). Unlike that study, in steep terrain experiencing stand-replacement fire (Bormann and others 2008), we did not observe severe erosion or changes in the soil surface between burned and unburned stands, and we detected no differences in

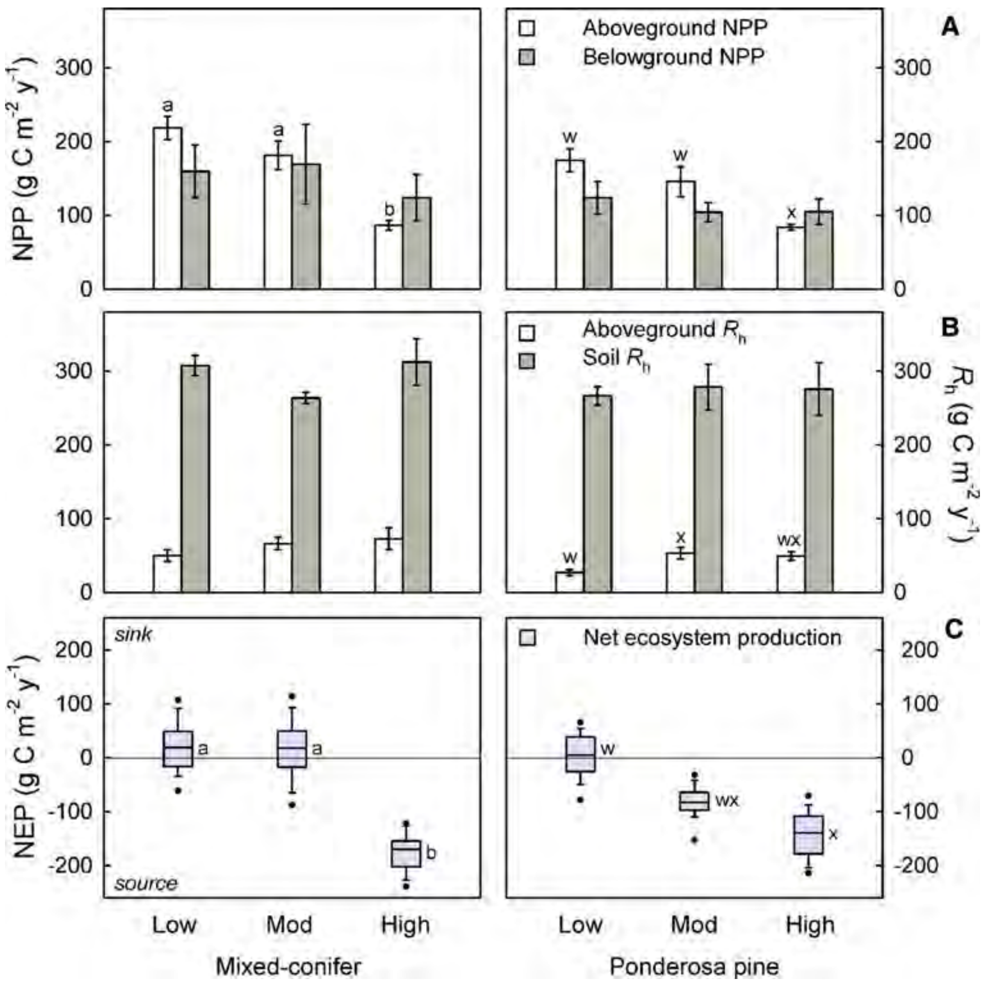

Figure 5. **A** Net primary productivity (NPP), **B** heterotrophic respiration (R_h), and **C** net ecosystem production (NEP) 4–5 years postfire by forest type and burn severity in the Metolius Watershed. Bars in **A** and **B** denote means; error bars denote ±1 SE from 8 plots in each forest type*burn severity treatment. Boxplots in **C** from Monte Carlo uncertainty propagation (see ''Methods''); line denotes median, box edges denote 25th and 75th percentiles, error bars denote 10th and 90th percentiles, and points denote 5th and 95th percentiles. Aboveground R_h includes all dead wood, shrubs, and herbaceous vegetation (Table 6). Soil R_h fractions from Irvine and others (2007). Lowercase letters denote statistically significant differences (Tukey-adjusted $P < 0.05$) among severities, tested with ANCOVA of each response variable given prefire biomass and burn severity.

mean or maximum soil depth among severities (Meigs 2009).

Our C pool estimates are consistent with previous estimates for PP in the Metolius area. Total aboveground C values for unburned and low-severity PP stands are similar to mature and young pine stands, respectively, whereas moderate- and high-severity stands fall between the values reported for initiation and young stands in a PP chronosequence (Law and others 2003). Our estimates of total ecosystem C in moderate- and high-severity PP stands are consistent with those reported by Irvine and others (2007). No analogous studies exist for the East Cascades MC forest type; the current study provides the first such estimates. The trends with burn severity were similar in both forest types, and the forest types differed consistently only in the magnitude of C pools. Total ecosystem C was 47% greater in MC forests than in PP forests (derived from Table 4).

Vegetation regeneration was generally robust but showed high variability and divergent responses of tree and non-tree functional types (Figure 4). Non-tree live biomass (that is, shrubs, forbs) was positively associated with burn severity, with significantly higher mass in high- versus low-severity stands ($P < 0.030$, Table 4, Figure 4). The strong shrub response—at or above prefire levels by 4–

5 years postfire—suggests important interactions with regenerating trees, which showed the opposite trend with burn severity. Tree seedling density (seedlings ha^{-1}) varied over 5 orders of magnitude (study wide range: 0–62,134) and, like shrub regeneration, was higher in MC than PP stands (Figure 4). This high variability is similar to studies of postfire conifer regeneration in the Klamath-Siskiyou and Rocky Mountain regions (5–6 orders of magnitude; Donato and others 2009b; Turner and others 2004), and the lack of PP regeneration in high-severity patches is consistent with previous studies reporting sparse regeneration beyond a generally short seed dispersal range (for example, Lentile and others 2005). Although regenerating vegetation represents a small C pool, it contributes to immediate postfire C uptake (described below) and sets the initial conditions for succession. The widespread presence of shrubs, particularly in high-severity stands, may initially reduce seedling growth through competition (Zavitkovski and Newton 1968), but over the long-term, understory shrubs play an important role in maintaining soil quality (C, N, microbial biomass C) in this ecoregion (Busse and others 1996). Because tree seedlings and shrubs were strongly correlated with overstory mortality, the burn severity mosaic could thus influence trajectories of C loss and accumulation for decades.

Postfire Carbon Balance (Biogenic C Fluxes and NEP)

Aboveground C Fluxes

Aboveground C fluxes followed the trends of live and dead C pools; NPP_A declined with increasing tree mortality (Figure 5A). In both forest types, NPP_A was significantly lower ($P < 0.015$) in high-severity versus moderate- and low-severity stands, which were not significantly different from each other ($P > 0.210$; overall range: 84–214 g C m^{-2} y^{-1}). Although NPP_A declined monotonically with burn severity, the sum of shrub and herbaceous NPP_A was about twofold higher in moderate- and high-severity versus low-severity stands, resulting in a dramatic increase in the non-tree proportion of NPP_A (Table 5). Thus, despite a reduction in live aboveground C of over 90% in both forest types in high-severity compared to low-severity stands, NPP_A was only 55% lower on average (Table 5). This trend, coupled with NPP_B (described below), resulted in a mean reduction of total NPP of about 40% from low- to high-severity, consistent with a strong compensatory effect of non-tree vegetation

Table 5. Annual Net Primary Productivity (NPP) of Burned Forest Stands in the Metolius Watershed

Forest type[1] / Burn severity	Aboveground				Belowground			Total NPP[7]	Non-tree[8] % of NPP_A	NPP_A:NPP_B ratio
	Tree[2]	Shrub	Herbaceous[3]	NPP_A^4	Coarse root[2]	Fine root[5]	NPP_B^6			
Mixed-conifer[1]	*93 (15)*	*20 (5)*	*46 (4)*	***159*** *(13)*	*18 (3)*	*132 (24)*	***150*** *(24)*	***309*** *(29)*	*42*	*1.06*
Low severity	$_{a}$173 (11)	8 (9)	33 (7)	$_{a}$**214** (15)	$_{a}$36 (3)	122 (44)	**159** (44)	**372** (47)	19	1.35
Mod severity	$_{b}$99 (11)	25 (9)	54 (7)	$_{a}$**178** (15)	$_{b}$18 (3)	151 (44)	**169** (43)	**347** (46)	44	1.05
High severity	$_{c}$12 (11)	27 (9)	51 (7)	$_{b}$**90** (15)	$_{c}$2 (3)	122 (44)	**125** (43)	**215** (46)	87	0.72
Ponderosa pine[1]	*68 (13)*	*10 (2)*	*57 (6)*	***135*** *(11)*	*10 (2)*	*96 (7)*	***107*** *(7)*	***242*** *(16)*	*50*	*1.26*
Low severity	$_{w}$135 (11)	3 (4)	$_{w}$34 (10)	$_{w}$**172** (15)	$_{w}$22 (2)	91 (13)	**113** (13)	$_{w}$**285** (24)	22	1.52
Mod severity	$_{x}$69 (12)	10 (4)	$_{x}$71 (10)	$_{w}$**151** (15)	$_{x}$9 (2)	101 (13)	**110** (13)	$_{wx}$**260** (24)	54	1.37
High severity	$_{y}$0 (0)	16 (4)	$_{wx}$68 (10)	$_{x}$**84** (15)	$_{y}$0 (0)	97 (13)	**97** (13)	$_{x}$**180** (24)	100	0.87

Notes: Values: mean NPP (g C m^{-2} y^{-1}). SE from ANCOVA in parentheses. Subscript letters indicate pairwise significant differences (Tukey-adjusted $P < 0.05$) between severities within each forest type. Summary fluxes bold.
[1]Forest type row: italics denote values from burned stands only (n = 24; most NPP components not surveyed in unburned stands).
[2]Tree: sum of bole and foliage NPP_A. Coarse root NPP modeled from live tree DBH (6th column).
[3]Herbaceous: sum of graminoid and forb NPP_A, equal to dry mass.
[4]NPP_A: annual aboveground net primary productivity (bold, shown in Figure 4).
[5]Fine root NPP_B to 100 cm depth based on published turnover index (Andersen and others 2008) and total fine root mass scaled from 20 cm depth.
[6]NPP_B: annual belowground net primary productivity (bold, shown in Figure 4).
[7]Total NPP: sum of all above- and belowground fluxes entering the system (bold).
[8]Non-tree NPP_A: sum of shrub and herbaceous NPP_A.

NPP_A. Previous studies in clearcut, thinned, and burned forests have shown the same pattern of rapid recolonization by non-trees contributing disproportionately to NPP (Campbell and others 2004; Gough and others 2007; Irvine and others 2007; Campbell and others 2009), and this study furthers the evidence across the severity gradient in two forest types. These findings suggest that fire studies focused solely on tree C pools (for example, Hurteau and others 2008) result in systematic biases and that C models and policies (for example, CCAR 2007) should encompass the full suite of ecosystem components and processes, including multiple vegetation functional types and rapid belowground recovery following disturbance.

Heterotrophic respiration of aboveground necromass (R_{hWD}), computed from C pools and decomposition constants, was a substantial component of C balance across both forest types but showed weak trends among severities (Figure 5B, Table 6). Despite the increase in dead wood mass with severity (Table 4), there were no significant differences in MC stands and only suggestive increases of R_{hWD} with severity in PP stands ($P = 0.031$–0.051). We attribute this surprising result to several factors: differing species- and decay class-specific constants and high variability among plots and severities; high retention and slow decomposition of snags; relatively high snag and dead shrub R_{hWD} in low-severity MC stands; relatively low CWD and dead shrub R_{hWD} in high-severity PP stands (Table 6). Although we expected that the immediate postfire period would exhibit maximum necromass over successional time (Wirth and others 2002; Hicke and others 2003), our R_{hWD} estimates were well less than both NPP_A and NPP_B ($R_{hWD} < 35\%$ of total NPP). In addition, R_{hWD} 4–5 years postfire constituted about 15% of total R_h across both forest types; R_{hsoil} (described below) accounted for approximately 85% (Table 6), demonstrating that belowground respiration processes are the predominant drivers of C loss.

Our range of R_{hWD} across the two forest types (28–75 g C m^{-2} y^{-1}; Table 6) is higher than estimates 2 years postfire in PP forest (Irvine and others 2007), similar to young PP stands in the Metolius area (Sun and others 2004) and an old-growth *Pseudotsuga-Tsuga* forest about 100 km away (Harmon and others 2004), and much less than untreated and thinned PP stands in Northern California (Campbell and others 2009). Our relatively low R_{hWD} estimates, particularly compared to C assimilation (NPP), illustrate the importance of decomposition lags in seasonally arid ecosystems, where microbial snag decomposition is moisture-limited. Other systems, such as sub-tropical humid zones where decomposition is not moisture- or temperature-limited and disturbance rapidly generates downed woody detritus (for example, hurricanes; Chambers and others 2007), may experience a more rapid pulse of C emission from necromass. The notion that fire-killed necromass represents a large, rapid C loss is unfounded, however, and warrants further investigation.

Woody detritus decomposition is a highly uncertain process, particularly in burned forests, where charring and snag fall play important, contrasting roles. For these R_{hWD} estimates, we used available decomposition constants derived from unburned forests. We believe that charring would likely reduce decomposition rates (DeLuca and Aplet 2008; Donato and others 2009a) but tested the sensitivity of our estimates by assuming snag decay rates equivalent to CWD. In this scenario, mean R_{hWD} would be approximately 125% and 50% higher in MC and PP stands, respectively, pushing low-severity stands into a net C source (negative NEP, although mean R_{hWD} would remain $<50\%$ of R_{hsoil} in both forest types). Our use of the 10% fraction is consistent with previous studies (Irvine and others 2007), and other studies have assumed zero snag decomposition (for example, Wirth and others 2002). Our short-term study precluded the assessment of snag fall, a stochastic process dependent on many factors (Russell and others 2006). The fall rates reported by Russell and others (2006)—snag half-lives for ponderosa pine and Douglas fir of 9–10 and 15–16 years, respectively—suggest that the majority of snags generated in the Metolius fires will stay standing for at least 10 years postfire. R_{hWD} may increase with accelerating snag fall (particularly in high-severity stands) but will remain small relative to R_{hsoil}, and NPP will likely increase over the same time period. Future studies are necessary to reduce the uncertainty of decomposition and snag dynamics in this area.

Belowground C Fluxes

Belowground C fluxes were by far the largest and most variable components of the annual C budget (NEP; Figure 5). Belowground NPP (NPP_B) was not significantly different across the entire study (overall mean: 284 g C m^{-2} y^{-1}; $P > 0.680$ in both forest types). Fine root NPP_B to 100 cm, based on total fine root mass and a constant turnover rate, accounted for about 90% of NPP_B, with increasing importance in high-severity stands, where very few live tree coarse roots survived. The apparent rapid establishment of fine roots in high-severity stands

Table 6. Annual Heterotrophic Respiration (R_h) and NEP of Forest Stands in the Metolius Watershed

Forest type[1] Burn severity	Aboveground (R_{hWD})						Belowground		Total R_h^7	NEP[8]	NPP:R_h ratio[8]
	Snag[2]	Stump[2]	CWD[3]	Dead shrub	Herbaceous[4]	R_{hWD}^5	R_{hsoil}^6	R_{hsoil}:R_{soil} ratio[6]			
Mixed-conifer[1]	7 (1)	5 (1)	24 (4)	3 (2)	22 (2)	**61** (6)	*294 (12)*	*na*	***357*** *(12)*	*−44 (28)*	*0.87*
Unburned	3 (2)	7 (1)	29 (9)	1 (4)	19 (4)	**59** (12)	na (na)	na	**na** (na)	na (na)	na
Low severity	7 (2)	3 (1)	14 (9)	7 (4)	17 (4)	**47** (12)	305 (21)	0.48	**353** (20)	$_{a}$21 (48)	1.05
Mod severity	9 (2)	5 (1)	22 (9)	1 (4)	27 (4)	**64** (12)	261 (21)	0.52	**327** (19)	$_{a}$21 (55)	1.06
High severity	9 (2)	5 (1)	32 (9)	3 (4)	26 (4)	**75** (12)	314 (21)	0.56	**388** (19)	$_{b}$-174 (32)	0.55
Ponderosa pine[1]	2 (1)	3 (1)	9 (2)	2 (1)	26 (3)	**42** (3)	*274 (15)*	*na*	***317*** *(17)*	*−76 (20)*	*0.76*
Unburned	$_{w}$0 (1)	4 (1)	$_{w}$18 (3)	2 (2)	$_{w}$16 (4)	**$_{wx}$39** (6)	na (na)	na	**na** (na)	na (na)	na
Low severity	$_{wx}$1 (1)	3 (1)	$_{x}$5 (3)	2 (2)	$_{w}$17 (4)	**$_{w}$27** (6)	262 (28)	0.48	**290** (30)	$_{w}$0 (33)	0.98
Mod severity	$_{wx}$2 (1)	3 (1)	$_{wx}$8 (3)	4 (2)	$_{x}$36 (4)	**$_{x}$53** (6)	286 (28)	0.52	**338** (31)	$_{wx}$-87 (35)	0.77
High severity	$_{x}$5 (1)	3 (1)	$_{wx}$7 (3)	1 (2)	$_{x}$34 (4)	**$_{wx}$49** (6)	274 (28)	0.56	**324** (30)	$_{x}$-142 (37)	0.56

Notes: Values: mean R_h ($g\ C\ m^{-2}\ y^{-1}$). SE from ANCOVA in parentheses, except NEP SE from Monte Carlo. Subscript letters Indicate pairwise significant differences (Tukey-adjusted $P < 0.05$) between severities within each forest type. Summary fluxes bold.

[1]Forest type row: non-italics denote all stands (unburned and burned, n = 32); italics denote burned stands only (n = 24, unburned stands not surveyed [na]).

[2]Snag R_h uses 10% of CWD decay rate and stump R_h uses 100% of CWD decay rate.

[3]CWD R_h includes FWD R_h, which was less than 0.15% of CWD R_h in all treatments.

[4]Herbaceous: forb and graminoid combined (assumed 50% of dry mass).

[5]R_{hWD}: sum of aboveground components (bold). Includes herbaceous annual decomposition (50% of dry mass).

[6]R_{hsoil}: heterotrophic soil respiration, based on total soil efflux and heterotrophic fractions from Irvine and others (2007). Moderate severity fraction is mean of unburned and high severity fractions.

[7]Total R_h: sum of all above- and belowground fluxes from land to atmosphere (bold).

[8]Net ecosystem production: sum of NPP (Table 5) and R_h fluxes. SE from Monte Carlo uncertainty propagation. NPP:R_h ratio < 1 if negative NEP.

contributed to the strong NPP compensatory effect of non-tree vegetation (Table 5). NPP_B accounted for approximately 50% of total NPP averaged across all severities and forest types, but high-severity stands in both forest types exhibited higher NPP_B than NPP_A (NPP_B = 58 and 54% of total NPP in MC and PP, respectively), indicating belowground C allocation values between those reported for grasslands and shrublands (67 and 50%, respectively; Chapin and others 2002). These estimates of fine root NPP_B are very similar to those reported for moderate- and high-severity PP by Irvine and others (2007), even though that study accounted for fire-induced fine root mortality and computed fine root NPP from live rather than total fine root stocks. Our estimated FR NPP is higher than a thinned PP forest in Northern California (Campbell and others 2009) and lower than a mixed-deciduous forest in Michigan (Gough and others 2007). Our estimates of total NPP (approximately 200–400 g C m^{-2} y^{-1}) and NPP_A:NPP_B ratio (overall mean: 1.15; Table 5) are within the range of previous studies in the area (Law and others 2003; Campbell and others 2004) and consistent with the postfire C allocation patterns described by Irvine and others (2007).

Heterotrophic soil respiration (R_{hsoil}) was not significantly different among burn severities and forest types ($P > 0.200$; Figure 5B, Table 6), consistent with the trends of forest floor, fine roots, and soil C (Table 4). Mean annual R_{hsoil} (g C m^{-2} y^{-1}, ±1 SE from regression) was 294 ± 12 and 274 ± 15 in MC and PP stands, respectively, very similar to previous estimates in mature unburned PP stands (Law and others 2003; Sun and others 2004). The lack of R_{hsoil} differences among severity classes and similarity to unburned forest suggests that this flux is resistant to disturbance-induced changes in these forests and supports the findings of previous studies (Irvine and others 2007; Campbell and others 2009). R_{hsoil} chamber measurements 1 year postfire in a nearby high-severity PP site on the 2006 Black Crater fire (J. Martin, unpublished data) were similar to unburned PP forest (Irvine and others 2008) and the values in the current study, indicating the lack of a large R_{hsoil} pulse from 1–5 years postfire. Although we did not find evidence of this postfire pulse in the absolute magnitude of R_{hsoil}, the conservation of R_{hsoil} across severities, coupled with declines in NPP, resulted in a large decline of the NPP:R_h ratio (approximately 0.55 in high-severity stands, both forest types; Table 6). This increase in relative R_{hsoil} equated to a muted postfire pulse that is reflected in our NEP estimates.

Implications for NEP

In both forest types, NPP_A was the principal driver of NEP trends, whereas R_{hsoil} controlled NEP magnitudes (Figure 5, Table 6). NEP was significantly lower in high- versus low-severity stands in both forest types ($P < 0.035$). In MC stands, mean NEP (g C m^{-2} y^{-1}, ± 1 SE from Monte Carlo simulations) varied from a slight sink (21 ± 48 and 21 ± 55) in low- and moderate-severity stands to a substantial source in high-severity stands (−174 ± 32). In PP forest, mean NEP declined from C neutral in low-severity stands (0 ± 33) to an intermediate source in moderate-severity stands (−87 ± 35) and substantial source in high-severity stands (−142 ± 37). Thus, mean annual NEP was similar in high-severity stands of both forest types 4–5 years after fire. These results are consistent with previous estimates of NPP, R_h, and NEP in unburned, moderate-, and high-severity PP stands within the study area (Irvine and others 2007), although our NEP estimate for high-severity stands is lower.

Previous studies quantified a NEP recovery period to a net sink of 20–30 years in PP forest following stand-replacement clearcutting (Law and others 2003; Campbell and others 2004). Longer-term measurements are necessary to determine the NEP fate of these postfire stands, but less than 30 years seems appropriate for high-severity stands, which are already closer to zero than initiation stands described by Law and others (2003), despite the removal of necromass via timber harvest in that study and higher R_{hWD} estimates here. In both forest types, low-severity NEP was not significantly different from zero (error estimates include zero; Table 6, Figure 5), which may be explained by limited fire effects and/or relatively rapid recovery of NEP. Although not a large C source to the atmosphere, C neutral stands represent a substantial decline from prefire NEP (unburned PP mean ± 1 SE for a range of age classes: 50 ± 14 g C m^{-2} y^{-1}, Irvine and others 2007). Management actions that mimic low-severity fire via prescribed burning or thinning (thus removing C) will likely reduce short-term NEP and long-term average C storage (Campbell and others 2009; Mitchell and others 2009), although strategic fuels treatments may help stabilize large tree C pools (North and others 2009).

Conclusion

The 2002–2003 wildfires across the Metolius Watershed generated a heterogeneous landscape pattern of overstory tree mortality and associated transformations of C pools and fluxes. Our results provide new constraints on short-term fire effects (4–5 years postfire) for regional C policy frameworks and underscore the importance of accounting for the full gradient of forest disturbance processes. Specifically, we found:

1. Stand-scale C combustion varied with burn severity from 13 to 35% of prefire aboveground C pools, with the largest emission proportion from combustion of surface/ground fuels and a study-wide average live tree stem consumption of 1.24%. Landscape-scale pyrogenic C emissions were equivalent to 2.5% of Oregon statewide anthropogenic CO_2 emissions from fossil fuel combustion and industrial processes for the same 2-year period.
2. Overstory live tree mass and seedling density decreased with increasing burn severity, whereas live shrub and herbaceous mass showed the opposite trend. From low- to moderate- to high-severity stands, average tree basal area mortality was 14, 49, and 100% in ponderosa pine, and 29, 58, and 96% in mixed-conifer forests.
3. Despite this decline in live aboveground C pools, total net primary productivity was only 40% lower in high- versus low-severity stands, reflecting a strong compensatory effect of non-tree productivity. Thus, the rapid response of early successional vegetation offset declines in NPP and NEP, buffering potential fire impacts on stand and landscape C storage, particularly when combined with the protracted decomposition of dead mass and conservation of belowground components (soil C, R_{hsoil}, and NPP_B).

With predictions of accelerating climate change and increasing fire extent and severity in western North American forests (IPCC 2007; Balshi and others 2009; Miller and others 2009), long-term field measurements are essential to assess trends in C storage and net annual C uptake over the course of several fire cycles, as well as any potential for directional ecosystem responses over time (for example, state change). Because non-stand-replacement fire accounts for the majority of the annual burned area in the Pacific Northwest Region (Schwind 2008), studies that focus exclusively on high-severity patches systematically underestimate pyrogenic C emission, mortality, and reduced C uptake following fire, impacts that will likely play an increasingly important role in regional and global carbon cycling.

ACKNOWLEDGMENTS

This research was supported by the Office of Science (BER), U.S. Department of Energy, Grant No. DE-FG02-06ER64318 and the College of Forestry, Oregon State University. We thank A. Pfleeger, P. Bozarth-Dreher, L. Gupta, R. Gupta, C. Sodemann, and C. Hebel for field and lab assistance. We acknowledge the insightful reviews of W. Cohen, C. Dunn, F. Gonçalves, C. Hebel, P. Hessburg, J. Meigs, D. Turner, and two anonymous reviewers. M. Huso provided invaluable statistical assistance, and the OSU Central Analytical Laboratory performed thorough, efficient chemical analysis. M. Duane, K. Howell, T. Hudiburg, J. Irvine, R. Kennedy, R. Ottmar, S. Powell, S. Prichard, C. Sierra, C. Thomas, H. Zald, and the OSU Pyro-maniacs assisted with data analysis. G. Fiske and K. Olsen helped with Figure 1 cartography. We thank the Deschutes National Forest for GIS data and access to field sites.

REFERENCES

Amiro BD, Todd JB, Wotton BM, Logan KA, Flannigan MD, Stocks BJ, Mason JA, Martell DL, Hirsch KG. 2001. Direct carbon emissions from Canadian forest fires, 1959–1999. Can J For Res 31:512–25.

Andersen CP, Phillips DL, Rygiewicz PT, Storm MJ. 2008. Fine root growth and mortality in different-aged ponderosa pine stands. Can J For Res 38:1797–806.

Balshi MS, McGuire AD, Duffy P, Flannigan M, Walsh J, Melillo JM. 2009. Assessing the response of area burned to changing climate in western boreal North America using a Multivariate Adaptive Regression Splines (MARS) approach. Glob Change Biol 15:578–600.

Birdsey RA, Jenkins JC, Johnston M, Huber-Sannwald E, Amiro BD, de Jong B, Barra JDE, French NHF, Garcia-Oliva F, Harmon ME, Heath LS, Jaramillo VJ, Johnsen K, Law BE, Marín-Spiotta E, Masera O, Neilson R, Pan Y, Pregitzer KS. 2007. North American forests. In: King AW, Dilling L, Zimmerman GP, Fairman DM, Houghton RA, Marland G, Rose AZ, Wilbanks TJ, Eds. The first State of the Carbon Cycle Report (SOCCR): The North American carbon budget and implications for the global carbon cycle. A report by the U.S. Climate Change Science Program and the Subcommittee on Global Change Research. Asheville: National Oceanic and Atmospheric Administration National Climatic Data Center. p 117–26.

Bork BJ. 1985. Fire history in three vegetation types on the eastern side of the Oregon Cascades. PhD Thesis, Oregon State University. 94 p.

Bormann BT, Homann PS, Darbyshire RL, Morrissette BA. 2008. Intense forest wildfire sharply reduces mineral soil C and N: the first direct evidence. Can J For Res 38:2771–83.

Brown JK. 1974. Handbook for inventorying downed woods material. USDA Forest Service General Technical Report INT-GTR-16. Ogden.

Busse MD, Cochran PH, Barren JW. 1996. Changes in ponderosa pine site productivity following removal of understory vegetation. Soil Sci Soc Am J 60:1614–21.

Campbell JL, Alberti G, Martin JG, Law BE. 2009. Carbon dynamics of a ponderosa pine plantation following a thinning treatment in the northern Sierra Nevada. For Ecol Manag 257:453–63.

Campbell JL, Donato DC, Azuma DL, Law BE. 2007. Pyrogenic carbon emission from a large wildfire in Oregon, United States. J Geophys Res 112:G04014.

Campbell JL, Law BE. 2005. Forest soil respiration across three climatically distinct chronosequences in Oregon. Biogeochemistry 73:109–25.

Campbell JL, Sun OJ, Law BE. 2004. Disturbance and net ecosystem production across three climatically distinct forest landscapes. Glob Biogeochem Cycles 18.

CCAR. 2007. Forest sector protocol version 2.1. California Climate Action Registry (CCAR). http://www.climateregistry.org/tools/protocols/industry-specific-protocols.html.

Chambers JQ, Fisher JI, Zeng HC, Chapman EL, Baker DB, Hurtt GC. 2007. Hurricane Katrina's carbon footprint on U. S. Gulf Coast forests. Science 318:1107.

Chapin FSIII, Matson PA, Mooney HA. 2002. Principles of terrestrial ecosystem ecology. New York: Springer.

Chapin FSIII, Woodwell GM, Randerson JT, Rastetter EB, Lovett GM, Baldocchi DD, Clark DA, Harmon ME, Schimel DS, Valentini R, Wirth C, Aber JD, Cole JJ, Goulden ML, Harden JW, Heimann M, Howarth RW, Matson PA, McGuire AD, Melillo JM, Mooney HA, Neff JC, Houghton RA, Pace ML, Ryan MG, Running SW, Sala OE, Schlesinger WH, Schulze ED. 2006. Reconciling carbon-cycle concepts, terminology, and methods. Ecosystems 9:1041–50.

Chen H, Harmon ME, Sexton JM, Fasth B. 2002. Fine-root decomposition and N dynamics in coniferous forests of the Pacific Northwest, USA. Can J For Res 32:320–31.

Cline SP, Berg AB, Wight HM. 1980. Snag characteristics and dynamics in Douglas-fir forests, western Oregon. J Wildlife Manag 44:773–86.

Daly C, Gibson WP, Taylor GH, Johnson GL, Pasteris P. 2002. A knowledge-based approach to the statistical mapping of climate. Clim Res 22:99–113.

DAYMET. 2009. Distributed climate data, http://www.daymet.org/.

DeLuca TH, Aplet GH. 2008. Charcoal and carbon storage in forest soils of the Rocky Mountain West. Front Ecol Environ 6:18–24.

Donato DC, Campbell JL, Fontaine JB, Law BE. 2009a. Quantifying char in postfire woody detritus inventories. Fire Ecol 5(2):104–115.

Donato DC, Fontaine JB, Campbell JL, Robinson WD, Kauffman JB, Law BE. 2009b. Early conifer regeneration in stand-replacement portions of a large mixed-severity wildfire in the Siskiyou Mountains, Oregon. Can J For Res 39:823–38.

Dore S, Kolb TE, Montes-Helu M, Sullivan BW, Winslow WD, Hart SC, Kaye JP, Koch GW, Hungate BA. 2008. Long-term impact of a stand-replacing fire on ecosystem CO_2 exchange of a ponderosa pine forest. Glob Change Biol 14:1801–20.

Eyre FH, Eds.1980. Forest cover types of the United States and Canada. Society of American Foresters, Washington, DC.

Fitzgerald SA. 2005. Fire ecology of ponderosa pine and the rebuilding of fire-resilient ponderosa pine ecosystems. In: Proceedings of the symposium on ponderosa pine: issues, trends, and management. USDA Forest Service General Technical Report PSW-GTR-198, 18–21 October 2004, Klamath Falls, OR, Albany.

Franklin JF, Dyrness CT. 1973. Natural vegetation of Oregon and Washington. USDA Forest Service General Technical Report PNW-GTR-8. Portland.

Franklin SE, Waring RH, McCreight RW, Cohen WB, Fiorella M. 1995. Aerial and satellite sensor detection and classification of western spruce budworm defoliation in a subalpine forest. Can J Remote Sens 21:299–308.

French NHF, Kasischke ES, Hall RJ, Murphy KA, Verbyla DL, Hoy EE, Allen JL. 2008. Using Landsat data to assess fire and burn severity in the North American boreal forest region: an overview and summary of results. Int J Wildland Fire 17:443–62.

Goward SN, Masek JG, Cohen WB, Moisen G, Collatz GJ, Healey SP, Houghton RA, Huang C, Kennedy RE, Law BE, Powell SL, Turner DP, Wulder MA. 2008. Forest disturbance and North American carbon flux Eos, transactions. Am Geophys Union 89:105–16.

Gough CM, Vogel CS, Harrold KH, George K, Curtis PS. 2007. The legacy of harvest and fire on ecosystem carbon storage in a north temperate forest. Glob Change Biol 13:1935–49.

Harmon ME, Bible K, Ryan MG, Shaw DC, Chen H, Klopatek J, Li X. 2004. Production, respiration, and overall carbon balance in an old-growth *Pseudotsuga-tsuga* forest ecosystem. Ecosystems 7:498–512.

Harmon ME, Fasth B, Sexton JM. 2005. Bole decomposition rates of seventeen tree species in Western U.S.A.: a report prepared for the Pacific Northwest Experiment Station, the Joint Fire Sciences Program, and the Forest Management Service Center of WO Forest Management Staff. http://andrewsforest.oregonstate.edu/pubs/webdocs/reports/decomp/cwd_decomp_web.htm.

Harmon ME, Sexton JM. 1996. Guidelines for measurements of woody detritus in forest ecosystems. U.S. long term ecological research program network, vol. 20. Albuquerque.

Hessburg PF, Salter RB, James KM. 2007. Re-examining fire severity relations in pre-management era mixed conifer forests: inferences from landscape patterns of forest structure. Landsc Ecol 22:5–24.

Hicke JA, Asner GP, Kasischke ES, French NHF, Randerson JT, Collatz GJ, Stocks BJ, Tucker CJ, Los SO, Field CB. 2003. Postfire response of North American boreal forest net primary productivity analyzed with satellite observations. Glob Change Biol 9:1145–57.

Hudiburg T. 2008. Climate, management, and forest type influences on carbon dynamics of West-Coast US forests. M.S. Thesis, Oregon State University. 86 p.

Hudiburg T, Law BE, Turner DP, Campbell JL, Donato DC, Duane M. 2009. Carbon dynamics of Oregon and Northern California forests and potential land-based carbon storage. Ecol Appl 19:163–80.

Hurteau MD, Koch GW, Hungate BA. 2008. Carbon protection and fire risk reduction: toward a full accounting of forest carbon offsets. Front Ecol Environ 6:493–8.

IPCC. 2007. Climate change 2007: the physical science basis. In: Solomon S, Qin D, Manning M, Chen Z, Marquis M, Averyt KB, Tignor M, Miller HL, Eds. Contribution of working group I to the fourth assessment report of the intergovernmental panel on climate change (IPCC). Cambridge University Press, Cambridge, United Kingdom and New York. http://www.ipcc.ch.

Irvine J, Law BE, Hibbard KA. 2007. Postfire carbon pools and fluxes in semiarid ponderosa pine in Central Oregon. Glob Change Biol 13:1748–60.

Irvine J, Law BE, Martin JG, Vickers D. 2008. Interannual variation in soil CO_2 efflux and the response of root respiration to climate and canopy gas exchange in mature ponderosa pine. Glob Change Biol 14:2848–59.

Kashian DM, Romme WH, Tinker DB, Turner MG, Ryan MG. 2006. Carbon storage on landscapes with stand-replacing fires. Bioscience 56:598–606.

Keane RE, Agee JK, Fulé P, Keeley JE, Key C, Kitchen SG, Miller R, Schulte LA. 2008. Ecological effects of large fires on US landscapes: benefit or catastrophe? Int J Wildland Fire 17:696–712.

Key CH, Benson NC. 2006. Landscape assessment: Ground measure of severity, the Composite Burn Index; and remote sensing of severity, the Normalized Burn Ratio. In Lutes DC, et al, Eds. FIREMON: Fire effects monitoring and inventory system. USDA Forest Service General Technical Report RMRS-GTR-164-CD. Fort Collins.

Kurz WA, Stinson G, Rampley GJ, Dymond CC, Neilson ET. 2008. Risk of natural disturbances makes future contribution of Canada's forests to the global carbon cycle highly uncertain. Proc Natl Acad Sci USA 105:1551–5.

Law BE, Arkebauer T, Campbell JL, Chen J, Sun O, Schwartz M, van Ingen C, Verma S. 2008. Terrestrial carbon observations: Protocols for vegetation sampling and data submission. Report 55, Global Terrestrial Observing System. FAO, Rome. 87 pp.

Law BE, Ryan MG, Anthoni PM. 1999. Seasonal and annual respiration of a ponderosa pine ecosystem. Glob Change Biol 5:169–82.

Law BE, Sun OJ, Campbell JL, Van Tuyl S, Thornton PE. 2003. Changes in carbon storage and fluxes in a chronosequence of ponderosa pine. Glob Change Biol 9:510–24.

Law BE, Thornton PE, Irvine J, Anthoni PM, Van Tuyl S. 2001a. Carbon storage and fluxes in ponderosa pine forests at different developmental stages. Glob Change Biol 7:755–77.

Law BE, Van Tuyl S, Cescatti A, Baldocchi DD. 2001b. Estimation of leaf area index in open-canopy ponderosa pine forests at different successional stages and management regimes in Oregon. Agric For Meteorol 108:1–14.

Law BE, Waring RH. 1994. Combining remote sensing and climatic data to estimate net primary production across Oregon. Ecol Appl 4:717–28.

Lentile LB, Smith FW, Shepperd WD. 2005. Patch structure, fire-scar formation, and tree regeneration in a large mixed-severity fire in the South Dakota Black Hills, USA. Can J For Res 35:2875–85.

Martin RE, Sapsis DB. 1991. Fires as agents of biodiversity: pyrodiversity promotes biodiversity. In: Harris RR, Erman DE, Kerner HM (technical coordinators), Eds. Proceedings of the symposium on biodiversity of northwestern California. Santa Rosa, CA: Wildland Resources Center, pp. 150–7.

Maser C, Anderson RG, Cromack Jr K, Williams JT, Martin RE. 1979. Dead and down woody material. Wildlife habitats in managed forests of the Blue Mountains of Oregon and Washington, USDA Forest Service Agriculture Handbook No. 553.

McIver JD, Ottmar RD. 2007. Fuel mass and stand structure after post-fire logging of a severely burned ponderosa pine forest in northeastern Oregon. For Ecol Manag 238:268–79.

Meigs GW. 2009. Carbon dynamics following landscape fire: influence of burn severity, climate, and stand history in the Metolius Watershed, Oregon. M.S. Thesis, Oregon State University. 147 p.

Miller JD, Safford HD, Crimmins M, Thode AE. 2009. Quantitative evidence for increasing forest fire severity in the Sierra Nevada and Southern Cascade Mountains, California and Nevada, USA. Ecosystems 12:16–32.

Mitchell SR, Harmon ME, O'Connell KEB. 2009. Forest fuel reduction alters fire severity and long-term carbon storage in three Pacific Northwest ecosystems. Ecol Appl 19:643–55.

Monsanto PG, Agee JK. 2008. Long-term post-wildfire dynamics of coarse woody debris after salvage logging and implications for soil heating in dry forests of the eastern Cascades, Washington. For Ecol Manag 255:3952–61.

North M, Hurteau M, Innes J. 2009. Fire suppression and fuels treatment effects on mixed-conifer carbon stocks and emissions. Ecol Appl 19:1385–96.

Ottmar RD, Sandberg DV, Riccardi CL, Prichard SJ. 2007. An overview of the fuel characteristic classification system—quantifying, classifying, and creating fuelbeds for resource planning. Can J For Res 37:2383–93.

Pierce LL, Running SW. 1988. Rapid estimation of coniferous forest leaf-area index using a portable integrating radiometer. Ecology 69:1762–7.

Prichard SJ, Ottmar RD, Anderson GK. 2006. Consume 3.0 user's guide. Pacific Wildland Fire Sciences Laboratory, USDA Forest Service, Pacific Northwest Research Station. Seattle, WA. http://www.fs.fed.us/pnw/fera/research/smoke/consume/index.shtml.

Rorig ML, Ferguson SA. 1999. Characteristics of lightning and wildland fire ignition in the Pacific Northwest. J Appl Meteorol 38:1565–75.

Roy DR, Boschetti L, Trigg SN. 2006. Remote sensing of fire severity: assessing the performance of the normalized burn ratio. IEEE Geosci Remote Sens Lett 3:112–6.

Running SW. 2008. Ecosystem disturbance, carbon, and climate. Science 321:652–3.

Russell RE, Saab VA, Dudley JG, Rotella JJ. 2006. Snag longevity in relation to wildfire and postfire salvage logging. For Ecol Manag 232:179–87.

Santantonio D, Hermann RK, Overton WS. 1977. Root biomass studies in forest ecosystems. Pedobiologia 17:1–31.

Savage M, Mast JN. 2005. How resilient are southwestern ponderosa pine forests after crown fires? Can J For Res 35:967–77.

Schoennagel T, Veblen TT, Romme WH. 2004. The interaction of fire, fuels, and climate across Rocky Mountain forests. Bioscience 54:661–76.

Schwind B. 2008. Monitoring trends in burn severity: report on the Pacific Northwest and Pacific Southwest fires—1984 to 2005. Available online: http://mtbs.gov.

Simon SA. 1991. Fire history in the Jefferson Wilderness area of east of the Cascade Crest. A final report to the Deschutes National Forest Fire Staff.

Soeriaatmadhe RE. 1966. Fire history of the ponderosa pine forests of the Warm Springs Indian Reservation Oregon. PhD Thesis, Oregon State University.

Sun OJ, Campbell JL, Law BE, Wolf V. 2004. Dynamics of carbon stocks in soils and detritus across chronosequences of different forest types in the Pacific Northwest, USA. Glob Change Biol 10:1470–81.

Swedberg KC. 1973. A transition coniferous forest in the Cascade Mountains of Northern Oregon. Am Midl Nat 89:1–25.

Thomas CK, Law BE, Irvine J, Martin JG, Pettijohn JC, Davis KJ. 2009. Seasonal hydrology explains inter-annual and seasonal variation in carbon and water exchange in a semi-arid mature ponderosa pine forest in Central Oregon. J Geophys Res Biogeosci. doi:10.1029/2009JG001010.

Thompson JR, Spies TA, Ganio LM. 2007. Reburn severity in managed and unmanaged vegetation in a large wildfire. Proc Natl Acad Sci USA 104:10743–8.

Thornton PE, Running SW, White MA. 1997. Generating surfaces of daily meteorological variables over large regions of complex terrain. J Hydrol 190:214–51.

Turner DP, Ritts WD, Law BE, Cohen WB, Yang Z, Hudiburg T, Campbell JL, Duane M. 2007. Scaling net ecosystem production and net biome production over a heterogeneous region in the western United States. Biogeosciences 4:597–612.

Turner MG, Tinker DB, Romme WH, Kashian DM, Litton CM. 2004. Landscape patterns of sapling density, leaf area, and aboveground net primary production in postfire lodgepole pine forests, Yellowstone National Park (USA). Ecosystems 7:751–75.

USDA. 2003. Field instructions for the annual inventory of Washington, Oregon, and California Forest Inventory and Analysis Program. USDA Forest Service Pacific Northwest Research Station. Portland.

Van Tuyl S, Law BE, Turner DP, Gitelman AI. 2005. Variability in net primary production and carbon storage in biomass across Oregon forests: an assessment integrating data from forest inventories, intensive sites, and remote sensing. For Ecol Manag 209:273–91.

Van Wagner CE. 1968. The line intersect method in forest fuel sampling. For Sci 14:20–6.

Weaver H. 1959. Ecological changes in the ponderosa pine forest of the Warm Springs Indian Reservation in Oregon. J For 57:15–20.

Westerling AL, Hidalgo HG, Cayan DR, Swetnam TW. 2006. Warming and earlier spring increase western US forest wildfire activity. Science 313:940–3.

Wirth C, Czimczik CI, Schulze ED. 2002. Beyond annual budgets: carbon flux at different temporal scales in fire-prone Siberian Scots pine forests. Tellus B Chem Phys Meteorol 54:611–30.

Zavitkovski J, Newton M. 1968. Ecological importance of snowbrush *Ceanothus velutinus* in the Oregon Cascades. Ecology 49:1134–45.

Comment on "Prescribed Fire As a Means of Reducing Forest Carbon Emissions in the Western United States"

Wiedinmyer and Hurteau (*1*) present a "preliminary sensitivity analysis" suggesting that a one-to-one replacement of wildfire with low-intensity prescribed fire in western U.S. forests between 2001 and 2008 would have substantially reduced pyrogenic carbon emissions over this period. We agree that prescribed burning is an important tool for restoring certain forests to the fire regimes in which they evolved. We further agree that pyrogenic carbon emissions must be considered in regional carbon accounting and commend the authors for highlighting the spatiotemporal variability and uncertainties associated with emissions estimates.

We have concerns, however, regarding the study's conclusions. Our basic argument is that a one-to-one substitution of prescribed fire for wildfire in both space and time is a fundamentally unrealistic scenario, even for a sensitivity analysis. For prescribed fire to preclude all wildfire, it would have to be applied both over larger areas and more frequently than wildfire would otherwise occur. Although Wiedinmyer and Hurteau (*1*) state that their simulations do not account for the feasibility or cumulative emissions of repeated prescribed burning, simply acknowledging these limitations does not justify the claim that "...Wide-scale prescribed fire application can reduce CO_2 fire emissions for the western U.S. by 18–25%...," even when labeled as an "upper bound." By underestimating the impacts of prescribed fire, the authors present misleading conclusions that could result in flawed forest carbon policies.

In simulating a one-to-one substitution of prescribed fire for wildfire, Wiedinmyer and Hurteau (*1*) take forests that historically experienced frequent, low- to mixed-severity fire and assume that all fires could instead be human-ignited, controlled, and low-intensity. In practice, this approach would require: (1) predicting where and when all wildfires occur; (2) implementing prescribed fire within these perimeters; (3) 100% efficacy of prescribed fire in eliminating wildfires; and (4) 0% escape of prescribed fires. This framework is completely unrealistic. Because wildfires affect a small and largely unpredictable proportion of the landscape, mitigating their impacts with prophylactic prescriptions requires treatment of a much larger proportion of the landscape. Treating this larger area would necessarily reduce the difference between the prescribed-fire and wildfire scenarios.

Even if one could predict where and when wildfires were to occur, the intrinsic reciprocality between fire frequency and intensity further invalidates a one-to-one substitution of low-intensity prescribed fire for high-intensity wildfire. Although low-intensity fire results in lower per-unit-area emissions than high-intensity fire (*2*), cumulative emissions over time are likely similar because high-intensity fire is by nature infrequent, whereas fuel treatment via thinning or prescribed fire must be applied frequently to remain effective (*3, 4*). We suggest that a more realistic temporal framework be based on the mass balance of fuel production and combustion over time. For example, the authors could have compared a single high-intensity wildfire in 100 years with four to five low-intensity prescribed fires over the same time period.

Wiedinmyer and Hurteau (*1*) have made some important improvements over previous studies. For instance, the removal of redundant and low-confidence fire detection by the MODIS sensor reduced estimated regional emissions by 40–56% compared to previous estimates (*5*). Also, the authors' determination that wildfire releases about twice as much carbon per-unit-area as prescribed fire (Table 1 in *1*) greatly improves upon earlier suggestions that high-intensity wildfire released over 10 times more carbon than surface fire (*6*). This correction much better reflects the fact that most pyrogenic emissions arise from the combustion of fine surface fuels, which are readily consumed in both surface and crown fire (*2*).

There is a strong consensus that vast areas of arid forests in the western U.S. have suffered both structurally and compositionally from a century of fire exclusion and that prescribed fire can be an effective tool for restoring historic functionality and resilience to these ecosystems. We agree with concerns that emerging policies aimed at reducing CO_2 emissions could threaten the ability of managers to apply prescribed fire at the spatial and temporal frequency necessary to achieve and sustain desired forest conditions. Nevertheless, unrealistic claims that fuel reduction treatments reduce overall forest carbon emissions do not serve this cause. It is more useful to demonstrate and champion the restoration of fire-prone forests despite what may be net carbon losses. While there do exist some negative feedbacks among thinning, prescribed fire, and wildfire, the increase of any of these will almost certainly lead to an overall reduction of carbon storage. More importantly, increases in all three may be necessary to bring about desired future conditions.

Literature Cited

(1) Wiedinmyer, C.; Hurteau, M. D. Prescribed fire as a means of reducing forest carbon emissions in the Western United States. *Environ. Sci. Technol.* **2010**, *44* (6), 1926–1932.
(2) Campbell, J. L.; Donato, D. C.; Azuma, D. L.; Law, B. E. Pyrogenic carbon emission from a large wildfire in Oregon, United States. *J. Geophys. Res.* **2007**, *112* (G04014), doi: 10.1029/2007JG000451.
(3) Ager, A. A.; McMahan, A. J.; Barrett, J. J.; McHugh, C. W. A simulation study of thinning and fuel treatments on a wildland–urban interface in eastern Oregon, USA. *Landsc. Urb. Plann.* **2007**, *80*, 292–300.
(4) Finney, M. A.; McHugh, C. W.; Grenfell, I. C. Stand- and landscape-level effects of prescribed burning on two Arizona wildfires. *Can. J. For. Res.* **2005**, *35*, 1714–1722.
(5) Wiedinmyer, C.; Neff, J. C. Estimates of CO_2 from fires in the United States: Implications for carbon management. *Carbon Balance Manage.* **2007**, *2* (10), 10.1186/1750-0680-2-10.
(6) Hurteau, M. D.; Koch, G. W.; Hungate, B. A. Carbon protection and fire risk reduction: Toward a full accounting of forest carbon offsets. *Front. Ecol. Environ.* **2008**, *6* (9), 493–498.

Garrett W. Meigs* and John L. Campbell

Department of Forest Ecosystems and Society, Oregon State University, Corvallis, Oregon

* Corresponding author e-mail: garrett.meigs@oregonstate.edu.

ES101595T

EXHIBIT 30